Université d'Aix-Marseille

École doctorale Science de l'environnement, ED 251

Thèse de doctorat

Présentée par Natascha SCHMIDT

Présence dans l'environnement et flux des contaminants organiques d'intérêt émergent dans la zone côtière nord-ouest de la Méditerranée et dans le Rhône.

Composition du jury :

Prof. Dr. Ralf Ebinghaus (Helmholtz-Zentrum Geesthacht)	Rapporteur
Dr. Sopheak Net (LASIR, Université de Lille)	Rapporteur
Prof. Jordi Dachs (Spanish National Research Council)	Examinateur
Dr. Hélène Budzinski (EPOC, Université de Bordeaux)	Examinateur
Dr. Madeleine Goutx (MIO, Université Aix-Marseille)	Examinateur
Dr. Richard Sempéré (MIO, Université Aix-Marseille)	Co-directeur de thèse
Dr. Javier Castro-Jiménez (MIO, Université Aix-Marseille)	Co-directeur de thèse

Université d'Aix-Marseille

École doctorale Science de l'environnement, ED 251

Thèse de doctorat

Présentée par Natascha SCHMIDT

Présence dans l'environnement et flux des contaminants organiques d'intérêt émergent dans la zone côtière nord-ouest de la Méditerranée et dans le Rhône.

Composition du jury :

Prof. Dr. Ralf Ebinghaus (Helmholtz-Zentrum Geesthacht)	Rapporteur
Dr. Sopheak Net (LASIR, Université de Lille)	Rapporteur
Prof. Jordi Dachs (Spanish National Research Council)	Examinateur
Dr. Hélène Budzinski (EPOC, Université de Bordeaux)	Examinateur
Dr. Madeleine Goutx (MIO, Université Aix-Marseille)	Examinateur
Dr. Richard Sempéré (MIO, Université Aix-Marseille)	Co-directeur de thèse
Dr. Javier Castro-Jiménez (MIO, Université Aix-Marseille)	Co-directeur de thèse

Abstract

Chemical pollution has become a global threat to the environment, including marine ecosystems, which receive important contaminant loads *via* wastewater and freshwater inputs, among others. Phthalates (PAEs), organophosphate esters (OPEs), bisphenols (BPs) and perfluoroalkyl substances (PFAS) are man-made organic chemicals used in a variety of products. PAEs and BPs are common plasticizers as well as non-halogenated OPEs. Halogenated OPEs are mainly used as flame retardants and are considered as substitutes of polybrominated diphenyl ethers (PBDEs), which were banned by the Stockholm Convention on Persistent Organic Pollutants. PFAS have water and oil repellent properties and are thus used in the manufacturing of resistant textiles and polytetrafluoroethylene, but also in fire-fighting foams. These organic compounds, which are widely distributed in the environment due to their high production and usage rates and the insufficient regulatory framework, give raise to growing concerns due to their proven or suspected endocrine disruptors and/or carcinogen properties. Together with other environmental pollutants, such as microplastics, they exert a growing anthropogenic pressure on aquatic environments. Their temporal and spatial variability, local occurrence and sources, distribution in different compartments and interactions with organisms, among others, are not well characterized and many open questions remain. In this thesis, several of these aspects were investigated at the scale of the Bay of Marseille (NW Mediterranean Sea) and the Rhône River. In a first investigation, daily microplastic transport rates for the Northern Mediterranean Current (NMC) (0.18-86.46 t) and the Rhône River (0.20-21.32 kg) were estimated based on the collection of 3,193 microplastic items in the NMC influence area, the Bay of Marseille and the Rhône River and its plume. Secondly, organic plastic additives were analyzed in the Rhône River and it was estimated that 13.7-148 kg of dissolved organic plastic additives are exported by the Rhône River each day, indicating that potential leaching from (surface) microplastics cannot entirely explain the additive concentrations present in the dissolved water phase. In the third part, PFAS were analyzed in Marseille Bay and the Rhône River and it was observed that perfluorooctanesulfonic acid (PFOS) concentrations exceeded the EU annual average Environmental Quality Standard in over 80% of samples. Furthermore, it was shown through numeric modelling that intrusions from the Rhône River can transport important PFOS quantities into Marseille Bay. In the fourth section, a focus on Marseille Bay showed that especially zooplankton samples exhibited high organic plastic additive amounts, while water and sediment samples were only moderately or slightly contaminated. Hereby, diethylhexyl

phthalate (DEHP) was most abundant in zooplankton samples, with a wide range of concentrations (309 ng g^{-1} dw - 40 µg g^{-1} dw). Finally, off-shore water samples from the tropical North Atlantic allowed to make comparisons between coastal (Bay of Marseille), riverine (Rhône River) and remote (tropical North Atlantic) regions. While in Marseille Bay coastal (WWTP outlet, harbor activities) and riverine inputs dominated contaminant dynamics, medium-/long-range transport occurred in the tropical North Atlantic where contaminants supposedly originated from the Amazon River and were further transported by the North Brazil Current.

This study allowed to get an overview of the organic contaminant situation in Marseille Bay, to investigate contaminant fluxes from the Rhône River – the main freshwater source of the Mediterranean Sea – and to provide original data from the tropical North Atlantic. Future efforts should concentrate on dedicated studies of zooplankton-contaminant interactions, increased temporal resolution and investigations in areas of special interest, such as the Amazon River.

Key words: Phthalates, organic contaminants, plasticizers, environmental pollution, microplastics, Bay of Marseille.

Résumé

La pollution chimique est devenue une menace mondiale pour l'environnement, y compris les écosystèmes marins, qui reçoivent d'importantes charges de contaminants par les eaux usées et les apports fluviaux, entre autres. Les phtalates (PAEs), les esters organophosphorés (OPEs), les bisphénols (BPs) et les composés perfluorés (PFAS) sont des produits chimiques organiques synthétiques utilisés dans divers produits. Les PAEs et les BPs sont des plastifiants courants ainsi que les OPE non halogénés. Les OPE halogénés sont principalement utilisés comme retardateurs de flamme et sont considérés comme des substituts des polybromodiphényléthers (PBDE), qui ont été interdits par la Convention de Stockholm sur les polluants organiques persistants. Les PFAS ont des propriétés hydrofuges et oléofuges et sont donc utilisés dans la fabrication de textiles résistants et de polytétrafluoroéthylène, mais aussi dans les mousses extinctrices. Ces composés organiques qui sont largement répandus dans l'environnement en raison de leurs taux élevés de production et d'utilisation et de l'insuffisance du cadre réglementaire, suscitent des inquiétudes croissantes en raison de leurs propriétés éprouvées ou soupçonnées de perturbateurs endocriniens et/ou cancérogènes. Avec d'autres polluants environnementaux, tels que les microplastiques, ils exercent une pression anthropique croissante sur les milieux aquatiques. Leur variabilité temporelle et spatiale, leur occurrence et leurs sources locales, leur distribution dans différents compartiments et leurs interactions avec les organismes, entre autres, ne sont pas bien caractérisées et de nombreuses questions demeurent ouvertes. Dans cette thèse, plusieurs de ces aspects ont été étudiés à l'échelle de la Baie de Marseille (Méditerranée Nord-Ouest) et du Rhône. Dans une première étude, les taux quotidiens de transport de microplastiques pour le Courant Nord de la Méditerranée (CNM) (0.18-86.46 t) et le Rhône (0.20-21.32 kg) ont été estimés à partir de la collecte de 3,193 microplastiques dans la zone d'influence du CNM, la baie de Marseille et le Rhône et son panache. Deuxièmement, des additifs plastiques organiques ont été analysés dans le Rhône et il a été estimé que 13.7 à 148 kg d'additifs plastiques organiques dissous sont exportés chaque jour par le Rhône, ce qui indique que le relargage potentiel par les microplastiques (de surface) ne peut pas expliquer entièrement les concentrations des additifs présents dans la phase aqueuse dissoute. Dans la troisième partie, les PFAS ont été analysés dans la baie de Marseille et dans le Rhône et il a été observé que les concentrations d'acide perfluorooctanesulfonique (PFOS) dépassaient la norme de qualité environnementale moyenne annuelle de l'UE dans plus de 80% des échantillons. De plus, il a été démontré par modélisation numérique que les intrusions du Rhône peuvent transporter d'importantes quantités de PFOS dans la baie de Marseille. Dans la

quatrième section, l'accent mis sur la baie de Marseille a montré que les échantillons de zooplancton en particulier présentaient des quantités élevées d'additifs plastiques organiques, tandis que les échantillons d'eau et de sédiments n'étaient que modérément ou légèrement contaminés. Ainsi, le phtalate de diéthylhexyle (DEHP) était le plus abondant dans les échantillons de zooplancton, avec une large gamme de concentrations (309 ng g^{-1} dw - 40 µg g^{-1} dw). Enfin, des échantillons d'eaux de l'Atlantique Nord tropical ont permis de faire des comparaisons entre les régions côtières (baie de Marseille), fluviales (Rhône) et éloignées (Atlantique Nord tropical). Alors que dans la baie de Marseille, la dynamique des contaminants était dominée par les apports côtiers (décharge de la STEP, activités portuaires) et fluviaux, le transport à moyenne et longue distance s'est produit dans l'Atlantique Nord tropical, où les contaminants provenaient du fleuve Amazone et étaient ensuite transportés par le courant du Nord Brésilien.

Cette étude a permis d'avoir un aperçu de la situation des contaminants organiques dans la baie de Marseille, d'étudier les flux de contaminants provenant du Rhône - la principale source d'eau douce de la Méditerranée - et de fournir des données originales sur l'Atlantique Nord tropical. Les efforts futurs devraient se concentrer sur des études spécialisées sur les interactions zooplancton-contaminants, une résolution temporelle accrue et des études dans des zones d'intérêt particulier, comme le fleuve Amazone.

Mots clés : phtalates, contaminants organiques, plastifiants, pollution environnementale, microplastiques, Baie de Marseille.

CONTENTS

INTRODUCTION....1
1. Organic contaminants studied....5
1.1 Phthalates (PAEs)....5
1.2. Organophosphate esters (OPEs)....8
1.3. Bisphenols (BPs)....10
1.4. Perfluoroalkyl substances (PFAS)....12
1.5. Microplastics....13
2. Environmental sources and fate....14
3. Environmental levels....17
3.1. In freshwater ecosystems....17
3.2. In coastal and open-ocean waters....20
3.3. In marine sediments and biota....22
5. Study area....24
6. Scopes of this thesis....28
References....29
MATERIAL & METHODS....44
Microplastic samples....45
Water samples (Solid Phase Extraction)....46
Sediment and zooplankton samples (ultrasound extraction)....47
GC/MS and LC-HRMS analysis....49
Recovery rates & blanks....51
CHAPTER I: Microplastics....54
1. Introduction....58
2. Materials and Methods....60
3. Results and Discussion....63
3.1. Microplastic abundance....63
3.2. Microplastic weight....69
3.3. Microplastic size distribution....70
4. Conclusions....74
References....75
CHAPTER II: PAEs, OPEs and BPs in the Rhône River....81
1. Introduction....84
2. Materials and Methods....86

2.1. Study area and sampling 86
2.2. Solvents and chemical standards 87
2.3. Sample processing and analysis 88
2.4. Quality Assurance / Quality Control 90
2.5. Data processing 91
3. Results and Discussion 91
3.1. Concentration levels and relative abundances 94
3.1.1. Phthalates 94
3.1.2. Organophosphate esters 96
3.1.3. Bisphenols 97
3.1.4. Relative importance of PAEs, OPEs and BPs in the Rhône River 98
3.2. Potential factors affecting contaminant variability 99
3.3. Fluxes and potential sources to the Rhône River and the Mediterranean Sea 101
4. Conclusions 102
References 104
CHAPTER III: Perfluorinated compounds 110
1. Introduction 113
2. Materials & Methods 116
2.1. Study area and sampling 116
2.2. Chemicals and standards 117
2.3. Chemical analysis 118
2.4. Quality Assurance / Quality Control (QA/QC) 119
2.5. Hydrodynamic model (MARS3D) 119
3. Results and discussion 120
3.1. Σ_4 PFAS concentrations and estimated flux to the Mediterranean Sea 120
3.2. Relative abundances of individual compounds 123
3.3. PFOS occurrence, estimated flux and modelled inputs to Marseille Bay via freshwater intrusions 126
4. Conclusion 132
References 134
CHAPTER IV: Plastic additives in the Bay of Marseille 139
1. Introduction 141
2. Material & Methods 143
2.1. Study area 143
2.2. Sampling and sample processing 144

2.3. Contaminant extraction 145
2.3.1. Water samples 145
2.3.2. Sediment and zooplankton samples 146
2.4. GC/MS analysis 146
2.5. Quality Assurance / Quality Control 147
3. Results & Discussion 148
3.1. Surface waters 148
3.2. Sediments 151
3.3. Zooplankton samples 153
3.4. Microplastics 157
4. Conclusion 159
References 161
CHAPTER V: Organic contaminants in the tropical North Atlantic 165
Introduction 169
Methods 170
Contaminant analysis 170
Quality assurance/quality control (QA/QC) 172
Solvents and reagents 173
Salinity and velocity maps 173
Backwards trajectories 174
Results and discussion 175
References 187
CONCLUSION & PERSPECTIVES 192
PUBLICATIONS 200
ANNEXES 230
Annex Chapter I 231
Annex Chapter II 234
Annex Chapter III 244
Annex Chapter IV 250
Annex Chapter V 255

Acknowledgements

Three people were essential for the success of this work: Richard Sempéré, Javier Castro-Jiménez and Pierre Boissery. I would like to thank Richard for his unwavering confidence in me, his guidance and many helpful advices. Javier taught me a lot about organic chemistry; moreover, his ideas and inputs throughout the project were crucial and I would like to thank him for that. Without Pierre Boissery and the Agence de l'Eau Rhône Mediterrannée Corse the Blue-POLUT project would simply not have existed and I want to thank Pierre for his trust in us and his interest in our work.

I would also like to thank Vincent Fauvelle for making the work so pleasant and yet productive and for always being there when help was needed. Special thank goes to my office mate Masha and the dear Katixa, for their support, for shared lunches, tea and chocolate breaks and many, many conversations.

Michel Fornier regularly accompanied me to the samplings in Arles and we shared many stories and lunches together. The captain and crew of the Antedon II were indispensable for the success of the sampling campaigns in the Bay of Marseille, together with Dorian Guillemain, Michel Lafont and Deny Malengros. The "Sargasses II" expedition was a unique experience and I am grateful to have had the chance to participate. Therefore, I would like to express my thank to Monaco Explorations, the captain and crew of the Yersin, the IRD, the land-based team, everybody involved in organizing the mission and the scientists onboard.

Thanks to Benjamin Oursel for help with extractions, to Anouck for sharing the ship's cabin with me and doing wonderful backwards trajectories, to Mélanie for help with statistics, to Sophie Guasco for her kindness, to Lars for organizing BBQs, to Jean-Francois and Fred for their GC/MS expertise, to Patrick Raimbault for POC and PON measurements, to Benjamin Girardot for climbing breaks, to the MIO running group for running breaks, to Salomé and

Guillermo for fun moments, to Andrea Paluselli for helpful advice, to Cathy for taking good care of the chemistry lab and always knowing where the glassware you are looking for can be found, to Sandrine Chifflet for solving all kinds of problems and thanks to my “comité de suivi de thèse” for following my progress and offering guidance. Thank you also to the whole chemistry “CEM” team and the administration staff.

I sincerely thank the members of my PhD jury for having agreed to evaluate my work and for their helpful comments and advices during the defense. Thanks to Madeleine Goutx for having agreed to be the president of the jury.

Finally, I would like to thank my parents, my sister and my nephew for their support, their visits and their patience. And last but not least, thank you, Ilja.

For those who are drawn to the sea, the attraction cannot be explained easily. It is an unseen force, a siren’s song that lures us to the water.

- Brian Skerry

INTRODUCTION

Environmental pollution has been recognized as one of the major threats to biodiversity, ecosystem functioning and human health. The pollution sources however are ever-changing: while some legacy contaminants like polychlorinated biphenyls (PCBs) and organochlorine pesticides like dichlorodiphenyltrichloroethane (DDT) have been banned for most uses (Stockholm Convention, 2001), "emerging" contaminants like perfluoroalkyl substances (PFAS), phthalate esters (PAEs), bisphenols (BPs), organophosphate esters (OPEs) and plastic fragments, particularly microplastics (MPs) have taken the lead. PFAS are used in functional clothing, firefighting foams or pesticides, among others (Paul et al., 2009), whereas OPEs are mostly used as plasticizers or as flame retardants in furniture, electronics and plastics (Reemtsma et al., 2008). PAEs can be found in detergents, cosmetics and solvents, but they mainly find application as plasticizers. BPs are used as color developers in thermal paper and as additives in polycarbonate plastics and epoxy resins (Björnsdotter et al., 2017; Pivnenko et al., 2018). These organic compounds can enter the environment *via* direct sources (e.g., from industrial effluents during manufacturing processes) or indirect sources (e.g., leaching from consumer goods). The presence of PFAS, BPs, OPEs, PAEs and MPs in the environment is causing growing concern, since toxicological effects have been described for a magnitude of organisms, including humans. In experimental studies, PFAS, BPs and PAEs were shown to have deleterious effects on bones and bone marrow (Agas et al., 2018), while a specific OPE (Tris(2-chloroethyl) phosphate; TCEP) was observed to cause seizures and acute intoxications in dogs (Lehner et al., 2010). Most studies however focus on the endocrine disrupting activities of these organic compounds (Aoki et al., 2011; Balbi et al., 2016; Canesi and Fabbri, 2015; Chen et al., 2014; Tranfo et al., 2012; Zhai et al., 2014). Hereby, contaminants such as PAEs, OPEs and BPs interfere with hormone action and are thus considered as endocrine disrupting compounds (EDCs). In the marine environment, coastal and estuarine ecosystems are probably particularly impacted, even though for a number of contaminants the possibility of long-range

transport has been demonstrated (Castro-Jiménez et al., 2016; Ma et al., 2017; Mulder et al., 2014; Xie et al., 2007).

Apart from chemical pollution, another aspect is reason for growing concern: plastics in the environment. While plastic and more precisely microplastic pollution was first a topic of scientific research in the 1970s, we only start to understand the full impact of it and to study the underlying processes (fragmentation and degradation, chemical leaching, ingestion by biota and trophic transfer, transport of invasive species, etc.). Moreover, plastic pollution and chemical pollution can be linked (Zhang et al., 2018). Recent studies showed that important quantities of plastic additives (e.g., PAEs) can be released from plastic debris into the marine environment (León et al., 2018; Paluselli et al., 2019). Moreover, plastic debris is suspected to influence the biochemical cycles in the oceans. For example, Romera-Castillo et al. (2018) estimated that 23 600 metric tons of dissolved organic carbon (DOC) are released from marine plastics each year, inducing unknown consequences for marine microbes.

Furthermore, living organisms of all sizes are impacted by the presence of microplastics in the oceans. It has been observed, that bacterial gene transfer was increased in the presence of microplastics and that the spread of antibiotic resistances could possibly be facilitated (Arias-Andres et al., 2018). Moreover, the presence of bacteria associated to plastics can increase the risk of diseases, as was suggested to be the case for coral reefs (Lamb et al., 2018). Zooplankton and several fish species have been shown to ingest microplastics (Bellas et al., 2016; Desforges et al., 2015; Neves et al., 2015), while larger organisms choke on macroplastics or get entangled (Duncan et al., 2017; Lawson et al., 2015; Nunes et al., 2018; Sigler, 2014; Waluda and Staniland, 2013). Finally, recent research suggests that the increasing amount of plastic litter in the oceans could change the amount of sunlight penetrating the water column and thus potentially alter physical processes at the surface, which could ultimately have an effect on the climate, if no action is taken against the “plastic problem” (VishnuRadhan et al., 2019) (Figure

1). It is estimated that about 10% of the annual plastic production enters the oceans (Avio et al., 2017).

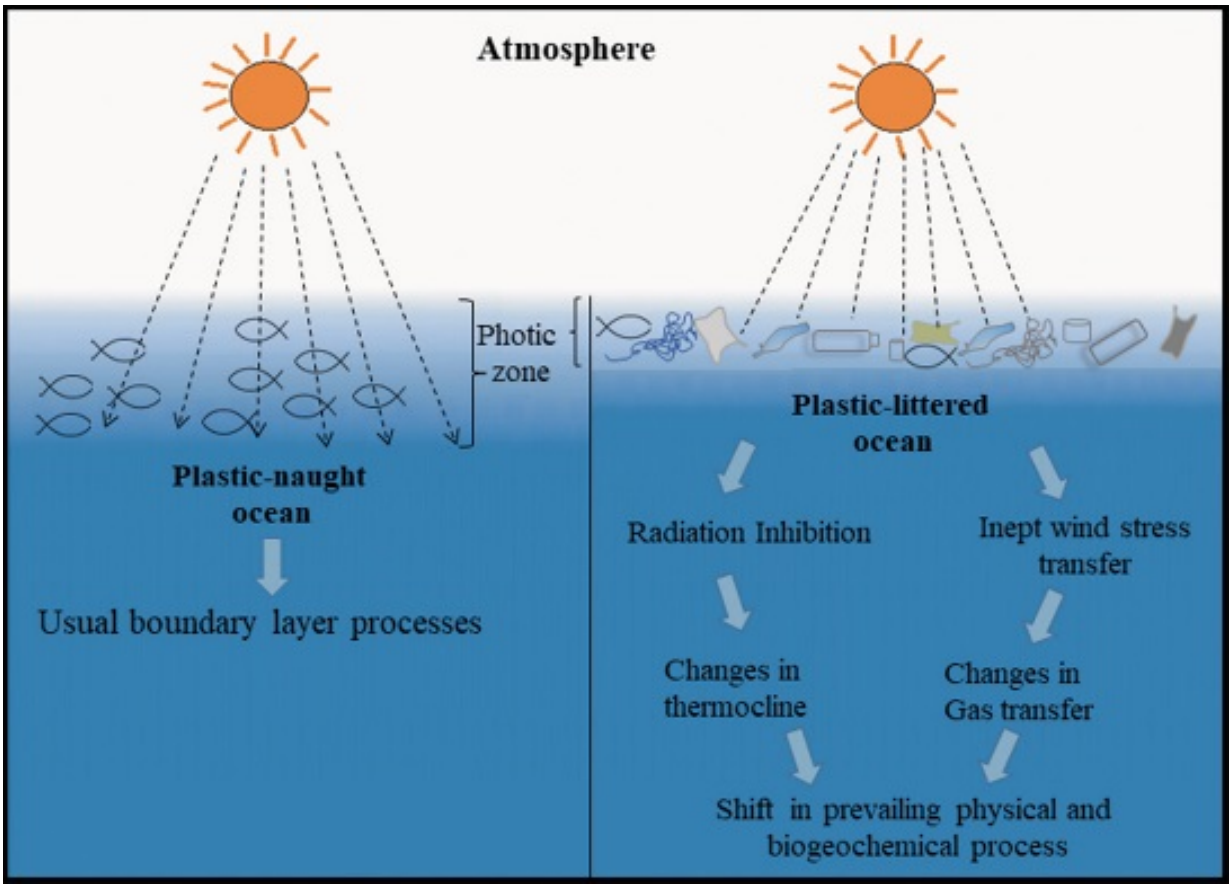

Figure 1: Schema describing how plastic litter on the ocean's surface could impact physical processes in the surface and near-surface layers. From VishnuRadhan et al. (2019).

1. Organic contaminants studied

1.1 Phthalates (PAEs)

Phthalate esters, or shortly phthalates, are organic compounds industrially produced through the reaction of alcohols with phthalic acid. Commonly two classes of PAEs are distinguished: low molecular weight (LMW) phthalates with less than 7 carbon atoms in their chemical backbone and high molecular weight (HMW) phthalates with 7-13 carbon atoms in their backbone. In Europe, HMW phthalates account for ~70% of the plasticizer market. The European Plasticizers Association stated that ~1 million tons of PAEs are annually produced in Western Europe, of which ~90% are used to soften polyvinyl chloride (PVC) (www.plasticisers.org). Other fields of application, especially for LMW phthalates such as DMP and DEP, include detergents, cosmetics and paints, among others (Net et al., 2015b). Since concerns regarding the effects of PAEs on human health have been raised, their use for certain products has been restricted or banned, e.g. the use of DEHP in children's toys. Main concerns are the endocrine disrupting activity of some PAEs as well as developmental toxicity (Chen et al., 2018; Chen et al., 2014; Okamoto et al., 2011). DEHP was included in the list of priority substances in the European Water Framework Directive (EU Water Framework Directive, 2000), a strategy aiming to achieve good chemical and ecological status of waterbodies.

Seven PAEs (DMP, DEP, DnBP, DiBP, DEHP, BzBP and DnOP) were chosen as target compounds in this study, due to their widespread use and/or suspected toxicological effects. Table 1 gives an overview of these PAEs, as well as additional information such as CAS numbers, molecular weight and log K_{OW} values. A compound's octanol-water partition coefficient (K_{OW}) gives important information, since it can be used to perform a first estimation

of the bioaccumulation potential of a compound. Under the Stockholm Convention (2001) chemicals are considered bioaccumulative if they have a log K_{OW} value > 5.

Table 1: Overview of the seven phthalates studied in this thesis.

Compound	Formula	Acronym	CAS N°	Molar Mass (g mol^{-1})	log K_{ow}	Chemical structure
Dimethyl phthalate	$C_{10}H_{10}O_4$	DMP	131-11-3	194.18	1.6	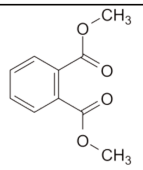
Diethyl phthalate	$C_{12}H_{14}O_4$	DEP	84-66-2	222.24	2.5	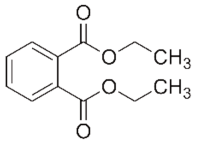
Di-n-butyl phthalate	$C_{16}H_{22}O_4$	DnBP	84-74-2	278.35	4.5	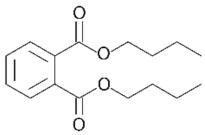
Di-iso-butyl phthalate	$C_{16}H_{22}O_4$	DiBP	84-69-5	278.35	4.1	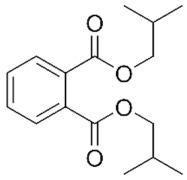
Benzylbutyl phthalate	$C_{19}H_{20}O_4$	BzBP	85-68-7	312.37	4.7	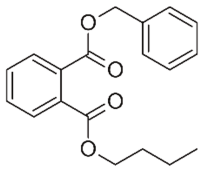
Diethylhexyl phthalate	$C_{24}H_{38}O_4$	DEHP	117-81-7	390.56	7.6	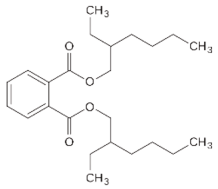
Di-n-octyl phthalate	$C_{24}H_{38}O_4$	DnOP	117-84-0	390.56	8.1	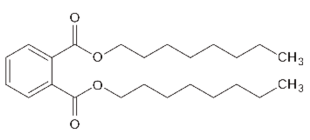

1.2. Organophosphate esters (OPEs)

Organophosphate esters, like PAEs, are high production volume chemicals commonly used in electronic devices, plastics, textiles and furniture (Reemtsma et al., 2008). Chlorinated OPEs, such as Tris(1-chloro-2-propyl) phosphate (TCPP), Tris-(2-chloroethyl) phosphate (TCEP) and Tris(1,3-dichloro-2-propyl) phosphate (TDCP) are mainly used as flame retardants, while non-chlorinated OPEs, such as Tri-n-butyl phosphate (TnBP) and Tri-iso-butyl phosphate (TiBP) are primarily used as plasticizers (Andresen et al., 2004). Chlorinated OPEs are less prone to degradation and are thus thought to have a higher potential for bioaccumulation and long-range transport (McDonough et al., 2018; Sühring et al., 2016; van der Veen and de Boer, 2012). Table 2 gives an overview of the nine OPEs, whose occurrence in the environment was investigated in this study. As can be observed, the selection includes a high structural diversity, representing non-chlorinated and chlorinated OPEs.

As for PAEs, OPEs are suspected to have endocrine disrupting activities and to have multiple adverse effects on human health (e.g., Wei et al., 2015 and references therein). For example, TDCP and Tripropyl phosphate (TPP) concentrations in house dust have been associated with a decrease in sperm concentration in men (Meeker and Stapleton, 2010). TPP has also been reported to cause allergic contact dermatitis after dermal exposure to plastic products (Camarasa and Serra-Baldrich, 1992).

WWTP effluents are thought to be a major source of OPEs in surface waters, but their presence is so ubiquitous, that special care needs to be taken when extracting and analyzing samples, since OPEs are also found in a magnitude of laboratory equipment (Pantelaki and Voutsa, 2019). Another important OPE source - especially in indoor environments - is the emission from electronic devices. A recent study linked human urinary OPE metabolites with the use of cell phones and suggested that dermal uptake and / or hand-to-mouth exposure occurs (Yang et al., 2019).

Table 2: Overview of the nine organophosphate esters studied in this thesis.

Compound	Formula	Acronym	CAS N°	Molar Mass (g mol^{-1})	log K_{ow}	Chemical structure
Tripropyl phosphate	$C_9H_{21}O_4P$	TPP	513-08-6	224.23	1.9	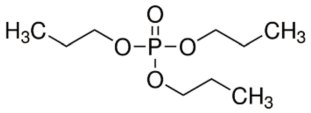
Tri-iso-butyl phosphate	$C_{12}H_{27}O_4P$	TiBP	126-71-6	266.32	3.5	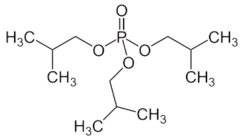
Tri-n-butyl phosphate	$C_{12}H_{27}O_4P$	TnBP	126-73-8	266.32	4.0	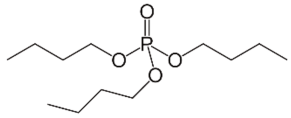
Tris-(2-chloroethyl) phosphate	$C_6H_{12}Cl_3O_4P$	TCEP	115-96-8	285.48	1.8	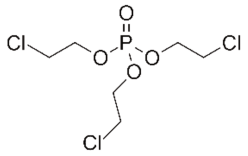
Tris(1-chloro-2-propyl) phosphate	$C_9H_{18}Cl_3O_4P$	TCPP	13674-84-5	327.56	2.6	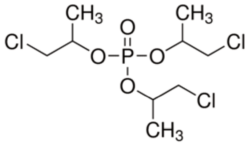
Tris(1,3-dichloro-2-propyl) phosphate	$C_9H_{15}Cl_6O_4P$	TDCP	13674-87-8	430.89	3.7	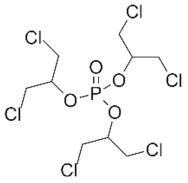
Triphenyl phosphate	$C_{18}H_{15}O_4P$	TPhP	115-86-6	326.29	4.6	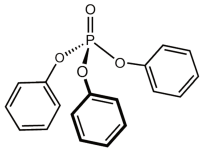
2- Ethylhexyl-diphenyl phosphate	$C_{20}H_{27}O_4P$	EHDPP	1241-94-7	362.41	5.7	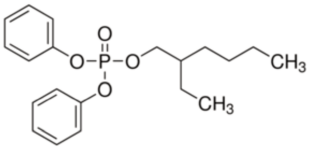
Tris(2-ethylhexyl) phosphate	$C_{24}H_{51}O_4P$	TEHP	78-42-2	434.63	9.5	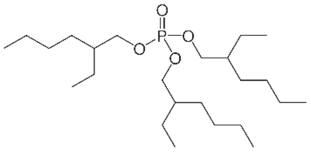

1.3. Bisphenols (BPs)

Bisphenols are synthetic compounds containing two phenol functional groups. The identification of BPA as an endocrine disruptor has received much public attention, mainly due to its use in the fabrication of baby bottles and their subsequent ban by governmental institutions. However, BPA is still used in a magnitude of products, primarily for polycarbonate plastics and epoxy resins. Furthermore, commonly used BPA alternatives, such as BPS and BPF, have been reported to interfere with hormone action, as well (Zhang et al., 2018) and evidence that BPA alternatives are not "safer" than the original is getting more abundant (Figure 2).

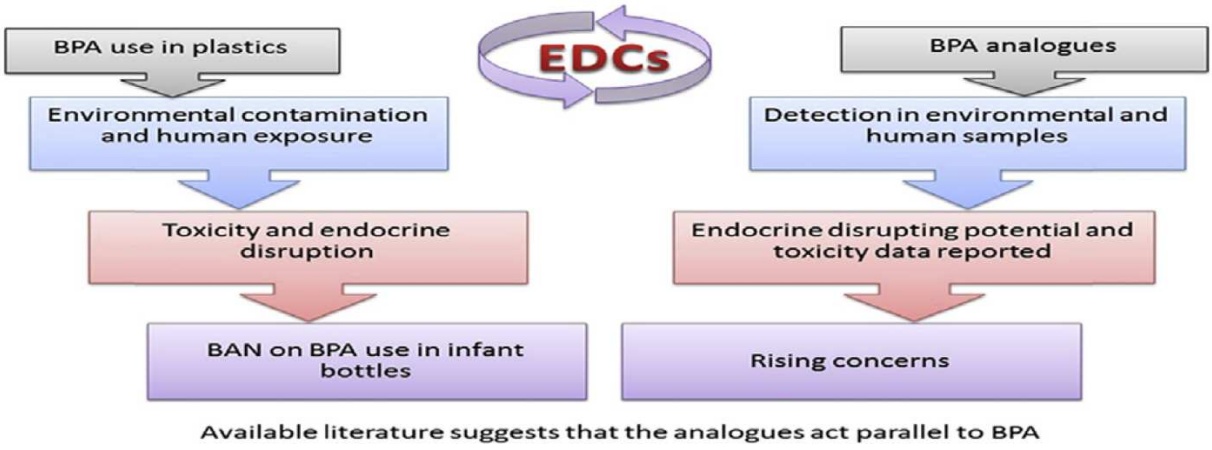

Figure 2: Scientific and public concern regarding BPA alternatives is growing, since an increasing number of studies suggest that they affect human health in the same way as BPA does. From Usman and Ahmad (2016).

Table 3 summarizes the six bisphenols (BPA, BPAF, BPAP, BPF, BPS and BPZ) which were studied in this thesis. Human exposure to bisphenols occurs mainly through ingesting of foods and beverages from epoxy lined tin cans or polycarbonate plastic bottles and from the handling of thermal paper (Björnsdotter et al., 2017).

Table 3: Overview of the six bisphenols studied in this thesis.

Compound	Formula	Acronym	CAS N°	Molar Mass (g mol^{-1})	log K_{ow}	Chemical structure
Bisphenol A	$C_{15}H_{16}O_2$	BPA	80-05-7	228.29	3.3	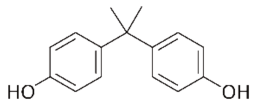
Bisphenol AF	$C_{15}H_{10}F_6O_2$	BPAF	14878-61-1	336.23	4.5	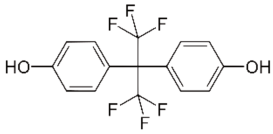
Bisphenol AP	$C_{20}H_{18}O_2$	BPAP	1571-75-1	290.36	4.4	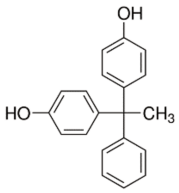
Bisphenol F	$C_{13}H_{12}O_2$	BPF	620-92-8	200.24	2.9	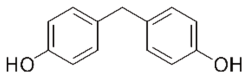
Bisphenol S	$C_{12}H_{10}O_4S$	BPS	80-09-1	250.27	1.9	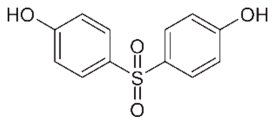
Bisphenol Z	$C_{18}H_{20}O_2$	BPZ	843-55-0	268.36	5.4	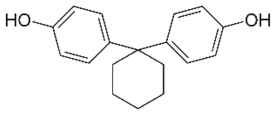

1.4. Perfluoroalkyl substances (PFAS)

The term perfluoroalkyl substances is used for a large variety of chemicals containing carbon-fluorine bonds. They include perfluoroalkyl carboxylic acids (PFCA), such as PFHA and PFOA, as well as perfluoroalkyl sulfonic acids (PFSA), such as PFOS and PFHS. Table 4 presents these four PFAS. Given their chemical stability, PFAS are used in a wide variety of products: from firefighting foams and inks to coatings and textiles (mainly because of their water and oil repelling characteristics) (Paul et al., 2009). Usually one of the most abundant PFAS in the environment, PFOS was produced at important quantities until regulations and restrictions were established in the early 2000's in the US and Europe. These restrictions are due to concerns of toxicity of PFOS. In fact, toxic effects of PFOS, ranging from altered gene expression to reduced feeding ability (Ding et al., 2015; Huang et al., 2011), have been described for a variety of organisms, including sea urchins, rats and even wheat plants, among others (Chen et al., 2012; Li et al., 2017; Qu et al., 2010; Ding et al., 2015).

Table 4: Overview of the four perfluoroalkyl substances studied in this thesis.

Compound	Formula	Acronym	CAS N°	Molar Mass (g mol^{-1})	log K_{ow}	Chemical structure
Perfluoro hexanoic acid	$C_6HF_{11}O_2$	PFHA	307-24-4	314.05	3.5	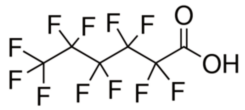
Perfluorohexane sulfonic acid	$C_6HF_{13}O_3S$	PFHS	3871-99-6	400.11	3.2	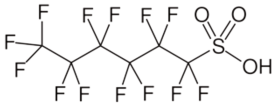
Perfluorooctanoic acid	$C_8HF_{15}O_2$	PFOA	335-67-1	414.07	4.8	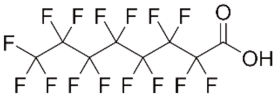
Perfluorooctane sulfonic acid	$C_8HF_{17}O_3S$	PFOS	1763-23-1	500.13	4.5	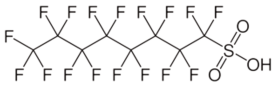

1.5. Microplastics

Microplastics are generally defined as plastics ≤ 5 mm and can have various shapes, such as spheres, fragments, fibers and films. Primary microplastics are conceived to be small-sized plastics and are thus intentionally produced this way (e.g., microbeads used in cosmetics and virgin plastic pellets used to produce larger items), while secondary microplastics are unintentionally produced and result from the degradation/fragmentation of larger plastics. Secondary microplastics can result from biotic degradation (e.g., through microorganisms and fungi) or abiotic degradation (i.e., thermal, photo-oxidative, hydrolytic or mechanical degradation). An important source for secondary microplastics are textiles, since with each washing up to 110,000 fibers per garment can enter the sewage systems, depending on the fabric type (Almroth et al., 2018). Just like microplastics can occur in all kinds of shapes and sizes, they are also differently colored. While this might seem trivial at first glance, it was observed that the color can indicate whether high amounts of contaminants are present or not (Endo et al., 2005) (e.g., black pellets from two Portuguese beaches had higher PCB concentrations than

white pellets; Frias et al., 2010). Furthermore, it was suggested that aquatic species - especially visual predators - might selectively ingest microplastics of certain colors. A study conducted in the Mediterranean Sea concluded that albacore, bluefin tuna and swordfish mainly ingested white and transparent plastics (Romeo et al., 2015).

2. Environmental sources and fate

Organic contaminants, such as PAEs, OPEs, BPs and PFAS, can leach from consumer goods, such as plastic materials, electronic devices and textiles. In the case of plastics, leaching can occur since the additives are only added physically to the polymeric matrix and are thus not bound chemically (Net et al., 2015b; Paluselli et al., 2019). As a reference, PAEs can represent up to 10-60% by weight of the final product (Net et al., 2015b), suggesting hence that large quantities of PAEs could reach the environment *via* leaching. Note that recent research revealed, that the leaching of PAEs from plastics can be enhanced by light and microorganisms, depending on the polymer type (Paluselli et al., 2019). In a study measuring PAEs in virgin and recycled plastics, up to 2700 µg DEHP per g plastic were detected and the authors suggested that PAE concentrations should be monitored if recycled plastics are used for the manufacturing of PAE-sensitive applications since leaching is possible (Pivnenko et al., 2016). In water, BPA was shown to leach more easily from plastic materials than PAEs, probably due to its higher solubility in water (Suhrhoff and Scholz-Böttcher, 2016). The same study also found that turbulence significantly increased the amount of leaching, while the effect of salinity was negligible. Apart from leaching, plastic additives can enter the environment by several pathways (i.e., migration, emissions, degradation and release) during the manufacturing process, the use and the disposal or reprocessing of plastic materials (Figure 3). An example for the emission/release of additives from plastic waste is plastic burning, which has been linked

to the occurrence of BPA in the atmosphere (Fu et al., 2013). In the case of PFAS, PFOA is used to solubilize fluorotelomers, but is not integrated into the polymer itself, meaning that it will then be discharged into the industrial effluents, consisting thus a direct input source (Dauchy et al., 2012). For the Seine River in Paris (France) it was concluded that DEHP and DnBP occurrence was driven by population density and the magnitude of industrial activity (Teil et al., 2007) and this statement can probably be generalized for most rivers. Another study calculated that French households introduced 2410 µg DEHP per day per capita into the sewer system *via* greywater; washing machines and showers being the main sources (Deshayes et al., 2017).

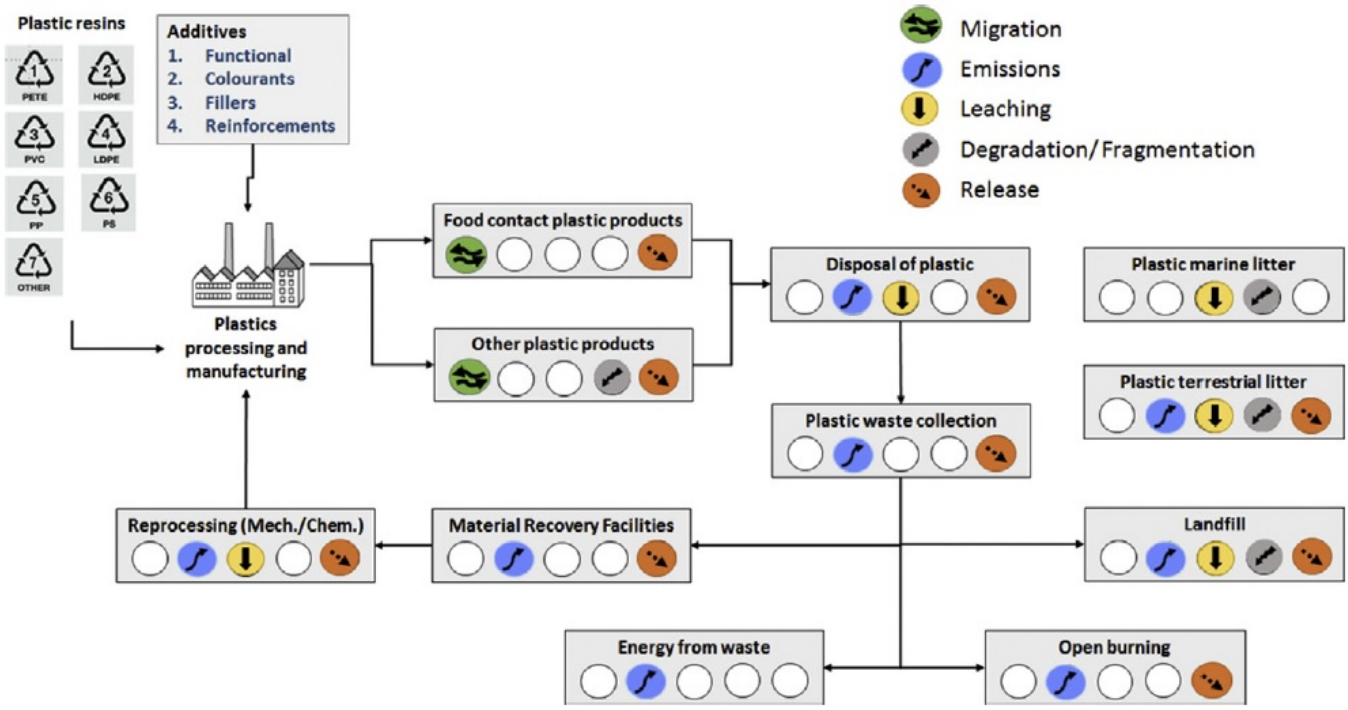

Figure 3: Schema of the pathways by which plastic additives can enter the environment. From Hahladakis et al. (2018).

Industrial and municipal wastewater treatment plants (WWTP) often receive important loads of (organic) contaminants and - depending on the techniques used to treat the wastewater

- significant or complete degradation or retaining of the compounds is not always obtained. Several techniques have been proposed for the removal of PAEs (Wang et al., 2014; Xu et al., 2009; Zhang et al., 2016) and OPEs (Pang et al., 2018; Yuan et al., 2015) from wastewater. A recent study related to the removal efficiency of a WWTP connected to the Charmoise River reported that BPA and several PAEs (including the seven PAEs focused on in this thesis) had decreased in concentration after biological treatment (i.e., microbial degradation) by ≥ 90% (Tran et al., 2015). In the natural environment, biotic degradation can occur, depending on the compounds and the environmental conditions. In laboratory experiments, it was shown that DMP and DEP can be biodegraded by 87% and 61% within four days by *Karenia brevis*, a single-celled dinoflagellate (Sun et al., 2019). Using an experimental approach including dark, biotic conditions in seawater, Paluselli et al. (2019) calculated half-lives of 15 days for DnBP, 21 days for BzBP, 26 days for DEHP, 29 days for DiBP, 53 days for DMP and 79 days for DEP. While PFAS are generally considered as persistent, a study using the microbe *Pseudomonas aeruginosa* claimed to have achieved biodegradation of high amounts of PFOS after 48 h of incubation (Kwon et al., 2014). This observation was, however, strongly questioned by peers (Avendaño et al., 2015).

Microplastics have been detected in all environmental compartments and are nowadays ubiquitous. Marine ecosystems are particularly at risk since they can receive important plastic loads *via* river discharges, coastal inputs and marine traffic, though some marine plastic debris can also be transferred to land, e.g. by tidal deposition (Figure 4). Beaches and shorelines are typical microplastic sinks, as well as seafloor sediments and the deep sea (Browne et al., 2011; Näkki et al., 2019; Woodall et al., 2014). Moreover, the Arctic Sea ice has been identified as a (temporal) sink for microplastics (Peeken et al., 2018), which are now increasingly being released due to the melting of sea ice caused by global warming (Obbard et al., 2014). Sedimentation of microplastics can occur if the polymer has a higher density than seawater,

through incorporation into phytoplankton aggregates or through colonization of the plastic (biofouling) (Kaiser et al., 2017; Long et al., 2015).

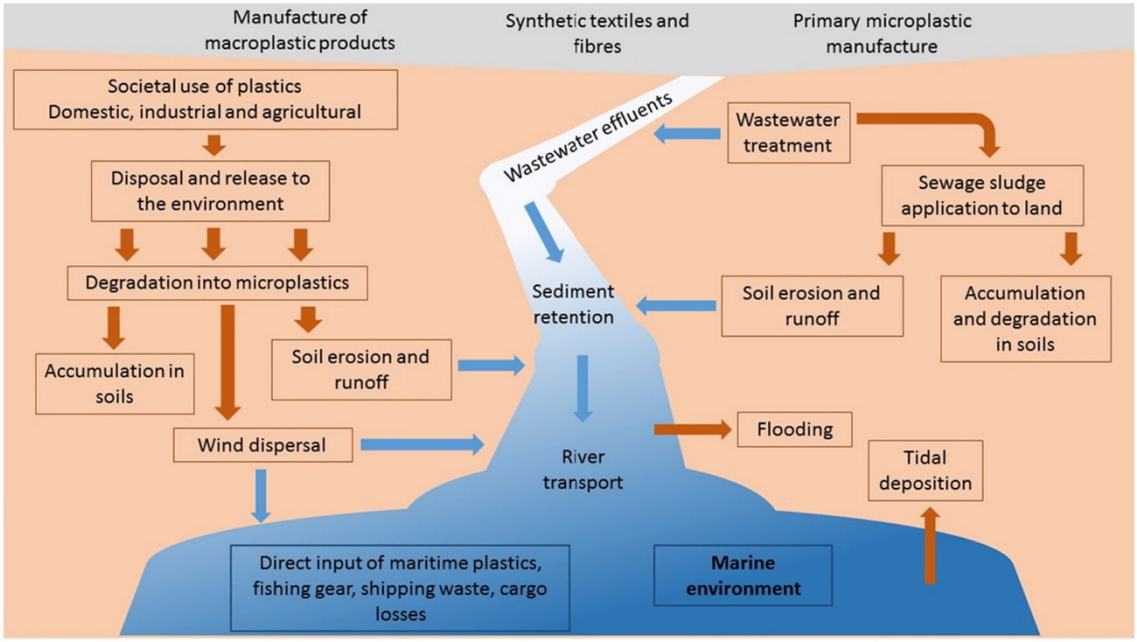

Figure 4: Microplastic sources and flows between the terrestrial, riverine and marine environment. From Horton et al. (2017).

3. Environmental levels

3.1. In freshwater ecosystems

In freshwater ecosystems, high amounts of organic contaminants can be detected, mainly through WWTP inputs. In river sediments from Taiwan (Love River, southern Taiwan), DEHP was detected (4.2-66.7 mg kg^{-1} dry weight (dw)) with concentrations being maximum in wet season (Chen et al., 2018). These values are comparable to those reported for Chinese river sediments (Jiangsu Province; Wang et al., 2014) (1.83-78.56 mg kg^{-1} dw DEHP; 79% average relative abundance), where the spatial PAE concentration variability was linked to different land uses (industrial, suburbs, agricultural areas). Li et al. (2017) suggested that river

sediment cores can be used to trace back historical PAE contamination levels (up to 26 years in their study) and thus to observe changes in single and total PAE inputs. A recent study at a freshwater aquafarm in China found that water and sediment samples were highly contaminated with PAEs (up to 35.7 µg L^{-1} DEHP in water), their levels exceeding Chinese environmental quality standards (Cheng et al., 2019). In Europe, DEHP was found at 160-314 ng L^{-1} in the Seine River estuary (France; Dargnat et al., 2009), at 407 ng L^{-1} in the Rhône River (France; Paluselli et al., 2018a) and at 0.05-4.96 µg L^{-1} in freshwater samples from the Netherlands (Peijnenburg and Struijs, 2006).

Concerning OPEs, Wolschke et al. (2018) observed that the overall pattern (i.e., relative abundance of individual OPEs) in European river sediments was significantly different from the pattern observed in a Chinese river, displaying different uses and legislations in China and Europe. In the Ruhr River (Germany) the presence of TCPP (20-200 ng L^{-1}) in water samples was suggested to origin from construction activities, since TCPP is primarily used for the manufacturing of rigid polyurethane foam plates (Andresen et al., 2004). In three Spanish rivers, 0.0083-1.8 µg L^{-1} of TCPP were measured and it was concluded that the OPE concentrations detected exhibited no acute toxicity risk for *Daphnia magna* (a planktonic crustacean commonly used for toxicity studies) (Cristale et al., 2013). Fries and Püttmann (2003) detected high OPE levels in the Oder River (Germany; mean 622 ng L^{-1} TBP and 352 ng L^{-1} TCEP) resulting from WWTP inputs and described the transport of OPEs from river water to ground water. In river water from the Danube and its tributaries, maximum TCPP concentrations of 603 ng L^{-1} were observed, while TiBP was present at up to 97 ng L^{-1} and TCEP at up to 41 ng L^{-1} (Loos et al., 2017).

In the Minho River basin (Iberian Peninsula), highest BPA concentrations attained 4.8 µg L^{-1} in water and 130 ng g^{-1} dw in sediment samples. The authors noted that certain sampling stations exhibited high BPA concentrations in water samples, while in the associated sediment

samples BPA was not detected, and concluded that point pollution and recent contamination were at the origin of this phenomenon (Salgueiro-González et al., 2015). In three freshwater ecosystems in China (Liaohe River, Hunhe River and Taihu Lake) BPA was the predominant bisphenol in water samples (mean 8.5-47 ng L^{-1}), followed by BPS (6-14 ng L^{-1}), reflecting the preferential use of these two bisphenols by industry (Jin and Zhu, 2016). In the same range is the BPA concentration detected by Carmona et al. (2017) (41 ng L^{-1}) in the Turia River (Spain). Extreme values have been measured in several rivers in Japan, Korea, China and India, where BPA reached maximum concentrations of 1950 ng L^{-1} and BPF up to 2850 ng L^{-1} (Yamazaki et al., 2015).

A nationwide study including over 100 French freshwater ecosystems concluded that PFOS was generally the predominant PFAS in the dissolved water phase, even though individual waterbodies or watersheds can show differing trends (Munoz et al., 2015). In the Danube River, a maximum concentration of 36.5 ng L^{-1} of PFOA and 26.2 ng L^{-1} of PFOS was detected (Loos et al., 2017), while in the UK rivers Aire and Calder maximum PFOS concentrations of 17.2 ng L^{-1} and 20.7 ng L^{-1} were measured, respectively (Earnshaw et al., 2014). The authors of the latter study also proposed a modelling approach (including the type of treatment used by WWTPs discharging their effluents into the rivers) to estimate spatial PFOS trends.

As for the other organic contaminants, WWTP are also an important entryway to rivers for microplastics (Kay et al., 2018), but recent research shows that even remote rivers can be affected by microplastic pollution, through atmospheric deposition (Allen et al., 2019). Thus, a multitude of rivers have been confirmed to be contaminated by microplastics, like rivers of the Tibet Plateau (483-967 items m^{-3}) or the Rhine River, where a peak concentration of 3.9 million particles km^{-2} was measured. Together with macroplastics, these microparticles are exported to the oceans at important quantities (Figure 5).

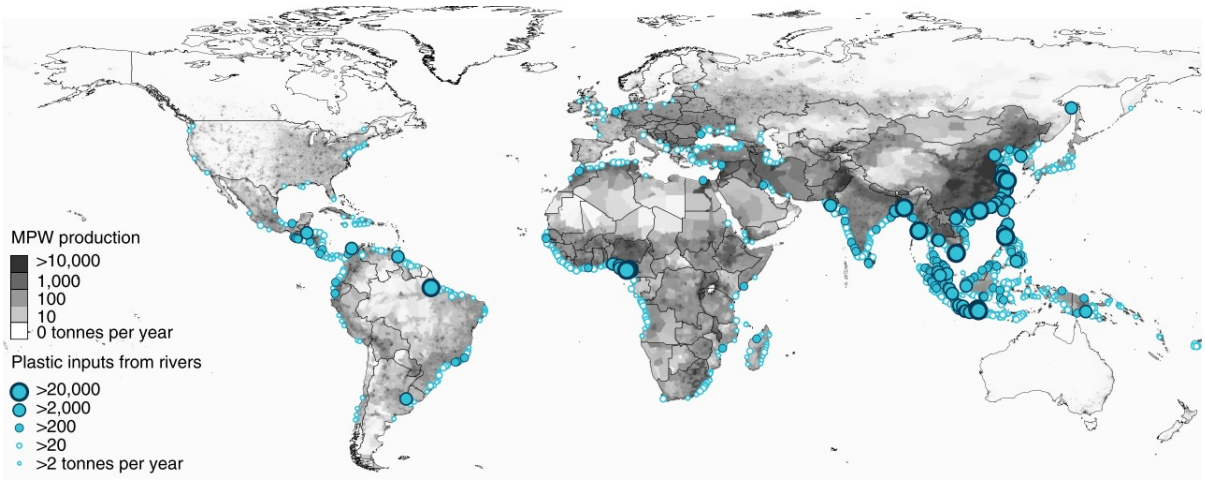

Figure 5: Modelled plastic inputs (in tons per year) from rivers into the oceans. MPW = mismanaged plastic waster. From Lebreton et al. (2017).

3.2. In coastal and open-ocean waters

Σ_6 PAEs were already reported in Marseille Bay surface seawater (NW Mediterranean Sea; 130.8-1330.7 ng L^{-1}), with DEHP being the most abundant PAE (Paluselli et al., 2018b). In coastal seawater from the Spanish part of the NW Mediterranean Sea, 31-617 ng L^{-1} (mean 145 ng L^{-1}) of DEHP were detected, while BPA concentrations ranged from 2.3-102 ng L^{-1} (mean 18 ng L^{-1}) (Sánchez-Avila et al., 2012). In water samples from the Gulf of Gdansk, a mean BPA concentration of 193.2 ± 128.1 ng L^{-1} was observed. Hereby, lower BPA concentrations were found in summer, when rising temperatures enhanced biodegradation activities (Staniszewska et al., 2015). Interestingly, BPA has also been detected in coastal seawater from the Antarctic (2.2-29.5 ng L^{-1}) and its presence in the environment was linked to two research stations based in Antarctica and their corresponding WWTP effluents (Emnet et al., 2014). In the Yellow Sea and East China Sea, mean concentrations of 134.44 ng L^{-1} of TCEP and 84.12 ng L^{-1} of TCPP were found in waters influenced by industrial activity (Hu et

al., 2014). In the Catalan coast, where river discharges were identified as more important PFAS sources than WWTP effluents, PFOS was detected in water samples with concentrations of <0.03-3.93 ng L^{-1} and PFOA with 0.07-1.86 ng L^{-1} (Sánchez-Avila et al., 2010). 2.67-7.83 ng L^{-1} of PFOA and 0.69-3.95 ng L^{-1} of PFOS were measured in the German Bight. Hereby, it was noted that concentrations decreased with increasing distance to the shore and that rivers had a major role concerning PFAS occurrence and spatial distribution. Furthermore, a positive correlation between PFOS and PFOA concentrations and DOC content was observed (Ahrens et al., 2009).

The occurrence of PAEs, OPEs and BPs in the open ocean has been poorly studied so far. Thanks to an expedition to the tropical and subtropical Atlantic, Pacific and Indian oceans, at least some PFAS data is available. Here, the PFOS concentrations varied between 14.8 and 6560 pg L^{-1}, while PFHA was detected at 0.06-296 pg L^{-1} (González-Gaya et al., 2014), with highest PFAS concentrations found in the Atlantic Ocean. Concerning OPEs, they were found in Arctic water, air and snow samples, indicating that long-range transport occurs, more importantly probably for chlorinated OPEs, which were detected at higher concentrations than non-halogenated OPEs (Li et al., 2017; McDonough et al., 2018).

Microplastic concentrations found in marine waters are very variable; nonetheless certain hotspots have been identified, such as the East Asian Seas, where 1,720,000 MPs km^{-2} were counted (Isobe et al., 2015). In open ocean waters, important plastic accumulation zones have been discovered (Figure 6).

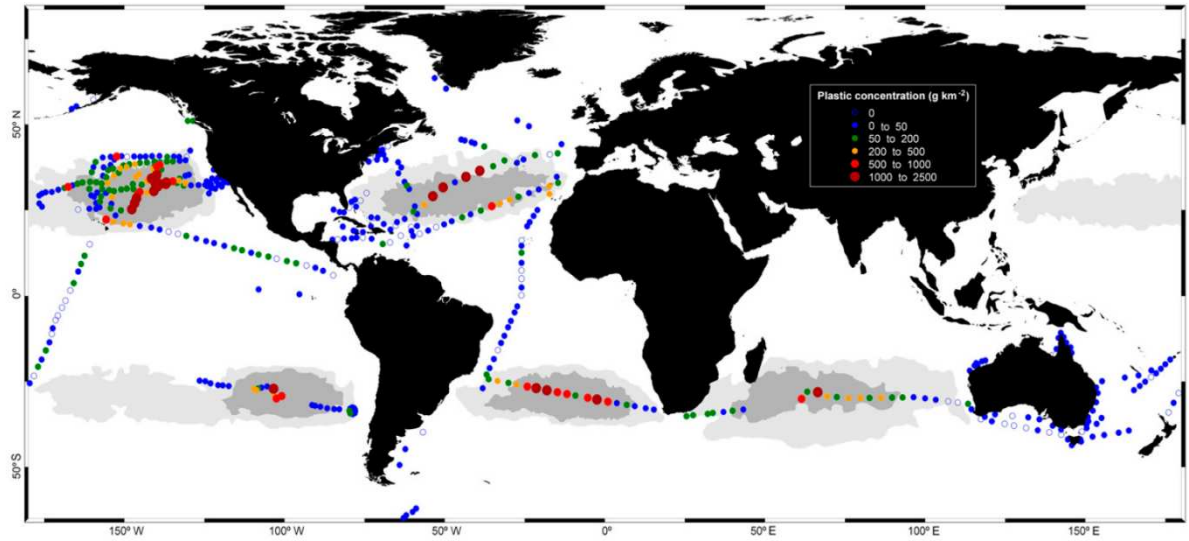

Figure 6: Plastic concentration (in g km^{-2}) in the global ocean. Data were obtained from > 3000 *in situ* measurements. Accumulation zones are indicated in gray. From Cozar et al. (2014).

3.3. In marine sediments and biota

In sediments from the North Pacific to the Arctic Ocean, halogenated OPEs dominated over non-halogenated OPEs, especially with increasing latitude, suggesting again that halogenated OPEs are more prone to be transported to remote regions (Ma et al., 2017). It was estimated, that the sediments of the Central Arctic Ocean contain 17-292 tons of Σ_7 OPEs, likely to increase in the future (Ma et al., 2017). In the Bohai and Yellow Seas, relatively low PAE concentrations were measured in sediments, with DEHP being dominant with a median concentration of 3.77 ng g^{-1} dw (Mi et al., 2019). In comparison, PAE concentrations in sediments from the Changjiang River Estuary (China) were much higher, with 0.26-8.55 µg g^{-1} dw (Zhang et al., 2018). In the Adriatic Sea no correlation of organic matter content and BPA concentrations in sediment was found, neither was a seasonality of BPA concentrations observed, with values ranging from 5.32-15.52 ng g^{-1} dw (Anđelić et al., 2015). Finally, PFOS concentrations in sediments of the German Bight (North Sea; 0.023–5.4 ng g^{-1} dw) were

comparable to those detected in a marine reserve in Italy (median values of 0.25-1.50 ng g^{-1} dw) (Perra et al., 2013; Zhao et al., 2015).

Organic contaminants have already been reported in zooplankton samples, even though data is rare. For instance, zooplankton samples from the Indian, Pacific and Atlantic Ocean exhibited PFOA concentrations of 0.1-43 ng g^{-1} dw and PFOS concentrations of 0.5-6.7 ng g^{-1} dw (Casal et al., 2017). Hereby, the average contribution of PFOS to the sum of PFCs analyzed was lower in zooplankton than in water samples. In a pooled sample near a WWTP outlet in China, PFOS represented 77% of Σ_7 PFAS (Li et al., 2008; 4.18 ng g^{-1} wet weight (ww)). In zooplankton samples from the Mediterranean Sea, DEHP concentrations of 20.36 ± 39.42 ng g^{-1} ww (Fossi et al., 2012), 35-2699 ng g^{-1} dw (Baini et al., 2017) and 9095 ± 4574 ng g^{-1} dw (Vered et al., 2019) have been reported so far. Furthermore, it was shown that mono-(2-ethylhexyl) phthalate (MEHP), the primary metabolite of DEHP, exhibited higher concentrations in plankton samples than DEHP (Fossi et al., 2012). Moreover, it was proposed that phthalate concentrations found in whale blubber could be used as a tracer of microplastic ingestion (Fossi et al., 2012).

Staniszewska et al. (2016) detected very high BPA concentrations in zooplankton samples of the Baltic Sea (up to 405.9 ng g^{-1} dw) and observed that the BPA concentrations depended on the species composition of plankton samples, where high BPA concentrations were linked to an increased amount of meroplankton, while lower concentrations were linked to a higher abundance of *Copepoda* and *Cladocera*. BPA was found to be more concentrated in fish livers than in muscle tissue, with up to ~6 ng g^{-1} liver tissue for *Sarpa salpa* individuals caught in the Mediterranean Sea close to the Italian coast (Mita et al., 2011). The plasma of harbor seals from Svalbard (Arctic Ocean) contained TCPP concentrations of 187.72 ± 184.7 ng g^{-1} lipid, indicating that food webs from remote areas are nowadays also impacted by the occurrence of OPEs (Hallanger et al., 2015). A study comparing wild-caught and aquaculture

fish (*Boops boops*) found that wild-caught fish had (for some individual compounds significantly) higher OPE concentrations than the aquaculture fish. Hereby, the TCPP concentrations ranged from 505.83–1832.00 ng g^{-1} lipid for wild-caught fish and from 344.02–686.40 ng g^{-1} lipid for aquaculture fish (Henríquez-Hernández et al., 2017). The authors suggested that this could probably be linked to the differing diets of wild-caught and aquaculture fish, though more research is needed before drawing conclusions.

5. Study area

The Bay of Marseille, at the eastern edge of the Gulf of Lion (north-western Mediterranean Sea), has a surface of ~90 km^2 and is strongly influenced by the city of Marseille, which is - after Paris - the second largest city of France. It receives high anthropogenic pressure from tourist and harbor activities and insufficient waste management. Nonetheless, a recent study reported that PFOS concentrations in shellfish (mussel and oyster) in Marseille were among the lowest detected along the French Mediterranean and Atlantic coasts (Munschy et al., 2019; < 0.05 ng g^{-1} ww). The microplastic concentration reported for Marseille Bay (0.01 items m^{-2}) is also quite low (Collignon et al., 2012), but no sampling efforts have so far been made to study the spatial and temporal variability of microplastic occurrence in Marseille Bay.

A major local pollution source is the municipal wastewater treatment plant (WWTP), which releases the treated wastewater into the sea at a natural inlet at the eastern edge of the city. This natural inlet ("Calanque de Cortiou", sampling site 1) is part of the marine section of the Calanques National Park (Figure 7) and receives approximately 250 000 m^3 wastewater per day (Savriama et al., 2015), representing about 1.7 million equivalent inhabitants. The installation of the WWTP in 1987 changed the resident macroalgal communities (Soltan et al.,

2001) and significantly improved the water quality, leading for example to a 75% reduction of lead concentrations in commercial sponges (Perez et al., 2005). However, the metal concentrations encountered are still fairly high and could explain the fluctuating asymmetry observed in sea urchins from Cortiou (Savriama et al., 2015). The leaves of the endemic seagrass species *Posidonia oceanica* were found to exhibit high concentrations of mercury in Cortiou (Pergent-Martini, 1998; 176.5 ng g^{-1}), whereas organochlorine pesticides and PCBs were detected in sediments (Syakti et al., 2012; Wafo et al., 2006). Concerning the organic contaminants studied in this thesis, Paluselli et al. (2018a) measured 213 ng L^{-1} of Σ_8 PAEs in surface waters near the WWTP outlet.

North-west of Cortiou and about 2 km off the coast lie the islands of Frioul (sampling site 2), which in ancient times had been used as quarantine stations in order to protect the city of Marseille from ship-borne illnesses such as the plague. Today, they are a popular destination for day-trippers, especially during summertime when tourist flows are highest. The islands have an own WWTP, which is, however, significantly smaller compared to the WWTP of Marseille, representing only about 200 equivalent inhabitants. A recent study using numeric modelling suggested that fine particles from the WWTP outlet in Cortiou can also be transported towards the inner bays of Marseille, including Frioul island, under certain conditions (SE wind regime coupled with an intrusion of the Northern Current on the continental shelf), possibly inducing health risks (Millet et al., 2018). Oursel et al. (2014) came to similar results and noted that with the export of fine particles from the WWTP outlet, the associated pollutants, including metals, are equally being transported. Research on hydrocarbons concluded that the waters near Frioul are moderately contaminated by aliphatic and polycyclic aromatic hydrocarbons, with rainfall increasing the concentrations detected in the dissolved phase (Guigue et al., 2011). Tiano et al. (2014) measured PCBs in plankton samples off Frioul (mean $\sum_7$ PCBs of 25-65.4 ng g^{-1} dw)

and suggested that planktonic PCB concentrations might be influenced by hydrodynamics generated through strong wind events.



Figure 7: Plan of the Calanques National Park. Cortiou, the natural inlet receiving Marseilles treated wastewater, is indicated by a red star; the islands of Frioul are indicated by a red dot. The light blue color indicates the adjacent maritime zone, the medium blue color represents the heart of the marine national park and the dark blue color indicates no-take areas within the heart of the marine reserve. From http://calanques-parcnational.fr/.

Still further north the district “L’Estaque” (sampling site 3), which has a rich history involving fishermen, tile producers and famous landscape painters, is situated. It holds a leisure

port, which in turn is adjacent to the ferry port of Marseille. The sediments of the port in L'Estaque have been reported to be highly polluted by arsenic and mineral oils (Mamindy-Pajany et al., 2013). Several times per year, intrusions of diluted water from the Rhône River (sampling site 4, at Arles city) can reach the Bay of Marseille, depending on wind forcing and the river's discharge volume, among others (Fraysse et al., 2014) and can generate phytoplankton blooms (Para et al., 2010). In 2018, the Rhône River had a mean annual water discharge of 1780 m^3 s^{-1} (http://www.hydro.eaufrance.fr). It is thus the main freshwater source of the Mediterranean Sea and an important carbon supplier (Sempéré et al., 2000). A few studies reported the presence of microplastics (De Alencastro, 2014) and organic contaminants (Miège et al., 2012; Mourier et al., 2014; Paluselli et al., 2018a) in the Rhône River, but corresponding monitoring programs do not yet exist.

Finally, the tropical North Atlantic (sampling site 5) was chosen as a contrasting study area to the coastal Bay of Marseille. Data on organic contaminants of emerging concern in open ocean environments is rare and this holds true for the tropical North Atlantic Ocean as well. A comparison between PFAS concentrations from the (sub-)tropical Atlantic, Pacific and Indian Oceans showed, that maximum concentrations were observed in the Atlantic, where furthermore a higher variability in concentrations was observed (González-Gaya et al., 2014).

6. Scopes of this thesis

The aim of this thesis, which was funded by the "Agence de l'eau Rhône Méditerranée Corse (AERMC)" was to study the occurrence and dynamic of contaminants of emerging concern, with focus on plastic additives (PAEs, OPEs, BPs), flame retardants (OPEs) and related contaminants such as PFAS and microplastics in the Bay of Marseille (North Western Mediterranean Sea) and the Rhône River. Furthermore, the comparison of the environmental occurrence of target compounds between the semi-enclosed Mediterranean Sea and an oceanic region in the North Atlantic was an objective of this work.

The first chapter deals with the occurrence of microplastics in several zones of the Gulf of Lion (Marseille Bay, the Mediterranean Northern Current and the Rhône River and its estuary), their size distribution, their spatial and temporal variability and possible sources. The second chapter presents the results of a one-year monitoring of PAEs, OPEs and BPs in surface water samples of the Rhône River. In chapter III the PFAS concentrations detected in the waters of the Rhône River and the Bay of Marseille are discussed and a risk assessment is provided by comparison with the Environmental Quality Standard (EQS) defined for PFOS. Chapter IV focuses on OPEs and PAEs in water, sediment and zooplankton samples from the Bay of Marseille and investigates the risk of bioconcentration and possible consequences for the local marine food web. Finally, in the last chapter, the focus widens from the local scale of the previous chapters to a transatlantic scale. Here, OPE, PFAS and BP concentrations are reported for the North Atlantic Ocean and it is demonstrated that the Amazon River is at the source of the observed contamination pattern and that long-range transport *via* ocean currents occurs. Lastly, the thesis closes with a conclusion and perspectives section.

References

Agas, D., Lacava, G., Sabbieti, M.G., 2018. Bone and bone marrow disruption by endocrine-active substances. J. Cell. Physiol. 234, 192–213. https://doi.org/10.1002/jcp.26837

Ahrens, L., Felizeter, S., Ebinghaus, R., 2009. Spatial distribution of polyfluoroalkyl compounds in seawater of the German Bight. Chemosphere 76, 179–184. https://doi.org/10.1016/j.chemosphere.2009.03.052

Alekseenko, E., Raybaud, V., Espinasse, B., Carlotti, F., Queguiner, B., Thouvenin, B., Garreau, P., Baklouti, M., 2014. Seasonal dynamics and stoichiometry of the planktonic community in the Northwestern Mediterranean Sea: a 3D modeling approach. Ocean Dyn. 64, 179–207.

Allen, S., Allen, D., Phoenix, V.R., Le Roux, G., Durántez Jiménez, P., Simonneau, A., Binet, S., Galop, D., 2019. Atmospheric transport and deposition of microplastics in a remote mountain catchment. Nat. Geosci. 12, 339–344.

Almroth, B.M.C., Åström, L., Roslund, S., Petersson, H., Johansson, M., Persson, N.-K., 2018. Quantifying shedding of synthetic fibers from textiles; a source of microplastics released into the environment. Environ. Sci. Pollut. Res. 25, 1191–1199. https://doi.org/10.1007/s11356-017-0528-7

Anđelić, I., Matijević, S., Ujević, I., 2015. Preliminary investigation of bisphenol A in sediments and suspended matter in Kaštela Bay (Adriatic Sea, Croatia). Acta Adriat. 56, 259–268.

Andresen, J.A., Grundmann, A., Bester, K., 2004. Organophosphorus flame retardants and plasticisers in surface waters. Sci. Total Environ. 332, 155–166. https://doi.org/10.1016/j.scitotenv.2004.04.021

Aoki, K.A.A., Harris, C.A., Katsiadaki, I., Sumpter, J.P., 2011. Evidence suggesting that di-n-butyl phthalate has antiandrogenic effects in fish. Environ. Toxicol. Chem. 30, 1338–1345. https://doi.org/10.1002/etc.502

Arias-Andres, M., Klümper, U., Rojas-Jimenez, K., Grossart, H.P., 2018. Microplastic pollution increases gene exchange in aquatic ecosystems. Environ. Pollut. 237, 253–261. https://doi.org/10.1016/j.envpol.2018.02.058

Avendaño, S.M., Zhong, G., Liu, J., 2015. Comment on ‘‘Biodegradation of perfluorooctanesulfonate (PFOS) as an emerging contaminant.’ Chemosphere 138, 1037–1038. https://doi.org/10.1016/j.chemosphere.2014.01.072

Avio, C.G., Gorbi, S., Regoli, F., 2017. Plastics and microplastics in the oceans: From emerging pollutants to emerged threat. Mar. Environ. Res. 128, 2–11. https://doi.org/10.1016/j.marenvres.2016.05.012

Baini, M., Martellini, T., Cincinelli, A., Campani, T., Minutoli, R., Panti, C., Finoia, M.G., Fossi, M.C., 2017. First detection of seven phthalate esters (PAEs) as plastic tracers in superficial neustonic/planktonic samples and cetacean blubber. Anal. Methods 9, 1512–1520. https://doi.org/10.1039/c6ay02674e

Balbi, T., Franzellitti, S., Fabbri, R., Montagna, M., Fabbri, E., Canesi, L., 2016. Impact of bisphenol A (BPA) on early embryo development in the marine mussel Mytilus

galloprovincialis: Effects on gene transcription. Environ. Pollut. 218, 996–1004. https://doi.org/10.1016/j.envpol.2016.08.050

Bellas, J., Martínez-Armental, J., Martínez-Cámara, A., Besada, V., Martínez-Gómez, C., 2016. Ingestion of microplastics by demersal fish from the Spanish Atlantic and Mediterranean coasts. Mar. Pollut. Bull. 109, 55–60. https://doi.org/10.1016/j.marpolbul.2016.06.026

Bergé, A., Gasperi, J., Rocher, V., Gras, L., Coursimault, A., Moilleron, R., 2014. Phthalates and alkylphenols in industrial and domestic effluents: Case of Paris conurbation (France). Sci. Total Environ. 488–489, 26–35. https://doi.org/10.1016/j.scitotenv.2014.04.081

Berrojalbiz, N., Dachs, J., Ojeda, M.J., Valle, M.C., Castro-Jiménez, J., Wollgast, J., Ghiani, M., Hanke, G., Zaldivar, J.M., 2011. Biogeochemical and physical controls on concentrations of polycyclic aromatic hydrocarbons in water and plankton of the Mediterranean and Black Seas. Global Biogeochem. Cycles 25, 1–14. https://doi.org/10.1029/2010GB003775

Björnsdotter, M.K., Jonker, W., Legradi, J., Kool, J., Ballesteros-Gómez, A., 2017. Bisphenol A alternatives in thermal paper from the Netherlands, Spain, Sweden and Norway. Screening and potential toxicity. Sci. Total Environ. 601–602, 210–221. https://doi.org/10.1016/j.scitotenv.2017.05.171

Browne, M.A., Crump, P., Niven, S.J., Teuten, E., Tonkin, A., Galloway, T., Thompson, R., 2011. Accumulation of Microplastic on Shorelines Woldwide: Sources and Sinks. Environ. Sci. Technol 45, 9175–9179. https://doi.org/10.1021/es201811s

Camarasa, J.G., Serra-Baldrich, E., 1992. Allergic contact dermatitis from triphenyl phosphate. Contact Dermatitis 26, 264–265.

Canesi, L., Fabbri, E., 2015. Environmental effects of BPA: Focus on aquatic species. Dose-Response 13. https://doi.org/10.1177/1559325815598304

Carmona, E., Andreu, V., Picó, Y., 2017. Multi-residue determination of 47 organic compounds in water, soil, sediment and fish—Turia River as case study. J. Pharm. Biomed. Anal. 146, 117–125. https://doi.org/10.1016/j.jpba.2017.08.014

Casal, P., González-Gaya, B., Zhang, Y., Reardon, A.J.F., Martin, J.W., Jiménez, B., Dachs, J., 2017. Accumulation of Perfluoroalkylated Substances in Oceanic Plankton. Environ. Sci. Technol. 51, 2766–2775. https://doi.org/10.1021/acs.est.6b05821

Castro-Jiménez, J., Barhoumi, B., Tedetti, M., Sempéré, R., 2018. Atmospheric particle-bound organophosphate ester flame retardants and plasticizers in a North African Mediterranean coastal city (Bizerte, Tunisia). Sci. Total Environ. 642, 383–393. https://doi.org/10.1016/j.scitotenv.2018.06.010

Castro-Jiménez, J., Berrojalbiz, N., Pizarro, M., Dachs, J., 2014. Organophosphate ester (OPE) flame retardants and plasticizers in the open mediterranean and black seas atmosphere. Environ. Sci. Technol. 48, 3203–3209. https://doi.org/10.1021/es405337g

Castro-Jiménez, J., Casal, P., González-Gaya, B., Pizarro, M., Dachs, J., 2016. Organophosphate ester flame retardants and plasticizers in the global oceanic atmosphere. Environ. Sci. Technol 50, 12831–12839.

Castro-Jiménez, J., González-Fernández, D., Fornier, M., Schmidt, N., Sempéré, R., n.d.

Macro-litter in surface waters from the Rhone River: Plastic pollution and flows to the NW Mediterranean Sea. Mar. Pollut. Bull.

Chen, C.F., Ju, Y.R., Lim, Y.C., Chang, J.H., Chen, C.W., Dong, C. Di, 2018. Spatial and temporal distribution of Di-(2-ethylhexyl) phthalate in urban river sediments. Int. J. Environ. Res. Public Health 15, 1–12. https://doi.org/10.3390/ijerph15102228

Chen, C.H., Jiang, S.S., Chang, I.S., Wen, H.J., Sun, C.W., Wang, S.L., 2018. Association between fetal exposure to phthalate endocrine disruptor and genome-wide DNA methylation at birth. Environ. Res. 162, 261–270. https://doi.org/10.1016/j.envres.2018.01.009

Chen, T., Zhang, L., Yue, J. qiu, Lv, Z. quan, Xia, W., Wan, Y. jian, Li, Y. yuan, Xu, S.Q., 2012. Prenatal PFOS exposure induces oxidative stress and apoptosis in the lung of rat off-spring. Reprod. Toxicol. 33, 538–545. https://doi.org/10.1016/j.reprotox.2011.03.003

Chen, X., Xu, S., Tan, T., Lee, S.T., Cheng, S.H., Lee, F.W.F., Xu, S.J.L., Ho, K.C., 2014. Toxicity and estrogenic endocrine disrupting activity of phthalates and their mixtures. Int. J. Environ. Res. Public Health 11, 3156–3168. https://doi.org/10.3390/ijerph110303156

Cheng, Z., Liu, J.B., Gao, M., Shi, G.Z., Fu, X.J., Cai, P., Lv, Y.F., Guo, Z.B., Shan, C.Q., Yang, Z.B., Xu, X.X., Xian, J.R., Yang, Y.X., Li, K. Bin, Nie, X.P., 2019. Occurrence and distribution of phthalate esters in freshwater aquaculture fish ponds in Pearl River Delta, China. Environ. Pollut. 245, 883–888. https://doi.org/10.1016/j.envpol.2018.11.085

Collignon, A., Hecq, J.H., Glagani, F., Voisin, P., Collard, F., Goffart, A., 2012. Neustonic microplastic and zooplankton in the North Western Mediterranean Sea. Mar. Pollut. Bull. 64, 861–864. https://doi.org/10.1016/j.marpolbul.2012.01.011

Constant, M., Kerhervé, P., Sola, J., Sanchez-Vidal, A., Canals, M., Heussner, S., 2018. Floating microplastics in the northwestern Mediterranean Sea: temporal and spatial heterogeneities, in: Proceedings of the International Conference on Microplastic Pollution in the Mediterranean Sea, Springer International Publishing. pp. 9–15. https://doi.org/10.1007/978-3-319-71279-6

Coste, B., Raimbault, P., 1993. Recent data on the nutrient input into the Mediterranean Sea by the Rhône river. Water Res. 30, 47–50.

Cozar, A., Echevarria, F., Gonzalez-Gordillo, J.I., Irigoien, X., Ubeda, B., Hernandez-Leon, S., Palma, A.T., Navarro, S., Garcia-de-Lomas, J., Ruiz, A., Fernandez-de-Puelles, M.L., Duarte, C.M., 2014. Plastic debris in the open ocean. Proc. Natl. Acad. Sci. 111, 10239–10244. https://doi.org/10.1073/pnas.1314705111

Cristale, J., García Vázquez, A., Barata, C., Lacorte, S., 2013. Priority and emerging flame retardants in rivers: Occurrence in water and sediment, Daphnia magna toxicity and risk assessment. Environ. Int. 59, 232–243. https://doi.org/10.1016/j.envint.2013.06.011

Danzl, E., Sei, K., Soda, S., Ike, M., Fujita, M., 2009. Biodegradation of bisphenol A, bisphenol F and bisphenol S in seawater. Int. J. Environ. Res. Public Health 6, 1472–1484. https://doi.org/10.3390/ijerph6041472

Dargnat, C., Blanchard, M., Chevreuil, M., Teil, M.J., 2009. Occurrence of phthalate esters in the Seine River estuary (France). Hydrol. Process. 23, 1192–1201.

https://doi.org/10.1002/hyp

Dauchy, X., Boiteux, V., Rosin, C., Munoz, J.F., 2012. Relationship between industrial discharges and contamination of raw water resources by perfluorinated compounds. Part I: Case study of a fluoropolymer manufacturing plant. Bull. Environ. Contam. Toxicol. 89, 525–530. https://doi.org/10.1007/s00128-012-0704-x

De Alencastro, L.F., 2014. Evaluation de la pollution par les plastiques dans les eaux de surface en Suisse. Rapp. Final. Sur mandat l'Office fédéral l'environnement 15–17.

Desforges, J.P.W., Galbraith, M., Ross, P.S., 2015. Ingestion of Microplastics by Zooplankton in the Northeast Pacific Ocean. Arch. Environ. Contam. Toxicol. 69, 320–330. https://doi.org/10.1007/s00244-015-0172-5

Deshayes, S., Eudes, V., Bigourie, M., Droguet, C., Moilleron, R., 2017. Alkylphenol and phthalate contamination of all sources of greywater from French households. Sci. Total Environ. 599–600, 883–890. https://doi.org/10.1016/j.scitotenv.2017.05.038

Ding, G., Wang, L., Zhang, J., Wei, Y., Wei, L., Li, Y., Shao, M., Xiong, D., 2015. Toxicity and DNA methylation changes induced by perfluorooctane sulfonate (PFOS) in sea urchin Glyptocidaris crenularis. Chemosphere 128, 225–230. https://doi.org/10.1016/j.chemosphere.2015.01.045

Domínguez-Morueco, N., González-Alonso, S., Valcárcel, Y., 2014. Phthalate occurrence in rivers and tap water from central Spain. Sci. Total Environ. 500–501, 139–146. https://doi.org/10.1016/j.scitotenv.2014.08.098

Duncan, E., Botterell, Z., Broderick, A., Galloway, T., Lindeque, P., Nuno, A., Godley, B., 2017. A global review of marine turtle entanglement in anthropogenic debris: a baseline for further action. Endanger. Species Res. 34, 431–448. https://doi.org/10.3354/esr00865

Earnshaw, M.R., Paul, A.G., Loos, R., Tavazzi, S., Paracchini, B., Scheringer, M., Hungerbühler, K., Jones, K.C., Sweetman, A.J., 2014. Comparing measured and modelled PFOS concentrations in a UK freshwater catchment and estimating emission rates. Environ. Int. 70, 25–31. https://doi.org/10.1016/j.envint.2014.05.004

Emnet, P., Gaw, S., Northcott, G., Storey, B., Graham, L., 2014. Personal care products and steroid hormones in the Antarctic coastal environment associated with two Antarctic research stations, McMurdo Station and Scott Base. Environ. Res. 136, 331–342. https://doi.org/10.1016/j.envres.2014.10.019

Endo, S., Takizawa, R., Okuda, K., Takada, H., Chiba, K., Kanehiro, H., Ogi, H., Yamashita, R., Date, T., 2005. Concentration of polychlorinated biphenyls (PCBs) in beached resin pellets: Variability among individual particles and regional differences. Mar. Pollut. Bull. 50, 1103–1114. https://doi.org/10.1016/j.marpolbul.2005.04.030

EU Water Framework Directive, T., 2000. Directive 2000/60/EC.

Fauvelle, V., Castro-Jiménez, J., Schmidt, N., Carlez, B., Panagiotopoulos, C., Sempéré, R., 2018. One-Single Extraction Procedure for the Simultaneous Determination of a Wide Range of Polar and Nonpolar Organic Contaminants in Seawater. Front. Mar. Sci. 5, 1–10. https://doi.org/10.3389/fmars.2018.00295

Fernández-Amado, M., Prieto-Blanco, M.C., López-Mahía, P., Muniategui-Lorenzo, S., Prada-Rodríguez, D., 2017. A comparative study of extractant and chromatographic phases for the rapid and sensitive determination of six phthalates in rainwater samples.

Chemosphere 175, 52–65. https://doi.org/10.1016/j.chemosphere.2017.02.001

Fossi, M.C., Panti, C., Guerranti, C., Coppola, D., Giannetti, M., Marsili, L., Minutoli, R., 2012. Are baleen whales exposed to the threat of microplastics? A case study of the Mediterranean fin whale (Balaenoptera physalus). Mar. Pollut. Bull. 64, 2374–2379. https://doi.org/10.1016/j.marpolbul.2012.08.013

Fraysse, M., Pairaud, I., Ross, O.N., Faure, V.M., Pinazo, C., 2014. Intrusion of Rhone River diluted water into the Bay of Marseille: Generation processes and impacts on ecosystem functioning. J. Geophys. Res. Ocean. 119, 6535–6556. https://doi.org/10.1002/2014JC010022.Received

Frias, J.P.G.L., Sobral, P., Ferreira, A.M., 2010. Organic pollutants in microplastics from two beaches of the Portuguese coast. Mar. Pollut. Bull. 60, 1988–1992. https://doi.org/10.1016/j.marpolbul.2010.07.030

Fries, E., Püttmann, W., 2003. Monitoring of the three organophosphate esters TBP, TCEP and TBEP in river water and ground water (Oder, Germany). J. Environ. Monit. 5, 346–352. https://doi.org/10.1039/b210342g

Fu, P.Q., Kawamura, K., Chen, J., Charrière, B., Sempéré, R., 2013. Organic molecular composition of marine aerosols over the Arctic Ocean in summer: Contributions of primary emission and secondary aerosol formation. Biogeosciences 10, 653–667. https://doi.org/10.5194/bg-10-653-2013

González-Gaya, B., Dachs, J., Roscales, J.L., Caballero, G., Jiménez, B., 2014. Perfluoroalkylated substances in the global tropical and subtropical surface oceans. Environ. Sci. Technol. 48, 13076–13084. https://doi.org/10.1021/es503490z

Guigue, C., Tedetti, M., Ferretto, N., Garcia, N., Méjanelle, L., Goutx, M., 2014. Spatial and seasonal variabilities of dissolved hydrocarbons in surface waters from the Northwestern Mediterranean Sea: Results from one year intensive sampling. Sci. Total Environ. 466–467, 650–662. https://doi.org/10.1016/j.scitotenv.2013.07.082

Guigue, C., Tedetti, M., Giorgi, S., Goutx, M., 2011. Occurrence and distribution of hydrocarbons in the surface microlayer and subsurface water from the urban coastal marine area off Marseilles, Northwestern Mediterranean Sea. Mar. Pollut. Bull. 62, 2741–2752. https://doi.org/10.1016/j.marpolbul.2011.09.013

Hahladakis, J.N., Velis, C.A., Weber, R., Iacovidou, E., Purnell, P., 2018. An overview of chemical additives present in plastics: Migration, release, fate and environmental impact during their use, disposal and recycling. J. Hazard. Mater. 344, 179–199. https://doi.org/10.1016/j.jhazmat.2017.10.014

Hallanger, I.G., Sagerup, K., Evenset, A., Kovacs, K.M., Leonards, P., Fuglei, E., Routti, H., Aars, J., Strøm, H., Lydersen, C., Gabrielsen, G.W., 2015. Organophosphorous flame retardants in biota from Svalbard, Norway. Mar. Pollut. Bull. 101, 442–447. https://doi.org/10.1016/j.marpolbul.2015.09.049

Henríquez-hernández, L.A., Montero, D., Camacho, M., Ginés, R., Boada, L.D., Ramírez, B., Valerón, P.F., Almeida-gonzález, M., Zumbado, M., Haroun, R., Luzardo, O.P., 2017. Comparative analysis of selected semi-persistent and emerging pollutants in wild-caught fi sh and aquaculture associated fi sh using Bogue (Boops boops) as sentinel species. Sci. Total Environ. 581–582, 199–208. https://doi.org/10.1016/j.scitotenv.2016.12.107

Hermabessiere, L., Dehaut, A., Paul-Pont, I., Lacroix, C., Jezequel, R., Soudant, P., Duflos, G., 2017. Occurrence and effects of plastic additives on marine environments and organisms: A review. Chemosphere 182, 781–793. https://doi.org/10.1016/j.chemosphere.2017.05.096

Herrero, A., Vila, J., Eljarrat, E., Ginebreda, A., Sabater, S., Batalla, R.J., Barceló, D., 2018. Transport of sediment borne contaminants in a Mediterranean river during a high flow event. Sci. Total Environ. 633, 1392–1402. https://doi.org/10.1016/j.scitotenv.2018.03.205

Horton, A.A., Walton, A., Spurgeon, D.J., Lahive, E., Svendsen, C., 2017. Microplastics in freshwater and terrestrial environments: Evaluating the current understanding to identify the knowledge gaps and future research priorities. Sci. Total Environ. 586, 127–141. https://doi.org/10.1016/j.scitotenv.2017.01.190

Hu, M., Li, J., Zhang, B., Cui, Q., Wei, S., Yu, H., 2014. Regional distribution of halogenated organophosphate flame retardants in seawater samples from three coastal cities in China. Mar. Pollut. Bull. 86, 569–574. https://doi.org/10.1016/j.marpolbul.2014.06.009

Huang, Q., Fang, C., Wu, X., Fan, J., Dong, S., 2011. Perfluorooctane sulfonate impairs the cardiac development of a marine medaka (Oryzias melastigma). Aquat. Toxicol. 105, 71–77. https://doi.org/10.1016/j.aquatox.2011.05.012

Ike, M., Chen, M.Y., Danzl, E., Sei, K., Fujita, M., 2006. Biodegradation of a variety of bisphenols under aerobic and anaerobic conditions. Water Sci. Technol. 53, 153–159.

Isobe, A., Uchida, K., Tokai, T., Iwasaki, S., 2015. East Asian seas: A hot spot of pelagic microplastics. Mar. Pollut. Bull. 101, 618–623. https://doi.org/10.1016/j.marpolbul.2015.10.042

Jin, H., Zhu, L., 2016. Occurrence and partitioning of bisphenol analogues in water and sediment from Liaohe River Basin and Taihu Lake, China. Water Res. 103, 343–351. https://doi.org/10.1016/j.watres.2016.07.059

Kaiser, D., Kowalski, N., Waniek, J.J., 2017. Effects of biofouling on the sinking behavior of microplastics. Environ. Res. Lett. 12. https://doi.org/10.1088/1748-9326/aa8e8b

Kang, J.H., Kondo, F., 2005. Bisphenol A degradation in seawater is different from that in river water. Chemosphere 60, 1288–1292. https://doi.org/10.1016/j.chemosphere.2005.01.058

Karlsson, T.M., Hassellöv, M., Jakubowicz, I., 2018. Influence of thermooxidative degradation on the in situ fate of polyethylene in temperate coastal waters. Mar. Pollut. Bull. 135, 187–194. https://doi.org/10.1016/j.marpolbul.2018.07.015

Kay, P., Hiscoe, R., Moberley, I., Bajic, L., McKenna, N., 2018. Wastewater treatment plants as a source of microplastics in river catchments. Environ. Sci. Pollut. Res. 25, 20264–20267. https://doi.org/https://doi.org/10.1007/s11356-018-2070-7

Kwon, B.G., Lim, H.J., Na, S.H., Choi, B.I., Shin, D.S., Chung, S.Y., 2014. Biodegradation of perfluorooctanesulfonate (PFOS) as an emerging contaminant. Chemosphere 109, 221–225. https://doi.org/10.1016/j.chemosphere.2014.01.072

Lamb, J.B., Willis, B.L., Fiorenza, E.A., Couch, C.S., Howard, R., Rader, D.N., True, J.D., Kelly, L.A., Ahmad, A., Jompa, J., Harvell, C.D., 2018. Plastic waste associated with disease on coral reefs. Sci. Reports 359, 460–462. https://doi.org/10.4081/aiol.2017.7211

Lawson, T.J., Wilcox, C., Johns, K., Dann, P., Hardesty, B.D., 2015. Characteristics of marine debris that entangle Australian fur seals (Arctocephalus pusillus doriferus) in southern Australia. Mar. Pollut. Bull. 98, 354–357. https://doi.org/10.1016/j.marpolbul.2015.05.053

Lebreton, L.C.M., Van Der Zwet, J., Damsteeg, J.W., Slat, B., Andrady, A., Reisser, J., 2017. River plastic emissions to the world's oceans. Nat. Commun. 8, 1–10. https://doi.org/10.1038/ncomms15611

Lehner, A.F., Samsing, F., Rumbeiha, W.K., 2010. Organophosphate Ester Flame Retardant-Induced Acute Intoxications in Dogs. J. Med. Toxicol. 6, 448–458. https://doi.org/10.1007/s13181-010-0105-7

León, V.M., García, I., González, E., Samper, R., Fernández-González, V., Muniategui-Lorenzo, S., 2018. Potential transfer of organic pollutants from littoral plastics debris to the marine environment. Environ. Pollut. 236, 442–453. https://doi.org/10.1016/j.envpol.2018.01.114

Li, J., Xie, Z., Mi, W., Lai, S., Tian, C., Emeis, K.C., Ebinghaus, R., 2017. Organophosphate Esters in Air, Snow, and Seawater in the North Atlantic and the Arctic. Environ. Sci. Technol. 51, 6887–6896. https://doi.org/10.1021/acs.est.7b01289

Li, R., Liang, J., Duan, H., Gong, Z., 2017a. Spatial distribution and seasonal variation of phthalate esters in the Jiulong River estuary, Southeast China. Mar. Pollut. Bull. 122, 38–46. https://doi.org/10.1016/j.marpolbul.2017.05.062

Li, R., Liang, J., Gong, Z., Zhang, N., Duan, H., 2017b. Occurrence, spatial distribution, historical trend and ecological risk of phthalate esters in the Jiulong River, Southeast China. Sci. Total Environ. 580, 388–397. https://doi.org/10.1016/j.scitotenv.2016.11.190

Li, X., Yin Yeung, L.W., Xu, M., Taniyasu, S., Lam, P.K.S., Yamashita, N., Dai, J., 2008. Perfluorooctane sulfonate (PFOS) and other fluorochemicals in fish blood collected near the outfall of wastewater treatment plant (WWTP) in Beijing. Environ. Pollut. 156, 1298–1303. https://doi.org/10.1016/j.envpol.2008.03.008

Li, Z., Liu, Q., Liu, C., Li, C., Li, Y., Li, S., Liu, X., Shao, J., 2017. Evaluation of PFOS-mediated neurotoxicity in rat primary neurons and astrocytes cultured separately or in co-culture. Toxicol. Vitr. 38, 77–90. https://doi.org/10.1016/j.tiv.2016.11.002

Liu, Y., Song, N., Guo, R., Xu, H., Zhang, Q., Han, Z., Feng, M., Li, D., Zhang, S., Chen, J., 2018. Occurrence and partitioning behavior of organophosphate esters in surface water and sediment of a shallow Chinese freshwater lake (Taihu Lake): Implication for eco-toxicity risk. Chemosphere 202, 255–263. https://doi.org/10.1016/j.chemosphere.2018.03.108

Long, M., Moriceau, B., Gallinari, M., Lambert, C., Huvet, A., Raffray, J., Soudant, P., 2015. Interactions between microplastics and phytoplankton aggregates: Impact on their respective fates. Mar. Chem. 175, 39–46. https://doi.org/10.1016/j.marchem.2015.04.003

Loos, R., Tavazzi, S., Mariani, G., Suurkuusk, G., Paracchini, B., Umlauf, G., 2017. Analysis of emerging organic contaminants in water, fish and suspended particulate matter (SPM) in the Joint Danube Survey using solid-phase extraction followed by UHPLC-MS-MS and GC–MS analysis. Sci. Total Environ. 607–608, 1201–1212. https://doi.org/10.1016/j.scitotenv.2017.07.039

Ma, Y., Xie, Z., Lohmann, R., Mi, W., Gao, G., 2017. Organophosphate Ester Flame Retardants and Plasticizers in Ocean Sediments from the North Pacific to the Arctic Ocean. Environ. Sci. Technol. 51, 3809–3815. https://doi.org/10.1021/acs.est.7b00755

Mamindy-Pajany, Y., Hurel, C., Géret, F., Galgani, F., Battaglia-Brunet, F., Marmier, N., Roméo, M., 2013. Arsenic in marine sediments from French Mediterranean ports: Geochemical partitioning, bioavailability and ecotoxicology. Chemosphere 90, 2730–2736. https://doi.org/10.1016/j.chemosphere.2012.11.056

Manikkam, M., Tracey, R., Guerrero-Bosagna, C., Skinner, M.K., 2013. Plastics Derived Endocrine Disruptors (BPA, DEHP and DBP) Induce Epigenetic Transgenerational Inheritance of Obesity, Reproductive Disease and Sperm Epimutations. PLoS One 8. https://doi.org/10.1371/journal.pone.0055387

Martínez-Carballo, E., González-Barreiro, C., Sitka, A., Scharf, S., Gans, O., 2007. Determination of selected organophosphate esters in the aquatic environment of Austria. Sci. Total Environ. 388, 290–299. https://doi.org/10.1016/j.scitotenv.2007.08.005

McDonough, C.A., De Silva, A.O., Sun, C., Cabrerizo, A., Adelman, D., Soltwedel, T., Bauerfeind, E., Muir, D.C.G., Lohmann, R., 2018. Dissolved Organophosphate Esters and Polybrominated Diphenyl Ethers in Remote Marine Environments: Arctic Surface Water Distributions and Net Transport through Fram Strait. Environ. Sci. Technol. 52, 6208–6216. https://doi.org/10.1021/acs.est.8b01127

Meeker, J.D., Stapleton, H.M., 2010. House dust concentrations of organophosphate flame retardants in relation to hormone levels and semen quality parameters. Environ. Health Perspect. 118, 318–323. https://doi.org/10.1289/ehp.0901332

Mi, L., Xie, Z., Zhao, Z., Zhong, M., Mi, W., Ebinghaus, R., Tang, J., 2019. Occurrence and spatial distribution of phthalate esters in sediments of the Bohai and Yellow seas. Sci. Total Environ. 653, 792–800. https://doi.org/10.1016/j.scitotenv.2018.10.438

Miège, C., Peretti, A., Labadie, P., Budzinski, H., Le Bizec, B., Vorkamp, K., Tronczynski, J., Persat, H., Coquery, M., Babut, M., 2012. Occurrence of priority and emerging organic compounds in fishes from the Rhone River (France). Anal. Bioanal. Chem. 404, 2721–2735. https://doi.org/10.1007/s00216-012-6187-0

Millet, B., Pinazo, C., Banaru, D., Pagès, R., Guiart, P., Pairaud, I., 2018. Unexpected spatial impact of treatment plant discharges induced by episodic hydrodynamic events: Modelling Lagrangian transport of fine particles by Northern current intrusions in the bays of marseille (France). PLoS One 13, 0–25. https://doi.org/10.1371/journal.pone.0195257

Mita, L., Bianco, M., Viggiano, E., Zollo, F., Bencivenga, U., Sica, V., Monaco, G., Portaccio, M., Diano, N., Colonna, A., Lepore, M., Canciglia, P., Mita, D.G., 2011. Bisphenol A content in fish caught in two different sites of the Tyrrhenian Sea (Italy). Chemosphere 82, 405–410. https://doi.org/10.1016/j.chemosphere.2010.09.071

Mourier, B., Desmet, M., Van Metre, P.C., Mahler, B.J., Perrodin, Y., Roux, G., Bedell, J.P., Lefèvre, I., Babut, M., 2014. Historical records, sources, and spatial trends of PCBs along the RhÔne River (France). Sci. Total Environ. 476–477, 568–576. https://doi.org/10.1016/j.scitotenv.2014.01.026

Mulder, M.D., Heil, A., Kukučka, P., Kuta, J., Påibylová, P., Prokeš, R., Lammel, G., 2014. Reprint of: Long-range atmospheric transport of PAHs, PCBs and PBDEs to the central

and eastern Mediterranean and changes of PCB and PBDE congener patterns in summer 2010. Atmos. Environ. 121, 66–74. https://doi.org/10.1016/j.atmosenv.2015.07.046

Munoz, G., Giraudel, J.L., Botta, F., Lestremau, F., Dévier, M.H., Budzinski, H., Labadie, P., 2015. Spatial distribution and partitioning behavior of selected poly- and perfluoroalkyl substances in freshwater ecosystems: A French nationwide survey. Sci. Total Environ. 517, 48–56. https://doi.org/10.1016/j.scitotenv.2015.02.043

Munschy, C., Bely, N., Pollono, C., Aminot, Y., 2019. Perfluoroalkyl substances (PFASs)in the marine environment: Spatial distribution and temporal profile shifts in shellfish from French coasts. Chemosphere 228, 640–648. https://doi.org/10.1016/j.chemosphere.2019.04.205

Näkki, P., Setälä, O., Lehtiniemi, M., 2019. Seafloor sediments as microplastic sinks in the northern Baltic Sea – Negligible upward transport of buried microplastics by bioturbation. Environ. Pollut. 249, 74–81. https://doi.org/10.1016/J.ENVPOL.2019.02.099

Net, S., Rabodonirina, S., Sghaier, R. Ben, Dumoulin, D., Chbib, C., Tlili, I., Ouddane, B., 2015a. Distribution of phthalates, pesticides and drug residues in the dissolved, particulate and sedimentary phases from transboundary rivers (France–Belgium). Sci. Total Environ. 521–522, 152–159. https://doi.org/10.1016/j.scitotenv.2015.03.087

Net, S., Sempéré, R., Delmont, A., Paluselli, A., Ouddane, B., 2015b. Occurrence, fate, behavior and ecotoxicological state of phthalates in different environmental matrices. Environ. Sci. Technol. 49, 4019–4035. https://doi.org/10.1021/es505233b

Neves, D., Sobral, P., Ferreira, J.L., Pereira, T., 2015. Ingestion of microplastics by commercial fish off the Portuguese coast. Mar. Pollut. Bull. 101, 119–126. https://doi.org/10.1016/j.marpolbul.2015.11.008

Noyes, P.D., McElwee, M.K., Miller, H.D., Clark, B.W., Van Tiem, L.A., Walcott, K.C., Erwin, K.N., Levin, E.D., 2009. The toxicology of climate change: Environmental contaminants in a warming world. Environ. Int. 35, 971–986. https://doi.org/10.1016/j.envint.2009.02.006

Nunes, J.A.C.C., Sampaio, C.L.S., Barros, F., Leduc, A.O.H.C., 2018. Plastic debris collars: An underreported stressor in tropical reef fishes. Mar. Pollut. Bull. 129, 802–805. https://doi.org/10.1016/j.marpolbul.2017.10.076

Obbard, R.W., Sadri, S., Wong, Y.Q., Khitun, A.A., Baker, I., Richard, C., 2014. Global warming releases microplastic legacy frozen in Arctic Sea ice. Earth'sFuture 2, 315–320. https://doi.org/10.1002/2014EF000240.Abstract

Okamoto, Y., Ueda, K., Kojima, N., 2011. Potential Risks of Phthalate Esters: Acquisition of Endocrine-disrupting Activity during Environmental and Metabolic Processing. J. Heal. Sci. 57, 497–503. https://doi.org/10.1248/jhs.57.497

Olivier, J., Lamouroux, N., Malard, F., Amoros, C., 2009. The Rhône River Basin. https://doi.org/10.1016/B978-0-12-369449-2.00007-2

Oursel, B., Garnier, C., Pairaud, I., Omanović, D., Durrieu, G., Syakti, A.D., Le Poupon, C., Thouvenin, B., Lucas, Y., 2014. Behaviour and fate of urban particles in coastal waters: Settling rate, size distribution and metals contamination characterization. Estuar. Coast. Shelf Sci. 138, 14–26. https://doi.org/10.1016/j.ecss.2013.12.002

Paluselli, A., Aminot, Y., Galgani, F., Net, S., Sempéré, R., 2018a. Occurrence of phthalate acid esters (PAEs) in the northwestern Mediterranean Sea and the Rhone River. Prog. Oceanogr. 163, 221–231. https://doi.org/10.1016/j.pocean.2017.06.002

Paluselli, A., Fauvelle, V., Galgani, F., Sempéré, R., 2019. Phthalate release from plastic fragments and degradation in seawater. Environ. Sci. Technol. 53, 166–175. https://doi.org/10.1021/acs.est.8b05083

Paluselli, A., Fauvelle, V., Schmidt, N., Galgani, F., Net, S., Sempéré, R., 2018b. Distribution of phthalates in Marseille Bay (NW Mediterranean Sea). Sci. Total Environ. 621, 578–587. https://doi.org/10.1016/j.scitotenv.2017.11.306

Panagiotopoulos, C., Sempéré, R., Para, J., Raimbault, P., Rabouille, C., Charrière, B., 2012. The composition and flux of particulate and dissolved carbohydrates from the Rhone River into the Mediterranean Sea. Biogeosciences 9, 1827–1844. https://doi.org/10.5194/bg-9-1827-2012

Pang, L., Ge, L., Yang, P., He, H., Zhang, H., 2018. Degradation of organophosphate esters in sewage sludge: Effects of aerobic/anaerobic treatments and bacterial community compositions. Bioresour. Technol. 255, 16–21. https://doi.org/10.1016/j.dib.2018.02.039

Pantelaki, I., Voutsa, D., 2019. Organophosphate flame retardants (OPFRs): A review on analytical methods and occurrence in wastewater and aquatic environment. Sci. Total Environ. 649, 247–263. https://doi.org/10.1016/j.scitotenv.2018.08.286

Para, J., Coble, P.G., Charrière, B., Tedetti, M., Fontana, C., Sempéré, R., 2010. Fluorescence and absorption properties of chromophoric dissolved organic matter (CDOM) in coastal surface waters of the northwestern Mediterranean Sea, influence of the Rhône River. Biogeosciences 7, 4083–4103.

Paul, A.G., Jones, K.C., Sweetman, A.J., 2009. A First Global Production , Emission And Environmental Inventory For Perfluorooctane Sulfonate 43, 386–392.

Peeken, I., Primpke, S., Beyer, B., Gütermann, J., Katlein, C., Krumpen, T., Bergmann, M., Hehemann, L., Gerdts, G., 2018. Arctic sea ice is an important temporal sink and means of transport for microplastic. Nat. Commun. 9. https://doi.org/10.1038/s41467-018-03825-5

Peijnenburg, W.J.G.M., Struijs, J., 2006. Occurrence of phthalate esters in the environment of the Netherlands. Ecotoxicol. Environ. Saf. 63, 204–215. https://doi.org/10.1016/j.ecoenv.2005.07.023

Perez, T., Longet, D., Schembri, T., Rebouillon, P., Vacelet, J., 2005. Effects of 12 years' operation of a sewage treatment plant on trace metal occurrence within a Mediterranean commercial sponge (Spongia officinalis, Demospongiae). Mar. Pollut. Bull. 50, 301–309. https://doi.org/10.1016/j.marpolbul.2004.11.001

Pergent-Martini, C., 1998. Posidonia oceanica: a Biological Indicator of Past and Present Mercury Contamination in the Mediterranean Sea. Mar. Environ. Res. 45, 101–111.

Perra, G., Focardi, E.S., Guerranti, C., 2013. Levels and spatial distribution of perfluorinated compounds (PFCs) in superficial sediments from the marine reserves of the Tuscan Archipelago National Park (Italy). Mar. Pollut. Bull. 76, 379–382. https://doi.org/10.1016/j.marpolbul.2013.07.051

Pivnenko, K., Eriksen, M.K., Martín-Fernández, J.A., Eriksson, E., Astrup, T.F., 2016.

Recycling of plastic waste: Presence of phthalates in plastics from households and industry. Waste Manag. 54, 44–52. https://doi.org/10.1016/j.wasman.2016.05.014

Pivnenko, K., Laner, D., Astrup, T.F., 2018. Dynamics of bisphenol A (BPA) and bisphenol S (BPS) in the European paper cycle: Need for concern? Resour. Conserv. Recycl. 133, 278–287. https://doi.org/10.1016/j.resconrec.2018.01.021

Pont, D., Simonnet, J.P., Walter, A. V., 2002. Medium-term changes in suspended sediment delivery to the ocean: Consequences of catchment heterogeneity and river management (Rhône River, France). Estuar. Coast. Shelf Sci. 54, 1–18. https://doi.org/10.1006/ecss.2001.0829

Qu, B., Zhao, H., Zhou, J., 2010. Toxic effects of perfluorooctane sulfonate (PFOS) on wheat (Triticum aestivum L.) plant. Chemosphere 79, 555–560. https://doi.org/10.1016/j.chemosphere.2010.02.012

Quinnies, K.M., Harris, E.P., Snyder, R.W., Sumner, S.S., Rissman, E.F., 2017. Direct and transgenerational effects of low doses of perinatal Di-(2-ethylhexyl) phthalate (DEHP) on social behaviors in mice. PLoS One 12, 1–19. https://doi.org/10.1371/journal.pone.0171977

Raimbault, P., Garcia, N., Cerutti, F., 2008. Distribution of inorganic and organic nutrients in the South Pacific Ocean − evidence for long-term accumulation of organic matter in nitrogen-depleted waters. Biogeosciences 5, 281–298. https://doi.org/10.5194/bg-5-281-2008

Reemtsma, T., Quintana, J.B., Rodil, R., García-López, M., Rodríguez, I., 2008. Organophosphorus flame retardants and plasticizers in water and air I. Occurrence and fate. Trends Anal. Chem. 27, 727–737. https://doi.org/10.1016/j.trac.2008.07.002

Revathi, P., Saipriya, K., Kumar, C.K., Kumar, T., 2014. Determination of dissolved TBP in PUREX process aqueous streams using ICP-AES. J. Radioanal. Nucl. Chem. 300, 93–98. https://doi.org/10.1007/s10967-014-2994-4

Romeo, T., Pietro, B., Pedà, C., Consoli, P., Andaloro, F., Fossi, M.C., 2015. First evidence of presence of plastic debris in stomach of large pelagic fish in the Mediterranean Sea. Mar. Pollut. Bull. 95, 358–361. https://doi.org/10.1016/j.marpolbul.2015.04.048

Romera-Castillo, C., Pinto, M., Langer, T.M., Álvarez-Salgado, X.A., Herndl, G.J., 2018. Dissolved organic carbon leaching from plastics stimulates microbial activity in the ocean. Nat. Commun. 9. https://doi.org/10.1038/s41467-018-03798-5

Salgueiro-González, N., Turnes-Carou, I., Besada, V., Muniategui-Lorenzo, S., López-Mahía, P., Prada-Rodríguez, D., 2015. Occurrence, distribution and bioaccumulation of endocrine disrupting compounds in water, sediment and biota samples from a European river basin. Sci. Total Environ. 529, 121–130. https://doi.org/10.1016/j.scitotenv.2015.05.048

Sánchez-Avila, J., Meyer, J., Lacorte, S., 2010. Spatial distribution and sources of perfluorochemicals in the NW Mediterranean coastal waters (Catalonia, Spain). Environ. Pollut. 158, 2833–2840. https://doi.org/10.1016/j.envpol.2010.06.022

Sánchez-Avila, J., Tauler, R., Lacorte, S., 2012. Organic micropollutants in coastal waters from NW Mediterranean Sea: Sources distribution and potential risk. Environ. Int. 46, 50–62. https://doi.org/10.1016/j.envint.2012.04.013

Savriama, Y., Stige, L.C., Gerber, S., Pérez, T., Alibert, P., David, B., 2015. Impact of sewage pollution on two species of sea urchins in the Mediterranean Sea (Cortiou, France): Radial asymmetry as a bioindicator of stress. Ecol. Indic. 54, 39–47. https://doi.org/10.1016/j.ecolind.2015.02.004

Schmidt, C., Krauth, T., Wagner, S., 2017. Export of Plastic Debris by Rivers into the Sea. Environ. Sci. Technol. 51, 12246–12253. https://doi.org/10.1021/acs.est.7b02368

Schmidt, N., Fauvelle, V., Ody, A., Castro-Jiménez, J., Jouanno, J., Changeux, T., Thibaut, T., Sempéré, R., 2019. The Amazon River – a major source of organic plastic additives to the tropical North Atlantic? Environ. Sci. Technol. https://doi.org/10.1021/acs.est.9b01585

Schmidt, N., Thibault, D., Galgani, F., Paluselli, A., Sempéré, R., 2018. Occurrence of microplastics in surface waters of the Gulf of Lion (NW Mediterranean Sea). Prog. Oceanogr. 163, 214–220. https://doi.org/10.1016/j.pocean.2017.11.010

Sempéré, R., Charrière, B., Castro-Jiménez, J., Kawamura, K., Panagiotopoulos, C., 2018. Occurrence of α, ω-dicarboxylic acids and ω-oxoacids in surface waters of the Rhone River and fluxes into the Mediterranean Sea. Prog. Oceanogr. 163, 136–146. https://doi.org/10.1016/j.pocean.2017.07.002

Sempéré, R., Charrière, B., Van Wambeke, F., Cauwet, G., 2000. Carbon inputs of the Rhône River to the Mediterranean Sea: Biogeochemical implications. Global Biogeochem. Cycles 14, 669–681. https://doi.org/10.1029/1999GB900069

Sempéré, R., Tedetti, M., Panagiotopoulos, C., Charrière, B., Van Wambeke, F., 2008. Distribution and bacterial availability of dissolved neutral sugars in the South East Pacific. Biogeosciences 5, 1165–1173.

Sigler, M., 2014. The effects of plastic pollution on aquatic wildlife: Current situations and future solutions. Water. Air. Soil Pollut. 225. https://doi.org/10.1007/s11270-014-2184-6

Slomberg, D.L., Ollivier, P., Radakovitch, O., Baran, N., Sani-Kast, N., Bruchet, A., Scheringer, M., Labille, J., 2017. Insights into natural organic matter and pesticide characterisation and distribution in the Rhone River. Environ. Chem. 14, 64–73. https://doi.org/10.1071/EN16038

Soltan, D., Verlaque, M., Boudouresque, C.F., Francour, P., 2001. Changes in Macroalgal Communities in the Vicinity of a Mediterranean Sewage Outfall After the Setting Up of a Treatment Plant. Mar. Pollut. Bull. 42, 59–70.

Staniszewska, M., Koniecko, I., Falkowska, L., Krzymyk, E., 2015. Occurrence and distribution of bisphenol A and alkylphenols in the water of the gulf of Gdansk (Southern Baltic). Mar. Pollut. Bull. 91, 372–379. https://doi.org/10.1016/j.marpolbul.2014.11.027

Staniszewska, M., Nehring, I., Mudrak-Cegiołka, S., 2016. Changes of concentrations and possibility of accumulation of bisphenol A and alkylphenols, depending on biomass and composition, in zooplankton of the Southern Baltic (Gulf of Gdansk). Environ. Pollut. 213, 489–501. https://doi.org/10.1016/j.envpol.2016.03.004

Stockholm Convention, T., 2001. Stockholm Convention on Persistent Organic Pollutants, http://www.pops.int.

Struglia, M.V., Mariotti, A., Filograsso, A., 2004. River discharge into the Mediterranean sea:

Climatology and aspects of the observed variability. J. Clim. 17, 4740–4751. https://doi.org/10.1175/JCLI-3225.1

Suhrhoff, T.J., Scholz-Böttcher, B.M., 2016. Qualitative impact of salinity, UV radiation and turbulence on leaching of organic plastic additives from four common plastics - A lab experiment. Mar. Pollut. Bull. 102, 84–94. https://doi.org/10.1016/j.marpolbul.2015.11.054

Sühring, R., Diamond, M.L., Scheringer, M., Wong, F., Pućko, M., Stern, G., Burt, A., Hung, H., Fellin, P., Li, H., Jantunen, L.M., 2016. Organophosphate esters in Canadian Arctic air: Occurrence, levels and trends. Environ. Sci. Technol. 50, 7409–7415. https://doi.org/10.1021/acs.est.6b00365

Sun, C., Zhang, G., Zheng, H., Liu, N., Shi, M., Luo, X., 2019. Fate of four phthalate esters with presence of Karenia brevis : Uptake and biodegradation. Aquat. Toxicol. 206, 81–90. https://doi.org/10.1016/j.aquatox.2018.11.010

Syakti, A.D., Asia, L., Kanzari, F., Umasangadji, H., Malleret, L., Ternois, Y., Mille, G., Doumenq, P., 2012. Distribution of organochlorine pesticides (OCs) and polychlorinated biphenyls (PCBs) in marine sediments directly exposed to wastewater from Cortiou, Marseille. Environ. Sci. Pollut. Res. 19, 1524–1535. https://doi.org/10.1007/s11356-011-0640-z

Teil, M.J., Blanchard, M., Chevreuil, M., 2006. Atmospheric fate of phthalate esters in an urban area (Paris-France). Sci. Total Environ. 354, 212–223. https://doi.org/10.1016/j.scitotenv.2004.12.083

Teil, M.J., Blanchard, M., Dargnat, C., Larcher-Tiphagne, K., Chevreuil, M., 2007. Occurrence of phthalate diesters in rivers of the Paris district (France). Hydrol. Process. 21, 2515–2525. https://doi.org/10.1002/hyp

Tiano, M., Tronczyński, J., Harmelin-Vivien, M., Tixier, C., Carlotti, F., 2014. PCB concentrations in plankton size classes, a temporal study in Marseille Bay, Western Mediterranean Sea. Mar. Pollut. Bull. 89, 331–339. https://doi.org/10.1016/j.marpolbul.2014.09.040

Tran, B.C., Teil, M.J., Blanchard, M., Alliot, F., Chevreuil, M., 2015. BPA and phthalate fate in a sewage network and an elementary river of France. Influence of hydroclimatic conditions. Chemosphere 119, 43–51. https://doi.org/10.1016/j.chemosphere.2014.04.036

Tranfo, G., Caporossi, L., Paci, E., Aragona, C., Romanzi, D., De Carolis, C., De Rosa, M., Capanna, S., Papaleo, B., Pera, A., 2012. Urinary phthalate monoesters concentration in couples with infertility problems. Toxicol. Lett. 213, 15–20. https://doi.org/10.1016/j.toxlet.2011.11.033

Usman, A., Ahmad, M., 2016. From BPA to its analogues: Is it a safe journey? Chemosphere 158, 131–142. https://doi.org/10.1016/j.chemosphere.2016.05.070

van der Veen, I., de Boer, J., 2012. Phosphorus flame retardants: properties, production, environmental occurrence, toxicity and analysis. Chemosphere 88, 1119–1153. https://doi.org/10.1016/j.chemosphere.2012.03.067

Van Sebille, E., Wilcox, C., Lebreton, L., Maximenko, N., Hardesty, B.D., Van Franeker, J.A., Eriksen, M., Siegel, D., Galgani, F., Law, K.L., 2015. A global inventory of small

floating plastic debris. Environ. Res. Lett. 10, 124006. https://doi.org/10.1088/1748-9326/10/12/124006

Vered, G., Kaplan, A., Avisar, D., Shenkar, N., 2019. Using solitary ascidians to assess microplastic and phthalate plasticizers pollution among marine biota: A case study of the Eastern Mediterranean and Red Sea. Mar. Pollut. Bull. 138, 618–625. https://doi.org/10.1016/j.marpolbul.2018.12.013

VishnuRadhan, R., Eldho, T.I., David, T.D., 2019. Can plastics affect near surface layer ocean processes and climate? Mar. Pollut. Bull. 140, 274–280. https://doi.org/10.1016/j.marpolbul.2019.01.052

Wafo, E., Sarrazin, L., Diana, C., Schembri, T., Lagadec, V., Monod, J.L., 2006. Polychlorinated biphenyls and DDT residues distribution in sediments of Cortiou (Marseille, France). Mar. Pollut. Bull. 52, 104–107. https://doi.org/10.1016/j.marpolbul.2005.09.041

Waluda, C.M., Staniland, I.J., 2013. Entanglement of Antarctic fur seals at Bird Island, South Georgia. Mar. Pollut. Bull. 74, 244–252. https://doi.org/10.1016/j.marpolbul.2013.06.050

Wang, J., Bo, L., Li, L., Wang, D., Chen, G., Christie, P., Teng, Y., 2014. Occurrence of phthalate esters in river sediments in areas with different land use patterns. Sci. Total Environ. 500–501, 113–119. https://doi.org/10.1016/j.scitotenv.2014.08.092

Wang, R., Tang, J., Xie, Z., Mi, W., Chen, Y., Wolschke, H., Tian, C., Pan, X., Luo, Y., Ebinghaus, R., 2015. Occurrence and spatial distribution of organophosphate ester flame retardants and plasticizers in 40 rivers draining into the Bohai Sea, north China. Environ. Pollut. 198, 172–178. https://doi.org/10.1016/j.envpol.2014.12.037

Wang, Y., Liu, Y., Liu, T., Song, S., Gui, X., Liu, H., Tsiakaras, P., 2014. Dimethyl phthalate degradation at novel and efficient electro-Fenton cathode. Appl. Catal. B Environ. 156–157, 1–7. https://doi.org/10.1016/j.apcatb.2014.02.041

Wei, G.L., Li, D.Q., Zhuo, M.N., Liao, Y.S., Xie, Z.Y., Guo, T.L., Li, J.J., Zhang, S.Y., Liang, Z.Q., 2015. Organophosphorus flame retardants and plasticizers: Sources, occurrence, toxicity and human exposure. Environ. Pollut. 196, 29–46. https://doi.org/10.1016/j.envpol.2014.09.012

Wolschke, H., Sühring, R., Massei, R., Tang, J., Ebinghaus, R., 2018. Regional variations of organophosphorus flame retardants - Fingerprint of large river basin estuaries/deltas in Europe compared with China. Environ. Pollut. 236, 391–395. https://doi.org/10.1016/j.envpol.2018.01.061

Wolschke, H., Sühring, R., Xie, Z., Ebinghaus, R., 2015. Organophosphorus flame retardants and plasticizers in the aquatic environment: A case study of the Elbe River, Germany. Environ. Pollut. 206, 488–493. https://doi.org/10.1016/j.envpol.2015.08.002

Wong, Y.M., Li, R., Lee, C.K.F., Wan, H.T., Wong, C.K.C., 2017. The measurement of bisphenol A and its analogues, perfluorinated compounds in twenty species of freshwater and marine fishes, a time-trend comparison and human health based assessment. Mar. Pollut. Bull. 124, 743–752. https://doi.org/10.1016/j.marpolbul.2017.05.046

Woodall, L.C., Sanchez-Vidal, A., Canals, M., Paterson, G.L.J., Coppock, R., Sleight, V., Calafat, A., Rogers, A.D., Narayanaswamy, B.E., Thompson, R.C., 2014. The deep sea

is a major sink for microplastic debris. R. Soc. Open Sci. 1, 140317. https://doi.org/10.1098/rsos.140317

Xie, Z., Ebinghaus, R., Temme, C., Lohmann, R., Caba, A., Ruck, W., 2007. Occurrence and air-sea exchange of phthalates in the arctic. Environ. Sci. Technol. 41, 4555–4560. https://doi.org/10.1021/es0630240

Xu, B., Gao, N. yun, Cheng, H., Xia, S. ji, Rui, M., Zhao, D. dan, 2009. Oxidative degradation of dimethyl phthalate (DMP) by UV/H2O2 process. J. Hazard. Mater. 162, 954–959. https://doi.org/10.1016/j.jhazmat.2008.05.122

Yamazaki, E., Yamashita, N., Taniyasu, S., Lam, J., Lam, P.K.S., Moon, H.B., Jeong, Y., Kannan, P., Achyuthan, H., Munuswamy, N., Kannan, K., 2015. Bisphenol A and other bisphenol analogues including BPS and BPF in surface water samples from Japan, China, Korea and India. Ecotoxicol. Environ. Saf. 122, 565–572. https://doi.org/10.1016/j.ecoenv.2015.09.029

Yang, C., Harris, S.A., Jantunen, L.M., Siddique, S., Kubwabo, C., Tsirlin, D., Latifovic, L., Fraser, B., St-Jean, M., De La Campa, R., You, H., Kulka, R., Diamond, M.L., 2019. Are cell phones an indicator of personal exposure to organophosphate flame retardants and plasticizers? Environ. Int. 122, 104–116. https://doi.org/10.1016/j.envint.2018.10.021

Yuan, X., Lacorte, S., Cristale, J., Dantas, R.F., Sans, C., Esplugas, S., Qiang, Z., 2015. Removal of organophosphate esters from municipal secondary effluent by ozone and UV/H2O2treatments. Sep. Purif. Technol. 156, 1028–1034. https://doi.org/10.1016/j.seppur.2015.09.052

Zhai, W., Huang, Z., Chen, L., Feng, C., Li, B., Li, T., 2014. Thyroid endocrine disruption in zebrafish larvae after exposure to mono-(2-ethylhexyl) phthalate (MEHP). PLoS One 9, 1–6. https://doi.org/10.1371/journal.pone.0092465

Zhang, H., Zhou, Q., Xie, Z., Zhou, Y., Tu, C., Fu, C., Mi, W., Ebinghaus, R., Christie, P., Luo, Y., 2018. Occurrences of organophosphorus esters and phthalates in the microplastics from the coastal beaches in north China. Sci. Total Environ. 616–617, 1505–1512. https://doi.org/10.1016/j.scitotenv.2017.10.163

Zhang, T., Huang, Z., Chen, X., Huang, M., Ruan, J., 2016. Degradation behavior of dimethyl phthalate in an anaerobic/anoxic/oxic system. J. Environ. Manage. 184, 281–288. https://doi.org/10.1016/j.jenvman.2016.10.008

Zhang, Y.F., Ren, X.M., Li, Y.Y., Yao, X.F., Li, C.H., Qin, Z.F., Guo, L.H., 2018. Bisphenol A alternatives bisphenol S and bisphenol F interfere with thyroid hormone signaling pathway in vitro and in vivo. Environ. Pollut. 237, 1072–1079. https://doi.org/10.1016/j.envpol.2017.11.027

Zhang, Z., Zhang, H., Zhang, J., Wang, Q., Yang, G., 2018. Occurrence , distribution , and ecological risks of phthalate esters in the seawater and sediment of Changjiang River Estuary and its adjacent area. Sci. Total Environ. 619–620, 93–102. https://doi.org/10.1016/j.scitotenv.2017.11.070

Zhao, Z., Xie, Z., Tang, J., Zhang, G., Ebinghaus, R., 2015. Spatial distribution of perfluoroalkyl acids in surface sediments of the German Bight, North Sea. Sci. Total Environ. 511, 145–152. https://doi.org/10.1016/j.scitotenv.2014.12.063

MATERIAL & METHODS

Microplastic samples

Marine microplastic samples were collected using Manta nets (0.50 m × 0.15 m opening, 780 µm or 330 µm mesh size (Chapter 1); opening area 0.40 × 0.70 m, mesh size 150 µm (Chapter 4)) towed horizontally at the surface. Sampling was only conducted under low swell conditions (< 1 m). The net was towed for 20 minutes at a speed of 2-3 knots, approximately 50 m behind the research vessel. It was towed at a slight angle to avoid disturbances caused by the boat's wake. Samples from the Rhône River were collected from a fixed location on the dock of the river.

The net was carefully rinsed, and the content of the cod-end was poured into 1 L glass bottles and kept in cold and dark conditions until further analysis. Samples were then sieved (mesh size 125 µm) and rinsed with ultrapure water (ISO 3696). Plastic debris were picked out with tweezers under a dissecting microscope. Fibers were not taken into account due to the high risk of contamination. The number, size and shape of each item was identified using a ZooScan© (HYDROPTIC SARL). Each item was placed on the screen of the ZooScan without any water (Figure 1). Plastic items ≤ 5 mm were considered.

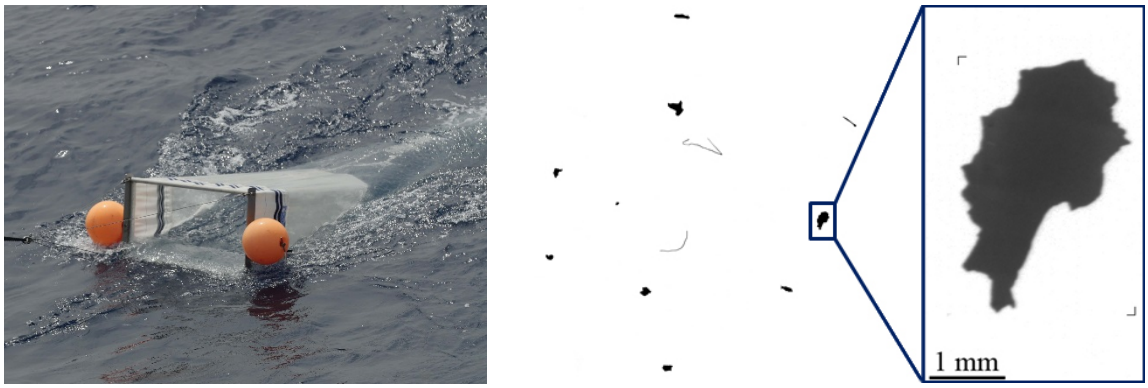

Figure 1: Picture of the Manta net used for microplastic sampling (left) and an example of a ZooScan image displaying different types of microplastics (right) with a zoom of one particle.

Water samples (Solid Phase Extraction)

Water samples were collected using a stainless-steel collector and poured into pre-combusted 1 L glass bottles (marine samples) or collected directly using the pre-combusted 1 L glass bottles (Rhône River). They were filtered through a glass fiber filter (GF/F, 0.7 µm) within three hours after collection and were either stored at 4 °C in the dark and extracted within 24 h or otherwise stored at -25 °C in the dark when immediate extraction was not possible. A schematic representation of the extraction process is given in Figure 2. Briefly, labeled surrogate standards were added (100 ng sample^{-1} of d_{27}-tri-n-butyl phosphate -d_{27}-TBP-, d_{18}-tris (2-chloroisopropyl) phosphate -d_{18}-TCPP-, d_{15}-tris (1,3-dichloro-2-propyl) phosphate -d_{15}-TDCP- and d_4-di-n-butyl phthalate -d_4-DnBP- and 20 ng sample^{-1} of 4-n-octylphenol-d_{17} -4nOP-d_{17}-) and the water was passed through pre-combusted and pre-cleaned glass cartridges containing 250 mg SPE sorbent (Oasis hydrophilic lipophilic balance HLB, Waters, Guyancourt, France) *via* polytetrafluoroethylene (PTFE) liners. Next, the cartridges were vacuum-dried for 2-3 hours to complete dryness. Molecules of interest were then sequentially eluted using a solvent polarity gradient resulting in two different fractions by using 5 mL of n-hexane followed by 5 mL of n-hexane/dichloromethane 50:50 (v/v) for PAEs and OPEs (F_a fraction) and 5 mL of ethyl acetate followed by 5 mL of methanol for BPs and PFAS (F_b fraction). The extracts were then evaporated using pure N_2 gas until a volume of approximately 1 mL was transferred into 2-mL conical glass vials. The extracts were further concentrated through gentle N_2 flux to (F_a) a final volume of approximately 100 µL or (F_b) dryness in which case the extract was then reconstituted with 990 µL of methanol.

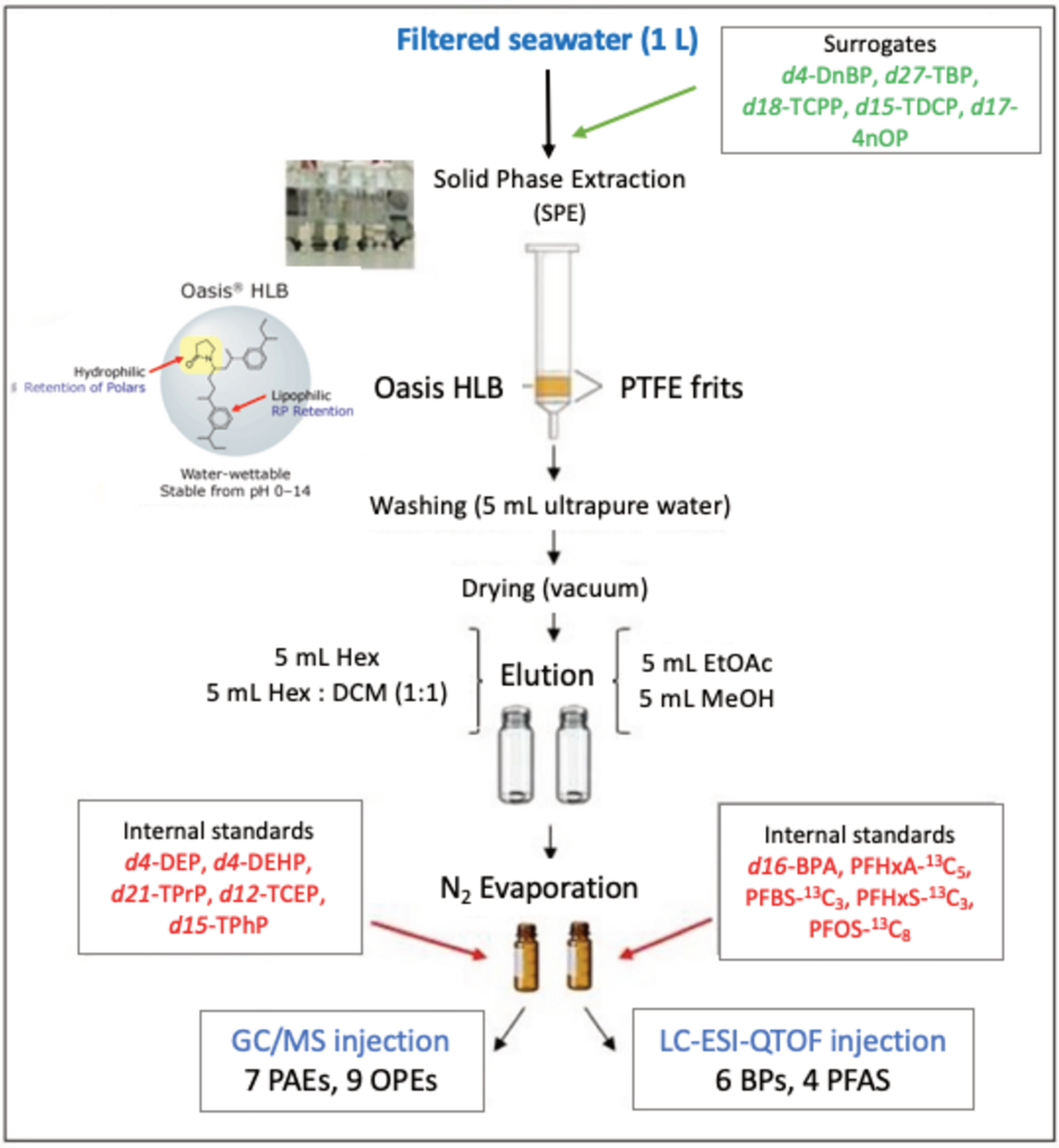

Figure 2: Schematic representation of the processing of water samples. Solid Phase Extraction (SPE) is used to extract target compounds.

Sediment and zooplankton samples (ultrasound extraction)

Sediments were sampled using a Van Veen grab. Approximately the upper 5 cm of the retrieved sediment were collected and put into pre-combusted (450 °C, 6 h) glass tubes. Once

in the laboratory, the sediments were stored in the freezer (-20 °C) and afterwards lyophilized. Next, they were sieved to a size class ≤ 500 µm using a metal sieve and debris was removed.

Zooplankton samples were collected using a Manta net (opening area 0.40 × 0.70 m, mesh size 150 µm), which was towed horizontally at a speed of 2-3 knots for 20 minutes. The samples were poured into glass bottles and kept under cool and dark conditions until reaching the laboratory. They were left for 24 h to enable the zooplankton to defecate, in order to avoid a falsification of the chemical analysis. Next, three size classes were established using metal sieves: 150-500 µm, 500-1000 µm and > 1000 µm. The samples were thoroughly rinsed using ultrapure water. Next, microplastics were sorted out using a dissecting microscope and tweezers. Other debris (e.g., plant debris) was also removed from the samples and a rough taxonomical identification was made. The plankton samples were then frozen (-20 °C), lyophilized and ground using an agate mortar and pestle.

3 g (dry weight) of sediments and 100 mg (dry weight) of zooplankton samples were used for the respective extraction of OPEs and PAEs. They were filled into glass tubes, spiked with surrogate standards (100 ng sample^{-1} of d_{27}-TBP, d_{18}-TCPP, d_{15}-TDCP and d_4-DnBP), vortexed and left to equilibrate for about 30 min. To sediment samples a spatula of activated copper was then added, while for zooplankton samples the activated copper was added to the final extract. Next, 5 mL of hexane were added and an ultrasound extraction (Elmasonic X-tra TT 120 H) was performed during 15 min without heating. Afterwards, the extract was collected with a Pasteur pipette and filled into glass cartridges containing 250 mg of Oasis MAX sorbent (Waters, Guyancourt, France), which were previously cleaned three times by a sequence of solvents (3 × 5 mL each of acetone, ethyl acetate and dichloromethane). The Oasis MAX sorbent was hereby used as a clean-up to reduce matrix effects that could interfere with the GC/MS analysis. The processed extracts were collected in glass tubes. The extraction and following procedure were repeated one more time with 5 mL of hexane and two more times

with 5 mL hexane/dichloromethane (50/50, v/v). The volume of the extracts was then reduced using subsequent N_2 evaporation until a final volume of approximately 100 µL (Figure 3).

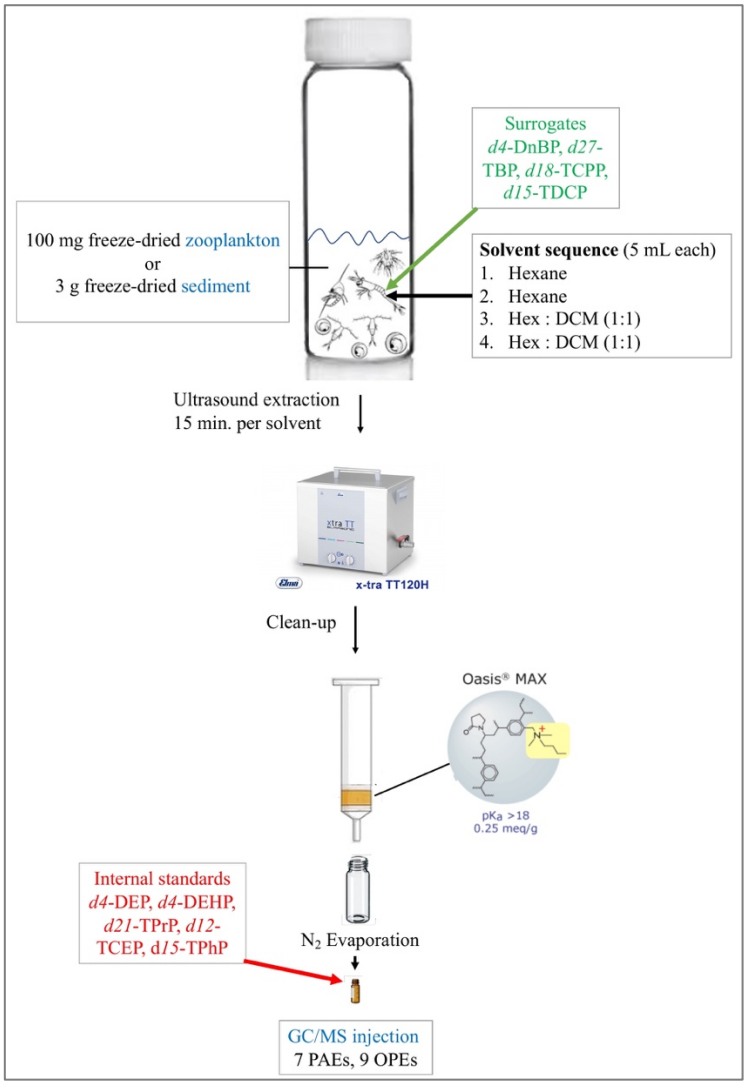

Figure 3: Schematic representation of the processing of zooplankton and sediment samples. Ultrasound extraction is used to extract target compounds.

GC/MS and LC-HRMS analysis

Internal standards for quantification were added to water (F_a fraction), sediment and zooplankton samples as follows: 100 ng sample^{-1} of d_4-diethyl phthalate (d_4-DEP), d_4-

diethylhexyl phthalate (d_4-DEHP), d_{21}-tri-n-propyl phosphate (d_{21}-TPrP), d_{12}-tris (2-chloroethyl) phosphate (d_{12}-TCEP) and d_{15}-triphenyl phosphate (d_{15}-TPhP). These samples were injected into a gas chromatograph coupled with a mass spectrometry detector (GC-MS, Agilent 7820A Series GC – Agilent 5977E MS) operating in selected ion monitoring (SIM) and electron impact (EI, 70 eV) modes, for the quantification of OPEs and PAEs. The separation was achieved in a 30 m × 0.25 mm i.d. × 0.25 μm HP-5MS capillary column (Agilent J&W). All target contaminants were quantified by the internal standard (IS) procedure. The injection volume was of 2 μL and the helium carrier gas flow was 1 mL min^{-1}. The temperatures of the MS transfer line and the ion source and the quadrupole were set at 300, 230 and 150 ºC, respectively. The following conditions were applied: injector temperature: 270 ºC (splitless) and the oven was programmed from 90 ºC to 132 ºC at 3 ºC min^{-1}, to 166 ºC at 10 ºC min^{-1}, to 175 at 1 ºC min^{-1} (holding time 2 min), to 232 ºC at 2 ºC min^{-1}, and then to 300 °C at 25 ºC min^{-1} (holding time 5 min).

To water samples (F_b fraction) 20 ng $sample^{-1}$ of d_{16}-bisphenol A (d_{16}-BPA), perfluorohexanoic acid-$^{13}C_5$ (PFHA-$^{13}C_5$), perfluoro butanesulfonate-$^{13}C_3$ (PFBS-$^{13}C_3$), perfluorohexane sulfonic acid-$^{13}C_3$ (PFHS-$^{13}C_3$) and perfluorooctane sulfonate-$^{13}C_8$ (PFOS-$^{13}C_8$) were added as internal standards. 10 μL of the extract were injected for the quantification of BPs and PFAS using LC-electrospray ionization quadrupole time of flight mass spectrometry (LC-ESI-QTOF, Agilent 1290 Infinity LC system coupled with Agilent 6530 Accurate-Mass Q-TOF, Agilent Technologies, Les Ulis, France). The syringe was washed externally with MeOH for 20 seconds before injection to avoid contamination of injection port or following samples. Separation was achieved on an Agilent Zorbax Eclipse XDB reversed phase column (50 mm × 2.1 mm, 1.8 μm), with temperature set at 30 °C. Elution was performed with ultrapure water (A) and MeOH (B) under gradient conditions: 0 min 95:5 A/B, 1 min 95:5 A/B, 10 min 0:100 A/B, 15 min 0:100 A/B, 15.1 min 95:5 A/B, 20 min 95:5 A/B. ESI interface was operated in negative mode

(3.5 kV capillary voltage), and MS TOF mass acquisition was performed in the range 50-600 m/z at a rate of 1 spectrum s^{-1}. ESI parameters were set as follows: 300 °C gas temperature, 11 L min^{-1} drying gas, 40 psig nebulizer, 350 °C sheath gas temperature, 11 L min^{-1} sheath gas flow. TOF parameters were: 1500 V nozzle voltage, 175 V fragmentor voltage, 65 V skimmer voltage, 750 V octopole voltage. Ion chromatogram extraction was performed with 10 ppm mass tolerance, based on exact monoisotopic mass and retention time.

Recovery rates & blanks

To obtain method recovery rates, spike experiments using native and surrogate compounds were performed. For water samples, samples (n=5) were spiked at a concentration level of 150 ng L^{-1} and recovery rates varied between 61-131% (OPEs; mean 101%), 52-89% (PAEs; mean 77%), 79-118% (BPs; mean 95%) and 73-124% (PAFS; mean 91%) (Figure 4). Real samples were systematically spiked with surrogate compounds (see description of extraction procedure) to monitor recovery rates of individual samples. Results were not recovery-corrected.

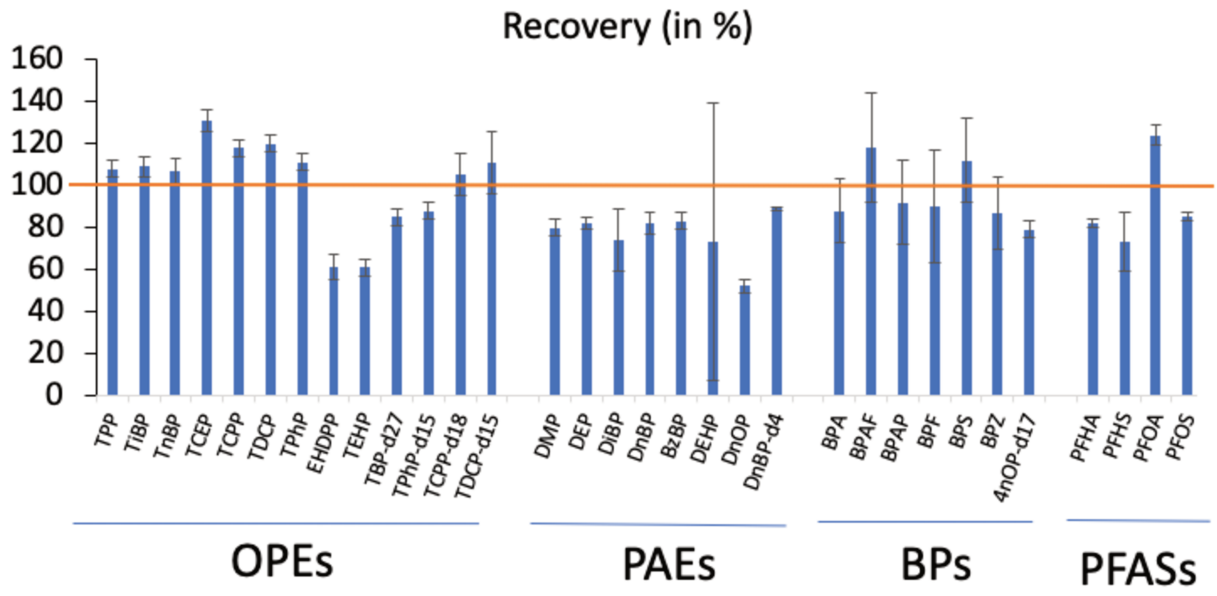

Figure 4: Graph showing the recovery rates of individual OPEs, PAEs, BPs and PFAS in water samples. The orange line indicates the 100% recovery mark. Error bars represent standard deviations.

Sediment (n=3) and zooplankton (n=3) samples were spiked with native and surrogate PAEs and OPEs at 50 ng sample^{-1} to obtain method recovery rates. Recovery rates varied between 72-103% (PAEs) and 46-104% (OPEs) for sediments, while they ranged from 58-97% (PAEs) and from 42-89% (OPEs) for zooplankton samples (Figure 5). Real samples were systematically spiked with surrogate compounds (see description of extraction procedure) to monitor recovery rates of individual samples. Results were not recovery-corrected.

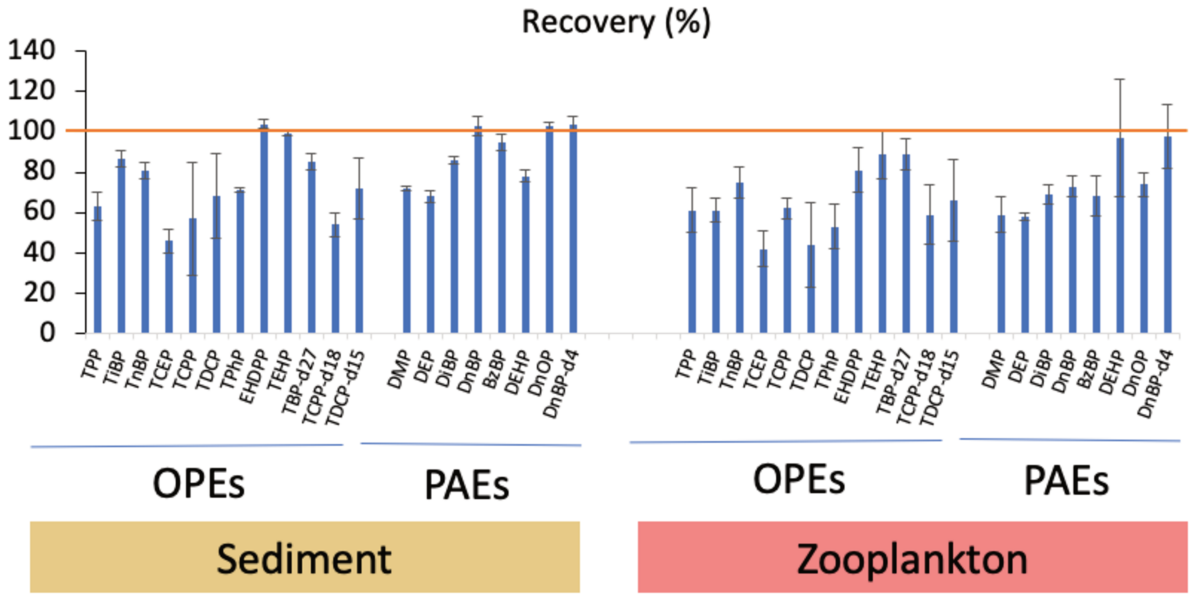

Figure 5: Graph showing the recovery rates of individual OPEs, PAEs, BPs and PFAS in sediment and zooplankton samples. The orange line indicates the 100% recovery mark. Error bars represent standard deviations.

For each extraction batch (usually containing 6-10 water, sediment or zooplankton samples) two extraction blanks were made in order to check for possible contamination. DEHP and TCPP were the compounds most prone to contamination, while BPs and PFAS were rarely detected in blanks. To reduce the effect of different blank values between batches, results were blank-corrected by using the blank values obtained during the same extraction as the corresponding sample batch. Average blank values or ranges are indicated in the Material & Methods section of each chapter, moreover tables with blank details are given in Annex IV, Table S3 (page 253; blanks made during water, sediment and zooplankton extraction) and Annex V, Table S5 (page 277; transport, laboratory and extraction blanks obtained for water samples).

CHAPTER I: Microplastics

Progress in Oceanography 163 (2018) 214–220

Contents lists available at ScienceDirect

Progress in Oceanography

journal homepage: www.elsevier.com/locate/pocean

Occurrence of microplastics in surface waters of the Gulf of Lion (NW Mediterranean Sea)

Natascha Schmidt[a], Delphine Thibault[a,b], François Galgani[c], Andrea Paluselli[a], Richard Sempéré[a,*]

[a] Aix Marseille Univ., Université de Toulon, CNRS, IRD, MIO, Marseille, France
[b] MARBEC, IRD, LMI ICEMASA, Cape Town, South Africa
[c] IFREMER, LER/PAC, 20600 Bastia, France

ARTICLE INFO

Keywords:
Marine litter
Microplastic
Mediterranean Sea
Gulf of Lion
Marseille Bay

ABSTRACT

Between 2014 and 2016 a total of 43 microplastic samples were collected at six sampling stations in the eastern section of the Gulf of Lion (located in the northwestern Mediterranean Sea), as well as upstream of the Rhône River. Microplastics were found in every sample with highly variable concentrations and masses. Concentrations ranged from $6 \cdot 10^3$ items km^{-2} to $1 \cdot 10^6$ items km^{-2} (with an average of $112 \cdot 10^3$ items km^{-2}), and mass ranged from 0.30 g km^{-2} to 1018 g km^{-2} DW (mean 61.92 ± 178.03 g km^{-2}). The samples with the highest and lowest microplastic count originate both from the Bay of Marseille. For the Bay of Marseille, it is estimated that the total microplastic load consist of $519 \cdot 10^3$ –$101 \cdot 10^6$ items weighing 0.07–118 kg. Estimations for daily microplastic transport by the Northern Current and the Rhône River, two important hydrologic features of the northwestern Mediterranean Sea, range from 0.18 to 86.46 t and from 0.20 to 21.32 kg, respectively. Particles < 1 mm^2 clearly dominated sampling stations in the Northern Current, the Rhône River and its plume (52, 53 and 61%, respectively), suggesting a long exposure time in the environment. Items between 1 mm^2 and 5 mm^2 in size were the most abundant microplastics in Marseille Bay (55%), which suggests coastal pollution sources or the removal of smaller particles from surface waters e.g. by ballasting owing to the presence of epibionts.

1. Introduction

Plastic and its chemical compounds have played an important role in the Anthropocene and might threaten human health (Kobrosly et al., 2014; Tranfo et al., 2012; Sathyanarayana 2008; Heudorf et al., 2007) and both terrestrial (Zhao et al., 2016; Lwanga et al., 2016; Oehlmann et al., 2009) and marine environments (Przybylinska and Wyszkowski, 2016; Van Franeker and Law, 2015; Sigler, 2014). In 2014, 311 million tons of plastic were produced worldwide, 15% of which were consumed in Europe (PlasticsEurope, 2015). The degradation of large plastic items into microplastics (≤5 mm) in the ocean is a slow and heterogeneous process, varying with respect to the quality, shape and size of the plastic. This process is driven by mechanical forcing (e.g., waves), salt water, and UV radiation (Ter Halle et al., 2016). Because of its small size, micro debris can easily be ingested (e.g., Desforges et al., 2015; Neves et al., 2015). Approximately $270 \cdot 10^3$ tons of plastic are suspected to float in the world's oceans (Eriksen et al., 2014). Estimates for floating microplastic loads range from $7 \cdot 10^3$ to $35 \cdot 10^3$ tons for global open-ocean surface waters (Cózar et al., 2014) or from $93 \cdot 10^3$ to $236 \cdot 10^3$ tons depending on the model used (Van Sebille et al., 2015). Plastic accounts for 60 to 80% of all marine litter, followed in quantity by glass and metal (UNEP, 2009). About $370 \cdot 10^9$ plastic particles or 1455 tons have been estimated to be floating on the surface of the Mediterranean Sea (Ruiz-Orejón et al., 2016). Other estimates range from 756 to 2969 tons (Cózar et al., 2015) and from 874 to 2576 tons (Suaria et al., 2016).

The Mediterranean Sea is a semi-enclosed basin subject to significant anthropogenic pressures (e.g., The MerMex group, 2011; Blanfuné et al., 2016; Hassoun et al., 2015; Casale et al., 2015). Marine debris, including microplastics, are a particularly important concern in this region (Deudero and Alomar, 2015; Cózar et al., 2015; Ioakeimidis et al., 2014; Faure et al., 2015; Pedrotti et al., 2016). Concerns about marine litter in the Mediterranean Sea were first expressed in 1976 when the Barcelona Convention was signed with the goal of preventing and abating marine and coastal pollution (UNEP, 2009). In subsequent years, studies have been undertaken to better understand pollution

* Corresponding author.
E-mail addresses: natascha.schmidt@mio.osupytheas.fr (N. Schmidt), delphine.thibault@ird.fr (D. Thibault), francois.galgani@ifremer.fr (F. Galgani), andrea.paluselli@mio.osupytheas.fr (A. Paluselli), richard.sempere@mio.osupytheas.fr (R. Sempéré).

https://doi.org/10.1016/j.pocean.2017.11.010

Available online 22 November 2017
0079-6611/ © 2017 Elsevier Ltd. All rights reserved.

Occurrence of microplastics in surface waters of the Gulf of Lion (NW Mediterranean Sea)

Natascha Schmidt [a], Delphine Thibault [a,b], François Galgani [c], Andrea Paluselli [a], Richard Sempéré [a, *]

[a] Aix Marseille Univ., Université de Toulon, CNRS, IRD, MIO, Marseille, France

[b] MARBEC, IRD, LMI ICEMASA, Cape Town, South Africa

[c] IFREMER, LER/PAC, 20600, Bastia, France

[*] Corresponding author

E-mail addresses: natascha.schmidt@mio.osupytheas.fr (N. Schmidt), delphine.thibault@ird.fr (D. Thibault), francois.galgani@ifremer.fr (F. Galgani), andrea.paluselli@mio.osupytheas.fr (A. Paluselli), richard.sempere@mio.osupytheas.fr (R. Sempéré).

Keywords: Marine litter, microplastic, Mediterranean Sea, Gulf of Lion, Marseille Bay

Abstract

Between 2014 and 2016 a total of 43 microplastic samples were collected at six sampling stations in the eastern section of the Gulf of Lion (located in the northwestern Mediterranean Sea), as well as upstream of the Rhône River. Microplastics were found in every sample with highly variable concentrations and masses. Concentrations ranged from 6 10^3 items km^{-2} to 1 10^6 items km^{-2} (with an average of 112 10^3 items km^{-2}), and mass ranged from 0.30 g km^{-2} to 1018 g km^{-2} DW (mean 61.92 ± 178.03 g km^{-2}). The samples with the highest and lowest microplastic count originate both from the Bay of Marseille. For the Bay of Marseille, it is estimated that the total microplastic load consist of 519 10^3 - 101 10^6 items weighing 0.07 - 118 kg. Estimations for daily microplastic transport by the Northern Current and the Rhône River, two important hydrologic features of the northwestern Mediterranean Sea, range from 0.18 to 86.46 t and from 0.20 to 21.32 kg, respectively. Particles < 1 mm^2 clearly dominated sampling stations in the Northern Current, the Rhône River and its plume (52, 53 and 61 %, respectively), suggesting a long exposure time in the environment. Items between 1 mm^2 and 5 mm^2 in size were the most abundant microplastics in Marseille Bay (55 %), which suggests coastal pollution sources or the removal of smaller particles from surface waters e.g. by ballasting owing to the presence of epibionts.

1. **Introduction**

Plastic and its chemical compounds have played an important role in the Anthropocene and might threaten human health (Kobrosly et al., 2014; Tranfo et al., 2012; Sathyanarayana 2008; Heudorf et al., 2007) and both terrestrial (Zhao et al., 2016; Lwanga et al., 2016; Oehlmann et al., 2009) and marine environments (Przybylinska & Wyszkowski, 2016; Van Franeker & Law, 2015; Sigler, 2014). In 2014, 311 million tons of plastic were produced worldwide, 15 % of which were consumed in Europe (PlasticsEurope, 2015). The degradation of large plastic items into microplastics (≤ 5 mm) in the ocean is a slow and heterogeneous process, varying with respect to the quality, shape and size of the plastic. This process is driven by mechanical forcing (e.g., waves), salt water, and UV radiation (Ter Halle et al., 2016). Because of its small size, micro debris can easily be ingested (e.g., Desforges et al., 2015; Neves et al., 2015). Approximately 270 10^3 tons of plastic are suspected to float in the world's oceans (Eriksen et al., 2014). Estimates for floating microplastic loads range from 7 10^3 to 35 10^3 tons for global open-ocean surface waters (Cózar et al., 2014) or from 93 10^3 to 236 10^3 tons depending on the model used (Van Sebille et al., 2015). Plastic accounts for 60 to 80 % of all marine litter, followed in quantity by glass and metal (UNEP, 2009). About 370 10^9 plastic particles or 1,455 tons have been estimated to be floating on the surface of the Mediterranean Sea (Ruiz-Orejón et al., 2016). Other estimates range from 756 to 2,969 tons (Cózar et al., 2015) and from 874 to 2,576 tons (Suaria et al., 2016).

The Mediterranean Sea is a semi-enclosed basin subject to significant anthropogenic pressures (e.g., The MerMex group, 2011; Blanfuné et al., 2016; Hassoun et al., 2015; Casale et al., 2015). Marine debris, including microplastics, are a particularly important concern in this region (Deudero & Alomar, 2015; Cózar et al., 2015; Ioakeimidis et al., 2014; Faure et al., 2015; Pedrotti et al., 2016). Concerns about marine litter in the Mediterranean Sea were first

expressed in 1976 when the Barcelona Convention was signed with the goal of preventing and abating marine and coastal pollution (UNEP, 2009). In subsequent years, studies have been undertaken to better understand pollution sources and trajectories, through approaches as modeling the transport of floating marine debris (Mansui et al., 2014). However, knowledges on the spatial and temporal microplastic distribution remain limited (Ruiz-Orejón et al., 2016; Suaria et al., 2016; Cózar et al., 2015). Their contents are highly variable, although the sea surface circulation seems to be the main driver on the distribution of floating marine litter whatever their sizes. Currents affect time-dependent movements that remain difficult to predict, and cause several non-trivial Lagrangian mechanisms (Zambianchi et al., 2014). In semi-enclosed seas, such as the Mediterranean Sea, aggregation patterns are not permanent and high variability is observed at a small scale (Suaria et al., 2016). Wind-induced effects on floating material and Stokes drift velocities require further investigation, such as refinement of regional models. Nevertheless, some available scenarios could be hypothesized with possible retention areas in the northwestern Mediterranean and the Tyrrhenian sub-basins (Poullain et al., 2012; Mansui et al., 2014). The Gulf of Lion is in the northwestern sector of the Mediterranean Sea, and its hydrodynamics are influenced by shallow water depths of the shelf, wind regimes (Mistral and Marin), the Northern Current (NC), and freshwater inputs from the Rhône River (Gatti et al., 2006; Fraysse et al., 2014). The NC has a high seasonal variability: while a decrease in intensity is observed in summer, it becomes faster, deeper and narrower in winter (Millot, 1991). Intrusion of the NC onto the shelf of the Gulf of Lion has been observed (Ross et al., 2016; Barrier et al., 2016 and references therein). This productive shelf is also highly exploited for commercial fishing (Bănaru et al., 2013) and the coastal area is strongly influenced by tourism activities. Given this areas great economic, touristic and environmental significance, monitoring threats, such as pollution sources, is essential. Therefore, the primary goal of this study was to provide insight into the temporal and spatial distribution of microplastics in the

eastern sector of the Gulf of Lion. Furthermore, we wanted to examine relationships between microplastic size distributions and possible pollution sources and transportation routes.

2. Materials and Methods

Following the framework of the Particule-MERMEX and PLASTOX projects, microplastic debris were collected at different times between February 2014 and April 2016 (Table S1) in three distinct areas with specific hydrodynamic characteristics (Figure 1) within the eastern sector of the Gulf of Lion (northwestern Mediterranean Sea). The first area is located 40 km offshore at the eastern part (station #1, also called 'Antares site') and is within the direct influence of the Northern Current, which runs east to west along the shelf break over 2,475 m of water (Martini et al., 2016). The second area includes the Bay of Marseille (stations #2, 3 and 4), which is significantly influenced by a population of approximately 1 million inhabitants and by the daily volume of about 250 10^3 m^3 of waste waters released from the Marseille-Cortiou wastewater treatment plant (WWTP) (Savriama et al., 2015; Tedetti et al., 2012). To the west, the third study area is the downstream part of the Rhône River (station #6, Arles, 48 km from the river mouth) and within the dilution plume (station #5, about 2.5 km from the mouth) (Sempéré et al., 2000). Sampling dates, GPS coordinates, microplastic concentration, mean wind speed and wind direction are provided in the supplementary data (Table S1) along with information on precipitation. Surface current speeds and directions were extracted from the Mars 3D model (http://marc.ifremer.fr).

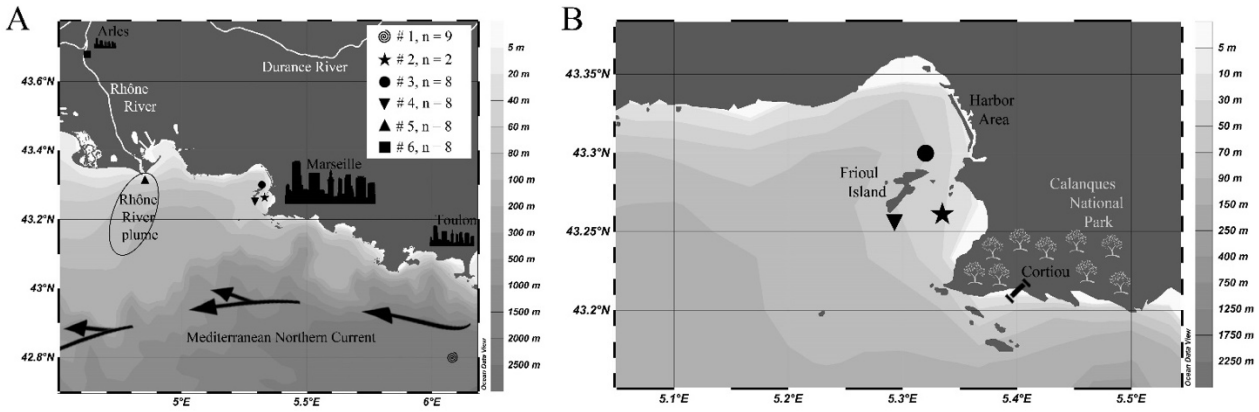

Fig. 1: The sampling stations situated in the eastern Gulf of Lion (A) including Antares site (station 1), Marseille Bay site (stations 2-4) and Rhône River site (stations 5-6). The Rhône River plume as observed during north/northwest wind conditions and the Northern Current (NC) are also indicated. Zoom of the Bay of Marseille (B) with the local WWTP (Cortiou). Map modified after Schlitzer, R., 2009.

Microplastic samples were collected using a Manta net (0.50 m x 0.15 m opening) mounted with a 780 µm mesh size and towed horizontally at the surface. Ten samples from March and April 2016 were collected (in Marseille at stations 3 and 4) with a 330 µm mesh size (Suppl. Table 1). Sampling was only conducted under low swell conditions (< 1 m). The net was towed for 20 minutes at an average speed of 2.5 knots approximately 50 m behind the research vessel. It was towed at a slight angle to avoid disturbances caused by the boat's wake. Samples from the Rhône River (station #6) were collected from a fixed location on the dock of the river. Sampled superficies at this station were calculated by comparing the flow rate during sampling with reference flow rates and river speeds. Lower-limit river speeds were used for estimates, since river speeds tend to be slower near the dock.

The net was carefully rinsed and the content of the cod-end was poured into a 1 L glass bottle, preserved with a buffered seawater formalin solution (final concentration 5 %), and kept

in cold and dark conditions until further analysis. Samples were then sieved (mesh size 125 µm), and rinsed with ultrapure water (ISO 3696). Plastic debris were picked out with tweezers under a dissecting microscope. Fibers were not taken into account due to the high risk of contamination. No Fourier Transform Infrared Spectroscopy (FTIR) Analysis was performed to verify the nature of the items, so despite all efforts to maximize result reliability, it cannot be excluded that some non-plastic items were estimated to be microplastics.

The number, size and shape of each item was identified using a ZooScan© (HYDROPTIC SARL). Each item was placed on the screen of the ZooScan without any water. Surface area measurements in pixels were obtained using the ImageJ software and then converted into mm^2 and the Equivalent Spherical Diameter (ESD). Plastic items ≤ 5 mm were considered. All microplastics from each sample were then weighed (Mettler AE 240, reliability ± 0.1 mg). Microplastic abundance (items km^{-2}) and dry weight (g km^{-2}) were calculated for each sample using the towing distance and the net opening surface. Analysis of variance (one-way and two-way ANOVA) with a 0.05 level of significance was performed to assess whether the microplastic abundance and size distribution varied with space (stations) and time. The Tukey test was used whenever significant differences were detected. All statistical analyses were performed using R version 3.3.2.

3. Results and Discussion

3.1. Microplastic abundance

Microplastic abundance ranged from 6 10^3 to 1 10^6 (mean 96 10^3) items km^{-2} in the Marseille Bay area, from 33 10^3 to 400 10^3 (mean 113 10^3) items km^{-2} in the Rhône River plume, from 7 10^3 to 69 10^3 (mean 34 10^3) items km^{-2} in the river itself and from 9 10^3 to 916 10^3 (mean 212 10^3) items km^{-2} off-shore (Fig. 2, top). The highest microplastic concentration (1 10^6 items km^{-2}) was observed at station #2 (Marseille Bay area). The day this sample was collected was characterized by calm conditions with no noteworthy surface currents near the station. In contrast, the other two stations on the coast of Marseille, stations #3 and #4, showed very low particle concentrations (averages 20 10^3 and 10 10^3 items km^{-2}, respectively). While a comparison between these both stations and the station #2 is difficult, because the samples were collected in different years (2016 *vs*. 2014), some assumptions can still be considered. Goldstein et al. (2013) reported that a high spatial heterogeneity for microplastic concentrations could be found not only at a large scale but also on a smaller scale for samples taken at distances of 10 km from one another. Heterogeneous spatial debris distribution can be the result of currents, wave- and wind-driven turbulences, river inputs or hydrodynamic features such as upwelling, downwelling, gyres or fronts (e.g., Kukulka et al., 2012; Suaria and Aliani, 2014; Collignon et al., 2012). More generally, high concentrations of microplastics, especially small fragments, are found in coastal waters because of the proximity of densely populated areas, (Pedrotti et al., 2016) and continental inputs from the atmosphere or rivers (Collignon et al., 2012). Point pollutions could also play an important role in the Bay of Marseille, where the fierce northwestern Mistral wind can transport litter from city streets into coastal waters. Another possible source of microplastics in the Bay of Marseille is the local sewage facility (Cortiou) where treated wastewater enters the sea in the southeastern part of the city. On March

17, 2016 a slight surface current coming from Cortiou at a speed of approximately 0.5 m s^{-1} entered the area of stations #3 and 4. The microplastic concentrations observed that day were the highest ever found at station #4 (15 10^3 items km^{-2}) and the second highest for station #3 (27 10^3 items km^{-2}). Interestingly, microplastic abundance was always higher at station #3 compared to station #4, in spite of their geographical proximity ($p < 0.05$).

Our median concentration (31 10^3 items km^{-2}) was about one third of the mean value, highlighting potential surges in microplastic presence, possibly linked to climatic and hydrodynamic events. Hydrodynamic processes influencing microplastic distribution are e.g. vertical mixing or eddies and anticyclonic gyres. The latter of which are unsteady formations in the Mediterranean Sea (Pedrotti et al., 2016), but could lead to punctual increases in regional microplastic abundances. Additionally, in our study area, there is the Northern Current, which varies greatly in intensity, depth, and position (Millot, 1991). Data collected at station #1 showed temporal variability, with concentrations of microplastics being significantly higher on March 10, 2014 ($p < 0.05$) when the Northern Current was fast and narrow with maximum speeds of approximately 0.9 m s^{-1}. However, triplicated trawls exhibited a range of microplastic abundances from 103 10^3 to 916 10^3 items km^{-2} at this sampling date, implying that a nine fold difference in abundances can be observed in the same sampling area within two hours. This further highlights the strong temporal variability observed for microplastic concentrations. Overall no seasonal differences were detected ($p > 0.05$), but the low number of observations limits the strength of any comparison. Goldstein et al. (2013) observed seasonal heterogeneity at much larger scale in the northeastern Pacific Ocean between summer 2009 and fall 2010.

Floating debris transported by the NC could be transported to the Balearic Islands, where models calculated high beaching probabilities (Mansui et al., 2014), or to the seafloor which is known to be a (micro-) plastic sink (Claessens et al., 2011; Ioakeimidis et al., 2014; Woodall et al., 2014). Reasons of microplastic sedimentation can be the nature of the plastic material, (if

its density is higher than the one of seawater, Tekman et al., 2017), the biofouling accumulation on microplastic surfaces (Woodall et al., 2014), the incorporation of free microplastics into marine aggregates or the incorporation of microplastics into fast-sinking faecal pellets after ingestion by zooplanktons and fishes (Cole et al., 2013).

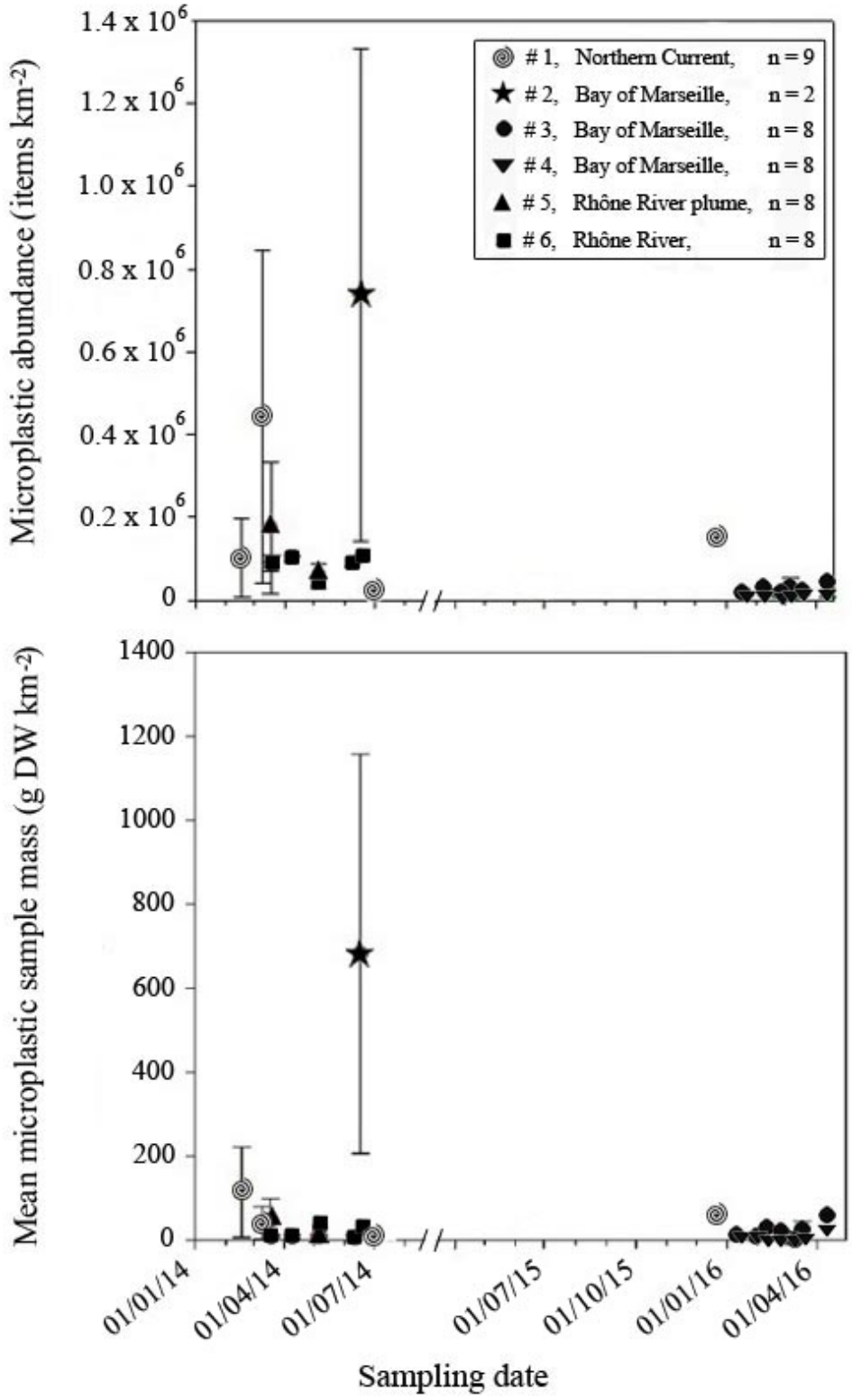

Fig. 2: Microplastic abundance (top; particles km^{-2}) and weight (bottom; g dry weight km^{-2}) for the six stations studied at the three sites. For samples collected the same day at the same station, points represent the averaged values and error bars the standard deviation. n = overall number

of samples taken at this station. *Note: the weight of one sample collected on 10/03/14 was not available and the data point hence only represents the weight of the two other samples collected this day at station #1.*

The overall average microplastic abundance for our samples was 112 10^3 items km^{-2}, which is in the same range as other areas in the northwestern basin, where mean densities have been estimated to 115 10^3 items km^{-2} (Collignon et al., 2012), 130 10^3 items km^{-2} (Faure et al., 2015) and 150 10^3 items km^{-2} (De Lucia et al., 2014). Higher amounts were measured for the entire Mediterranean basin (243 10^3 items km^{-2}, Cózar et al., 2015), due to high concentrations in some Mediterranean areas. Densely populated areas as the semi-enclosed Adriatic Sea and the Levantine Basin were characterized by high densities of 1,050 10^3 (max: 4,600 10^3; Suaria et al., 2015) and 1,518 10^3 (max: 65 10^6; Van der Hal, 2017) items km^{-2}, respectively. Our results are consistent with previous studies and indicate that the northwestern Mediterranean Sea contains similar mean microplastic concentrations as the Atlantic and Pacific Oceans (mean: 134 10^3 items km^{-2} and 124 10^3 items km^{-2}, respectively, Eriksen et al., 2014). Hereby it needs to be considered that the Atlantic and Pacific Oceans are also known to be highly heterogeneous, with microplastic accumulation and non-accumulation zones. Examples for a heavily contaminated area are the East Asian Seas, where a mean microplastic abundance of 1,720 10^3 items km^{-2} was measured (Isobe et al., 2015).

Microplastic abundances in the Rhône River at Arles (station #6; 34 10^3 ± 19 10^3 items km^{-2}; net size 0.50 m x 0.15 m, mesh size 780 µm) were relatively low, but were similar to values reported by De Alencastro (2014) upstream at Chancy (~ 52 10^3 items km^{-2}; net size 0.60 m x 0.18 m, mesh size 300 µm). In comparison, a mean microplastic abundance of 893 10^3 items km^{-2} was found in the Rhine River, a watercourse flowing through highly industrialized areas, such as North-Rhine Westphalia (Germany), where many plastic factories

are located (Mani et al., 2015). Concentrations observed in the Rhône River plume (station #5, up to 400 10^3 items km^{-2}) were higher than in the river itself, suggesting that the Rhône River – sea interface may generate a temporal accumulation zone for debris. In general, however, the area covered by our six sampling stations is not considered to be a retention area, but can better be described as a "transit area". The size of the Mediterranean basin reduces the potential for formation of permanent gyres as in the Atlantic, Pacific and Indian Oceans, where plastic often concentrates (Cózar et al., 2015).

At the river mouth, microplastic concentrations were either significantly greater ($p < 0.05$) or similar to those observed upstream in the Rhône River. Concerning the river plume, we should highlight the similitude in zooplankton composition of two samples collected with the same Manta trawl, first, on the 10/03/14 at the station #1 (NC) and then (18/03/14), at the Rhône River Plume station (station #5). High abundances (> 1,000 individuals per sample) of *Velella velella*, a free-floating hydrozoan, were observed at both dates (Thibault D. pers. com.), implying a potential intrusion of water masses from the NC onto the shelf. Such intrusions have already been observed before (Barrier et al., 2016). Salinity data from the Mars 3D model support the hypothesis: while the Rhône River plume was extended in all directions on 10/03/14 and the following days, saltier surface waters pushed from the eastern direction into the area from 16/03/14 on and thus, reduced the extension area of the river plume. During the period examined, the velocity of the NC flowing through station #1 was about 0.4 m s^{-1} (Suppl. Table 1), but currents leaving the main branch in northwestern directions flowed at reduced speeds of about 0.2 m s^{-1}. At this speed range (0.2-0.4 m s^{-1}), water masses could have travelled about 140-275 km in eight days, which is consistent with the straight line distance (120 km) between both stations. However, we would like to point out that these are only indications, since an accurate model would be needed to simulate the exact trajectory of the water masses and microplastics in question.

3.2. Microplastic weight

Microplastic dry weight showed a similar variability, ranging from 0.30 g DW km^{-2} to 1018 g DW km^{-2}, with the maximum observed in Marseille Bay (Fig. 2, bottom). An average of 61.92 g DW km^{-2} (± 178.03 g DW km^{-2}) was found in the study area. This value is similar to averages of 60 and 63 g DW km^{-2} reported for the western part of the northwestern Mediterranean Sea (Collignon et al., 2012) and the upstream part of the Rhône River (De Alencastro, 2014), respectively.

An estimated surface area of 87 km^2 of the Bay of Marseille would provide a total microplastic load of 0.07 to 118 kg (mean 9.94 kg), representing a range of concentrations from 0.5 10^6 to 101 10^6 (mean 8 10^6) microplastic pieces in surface waters. For the Rhône River, the flow rate used for calculations varied between 1,150 m^3 s^{-1} and 1,600 m^3 s^{-1} during the sampling period. Using minimum and maximum concentration and weight values, we calculated a daily microplastic spill of 0.20 – 21.32 kg (dry weight), representing 10 10^6 - 40 10^6 items discharged by the Rhône River into the Mediterranean Sea. Similarly, microplastic loads for the Northern Current were calculated using volumetric transport rates of 0.7 Sv (Conan and Millot, 1995) and 2 Sv (Petrenko, 2003) and the minimum and maximum concentration and weight values. This method provided an estimate of daily transport ranging from 0.18 to 86.46 tons (dry weight) of microplastic, representing 4 10^9 to 1 10^{12} items. These calculations give minimum ranges, since they are based on the assumption that microplastics concentrate within 15 cm under the surface. Turbulences, especially in rivers, may however transfer microplastics through several meters of the water column. As interesting as they are, these extrapolations should be considered with caution, since microplastic abundances show a high amount of variability and are difficult to predict.

3.3. Microplastic size distribution

The mean size of microplastic was 1.48 ± 0.88 mm, however significant differences ($p < 0.01$) were observed between samples from the Bay of Marseille (stations # 2-4) and all other sampling stations. For better visualization of the size distribution of our samples, we calculated the equivalent spherical diameter (ESD) of each microplastic particle (Figure 3). A general exponential distribution curve was observed with the smallest items being the most important, except in the Bay of Marseille, where microplastics were more evenly distributed over the size range. The overall size distribution observed in this study closely resembles those observed for the Mediterranean Sea (Ruiz-Orejón et al., 2016; Cózar et al., 2015), open ocean waters (Cózar et al., 2014) and the Northeast Pacific Ocean (Goldstein et al., 2013). Manta nets are the most commonly used sampling device for microplastic sampling in aquatic ecosystems and were also used in this study. The mesh size of the net can influence the size distribution as well as the speed of the tow, as smaller particles avoiding the net can be forced aside from the net opening or large particles can squeeze out through the mesh. This study used mainly a 780 µm mesh sized net and a 330 µm mesh sized net only for ten sampling events at stations # 3 and #4 (Suppl. Table 1). We expected to collect more 0.0-0.4 mm items at both concerned stations (#3 and #4) by using the 330 µm mesh sized net, but microplastics of this size class were observed neither in samples from the 330 µm mesh size, nor in samples from the 780 µm mesh size. No influence on the microplastic size distribution caused by the use of these different mesh sizes was hence observed. This was statistically confirmed by removing all samples collected with the 330 µm net from the dataset and repeating the one-way ANOVA with the following post-hoc test and obtaining the same significant results.

Size distribution can be an indicator of the source of marine debris and of its distance to the shoreline. While Pedrotti et al. (2016) observed that small sized microplastics were more abundant within the first kilometre adjacent to the coastline, Isobe et al. (2015) found that the percentage of larger plastic particles is typically greater in areas close to the pollution source.

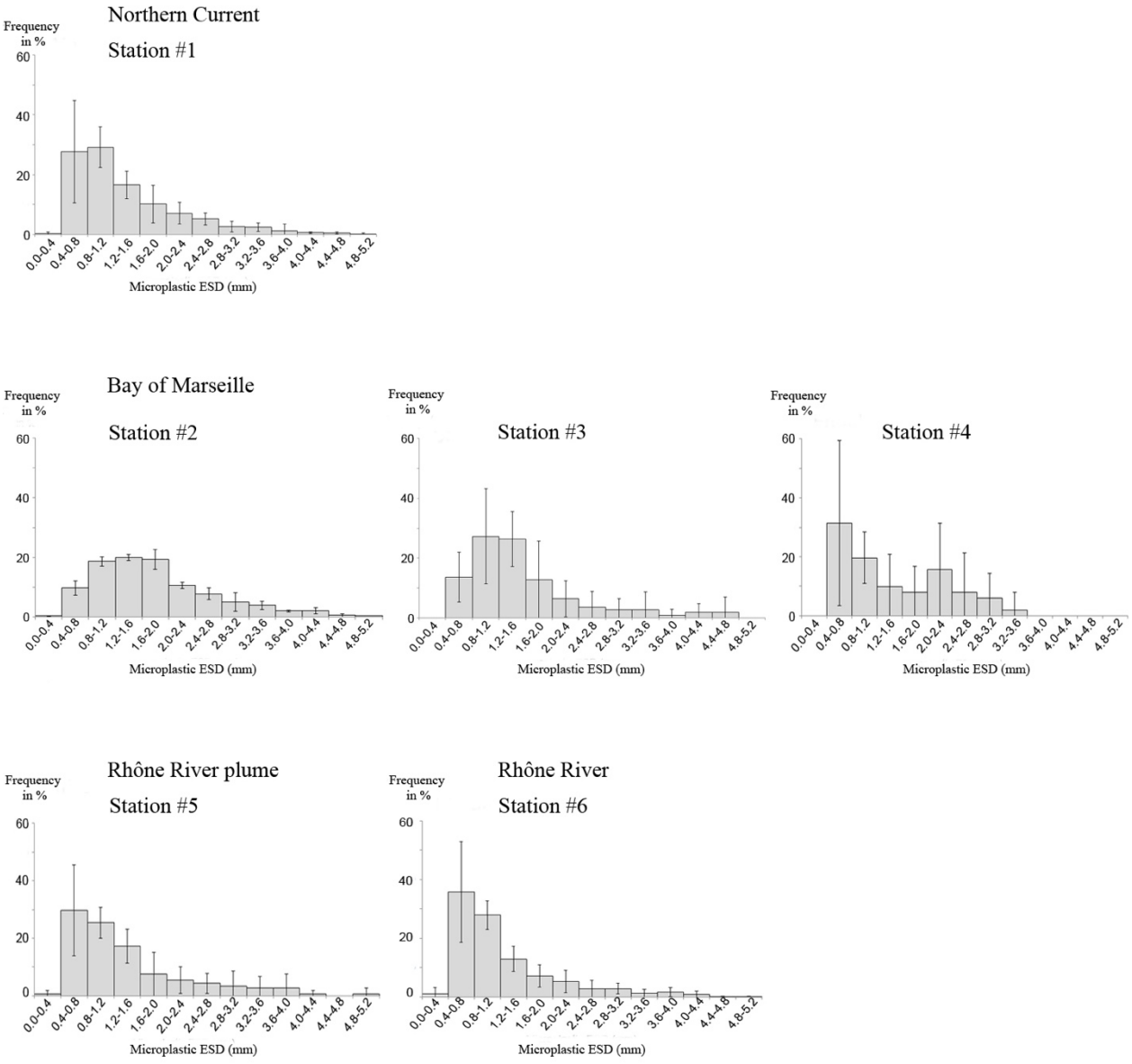

Fig. 3: Microplastic size distributions (ESD in mm) measured at six sampling stations with a ZooScan apparatus. Error bars represent the standard deviation.

The surface area distributions of stations #1 (NC) and 6 (Rhône River) clearly resemble each other. Both are dominated by small particles (< 1 mm^2: 52 and 53 %, respectively, Figure 4). This size class only represented 27 % for stations in the Bay of Marseille, but represented 61 % of microplastic particles at the Rhône River plume. The second size class (1-5 mm^2) was the most abundant in Marseille Bay (55 %). The largest pieces (> 10 mm^2) were poorly represented (< 5 %) at all stations. The size class distributions are likely related to the distance of the collected particles from pollution sources. In the case of station #1 (NC), it is likely that microplastics were transported by the Northern Current and may have originated in regions farther east, such as the Italian coast. At station #6 (Rhône River), the size distribution suggests that the collected microplastics were in the Rhône River watershed for some time and certainly originated from highly industrialized and/or populated regions higher upstream (e.g., Lyon with ~ 500,000 inhabitants). The position of the Rhône River plume varies based on wind and river flow; therefore, debris will be contributed from both the river itself and surrounding coastal areas in variable amounts. Since the smallest particles are most abundant here, it is probable that these microplastics, have also been transported by water masses for some time before collection. In the Bay of Marseille (stations #2-4) the dominance of larger particles (1-5 mm^2) suggests that the microplastics collected in this area were closer to their source and mainly originate from the urban area. A more efficient removal of the smallest floating particles in this region, via ballasting due to epiphytic growth, could also be a possible explanation (Ryan, 2015).

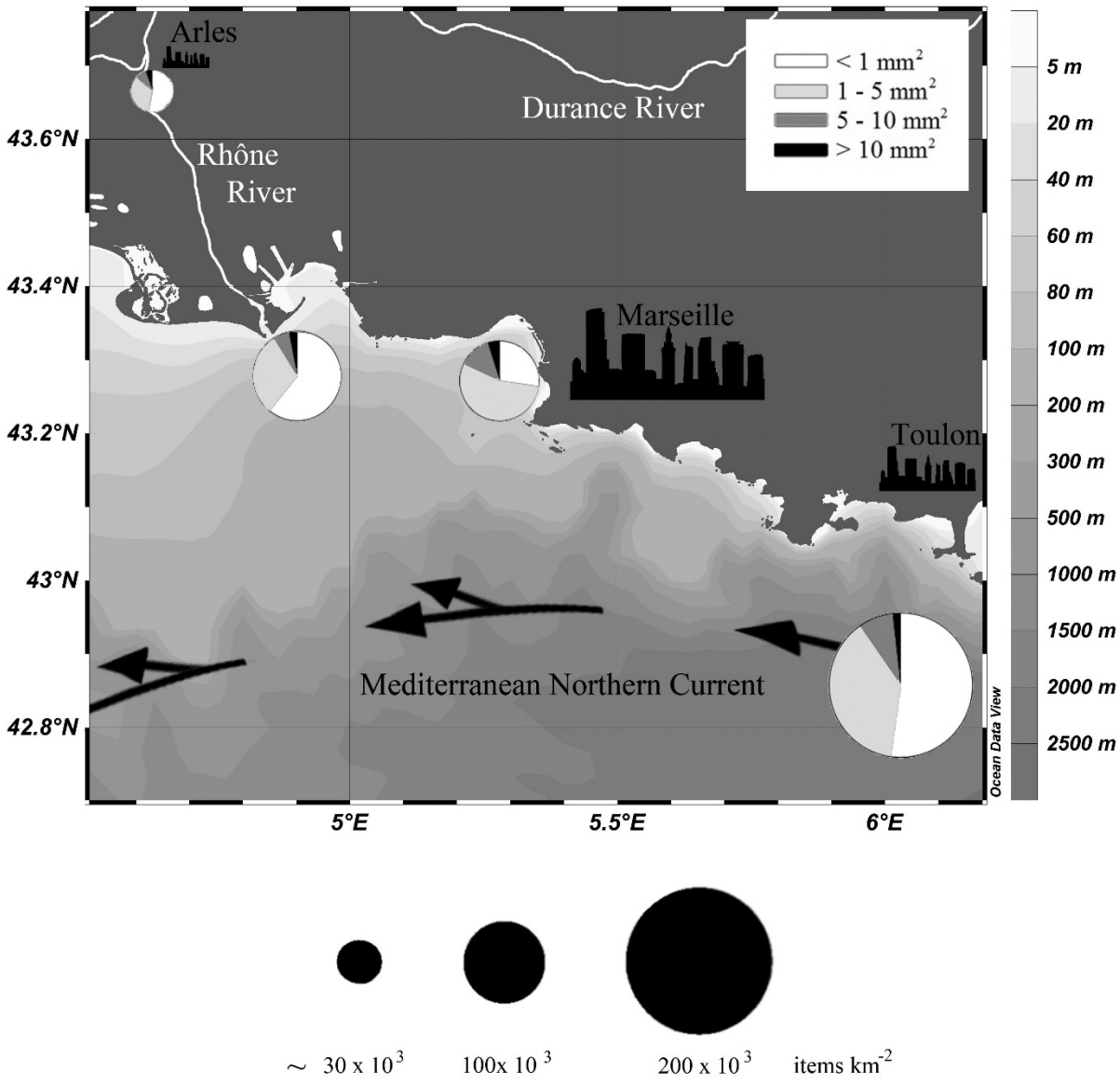

Fig. 4: Spatial occurrence of microplastics and surface area distribution in the Northern Current (station #1), the Bay of Marseille (stations #2-4), the Rhône River plume (station #5) and the Rhône River (station #6). The size of the pie charts is hereby proportional to overall particle concentrations. Map modified after Schlitzer, R., 2009.

4. Conclusions

This study provides additional data on microplastic occurrence in the eastern Gulf of Lion. Our results revealed that surface water microplastic concentrations and size distributions in this area affected by anthropogenic impacts are consistent with those already published for the western Mediterranean Sea. Significant temporal and spatial heterogeneity was observed for microplastic abundances. Our results confirm that the Rhône River, large cities, such as Marseille, and the Northern Current act as sources and/or transportation routes of microplastics collected in the northwestern basin of the Mediterranean Sea. As our microplastics are floating, it was shown that it can be pertinent to study the zooplankton composition of samples additionally to currentology data, in order to improve our knowledge on microplastic transport in the sea.

Acknowledgments

This study was conducted as part of the PARTICULE-region PACA, MERMEX/MISTRALS and JPI Oceans PLASTOX projects. We acknowledge the technical support provided by the Service Atmosphere Mer (SAM) and the Microscopie et Imagerie (MIM) and Marine Environmental Chemistry (PACEM) M I O platforms. We sincerely thank the captain and crew of N. O. Antedon II and Thethys, as well as Sandrine Ruitton, who kindly allowed sampling time during her diving trips. We thank Maryvonne Henry and Anne Delmont for help with sample collection. Maria Luiza Pedrotti's work group from LOV laboratory in Villefranche-sur-Mer kindly shared their ZooScan expertise. Thanks to Javier Castro-Jimenez and Vincent Fauvelle for revising an earlier version of the manuscript. The project leading to this publication has received funding from European FEDER Fund under project 1166-39417. A PhD scholarship for N. Schmidt was provided by Agence de l'Eau.

References

Bănaru, D., Mellon-Duval, C., Roos, D., Bigot, J.-L., Souplet, A., Jadaud, A., Beaubrun, P., Fromentin, J.-M., 2013. Trophic structure in the Gulf of Lions marine ecosystem (north-western Mediterranean Sea) and fishing impacts. Journal of Marine Systems 111-112, 45-68.

Barrier, N., Petrenko, A.A., Ourmières, Y., 2016. Strong intrusions of the Northern Mediterranean Current on the eastern Gulf of Lion: insights from in-situ observations and high resolution numerical modelling. Ocean Dynamics 66, 313-327.

Blanfuné, A., Boudouresque, C.F., Verlaque, M., Beqiraj, S., Kashta, L., Nasto, I., Ruci, S., Thibaut, T., 2016. Response of rocky shore communities to anthropogenic pressures in Albania (Mediterranean Sea): Ecological status assessment through the CARLIT method. Marine Pollution Bulletin 109, 409-418.

Casale, P., Freggi, D., Furii, G., Vallini, C., Salvemini, P., Deflorio, M., Totaro, G., Raimondi, S., Fortuna, C., Godley, B.J., 2015. Annual survival probabilities of juvenile loggerhead sea turtles indicate high anthropogenic impact on Mediterranean populations. Aquatic Conservation: Marine and Freshwater Ecosystems 25, 690-700.

Claessens, M., De Meester, S., Van Landuyt, L., De Clerck, K., Janssen, C.R., 2011. Occurrence and distribution of microplastics in marine sediments along the Belgian coast. Marine Pollution Bulletin 62, 2199-2204.

Cole, M., Lindeque, P., Fileman, E., Halsband, C., Goodhead, R., Moger, J., Galloway, T.S., 2013. Microplastic Ingestion by Zooplankton. Environmental Science and Technology 47 (12), 6646–6655.

Collignon, A., Hecq, J.-H., Glagani, F., Voisin, P., Collard, F., Goffart, A., 2012. Neustonic microplastic and zooplankton in the North Western Mediterranean Sea. Marine Pollution Bulletin 64, 861-864.

Conan, P., Millot, C., 1995. Variability of the Northern Current off Marseilles, western Mediterranean Sea, from February to June 1992. Oceanologica Acta 18 (2), 193-205.

Cózar, A., Echevarría, F., González-Gordillo, J.I., Irigoien, X., Úbeda, B., Hernández-León, S., Palma, A.T., Navarro, S., García-de-Lomas, J., Ruiz, A., Fernández-de-Puelles, M.L., Duarte, C.M., 2014. Plastic debris in the open ocean. PNAS 111 (28), 10239-10244.

Cózar, A., Sanz-Martín, M., Martí, E., González-Gordillo, J.I., Ubeda, B., Gálvez, J.Á., Irigoien, X., Duarte, C.M., 2015. Plastic Accumulation in the Mediterranean Sea. PLoS ONE 10(4), 1-12.

De Alencastro, L.F., 2014. Evaluation de la pollution par les plastiques dans les eaux de surface en Suisse. Rapport final. Sur mandat de l'Office fédéral de l'environnement (OFEV) 22-23.

De Lucia, G. A., Caliani, I., Marra, S., Camedda, A., Coppa, S., Alcaro, L., et al., 2014. Amount and distribution of neustonic micro-plastic off the Western Sardinian coast (Central-Western Mediterranean Sea). Marine Environmental Research 100, 10-16.

Desforges, J.-P.W., Galbraith, M., Ross, P.S., 2015. Ingestion of Microplastics by Zooplankton in the Northeast Pacific Ocean. Archives of Environmental Contamination and Toxicology 69, 320-330.

Deudero, S., Alomar, C., 2015. Mediterranean marine biodiversity under threat: Reviewing influence of marine litter on species. Marine Pollution Bulletin 98, 58-68.

Eriksen, M., Lebreton, L.C.M., Carson, H.S., Thiel, M., Moore, C.J., Borerro, J.C., Galgani, F., Ryan, P.G., Reisser, J., 2014. Plastic Pollution in the World's Oceans: More than 5 Trillion Plastic Pieces Weighing over 250,000 Tons Afloat at Sea. PLoS ONE 9(12), 1-15.

Faure, F., Saini, C., Potter, G., Galgani, F., De Alencastro, L.F., Hagmann, P., 2015. An evaluation of surface micro- and mesoplastic pollution in pelagic ecosystems of the Western Mediterranean Sea. Environmental Science and Pollution Research 22(16), 12190-12197.

Fraysse, M., Pairaud, I., Ross, O.N., Faure, V.M., Pinazo, C., 2014. Intrusion of Rhone River diluted water into the Bay of Marseille: Generation processes and impacts on ecosystem functioning. Journal of Geophysical Research: Oceans 119, 6535-6556.

Gatti, J., Petrenko, A. , Leredde, Y., Devenon, J.-L. & Ulses, C., 2006. The Rhone river dilution zone present in the northeastern shelf of the Gulf of Lion in December 2003. Continental Shelf Research 26(15), 1794-1805.

Goldstein, M.C., Titmus, A.J., Ford, M., 2013. Scales of Spatial Heterogeneity of Plastic Marine Debris in the Northeast Pacific Ocean. PLoS ONE 8(11), 1-11.

Hassoun, A.E.R., Gemayel, E., Krasakopoulou, E., Goyet, C., Saab, M.A.-A., Guglielimi, V., Touratier, F., Falco, C., 2015. Acidification of the Mediterranean Sea from anthropogenic carbon penetration. Deep-Sea Research I 102, 1-15.

Heudorf, U., Mersch-Sundermann, V., Angerer, J., 2007. Phthalates: Toxicology and Exposure. International Journal of Hygiene and Environmental Health 210(5), 623-634.

Ioakeimidis, C., Zeri, C., Kaberi, H., Galatchi, M., Antoniadis, K., Streftaris, N., Galgani, F., Papathanassiou, E., Papatheodorou, G., 2014. A comparative study of marine litter on the seafloor of coastal areas in the Eastern Mediterranean and Black Seas. Marine Pollution Bulletin 89, 296-304.

Isobe, A., Uchida, K., Tokai, T., Iwasaki, S., 2015. East Asian seas: A hot spot of pelagic microplastics. Marine Pollution Bulletin 101, 618-623.

Kobrosly, R.W., Evans, S., Miodovnik, A., Barrett, E.S., Thurston, S.W., Calafat, A.M., Swan, S.H., 2014. Prenatal Phthalate Exposures and Neurobehavioral Development Scores in Boys and Girls at 6-10 Years of Age. Environmental Health Perspectives 122(5), 521-528.

Kukulka, T., Proskurowski, G., Morét-Ferguson, S., Meyer, D.W., Law, K.L., 2012. The effect of wind mixing on the vertical distribution of buoyant plastic debris. Geophysical Research Letters 39, 1-6.

Lwanga, E.H., Gersten, H., Gooren, H., Peters, P., Salánki, T., van der Ploeg, M., Besseling, E., Koelmans, A.A., Geissen, V., 2016. Microplastics in the Terrestrial Ecosystem: Implications for *Lumbricus terrestris* (Oligochaeta, Lumbricidae). Environmental Science and Technology 50, 2685-2691.

Mani, T., Hauk, A., Walter, U., Burkhardt-Holm, P., 2015. Microplastics profile along the Rhine River. Nature Scientific Reports 5:17988, DOI: 10.1038/srep17988

Mansui, J., Molcard, A., Ourmières, Y., 2014. Modelling the transport and accumulation of floating marine debris in the Mediterranean basin. Marine Pollution Bulletin 91, 249-257.

Martini, S., Michotey, V., Casalot, L., Bonin, P., Guasco, S., Garel, M., Tamburini, C. 2016. Bacteria as part of bioluminescence emission at the deep ANTARES station (North-Western Mediterranean Sea) during a one-year survey. Deep-Sea Research I 116, 33-40.

Millot, C., 1991. Mesoscale and seasonal variabilities of the circulation in the western Mediterranean. Dynamics of Atmospheres and Oceans 15, 179-214.

Neves, D., Sobral, P., Ferreira, J.L., Pereira, T., 2015. Ingestion of microplastics by commercial fish off the Portuguese coast. Marine Pollution Bulletin 101, 119-126.

Oehlmann, J., Schulte-Oehlmann, U., Kloas, W., Jagnytsch, O., Lutz, I., Kusk, K.O., Wollenberger, L., Santos, E.M., Paull, G.C., Van Look, K.J.W., Tyler, C.R., 2009. A critical analysis of the biological impacts of plasticizers on wildlife. Philosophical Transactions of the Royal Society B 364, 2047-2062.

Pedrotti, M., Petit, S., Elineau, A., Bruzaud, S., Crebassa, J., Dumontet, B., Marti, E., Gorsky, G., Cozar, A., 2016. Changes in the Floating Plastic Pollution of the Mediterranean Sea in Relation to the Distance to land. PLoS ONE 11(8): e0161581.

Petrenko, A.A., 2003. Variability of circulation features in the Gulf of Lion NW Mediterranean Sea. Importance of inertial currents. Oceanologica Acta 26, 323-338.

Poullain, P., Menna, M., Mauri, E., 2012. Surface Geostrophic Circulation of the Mediterranean Sea Derived from Drifter and Satellite Altimeter Data. Journal of Physical Oceanography 42(6), 973-990.

Przybylinska, P.A., Wyszkowski, M., 2016. Environmental Contamination with Phthalates and its Impact on Living Organisms. Ecological Chemistry and Engineering Society 23(2), 347-356.

PlasticsEurope, 2015. Plastics – the Facts 2015: An analysis of European plastics production, demand and waste data. http://www.plasticseurope.org/Document/plastics---the-facts-2015.aspx (accessed 11.01.2016)

Ruiz-Orejón, L.F., Sardá, R., Ramis-Pujol, J., 2016. Floating plastic debris in the Central and Western Mediterranean Sea. Marine Environmental Research 120, 136-144.

Ross, O.N., Fraysse, M., Pinazo, C., Pairaud, I., 2016. Impact of an intrusion by the Northern Current on the biogeochemistry in the eastern Gulf of Lion, NW Mediterranean. Estuarine and Continental Shelf Research 170, 1-9.

Ryan, P.G., 2015. Does size and buoyancy affect the long-distance transport of floating debris? Environmental Research Letters 10, 084019.

Sathyanarayana, S., 2008. Phthalates and Children's Health. Current Problems in Pediatric and Adolescent Health Care 38(2), 34-49.

Savriama, Y., Stige, L.C., Gerber, S., Pérez, T., Alibert, P., David, B., 2015. Impact of sewage pollution on two species of sea urchins in the Mediterranean Sea (Cortiou, France): Radial asymmetry as a bioindicator of stress. Ecological Indicators 54, 39-47.

Schlitzer, R., Ocean Data View, http://odv.awi.de, 2009.

Sempéré, R., Charrière, B., Cauwet, G., Van Wambeke, F., 2000. Carbon inputs of the Rhône River to the Mediterranean Sea: Biogeochemical implications. Global Biogeochemical Cycles 14, 669-681.

Sigler, M., 2014. The Effects of Plastic Pollution on Aquatic Wildlife: Current Situations and Future Solutions. Water Air Soil Pollution 225, 2184.

Suaria, G., Aliani, S., 2014. Floating debris in the Mediterranean Sea. Marine Pollution Bulletin 86, 494-504.

Suaria, G., Avio, C.G., Lattin, G.L., Regoli, F., and Aliani, S., 2015. Neustonic microplastics in the Southern Adriatic Sea. Preliminary results. Micro 2015, in Seminar of the Defishgear Project, Abstract Book (Piran), 42.

Suaria, G., Avio, C.G., Mineo, A., Lattin, G.L., Magaldi, M.G., Belmonte, G., Moore, C.J., Regoli, F., Aliani, S., 2016. The Mediterranean Plastic Soup: synthetic polymers in Mediterranean surface waters. Nature Scientific Reports 6:37551, DOI: 10.1038/srep37551

Tedetti, M., Longhitano, R., Garcia, N., Guigue, C., Ferretto, N., Goutx., M. 2012. Fluorescence properties of dissolved organic matter in coastal Mediterranean waters influenced by a municipal sewage effluent (Bay of Marseilles, France). Environmental Chemistry 9 (5), 438-449.

Tekman, M.B., Krumpen, T., Bergmann, M., 2017. Marine litter on deep Arctic seafloor continues to increase and spreads to the North at the HAUSGARTEN observatory. Deep Sea Research Part I: Oceanographic Research Papers 120, 88-99.

Ter Halle, A., Ladirat, L., Gendre, X., Goudouneche, D., Pusineri, C., Routaboul, C., Tenailleau, C., Duployer, B., Perez, E., 2016. Understanding the Fragmentation Pattern of Marine Plastic Debris. Environmental Science & Technology 50, 5668-5675.

The MerMex Group, 2011. Marine ecosystems' responses to climatic and anthropogenic forcings in the Mediterranean. Progress in Oceanography 91, 97-166.

Tranfo, G., Caporossi, L., Paci, E., Aragona, C., Romanzi, D., de Carolis, C., de Rosa, M., Capanna, S., Papaleo, B., Pera, A., 2012. Urinary phthalate monoesters concentration in couples with infertility problems. Toxicology Letters 213, 15-20.

UNEP, 2009. Marine Litter: A Global Challenge, 232.

Van der Hal, N., Asaf, A., Dror, A., 2017. Exceptionally high abundances of microplastics in the oligotrophic Israeli Mediterranean coastal waters. Marine Pollution Bulletin, in press.

Van Franeker, J.A., Law, K.L., 2015. Seabirds, gyres and global trends in plastic pollution. Environmental Pollution 203, 89-96.

Van Sebille, E., Wilcox, C., Lebreton, L., Maximenko, N., Hardesty, B.D., van Franeker, J.A., Eriksen, M., Siegel, D., Galgani, F., Law, K.L., 2015. A global inventory of small floating plastic debris. Environonmental Research Letters 10, 124006.

Woodall, L.C., Sanchez-Vidal, A., Canals, M., Paterson, G.L.J., Coppock, R., Sleight, V., Calafat, A., Rogers, A.D., Narayanaswamy, B.E., Thompson, R.C., 2014. The deep sea is a major sink for microplastic debris. Royal Society Open Science 1, 140317.

Zambianchi, E., Iermano, I., Aliani, S., 2014. Marine litter in the Mediterranean Sea, An Oceanographic perspective. In Ciesm Workshop N°46 (Coordination F Galgani), Tirana, 18-21 juin 2014, 172 pages.

Zhao, S., Zhu, L., Li, D., 2016. Microscopic anthropogenic litter in terrestrial birds in Shanghai, China: Not only plastics but also natural fibers. Science of the Total Environment 550, 1110-1115.

CHAPTER II:
PAEs, OPEs and BPs in the Rhône River

Occurrence of organic plastic additives in surface waters of the Rhône River (France)

Natascha Schmidt [a], Javier Castro-Jiménez [a], Vincent Fauvelle [a], Mélanie Ourgaud [a], Richard Sempéré [a,*]

[a] *Aix-Marseille Univ., Toulon Univ., CNRS, IRD, Mediterranean Institute of Oceanography (M I O), UM 110, Marseille, France*

* corresponding author

richard.sempere@mio.osupytheas.fr

Richard Sempéré

Mediterranean Institute of Oceanography

163 Av. de Luminy

13288 Marseille cedex 09

Tel.: +33 (0) 4 86 09 05 88

Journal: Environmental Pollution

Status: Under revision.

Abstract

Organic plastic additives are nowadays frequently detected in the environment, but monitoring programs and comprehensive data on local occurrences and sources are often missing. To gain information on their presence in the Rhône River, possible sources and export rates to the Mediterranean Sea, riverine surface water samples were collected monthly for one year. The dissolved phase was analyzed for 22 organic additives mainly used in the plastic industry, including organophosphate esters (OPEs), phthalates (PAEs) and bisphenols (BPs), by GC-MS and LC-HRMS. Our results indicate that PAEs were the most abundant class, with concentrations ranging from 97 to 541 ng L^{-1}, followed by OPEs (85-265 ng L^{-1}) and BPs (4-21 ng L^{-1}). Among PAEs, diethylhexyl phthalate (DEHP) was the most abundant compound, whereas TCPP (Tris(1-chloro-2-propyl) phosphate) and TnBP (Tri(n-butyl)phosphate) were the predominant OPEs. Bisphenol S was the only BP detected. 5-54 metric tons $year^{-1}$ of dissolved organic plastic additives of emerging concern are estimated to be exported to the Gulf of Lion by the Rhône River, which is the main freshwater source of the Mediterranean Sea.

Capsule

Organic plastic additives were present in all water samples from the Rhône River, with concentrations of up to ~830 ng L^{-1} for Σ_{17} compounds. Phthalates were most abundant.

Keywords: organophosphate esters; phthalates; bisphenols; river inputs; plastic additives

1. Introduction

Organic contaminants such as organophosphate esters (OPEs), phthalates (PAEs) and bisphenols (BPs) have been widely used in the last decade as additives in a broad range of products, such as detergents (PAEs), textiles (OPEs, PAEs), paints (OPEs, PAEs, BPs), food containers (PAEs, BPs) and plastics above all (OPEs, PAEs, BPs) (Hahladakis et al., 2018; Net et al., 2015b; Wei et al., 2015). These contaminants are commonly detected in marine and freshwater environments (Hermabessiere et al., 2017; Net et al., 2015b; Paluselli et al., 2018b; Pantelaki and Voutsa, 2019; Schmidt et al., 2019), and some of them have been classified or are suspected to act as endocrine disruptors (e.g., diethylhexyl phthalate, DEHP; tris(1-chloro-2-propyl) phosphate, TCPP). Even transgenerational effects have been shown to occur, e.g., through the exposure of mice to DEHP during pregnancy (Manikkam et al., 2013; Quinnies et al., 2017). However, Environmental Quality Standards (EQS) (i.e., maximum acceptable concentration thresholds in water, biota and sediments) have been derived (Directive 2008/105/EC) or proposed for only a few of them.

Rivers are known to be vectors for plastic debris (Horton et al., 2017; Schmidt et al., 2017), legacy contaminants such as polychlorinated biphenyls (PCBs) (Herrero et al., 2018) and contaminants considered of emerging concern, like PAEs (Paluselli et al., 2018a). Sánchez-Avila et al. (2012) concluded that rivers (along with wastewater treatment plants) are the main source of organic micropollutants, including BPs and PAEs, to the North Western Mediterranean coast. The knowledge of current environmental levels and fluxes is an important first step to identify contamination hot spots, estimate loadings to coastal areas and perform risk assessments. A limited number of studies have investigated the occurrence of OPEs in surface water from European rivers; for example, data exists for the Ruhr (Andresen et al., 2004), the Elbe (Wolschke et al., 2015) and the Danube rivers (Loos et al., 2017), whereas smaller datasets are available for others (Cristale et al., 2013; Fries and Püttmann, 2003; Martínez-Carballo et

al., 2007). To our knowledge, no data considering OPEs in the Rhône River have been reported thus far.

DEHP, generally the most abundant PAE in the environment, was detected at concentrations of 160-1,700 ng L^{-1} in the Charmoise River, France (Tran et al., 2015) and 540-920 ng L^{-1} in the Rhine River, the Netherlands (Peijnenburg and Struijs, 2006). PAEs were previously analyzed in the Rhône River by Paluselli et al. (2018), but only for one sampling date (March 2014; Σ_8 PAEs: 615 ng L^{-1}). Miège et al. (2012) measured bisphenol A (BPA) in fish samples from the Rhône River (mean BPA concentration of 13.7 ng g^{-1} dry weight), but no data for river water samples has been reported, neither concerning other bisphenols (such as bisphenol S), which are increasingly used to replace BPA (Wong et al., 2017).

The Rhône River, linking the Swiss Alps with the Mediterranean Sea, is 816 km long and is the main freshwater source of the NW Mediterranean Sea (Sempéré et al., 2000; Struglia et al., 2004). It has historically been of significant economic importance and has been highly modified by humankind (riverbed regulation, hydropower developments, etc.) over the course of time, passing through a heavily industrialized area with petrochemical industries and several nuclear plants. The Rhône River has already been studied on an annual basis for natural organic compounds, nutrients, dissolved inorganic carbon (DIC), chromophoric dissolved organic matter (CDOM), dicarboxylic acids, total suspended matter (TSM) fluxes and freshwater discharges (Coste and Raimbault, 1993; Panagiotopoulos et al., 2012; Para et al., 2010; Pont et al., 2002; Sempéré et al., 2018, 2000). In addition, recent studies showed that this river is a significant source of microplastics (Constant et al., 2018; Schmidt et al., 2018) and macroplastics to the Mediterranean Sea (Castro-Jiménez et al., submitted). However, available data on anthropogenic organic compounds rely mostly on punctual or short-term measurements. In this study, our objectives were (i) to quantify OPEs, PAEs and BPs in water samples from the Rhône River during a one-year period, (ii) to identify possible sources and/or environmental

drivers influencing contaminant concentrations and (iii) to provide a first estimate of fluxes into the NW Mediterranean Sea.

2. Materials and Methods

2.1. Study area and sampling

One-liter surface water samples were collected monthly in duplicate from May 2017 to April 2018 (see Supplementary Material for sampling dates, water temperature and river flow rates). All samples were taken at arm-length from the dock in the Rhône River in Arles city (France) at 43.67858° N, 4.62073° E (Figure 1) using precombusted (450 °C, 6 h) 1-L glass bottles. The samples were filtered through a glass fiber filter (GF/F, 0.7 µm) within three hours after collection and were either stored at 4 °C in the dark and extracted within 24 h or otherwise stored at -25 °C in the dark (for three months max.) when immediate extraction was not possible. River water temperature was measured using a handheld electronic thermometer, and river flow data were extracted from the French "Banque Hydro" (http://www.hydro.eaufrance.fr/). The river flow data used originate from a measuring station (in the commune of Tarascon) approximately 16 km upstream of Arles. Just upstream of Arles, the river separates into the "Petit Rhône" (representing ~10% of the total water flow; Sempéré et al., 2000) and the "Grand Rhône". Since this division is downstream of the flow-measuring station, but upstream of the water sampling station, the river flow at the water sampling station was considered to correspond to approximately 90% of the flow measured in Tarascon. The daily river flow during the whole sampling period is shown in Figure S1 A. All six wastewater treatment plants (WWTPs) situated in the commune of Arles are located downstream of our sampling station. However, about 15 km upstream of the sampling station, the WWTP effluents

from Tarascon (17,583 inhabitant equivalent) and Beaucaire (29,246 inhabitant equivalent) enter the Rhône River.

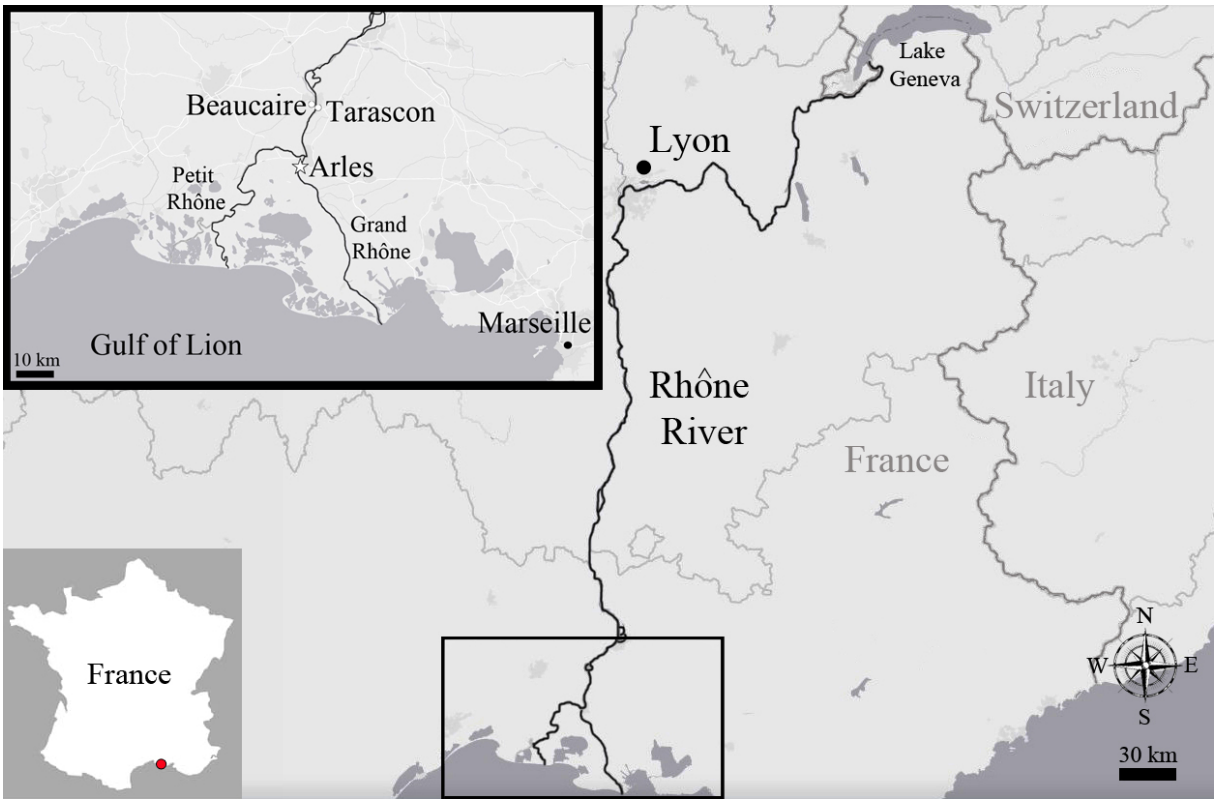

Figure 1: Map showing the French part of the Rhône River after leaving Lake Geneva until its estuary in the Gulf of Lion (NW Mediterranean Sea). A zoomed image in the left corner shows the position of the river discharge measuring station at Tarascon, the water sampling station (star) in Arles and the two river branches "Petit Rhône" (left) and "Grand Rhône" (right) representing ~10% and 90% of the total water flow, respectively.

2.2. Solvents and chemical standards

Solvents were purchased from Biosolve (ULC-MS grade methanol) and Promochem (Picograde, LGC n-hexane, ethyl acetate and dichloromethane). Isotope-labeled and native bisphenols were obtained from AccuStandard (USA); labeled and native phthalates from

Supelco (USA). Isotope-labeled OPEs were purchased from C/D/N Isotopes Inc. (Canada) (D_{27}-Tri-n-butyl phosphate -D_{27}-TBP-, D_{15}-Triphenyl phosphate -D_{15}-TPhP-, D_{21}-Tri-n-propyl phosphate -D_{21}-TPrP- and D_7Malathion -D_7-MAL-) and from Cambridge Isotope Laboratories, Inc. (USA) (D_{18}-Tris(1-chloro-2-propyl) phosphate -D_{18}-TCPP-, D_{15}-Tris (1,3-dichloro-2-propyl) phosphate -D_{15}-TDCP- and D_{12}-Tris (2-chloroethyl) phosphate -D_{12}-TCEP-). Native OPEs were obtained from Dr. Ehrenstorfer GmbH (Germany). CAS numbers of all compounds, as well as their monoisotopic masses and log K_{ow} values are given in Supplementary Material (Table S1).

2.3. Sample processing and analysis

Solid phase extraction (SPE) was carried out following a protocol described elsewhere (Fauvelle et al., 2018). Briefly, after filtration (GF/F, 0.7 µm) and the addition of labeled surrogate standards for the three organic classes (100 ng sample^{-1} of D_{27}-TBP, D_{18}-TCPP, D_{15}-TDCP, D_{15}-TPhP and D_4-di-n-butyl phthalate -D_4-DnBP- and 20 ng sample^{-1} of 4-n-octylphenol-D_{17} -4nOP-D_{17}-), the water was passed through precombusted and precleaned glass cartridges containing 250 mg SPE sorbent (Oasis hydrophilic lipophilic balance HLB, Waters, Guyancourt, France) *via* polytetrafluoroethylene (PTFE) liners. Next, the cartridges were vacuum-dried for 2-3 hours to complete dryness.

Molecules of interest were then sequentially eluted using a solvent polarity gradient resulting in two different fractions by using 5 mL of n-hexane followed by 5 mL of n-hexane/dichloromethane 50:50 (v/v) for PAEs and OPEs (F_a fraction) and 5 mL of ethyl acetate followed by 5 mL of methanol for BPs (F_b fraction). The extracts were then evaporated using pure N_2 gas until a volume of approximately 1 mL was transferred into 2-mL conical glass vials. The extracts were further concentrated through gentle N_2 flux to (F_a) a final volume of approximately 100 µL or (F_b) dryness in which case the extract was then reconstituted with 990

µL of methanol. Internal standards for quantification were then added as follows: (F_a) 100 ng sample^{-1} of D_4-diethyl phthalate (D_4-DEP), D_4-diethylhexyl phthalate (D_4-DEHP), D_{21}-TPrP, D_{12}-TCEP and D_7-MAL and (F_b) 20 ng sample^{-1} of D_{16}-bisphenol A (D_{16}-BPA).

For PAEs and OPEs, F_a was injected into a gas chromatograph coupled with a mass spectrometry detector (GC-MS, Agilent 7820A Series GC – Agilent 5977E MS) for the quantification of nine organophosphate esters (tripropyl phosphate -TPP-, tri-iso-buthyl phosphate -TiBP-, tri-n-butyl phosphate -TnBP-, tris-(2-chloroethyl) phosphate -TCEP-, tris-(2-chloro, 1-methylethyl) phosphate -TCPP-, tris-(2-chloro-, 1-chloromethylethyl) phosphate -TDCP-, triphenyl phosphate -TPhP-, 2-ethylhexyl-diphenyl phosphate -EHDPP- and tris(2-ethylhexyl) phosphate -TEHP-) and seven phthalates (dimethyl phthalate -DMP-, diethyl phthalate -DEP-, diisobutyl phthalate -DiBP-, di-n-butyl phthalate -DnBP-, benzylbutyl phthalate -BzBP-, diethylhexyl phthalate -DEHP- and di-n-octyl phthalate -DnOP-); while for the quantification of six bisphenols (bisphenol A -BPA-, bisphenol AF -BPAF-, bisphenol AP -BPAP-, bisphenol F -BPF-, bisphenol S -BPS- and bisphenol Z -BPZ-) F_b was injected into a liquid chromatograph coupled to a high-resolution time-of-flight mass spectrometer *via* an electrospray ionization interface (LC-ESI-QTOF, Agilent 1290 Infinity LC system coupled with Agilent 6530 Accurate-Mass Q-TOF). All details on GC-MS and LC-ESI-QTOF analyses can be found in the Supplementary Material (Text S1).

Dissolved organic carbon (DOC) was measured from filtered (GF/F, 0.7 µm), acidified (by 20 µL of 85% H_3PO_4 acid) Rhône River water subsamples using a Shimadzu TOC-5000 carbon analyzer (Sempéré et al., 2008). The instrument blank (≤ 5 µM) was subtracted from all measured data. GF/F filters were acidified with 50 µL H_2SO_4 (0.5 N) to remove inorganic carbon and analyzed for particulate organic carbon (POC) and nitrogen (PON) using high combustion (1000 °C) on a CN Integra mass spectrometer (SERCON), calibrated using glycine references for every batch of 10–15 samples (Raimbault et al., 2008).

2.4. Quality Assurance / Quality Control

The extractions were carried out in an ISO class 6 cleanroom equipped for organic trace analysis. All glassware used was carefully cleaned, rinsed with demineralized and ultrapure water and burned at 450 °C for 6 h. All plastic material was avoided during sampling, extraction and analysis. All organic contaminants and DOC analyses were performed in duplicate. Surrogate recoveries ranged from 83-119% (D_4-DnBP), 85-102% (D_{27}-TBP), 68-96% (D_{18}-TCPP), 83-104% (D_{15}-TDCP), 72-95% (D_{15}-TPhP) and 64-79% (4nOP-D_{17}). Native spike experiments performed in a previous study also showed good method recoveries, ranging from 61±4 to 131±5% for OPEs, from 52±3 to 89±1% for PAEs and from 79±4 to 118±26% for BPs (Fauvelle et al., 2018). Duplicate extraction blanks were made for each extraction batch (containing 6-8 duplicate samples) to detect potential contaminations during the sample extraction and processing. Samples were blank corrected by subtracting the averaged blank value of the specific batch. No particular blank issues were detected. PAE concentrations in blanks were as follows: DEP n.d.-2.0 ng L^{-1}, DiBP 1.8-5.0 ng L^{-1}, DnBP n.d.-2.9 ng L^{-1} and DEHP 7.0-37.0 ng L^{-1}. DMP, BzBP and DnOP were not detected in blanks. OPEs were detected in blanks at levels lower than the limits of quantification (LOQs) (TiBP, TnBP and EHDPP), not detected at all (TPP, TCEP, TDCP, TPhP and TEHP) or, in the case of TCPP, were detected at constantly low concentrations of 3.6-4.0 ng L^{-1}. BPs were either not detected in blanks or were present at low concentrations (n.d.-0.1 ng L^{-1} for BPS, n.d.-6.7 ng L^{-1} for BPZ). Method LOQs ranged from 0.03-0.75 ng L^{-1} for OPEs, from 0.03-0.25 ng L^{-1} for PAEs and from 0.1-5.0 ng L^{-1} for BPs (Table S2). The average DOC concentration measured in the Deep Seawater reference material (batch 17, lot# 04-17; D. Hansell, Rosenstiel School of Marine and Atmospheric Science, Miami, USA) was 45±1 µM C (n = 8).

2.5. Data processing

Correlations between PAEs, OPEs, BPs, DOC, POC, PON and river discharge were assessed through a correlation matrix using linear correlation coefficients. Correlations were considered strong if $\geq \pm 0.7$. To perform a rough estimation of the dissolved organic additive inputs of the Rhône River to the NW Mediterranean Sea contaminant fluxes were estimated. For this, the concentrations measured at each sampling day was multiplied with the corresponding daily river flow. The daily river flows are presented in Table 1.

3. Results and Discussion

Table 1: Sampling time and date, water temperature (°C), dissolved organic carbon (µM) and river discharge (m^3 s^{-1}). River discharge data were extracted from "Hydro Banque" (http://www.hydro.eaufrance.fr) from their measuring station at Tarascon, approximately 16 km upstream of our sampling station. Since the Rhône River separates into two branches (Petit Rhône and Grand Rhône) after the discharge measuring station, we estimated that the flow rate at our sampling station amounted to approximately 90% of the original value.

Date	Time of day	Water temperature (°C)	DOC (µM)	Approx. discharge rate (m^3 s^{-1})
05/23/2017	09:00	18.3	114	1116
06/22/2017	10:24	24.6	80	785
08/24/2017	11:38	23.5	117	470
09/19/2017	08:39	20.9	100	626
11/03/2017	09:08	14.0	118	460
11/30/2017	10:53	9.4	134	1026
12/12/2017	10:13	8.2	164	2772
01/05/2018	10:11	8.6	162	3960
02/13/2018	12:04	7.3	145	1521
03/01/2018	10:46	5.0	n.a.	1566
04/09/2018	12:57	11.7	131	2340

n.a. = not available

River discharge varied on sampling days between 460 and 3960 m^3 s^{-1}, water temperature between 5 and 25 °C and DOC concentrations between 80 and 164 µM (average 127±26 µM or 1517 ± 315 µg L^{-1}) (Table 1, Figure 2A). These values are in line with DOC concentrations measured at the same sampling station between 2006 and 2009 (80-216 µM; Sempéré et al., 2018) and with those reported by Panagiotopoulos et al. (2012) (average 134 µM). POC and PON ranged from 185-2134 µg L^{-1} and from 47-303 µg L^{-1}, respectively. More importantly, they followed the same dynamic as the river discharge (Figure 2A) and were thus positively correlated with it ($p < 0.01$). Our average POC concentration (667 µg L^{-1}) is notably lower than the one observed by Panagiotopoulos et al. (2012) (3096 µg L^{-1}), and in their study, a correlation between POC concentrations and river discharge could not be observed, probably due to incoherent POC dynamics during flood events.

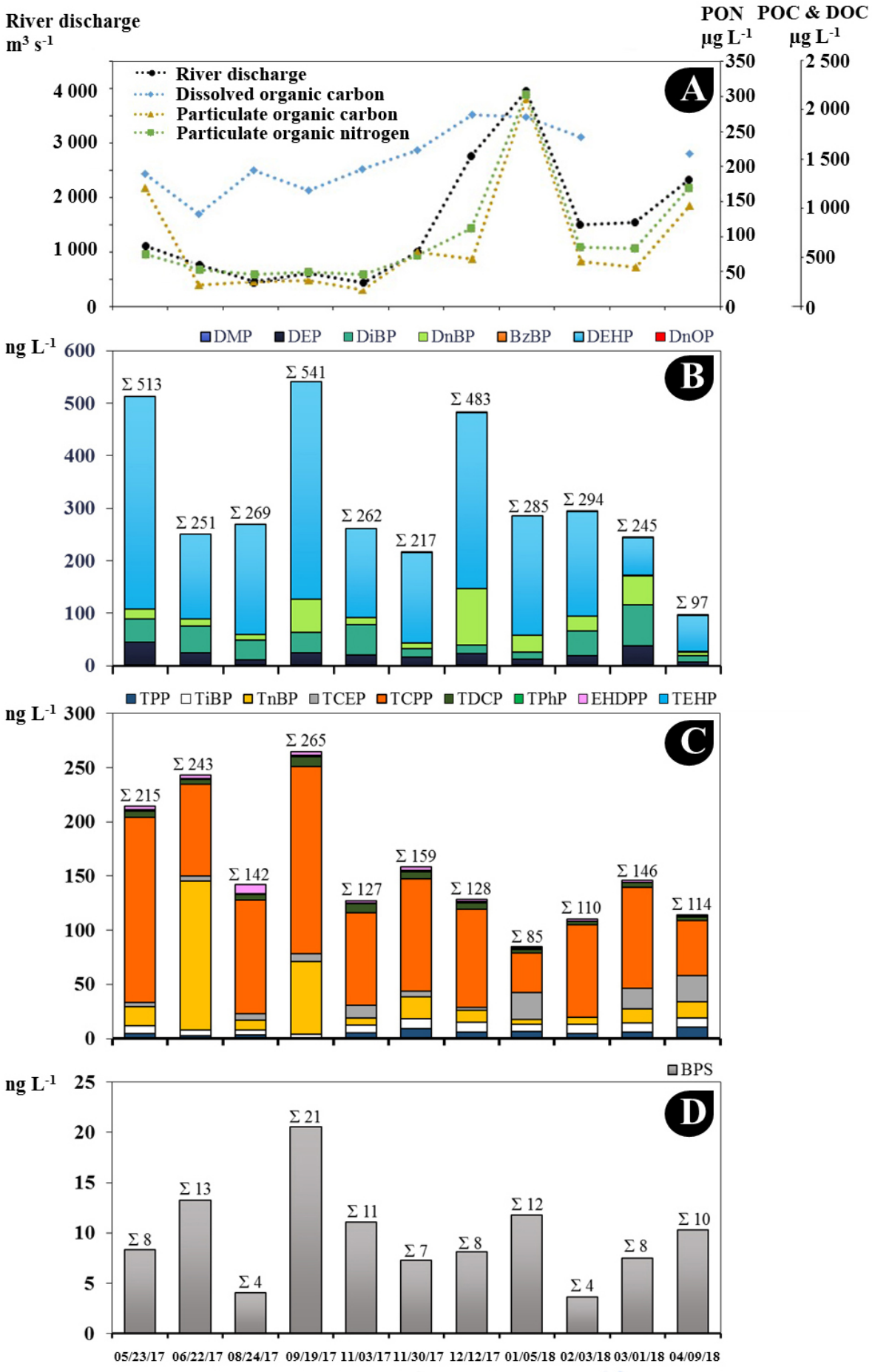
River discharge
m³ s⁻¹
PON
µg L⁻¹
POC & DOC
µg L⁻¹
River discharge
Dissolved organic carbon
Particulate organic carbon
Particulate organic nitrogen
A
4 000
3 000
2 000
1 000
0
350
300
250
200
150
100
50
0
2 500
2 000
1 500
1 000
500
0
DMP
DEP
DiBP
DnBP
BzBP
DEHP
DnOP
ng L⁻¹
600
500
400
300
200
100
0
B
Σ 513
Σ 251
Σ 269
Σ 541
Σ 262
Σ 217
Σ 483
Σ 285
Σ 294
Σ 245
Σ 97
TPP
TiBP
TnBP
TCEP
TCPP
TDCP
TPhP
EHDPP
TEHP
ng L⁻¹
300
250
200
150
100
50
0
C
Σ 215
Σ 243
Σ 142
Σ 265
Σ 127
Σ 159
Σ 128
Σ 85
Σ 110
Σ 146
Σ 114
BPS
ng L⁻¹
25
20
15
10
5
0
D
Σ 8
Σ 13
Σ 4
Σ 21
Σ 11
Σ 7
Σ 8
Σ 12
Σ 4
Σ 8
Σ 10
05/23/17
06/22/17
08/24/17
09/19/17
11/03/17
11/30/17
12/12/17
01/05/18
02/03/18
03/01/18
04/09/18

Figure 2: (A) River discharge (m^3 s^{-1}), PON (µg L^{-1}), POC (µg L^{-1}) and DOC (µg L^{-1}) concentrations measured during the sampling events, (B) concentrations (in ng L^{-1}) of the seven phthalates, (C) nine organophosphate esters and (D) six bisphenols. BPS was the only bisphenol detected. The March DOC sample was excluded due to contamination issues. Σ means sum of the concentrations of all individual molecules within each class of compounds. The dotted lines in (A) are there to facilitate the reading of the graph, but do not indicate an extrapolation between individual measurements.

3.1. Concentration levels and relative abundances

PAEs, OPEs and BPs were, for the first time, simultaneously measured in the Rhône River on a monthly basis. PAEs were the compound class reaching the highest concentrations compared to the other two contaminant families (97-541 ng L^{-1}; av. relative abundance 64% ± 10% standard deviation SD) followed by OPEs (85-265 ng L^{-1}; av. relative abundance 34% ± 10% SD) and BPs (4-21 ng L^{-1}; av. relative abundance 2% ± 1% SD), except in April 2018 when OPEs were predominant with ~52% relative abundance (Table S3). Hereby, the predominance of OPEs in April 2018 is mainly due to the lowest PAE concentration measured throughout the study. Overall, the highest plastic additive concentrations in surface water from the Rhône River were measured in September 2017, with ~830 ng L^{-1} for $\sum_{17}$ compounds.

3.1.1. Phthalates

The highest $\sum_7$ PAE levels were found in the months of May, September and December 2017 (Figure 2B), with values in the range of those reported by Paluselli et al. (2018) (615 ng L^{-1}, $\sum_7$ PAEs) for March 2014 at the same sampling site. DEHP, generally the most abundant

PAE, was found at concentrations ranging from 70 to 405 ng L^{-1} (mean 221 ng L^{-1}). Previous studies in French water courses reported higher concentrations in three rivers in the Parisian area (average 323-779 ng L^{-1} DEHP; Teil et al., 2007) and in several French-Belgian transboundary rivers (0.8-126 µg L^{-1} DEHP; Net et al., 2015a). Domínguez-Morueco et al. (2014) did not detect DEHP in any river or tap water samples from Spain and attributed this condition to the existing regulations restricting the use of DEHP for certain products (e.g., plastic toys). However, their LOD (460 ng L^{-1}) and LOQ (970 ng L^{-1}) values were quite elevated and they may have missed trace level concentrations.

Branched chain PAEs, including DEHP and DiBP, were found to be the most abundant PAEs, with DEHP being predominant with its relative abundance varying between 29.5–79.6% (mean 69%) of total PAEs, which is in line with the 66% and 54% relative DEHP abundance reported by Paluselli et al. (2018) and Net et al. (2015a), respectively. DMP, BzBP and DnOP were only detected at low concentrations (≤ 1 ng L^{-1}) or were not detected at all. DEP abundance varied between 3.6–14.7% of Σ_7 PAEs, whereas DiBP and DnBP relative abundances were between 3.2–31.9% and 3.7–22.6%, respectively (Table S3). Interestingly, the sample collected in March (03/01/2018) exhibited a different pattern, with a remarkably low DEHP relative abundance (29.5%) compared to the other months (64.7-79.6%) and with higher DEP and DiBP percentages (Figure 2B, Table S3). A possible explanation could be the rainfall (3.2 mm) observed on this given day, representing the only real rain event during the sampling days (daily precipitation data for the whole study period is shown in Figure S1 B). Previous works indicated that DEHP is less abundant in rainwater compared to other PAEs, possibly due to the short half-life of DEHP in the atmosphere (Fernández-Amado et al., 2017; Teil et al., 2006). This could possibly explain our observation; however, our present dataset is too limited to draw valid conclusions on this matter. Higher sampling frequencies and a detailed investigation of the particulate-dissolved partitioning of PAEs, particularly DEHP, would be needed.

WWTP effluents are major PAE sources to rivers and previous studies have reported that the relative abundances of individual PAEs depended on the effluent type. For example, industrial laundries were shown to be the main DEHP and DEP source in industrial effluents, while DnBP was mostly associated with the pharmaceutical industry (Bergé et al., 2014). Concerning domestic effluents, dishwater graywater was reported as an important DnBP source (54% relative abundance), while DEHP was predominant in all other types of graywater (Deshayes et al., 2017). In the case of our sampling station, two WWTPs are situated ~ 15 km upstream and are probable sources of the organic contaminants measured in this study, as well as the plastic packaging and plastic material industry located in the commune of Avignon (~ 35 km upstream). Furthermore, direct leaching from floating plastic debris present in the watercourse could contribute to the PAE, and other plastic additive, stocks in surface waters (León et al., 2018; Paluselli et al., 2019). Recent studies reported the widespread presence of macro- and microplastics in surface waters of the Rhône River (Castro-Jiménez et al., 2019; Constant et al., 2018; Schmidt et al., 2018).

3.1.2. Organophosphate esters

Total OPE concentrations were generally slightly lower than total PAE concentrations. They reached a maximum in September 2017, while the lowest concentration was measured in January 2018 (Figure 2C). Highest Σ_9 OPEs concentrations were found when water temperature was highest (May-September, 18.3-24.6 °C; Table 1), suggesting that temporal variability depending on water temperature occurs (see section 3.2). TCPP was predominant in this study, with concentrations of 37-173 ng L^{-1} (mean 98 ng L^{-1}). Such TCPP concentration levels are in the lower range of those previously reported in other rivers: 126±14 ng L^{-1} in the Elbe River (Germany) (Wolschke et al., 2015), and 28-603 ng L^{-1} in the Danube River (Loos et al., 2017).

In 40 rivers in China TCPP was the most abundant OPE, with concentrations of 5-921 ng L^{-1} (Wang et al., 2015). TCPP was also the most abundant OPE in this study (av. relative abundance 62% ± 15% SD), followed by TnBP (av. relative abundance 14% ± 15% SD) and TCEP (av. relative abundance 9% ± 10% SD) (Table S3). Interestingly, the sample collected in June 2017 exhibited a different pattern, with a much higher TnBP relative abundance (56.8%) compared to the rest of the samples (4.8-25.5%) and the lowest TCPP abundance (34.9%) of the sample period (Figure 2C, Table S3). Overall, TnBP concentrations varied between 4-138 ng L^{-1}. TnBP is used as a plasticizer, corrosion inhibitor and antifoaming agent, among other things. It is also used in the nuclear industry to reprocess spent fuel by a process called PUREX (Revathi et al., 2014). Note that nuclear power is the main energy source in France and the Rhône watershed has the highest concentration of nuclear power plants in Europe. Furthermore, the Rhône River accommodates an ancient nuclear fuel reprocessing plant (Olivier et al., 2009), which could thus be a TnBP source. The fluctuating abundance of TnBP (including its high abundance in the June 2017 sample) could therefore be linked to varying inputs from the nuclear industry, though other sources cannot be excluded and a dedicated study should investigate these inputs. TEHP was not detected in water samples from this campaign (see Figure S2 for detection frequencies). This was expected since TEHP tends to concentrate in sediments instead of in the dissolved water phase (Liu et al., 2018).

3.1.3. Bisphenols

Of the six different BPs screened for, only BPS was detected in our samples. The concentrations ranged between 4 and 21 ng L^{-1}, with a mean of 10 ng L^{-1} (Figure 2D). These values are comparable to those of other studies investigating BPs in river water (Jin and Zhu, 2016; Yamazaki et al., 2015). The highest concentration was found on September 19th, 2017,

as was the case for Σ PAEs and Σ OPEs (Figure 2). While BPS can be used as a substitute for BPA in certain products (e.g., as a color developer in thermal paper or as an additive in polycarbonate plastics), BPA still dominates these sectors (Björnsdotter et al., 2017; Pivnenko et al., 2018) and a higher BPA than BPS concentration could thus probably be expected in the environment. Therefore, it is remarkable that we did not detect any BPA in our samples. However, it is noteworthy that BPA is rapidly degraded in river water under aerobic conditions (e.g., 1 000 ng mL^{-1} can be reduced to < 0.5 ng mL^{-1} in seven days; Kang and Kondo, 2005), while BPS is significantly less biodegradable (Danzl et al., 2009; Ike et al., 2006). This could explain the lack of BPA in our samples, but other reasons cannot be excluded (e.g., differences in physicochemical properties or sorption behavior).

3.1.4. Relative importance of PAEs, OPEs and BPs in the Rhône River

A comparison with available scientific literature was made to assess the relative importance of PAE, OPE and BP concentrations compared to other anthropogenic dissolved organic compounds in the Rhône River (Figure 3). Using average concentrations, it was observed that bi-functional carboxylic acids (BCAs) represent 97% of dissolved organic compounds present in surface waters of the Rhône River. While BCAs in aquatic systems are not considered as typical contaminants, they can be generated from the incomplete combustion of fossil fuels, biomass burning and photooxidation of precursor organic compounds (Sempéré et al., 2018 and references therein) and their relative origin (natural versus anthropogenic) is not perfectly established in the aquatic ecosystem. The remaining 3% of organic compounds are mainly made up by pesticides and pesticide metabolites (PEST; 38.6%), PAEs (26.9%), aliphatic hydrocarbons (AHs; 14.6%), OPEs (13.5%) and polycyclic aromatic hydrocarbons

(PAHs; 4.9%). BPS, perfluorooctanoic acid (PFOA) and perfluorooctane sulfonate (PFOS) are minor contributors (<1% each).

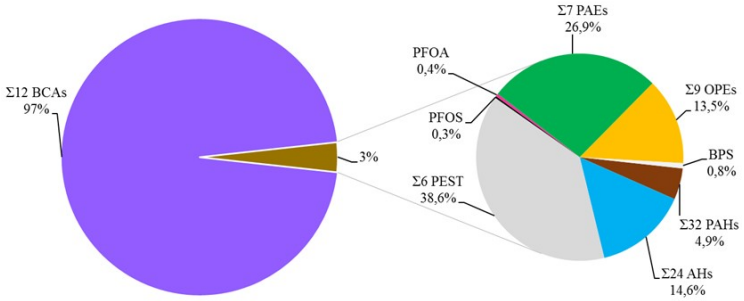

Abbreviation	*Full name*	*Reference*
BCAs	Bi-functional carboxylic acids	Sempéré et al., 2018
PAHs	Polycyclic aromatic hydrocarbons	Guigue et al., 2014
AHs	Aliphatic hydrocarbons	Guigue et al., 2014
PEST	Pesticides & metabolites	Slomberg et al., 2017
PFOS	Perfluorooctane sulfonate	Munoz et al., 2015
PFOA	Perfluorooctanoic acid	Munoz et al., 2015
PAEs	Phthalates	This study
OPEs	Organophosphate esters	This study
BPS	Bisphenol S	This study

Figure 3: Relative abundance (in %) of dissolved organic compounds in Rhône River surface waters.

3.2. Potential factors affecting contaminant variability

The highest contaminant concentrations observed in September 2017 do not correspond to the highest river discharge, nor to the maximum or minimum DOC, POC or PON concentrations. Actually, the September sample corresponded to one of the lowest river discharge values and to the higher values of water temperature registered during the sampling period. Temperature is known to be a key factor affecting the dissolved-particulate partition of semivolatile organic contaminants (Berrojalbiz et al., 2011). Higher water temperatures could have favored the partitioning of some of the organic additives towards the dissolved water phase, but since the particulate phase was not analyzed in this study, we cannot evaluate this. Furthermore, this situation was not observed for the months of June and August, which also had conditions of high temperature and low water discharge, suggesting that other factors (e.g.,

changes in emission sources, precipitation or water flow) are probably more important drivers. Moreover, high water temperatures are rather expected to stimulate PAE biodegradation processes (by increasing bacterial activity), and thus to lower PAE concentrations (Net et al., 2015a). High PAE concentrations observed in September, June and December (541, 513 and 483 ng L^{-1}, respectively) might also be due to peaks in plastic concentrations that may release PAEs into surrounding waters (Paluselli et al., 2019).

A correlation matrix (Table S4) confirmed the correlation between river discharge and POC and PON. Furthermore, DOC was positively correlated with river discharge and negatively correlated with water temperature. Σ OPEs was negatively correlated with DOC and positively correlated with water temperature. For Σ PAEs and BPS, no such correlation was observed, indicating that the three contaminant families are not influenced in the same manner by environmental drivers, such as temperature and DOC. When examining individual contaminants, TiBP was negatively correlated with water temperature. Water temperature could potentially be considered a proxy for seasonality, including primary production, UV intensity and recreational activities. Moreover, several individual contaminants were positively correlated (TCPP with DMP and DEHP, TPhP with DEHP, DMP with DEHP and DiBP with DnOP), indicating that they follow the same dynamics but are not necessarily (or not exclusively) forced by river discharge, water temperature or carbon and nitrogen concentrations in the water column. Most likely, a combination of various factors (including phenomena such as biotransformation and photolytic transformation, which were not investigated in this study) as well as varying contaminant inputs resulted in the temporal variability observed. A correlation between mean concentrations of target compounds and their corresponding log K_{ow} value was not observed (p-value > 0.05).

3.3. Fluxes and potential sources to the Rhône River and the Mediterranean Sea

We calculated daily fluxes of 10-116 kg, 5-31 kg and of 0.2-4 kg for PAEs, OPEs and BPS, respectively. Finally, using the same calculation method for all organic contaminants combined (Σ OPEs + Σ PAEs + Σ BPs), we achieved a daily flux of 15-149 kg. Table S5 summarizes the estimated fluxes. Assuming that this range of daily contaminant flux is representative for the whole year, an annual input ranging from 5 to 54 t of plastic additives is expected from the Rhône River to the Gulf of Lion in the NW Mediterranean Sea. Such kind of calculations have an important uncertainty associated with the large variation of contaminant concentrations depending on the pollution source (sporadic *vs.* chronic pollution) and environmental factors such as river flow (see section 3.2.), rain, UV radiation, temperature or pH (Li et al., 2017; Noyes et al., 2009). Furthermore, the contaminants associated with the particle water phase were not measured in our study, most likely leading to an underestimation of total contaminant fluxes, especially regarding hydrophobic substances.

Plastic debris can be a source of organic plastic additives through leaching (Net et al., 2015b). Recent estimations based on field observations of floating macro- and microplastics in the Rhône River suggested plastic fluxes of 0.73 t $year^{-1}$ and 0.07-7.8 t $year^{-1}$, respectively (Castro-Jiménez et al., 2019; Schmidt et al., 2018). Both studies focused on the observation of floating plastic debris only and included a limited amount of samples, but suggest that the additive concentrations in the dissolved water phase cannot be entirely explained by the leaching from floating plastic waste. Furthermore, a recent experimental study points to low PAE release rates from plastic materials (e.g., ~120 ng DnBP g^{-1} plastic bag after 4 weeks in dark, biotic conditions, Paluselli et al. (2019)), supporting this hypothesis, even though seawater was used in this study and similar experiments with riverine water remain yet to be done. However, non-floating plastic can also contribute to this "leaching source" and increasing evidence suggests

that this non-floating plastic burden is potentially more important than so far assumed (Karlsson et al., 2018; Van Sebille et al., 2015). In addition, other possible sources of contaminants to the Rhône River include inputs during the manufacturing of plastic materials, graywater and effluents from WWTPs and atmospheric deposition.

For the Mediterranean Sea, other important rivers, such as the Nile and Po rivers, could furthermore constitute important organic contaminant sources, alongside with highly inhabited and/or industrialized cities. Furthermore, atmospheric deposition has been confirmed as an efficient input pathway for OPEs in the Mediterranean Sea (Castro-Jiménez et al., 2014) and also in other marine environments (Castro-Jiménez et al., 2016). There are no available data from the atmospheric inputs of OPEs close to the Rhône area; however, recent estimations performed in another coastal site in the Western Mediterranean Sea point to dry deposition fluxes ranging from 18-180 ng m^{-2} d^{-1} for $\sum_9$ OPEs (Castro-Jiménez et al., 2018). If we consider these fluxes to be representative of Western Mediterranean coastal areas and extrapolate them to the whole Gulf of Lion (1.6 x 10^{10} m^2; Alekseenko et al., 2014), 0.1 to 1.1 t y^{-1} of OPEs (median value of 0.5 t y^{-1}) could be loaded from the atmosphere to the Gulf of Lion *via* dry deposition. However, a more representative assessment of the atmospheric inputs of plastic additives in the Gulf of Lion area, also including air-sea gas exchanges, is needed to constraint the uncertainty.

4. Conclusions

PAEs, OPEs and BPs were measured in dissolved phase surface waters from the Rhône River and detected in all samples, with DEHP and TCPP being the most abundant compounds. Temporal fluctuations in contaminant concentrations, which were not clearly linked to river discharge or other bulk parameters, were observed. A combination of sources such as WWTPs,

leaching from plastic debris, atmospheric deposition and the nuclear industry would most probably explain the occurrence of these organic contaminants in surface waters of the Rhône River. Rough flux estimations indicated that the Rhône River could be an important source of organic plastic additives *via* dissolved water phase transport to the NW Mediterranean Sea, which could certainly contribute to the contaminant cocktail potentially affecting the local food web, at least in the vicinity of the Rhône River mouth. However, data from other important rivers entering the Mediterranean Sea are needed for comparison. To the best of our knowledge, these are the first measurements of OPEs and BPS in the Rhône River, the main freshwater supplier of the Mediterranean Sea. Given the semi-enclosed nature of the Mediterranean Sea, the high anthropogenic pressure it receives and the scarcity of water resources in the Mediterranean, high contaminant fluxes *via* freshwater inputs could have more severe impacts on the ecosystem than they would have in the case of the global ocean.

Acknowledgements

Thanks to Michel Fornier for his help during sampling and Patrick Raimbault and the PAPB-MIO platform for POC and PON measurements. Thanks to METEO-FRANCE for precipitation data. Funding: the project leading to this publication was supported by the Agence de l'Eau Rhône Méditerranée Corse projects Blue-POLUT and Caremed, the JPI Oceans PLASTOX project and from European FEDER Fund under project 1166-39417.

References

Alekseenko, E., Raybaud, V., Espinasse, B., Carlotti, F., Queguiner, B., Thouvenin, B., Garreau, P., Baklouti, M., 2014. Seasonal dynamics and stoichiometry of the planktonic community in the Northwestern Mediterranean Sea: a 3D modeling approach. Ocean Dyn. 64, 179–207.

Andresen, J.A., Grundmann, A., Bester, K., 2004. Organophosphorus flame retardants and plasticisers in surface waters. Sci. Total Environ. 332, 155–166. https://doi.org/10.1016/j.scitotenv.2004.04.021

Bergé, A., Gasperi, J., Rocher, V., Gras, L., Coursimault, A., Moilleron, R., 2014. Phthalates and alkylphenols in industrial and domestic effluents: Case of Paris conurbation (France). Sci. Total Environ. 488–489, 26–35. https://doi.org/10.1016/j.scitotenv.2014.04.081

Berrojalbiz, N., Dachs, J., Ojeda, M.J., Valle, M.C., Castro-Jiménez, J., Wollgast, J., Ghiani, M., Hanke, G., Zaldivar, J.M., 2011. Biogeochemical and physical controls on concentrations of polycyclic aromatic hydrocarbons in water and plankton of the Mediterranean and Black Seas. Global Biogeochem. Cycles 25, 1–14. https://doi.org/10.1029/2010GB003775

Björnsdotter, M.K., Jonker, W., Legradi, J., Kool, J., Ballesteros-Gómez, A., 2017. Bisphenol A alternatives in thermal paper from the Netherlands, Spain, Sweden and Norway. Screening and potential toxicity. Sci. Total Environ. 601–602, 210–221. https://doi.org/10.1016/j.scitotenv.2017.05.171

Castro-Jiménez, J., Barhoumi, B., Tedetti, M., Sempéré, R., 2018. Atmospheric particle-bound organophosphate ester flame retardants and plasticizers in a North African Mediterranean coastal city (Bizerte, Tunisia). Sci. Total Environ. 642, 383–393. https://doi.org/10.1016/j.scitotenv.2018.06.010

Castro-Jiménez, J., Berrojalbiz, N., Pizarro, M., Dachs, J., 2014. Organophosphate ester (OPE) flame retardants and plasticizers in the open mediterranean and black seas atmosphere. Environ. Sci. Technol. 48, 3203–3209. https://doi.org/10.1021/es405337g

Castro-Jiménez, J., Casal, P., González-Gaya, B., Pizarro, M., Dachs, J., 2016. Organophosphate ester flame retardants and plasticizers in the global oceanic atmosphere. Environ. Sci. Technol 50, 12831–12839.

Castro-Jiménez, J., González-Fernández, D., Fornier, M., Schmidt, N., Sempéré, R., 2019. Macro-litter in surface waters from the Rhone River: Plastic pollution and flows to the NW Mediterranean Sea. Mar. Pollut. Bull. 146, 60–66. https://doi.org/10.1016/j.marpolbul.2019.05.067

Constant, M., Kerhervé, P., Sola, J., Sanchez-Vidal, A., Canals, M., Heussner, S., 2018. Floating microplastics in the northwestern Mediterranean Sea: temporal and spatial heterogeneities, in: Proceedings of the International Conference on Microplastic Pollution in the Mediterranean Sea, Springer International Publishing. pp. 9–15. https://doi.org/10.1007/978-3-319-71279-6

Coste, B., Raimbault, P., 1993. Recent data on the nutrient input into the Mediterranean Sea by the Rhône river. Water Res. 30, 47–50.

Cristale, J., García Vázquez, A., Barata, C., Lacorte, S., 2013. Priority and emerging flame retardants in rivers: Occurrence in water and sediment, Daphnia magna toxicity and risk assessment. Environ. Int. 59, 232–243. https://doi.org/10.1016/j.envint.2013.06.011

Danzl, E., Sei, K., Soda, S., Ike, M., Fujita, M., 2009. Biodegradation of bisphenol A, bisphenol F and bisphenol S in seawater. Int. J. Environ. Res. Public Health 6, 1472–1484. https://doi.org/10.3390/ijerph6041472

Deshayes, S., Eudes, V., Bigourie, M., Droguet, C., Moilleron, R., 2017. Alkylphenol and phthalate contamination of all sources of greywater from French households. Sci. Total Environ. 599–600, 883–890. https://doi.org/10.1016/j.scitotenv.2017.05.038

Domínguez-Morueco, N., González-Alonso, S., Valcárcel, Y., 2014. Phthalate occurrence in rivers and tap water from central Spain. Sci. Total Environ. 500–501, 139–146. https://doi.org/10.1016/j.scitotenv.2014.08.098

Fauvelle, V., Castro-Jiménez, J., Schmidt, N., Carlez, B., Panagiotopoulos, C., Sempéré, R., 2018. One-Single Extraction Procedure for the Simultaneous Determination of a Wide Range of Polar and Nonpolar Organic Contaminants in Seawater. Front. Mar. Sci. 5, 1–10. https://doi.org/10.3389/fmars.2018.00295

Fernández-Amado, M., Prieto-Blanco, M.C., López-Mahía, P., Muniategui-Lorenzo, S., Prada-Rodríguez, D., 2017. A comparative study of extractant and chromatographic phases for the rapid and sensitive determination of six phthalates in rainwater samples. Chemosphere 175, 52–65. https://doi.org/10.1016/j.chemosphere.2017.02.001

Fries, E., Püttmann, W., 2003. Monitoring of the three organophosphate esters TBP, TCEP and TBEP in river water and ground water (Oder, Germany). J. Environ. Monit. 5, 346–352. https://doi.org/10.1039/b210342g

Guigue, C., Tedetti, M., Ferretto, N., Garcia, N., Méjanelle, L., Goutx, M., 2014. Spatial and seasonal variabilities of dissolved hydrocarbons in surface waters from the Northwestern Mediterranean Sea: Results from one year intensive sampling. Sci. Total Environ. 466–467, 650–662. https://doi.org/10.1016/j.scitotenv.2013.07.082

Hahladakis, J.N., Velis, C.A., Weber, R., Iacovidou, E., Purnell, P., 2018. An overview of chemical additives present in plastics: Migration, release, fate and environmental impact during their use, disposal and recycling. J. Hazard. Mater. 344, 179–199. https://doi.org/10.1016/j.jhazmat.2017.10.014

Hermabessiere, L., Dehaut, A., Paul-Pont, I., Lacroix, C., Jezequel, R., Soudant, P., Duflos, G., 2017. Occurrence and effects of plastic additives on marine environments and organisms: A review. Chemosphere 182, 781–793. https://doi.org/10.1016/j.chemosphere.2017.05.096

Herrero, A., Vila, J., Eljarrat, E., Ginebreda, A., Sabater, S., Batalla, R.J., Barceló, D., 2018. Transport of sediment borne contaminants in a Mediterranean river during a high flow event. Sci. Total Environ. 633, 1392–1402. https://doi.org/10.1016/j.scitotenv.2018.03.205

Horton, A.A., Walton, A., Spurgeon, D.J., Lahive, E., Svendsen, C., 2017. Microplastics in freshwater and terrestrial environments: Evaluating the current understanding to identify the knowledge gaps and future research priorities. Sci. Total Environ. 586, 127–141. https://doi.org/10.1016/j.scitotenv.2017.01.190

Ike, M., Chen, M.Y., Danzl, E., Sei, K., Fujita, M., 2006. Biodegradation of a variety of bisphenols under aerobic and anaerobic conditions. Water Sci. Technol. 53, 153–159.

Jin, H., Zhu, L., 2016. Occurrence and partitioning of bisphenol analogues in water and sediment from Liaohe River Basin and Taihu Lake, China. Water Res. 103, 343–351. https://doi.org/10.1016/j.watres.2016.07.059

Kang, J.H., Kondo, F., 2005. Bisphenol A degradation in seawater is different from that in river water. Chemosphere 60, 1288–1292. https://doi.org/10.1016/j.chemosphere.2005.01.058

Karlsson, T.M., Hassellöv, M., Jakubowicz, I., 2018. Influence of thermooxidative degradation on the in situ fate of polyethylene in temperate coastal waters. Mar. Pollut. Bull. 135, 187–194. https://doi.org/10.1016/j.marpolbul.2018.07.015

León, V.M., García, I., González, E., Samper, R., Fernández-González, V., Muniategui-Lorenzo, S., 2018. Potential transfer of organic pollutants from littoral plastics debris to the marine environment. Environ. Pollut. 236, 442–453. https://doi.org/10.1016/j.envpol.2018.01.114

Li, R., Liang, J., Duan, H., Gong, Z., 2017. Spatial distribution and seasonal variation of phthalate esters in the Jiulong River estuary, Southeast China. Mar. Pollut. Bull. 122, 38–46. https://doi.org/10.1016/j.marpolbul.2017.05.062

Liu, Y., Song, N., Guo, R., Xu, H., Zhang, Q., Han, Z., Feng, M., Li, D., Zhang, S., Chen, J., 2018. Occurrence and partitioning behavior of organophosphate esters in surface water and sediment of a shallow Chinese freshwater lake (Taihu Lake): Implication for eco-toxicity risk. Chemosphere 202, 255–263. https://doi.org/10.1016/j.chemosphere.2018.03.108

Loos, R., Tavazzi, S., Mariani, G., Suurkuusk, G., Paracchini, B., Umlauf, G., 2017. Analysis of emerging organic contaminants in water, fish and suspended particulate matter (SPM) in the Joint Danube Survey using solid-phase extraction followed by UHPLC-MS-MS and GC–MS analysis. Sci. Total Environ. 607–608, 1201–1212. https://doi.org/10.1016/j.scitotenv.2017.07.039

Manikkam, M., Tracey, R., Guerrero-Bosagna, C., Skinner, M.K., 2013. Plastics Derived Endocrine Disruptors (BPA, DEHP and DBP) Induce Epigenetic Transgenerational Inheritance of Obesity, Reproductive Disease and Sperm Epimutations. PLoS One 8. https://doi.org/10.1371/journal.pone.0055387

Martínez-Carballo, E., González-Barreiro, C., Sitka, A., Scharf, S., Gans, O., 2007. Determination of selected organophosphate esters in the aquatic environment of Austria. Sci. Total Environ. 388, 290–299. https://doi.org/10.1016/j.scitotenv.2007.08.005

Miège, C., Peretti, A., Labadie, P., Budzinski, H., Le Bizec, B., Vorkamp, K., Tronczynski, J., Persat, H., Coquery, M., Babut, M., 2012. Occurrence of priority and emerging organic compounds in fishes from the Rhone River (France). Anal. Bioanal. Chem. 404, 2721–2735. https://doi.org/10.1007/s00216-012-6187-0

Munoz, G., Giraudel, J.L., Botta, F., Lestremau, F., Dévier, M.H., Budzinski, H., Labadie, P., 2015. Spatial distribution and partitioning behavior of selected poly- and perfluoroalkyl substances in freshwater ecosystems: A French nationwide survey. Sci. Total Environ. 517, 48–56. https://doi.org/10.1016/j.scitotenv.2015.02.043

Net, S., Rabodonirina, S., Sghaier, R. Ben, Dumoulin, D., Chbib, C., Tlili, I., Ouddane, B., 2015a. Distribution of phthalates, pesticides and drug residues in the dissolved, particulate and sedimentary phases from transboundary rivers (France–Belgium). Sci. Total Environ. 521–522, 152–159. https://doi.org/10.1016/j.scitotenv.2015.03.087

Net, S., Sempéré, R., Delmont, A., Paluselli, A., Ouddane, B., 2015b. Occurrence, fate, behavior and ecotoxicological state of phthalates in different environmental matrices. Environ. Sci. Technol. 49, 4019–4035. https://doi.org/10.1021/es505233b

Noyes, P.D., McElwee, M.K., Miller, H.D., Clark, B.W., Van Tiem, L.A., Walcott, K.C., Erwin, K.N., Levin, E.D., 2009. The toxicology of climate change: Environmental contaminants in a warming world. Environ. Int. 35, 971–986. https://doi.org/10.1016/j.envint.2009.02.006

Olivier, J., Lamouroux, N., Malard, F., Amoros, C., 2009. The Rhône River Basin. https://doi.org/10.1016/B978-0-12-369449-2.00007-2

Paluselli, A., Aminot, Y., Galgani, F., Net, S., Sempéré, R., 2018a. Occurrence of phthalate acid esters (PAEs) in the northwestern Mediterranean Sea and the Rhone River. Prog. Oceanogr. 163, 221–231. https://doi.org/10.1016/j.pocean.2017.06.002

Paluselli, A., Fauvelle, V., Galgani, F., Sempéré, R., 2019. Phthalate release from plastic fragments and degradation in seawater. Environ. Sci. Technol. 53, 166–175. https://doi.org/10.1021/acs.est.8b05083

Paluselli, A., Fauvelle, V., Schmidt, N., Galgani, F., Net, S., Sempéré, R., 2018b. Distribution of phthalates in Marseille Bay (NW Mediterranean Sea). Sci. Total Environ. 621, 578–587. https://doi.org/10.1016/j.scitotenv.2017.11.306

Panagiotopoulos, C., Sempéré, R., Para, J., Raimbault, P., Rabouille, C., Charrière, B., 2012. The composition and flux of particulate and dissolved carbohydrates from the Rhone River into the Mediterranean Sea. Biogeosciences 9, 1827–1844. https://doi.org/10.5194/bg-9-1827-2012

Pantelaki, I., Voutsa, D., 2019. Organophosphate flame retardants (OPFRs): A review on analytical methods and occurrence in wastewater and aquatic environment. Sci. Total Environ. 649, 247–263. https://doi.org/10.1016/j.scitotenv.2018.08.286

Para, J., Coble, P.G., Charrière, B., Tedetti, M., Fontana, C., Sempéré, R., 2010. Fluorescence and absorption properties of chromophoric dissolved organic matter (CDOM) in coastal surface waters of the northwestern Mediterranean Sea, influence of the Rhône River. Biogeosciences 7, 4083–4103.

Peijnenburg, W.J.G.M., Struijs, J., 2006. Occurrence of phthalate esters in the environment of the Netherlands. Ecotoxicol. Environ. Saf. 63, 204–215. https://doi.org/10.1016/j.ecoenv.2005.07.023

Pivnenko, K., Laner, D., Astrup, T.F., 2018. Dynamics of bisphenol A (BPA) and bisphenol S (BPS) in the European paper cycle: Need for concern? Resour. Conserv. Recycl. 133, 278–287. https://doi.org/10.1016/j.resconrec.2018.01.021

Pont, D., Simonnet, J.P., Walter, A. V., 2002. Medium-term changes in suspended sediment delivery to the ocean: Consequences of catchment heterogeneity and river management (Rhône River, France). Estuar. Coast. Shelf Sci. 54, 1–18. https://doi.org/10.1006/ecss.2001.0829

Quinnies, K.M., Harris, E.P., Snyder, R.W., Sumner, S.S., Rissman, E.F., 2017. Direct and transgenerational effects of low doses of perinatal Di-(2-ethylhexyl) phthalate (DEHP) on social behaviors in mice. PLoS One 12, 1–19. https://doi.org/10.1371/journal.pone.0171977

Raimbault, P., Garcia, N., Cerutti, F., 2008. Distribution of inorganic and organic nutrients in the South Pacific Ocean − evidence for long-term accumulation of organic matter in nitrogen-depleted waters. Biogeosciences 5, 281–298. https://doi.org/10.5194/bg-5-281-2008

Revathi, P., Saipriya, K., Kumar, C.K., Kumar, T., 2014. Determination of dissolved TBP in PUREX process aqueous streams using ICP-AES. J. Radioanal. Nucl. Chem. 300, 93–98. https://doi.org/10.1007/s10967-014-2994-4

Sánchez-Avila, J., Tauler, R., Lacorte, S., 2012. Organic micropollutants in coastal waters from NW Mediterranean Sea: Sources distribution and potential risk. Environ. Int. 46, 50–62. https://doi.org/10.1016/j.envint.2012.04.013

Schmidt, C., Krauth, T., Wagner, S., 2017. Export of Plastic Debris by Rivers into the Sea. Environ. Sci. Technol. 51, 12246–12253. https://doi.org/10.1021/acs.est.7b02368

Schmidt, N., Fauvelle, V., Ody, A., Castro-Jiménez, J., Jouanno, J., Changeux, T., Thibaut, T., Sempéré, R., 2019. The Amazon River: A Major Source of Organic Plastic Additives to the Tropical North Atlantic? Environ. Sci. Technol 53, 7513–7521. https://doi.org/https://doi.org/10.1021/acs.est.9b01585

Schmidt, N., Thibault, D., Galgani, F., Paluselli, A., Sempéré, R., 2018. Occurrence of microplastics in surface waters of the Gulf of Lion (NW Mediterranean Sea). Prog. Oceanogr. 163, 214–220. https://doi.org/10.1016/j.pocean.2017.11.010

Sempéré, R., Charrière, B., Castro-Jiménez, J., Kawamura, K., Panagiotopoulos, C., 2018. Occurrence of α, ω-dicarboxylic acids and ω-oxoacids in surface waters of the Rhone River and fluxes into the Mediterranean Sea. Prog. Oceanogr. 163, 136–146. https://doi.org/10.1016/j.pocean.2017.07.002

Sempéré, R., Charrière, B., Van Wambeke, F., Cauwet, G., 2000. Carbon inputs of the Rhône River to the Mediterranean Sea: Biogeochemical implications. Global Biogeochem. Cycles 14, 669–681. https://doi.org/10.1029/1999GB900069

Sempéré, R., Tedetti, M., Panagiotopoulos, C., Charrière, B., Van Wambeke, F., 2008. Distribution and bacterial availability of dissolved neutral sugars in the South East Pacific. Biogeosciences 5, 1165–1173.

Slomberg, D.L., Ollivier, P., Radakovitch, O., Baran, N., Sani-Kast, N., Bruchet, A., Scheringer, M., Labille, J., 2017. Insights into natural organic matter and pesticide characterisation and distribution in the Rhone River. Environ. Chem. 14, 64–73. https://doi.org/10.1071/EN16038

Struglia, M.V., Mariotti, A., Filograsso, A., 2004. River discharge into the Mediterranean sea: Climatology and aspects of the observed variability. J. Clim. 17, 4740–4751. https://doi.org/10.1175/JCLI-3225.1

Teil, M.J., Blanchard, M., Chevreuil, M., 2006. Atmospheric fate of phthalate esters in an urban area (Paris-France). Sci. Total Environ. 354, 212–223. https://doi.org/10.1016/j.scitotenv.2004.12.083

Teil, M.J., Blanchard, M., Dargnat, C., Larcher-Tiphagne, K., Chevreuil, M., 2007. Occurrence of phthalate diesters in rivers of the Paris district (France). Hydrol. Process. 21, 2515–2525. https://doi.org/10.1002/hyp

Tran, B.C., Teil, M.J., Blanchard, M., Alliot, F., Chevreuil, M., 2015. BPA and phthalate fate in a sewage network and an elementary river of France. Influence of hydroclimatic conditions. Chemosphere 119, 43–51. https://doi.org/10.1016/j.chemosphere.2014.04.036

Van Sebille, E., Wilcox, C., Lebreton, L., Maximenko, N., Hardesty, B.D., Van Franeker, J.A., Eriksen, M., Siegel, D., Galgani, F., Law, K.L., 2015. A global inventory of small floating plastic debris. Environ. Res. Lett. 10, 124006. https://doi.org/10.1088/1748-9326/10/12/124006

Wang, R., Tang, J., Xie, Z., Mi, W., Chen, Y., Wolschke, H., Tian, C., Pan, X., Luo, Y., Ebinghaus, R., 2015. Occurrence and spatial distribution of organophosphate ester flame retardants and plasticizers in 40 rivers draining into the Bohai Sea, north China. Environ. Pollut. 198, 172–178. https://doi.org/10.1016/j.envpol.2014.12.037

Wei, G.L., Li, D.Q., Zhuo, M.N., Liao, Y.S., Xie, Z.Y., Guo, T.L., Li, J.J., Zhang, S.Y., Liang, Z.Q., 2015. Organophosphorus flame retardants and plasticizers: Sources, occurrence, toxicity and human exposure. Environ. Pollut. 196, 29–46. https://doi.org/10.1016/j.envpol.2014.09.012

Wolschke, H., Sühring, R., Xie, Z., Ebinghaus, R., 2015. Organophosphorus flame retardants and plasticizers in the aquatic environment: A case study of the Elbe River, Germany. Environ. Pollut. 206, 488–493. https://doi.org/10.1016/j.envpol.2015.08.002

Wong, Y.M., Li, R., Lee, C.K.F., Wan, H.T., Wong, C.K.C., 2017. The measurement of bisphenol A and its analogues, perfluorinated compounds in twenty species of freshwater and marine fishes, a time-trend comparison and human health based assessment. Mar. Pollut. Bull. 124, 743–752. https://doi.org/10.1016/j.marpolbul.2017.05.046

Yamazaki, E., Yamashita, N., Taniyasu, S., Lam, J., Lam, P.K.S., Moon, H.B., Jeong, Y., Kannan, P., Achyuthan, H., Munuswamy, N., Kannan, K., 2015. Bisphenol A and other bisphenol analogues including BPS and BPF in surface water samples from Japan, China, Korea and India. Ecotoxicol. Environ. Saf. 122, 565–572. https://doi.org/10.1016/j.ecoenv.2015.09.029

CHAPTER III:
Perfluorinated compounds

Marine Pollution Bulletin 149 (2019) 110491

Contents lists available at ScienceDirect

Marine Pollution Bulletin

journal homepage: www.elsevier.com/locate/marpolbul

Occurrence of perfluoroalkyl substances in the Bay of Marseille (NW Mediterranean Sea) and the Rhône River

Natascha Schmidt[a], Vincent Fauvelle[a], Javier Castro-Jiménez[a,*], Katixa Lajaunie-Salla[a], Christel Pinazo[a], Christophe Yohia[b], Richard Sempéré[a,*]

[a] Aix-Marseille Univ., Toulon Univ., CNRS, IRD, Mediterranean Institute of Oceanography (MIO), Marseille, France
[b] Aix-Marseille Univ., Toulon Univ., CNRS, IRD, OSU-Intitut Pytheas, Marseille, France

ARTICLE INFO

Keywords:
Perfluorooctane sulfonate (PFOS)
Perfluorohexanoic acid (PFHxA)
Environmental Quality Standard
Surface water pollution
Mediterranean Sea

ABSTRACT

Four perfluoroalkyl substances (PFAS) were analyzed in 62 duplicate surface water samples from the Rhône River and Marseille Bay (France; NW Mediterranean Sea). Perfluorooctane sulfonate (PFOS) was detected in all samples and exceeded the European Environmental Quality Standard (EQS) values in over 80% of the cases. The most contaminated samples were from the Rhône River (up to 200 ng L^{-1} Σ_4 PFAS), as well as those collected near a wastewater treatment plant outlet in Marseille Bay (up to 9 ng L^{-1} Σ_4 PFAS). While PFOS was the predominant PFAS in Marseille Bay, remarkably high concentrations of perfluorohexanoic acid (PFHxA) were measured in the Rhône River (8–193 ng L^{-1}). The relative abundances of individual compounds differed thus significantly between the Rhône River and Marseille Bay, indicating different sources. A simulation made with the MARS3D model showed that PFOS inputs from the Rhône River can enter Marseille Bay at levels > EQS.

1. Introduction

Perfluoroalkyl substances (PFAS) are a group of chemicals containing carbon-fluorine bonds, with varying perfluoroalkyl chain lengths. They show water and oil repellent properties and are used in a wide variety of application sectors: from textiles, inks and varnishes to firefighting foams (aqueous film forming foams, AFFFs) and for metal plating (Paul et al., 2009). They are also used as additives in pesticides (Sánchez-Avila et al., 2010). Perfluorooctane sulfonate (PFOS) is a widely used PFAS, which has been detected in freshwater and marine environments as well as in biota and humans (Earnshaw et al., 2014; Kärrman et al., 2007; Naile et al., 2010; Sánchez-Avila et al., 2010). Historically, the US enterprise 3 M™ was the main producer of PFOS, but in 2000 the company declared to phase PFOS out. Since the demand for PFOS and PFOS-related compounds remained high, this phase-out led to a dramatic increase in the production of these chemicals in China (Lim et al., 2011). PFOS has been identified as a Persistent Organic Pollutant (POP) and was thus included in the Annex B of the Stockholm Convention in 2010, leading to restrictions in use and production. While PFOS in the environment can originate directly from industrial production and consumer goods, it can also be the result of degradation of its precursors. PFOS-precursors are usually substituted perfluorooctyl sulfonamides and a high variety of structures and degradation pathways exists (Asher et al., 2012). Perfluorooctanoic acid (PFOA) is another highly persistent PFAS under natural conditions. In addition to historical uses, PFOA can be generated from degradation of long-chain fluorotelomer precursor types and perfluorooctane amide related compounds (Dasu et al., 2012; Mejia-Avendaño et al., 2016).

Growing evidence suggests toxicological effects of PFOS and PFOA on a variety of organisms (Hagenaars et al., 2008; Xia et al., 2014; Zhang et al., 2013). For example, it is suggested that PFOS exposure (depending on exposure time and concentration levels) can lead to epigenetic changes in sea urchins and affect the cardiac development in fish (Ding et al., 2015; Huang et al., 2011). Annual average Environmental Quality Standards (EQS) have thus been derived for biota (9.1 μg kg^{-1} biota wet weight), freshwater (0.00065 μg L^{-1}) and marine waters (0.00013 μg L^{-1}) in the European Union (Directive 2013/39/EU).

The Bay of Marseille in the NW Mediterranean Sea is subject to different anthropogenic pressures including touristic activity on the coastline (especially during high season in summer) recreational and commercial activities in the Old Harbor ("Vieux Port"), as well as ferry, leisure and commercial harbors (e.g., at L'Estaque). Additionally, the local wastewater treatment plant rejects from 0.4 to 3.8 m^3 s^{-1} wastewater (Oursel et al., 2013) into the sea at its outlet (Cortiou) eastwards of the city in the Calanques National Park. At Cortiou, the small rivers

* Corresponding authors.
E-mail addresses: javier.castro-jimenez@mio.osupytheas.fr (J. Castro-Jiménez), richard.sempere@mio.osupytheas.fr (R. Sempéré).

https://doi.org/10.1016/j.marpolbul.2019.110491
Received 2 July 2019; Received in revised form 2 August 2019; Accepted 2 August 2019
Available online 08 August 2019
0025-326X/ © 2019 Elsevier Ltd. All rights reserved.

Occurrence of perfluorinated compounds in the Bay of Marseille (NW Mediterranean Sea) and the Rhône River

Natascha Schmidt [a], Vincent Fauvelle [a], Javier Castro-Jiménez [a,*], Katixa Lajaunie-Salla [a], Christel Pinazo [a], Christophe Yohia [b], Richard Sempéré [a,*]

[a] *Aix-Marseille Univ., Toulon Univ., CNRS, IRD, Mediterranean Institute of Oceanography (M I O), Marseille, France*

[b] *Aix-Marseille Univ., Toulon Univ., CNRS, IRD, OSU-Intitut Pytheas, Marseille, France*

* *corresponding authors*

Richard Sempéré, mail: richard.sempere@mio.osupytheas.fr

Javier Castro-Jiménez, mail: javier.castro-jimenez@mio.osupytheas.fr

Abstract

Four perfluoroalkyl substances (PFAS) were analyzed in 62 duplicate surface water samples from the Rhône River and Marseille Bay (France; NW Mediterranean Sea). Perfluorooctane sulfonate (PFOS) was detected in all samples and exceeded the European Environmental Quality Standard (EQS) values in over 80% of the cases. The most contaminated samples were from the Rhône River (up to 200 ng L^{-1} $\sum_4$ PFAS), as well as those collected near a wastewater treatment plant outlet in Marseille Bay (up to 9 ng L^{-1} $\sum_4$ PFAS). While PFOS was the predominant PFAS in Marseille Bay, remarkably high concentrations of perfluorohexanoic acid (PFHxA) were measured in the Rhône River (8-193 ng L^{-1}). The relative abundances of individual compounds differed thus significantly between the Rhône River and Marseille Bay, indicating different sources. A simulation made with the MARS3D model showed that PFOS inputs from the Rhône River can enter Marseille Bay at levels > EQS.

Keywords: Perfluorooctane sulfonate (PFOS), Perfluorohexanoic acid (PFHxA), Environmental Quality Standard, surface water pollution, Mediterranean Sea

1. **Introduction**

Perfluoroalkyl substances (PFAS) are a group of chemicals containing carbon-fluorine bonds, with varying perfluoroalkyl chain lengths. They show water and oil repellent properties and are used in a wide variety of application sectors: from textiles, inks and varnishes to firefighting foams (aqueous film forming foams, AFFFs) and for metal plating (Paul et al., 2009). They are also used as additives in pesticides (Sánchez-Avila et al., 2010). Perfluorooctane sulfonate (PFOS) is a widely used PFAS, which has been detected in

freshwater and marine environments as well as in biota and humans (Earnshaw et al., 2014; Kärrman et al., 2007; Naile et al., 2010; Sánchez-Avila et al., 2010). Historically, the US enterprise 3M™ was the main producer of PFOS, but in 2000 the company declared to phase PFOS out. Since the demand for PFOS and PFOS-related compounds remained high, this phase-out led to a dramatic increase in the production of these chemicals in China (Lim et al., 2011). PFOS has been identified as a Persistent Organic Pollutant (POP) and was thus included in the Annex B of the Stockholm Convention in 2010, leading to restrictions in use and production. While PFOS in the environment can originate directly from industrial production and consumer goods, it can also be the result of degradation of its precursors. PFOS-precursors are usually substituted perfluorooctyl sulfonamides and a high variety of structures and degradation pathways exists (Asher et al., 2012). Perfluorooctanoic acid (PFOA) is another highly persistent PFAS under natural conditions. In addition to historical uses, PFOA can be generated from degradation of long-chain fluorotelomer precursor types and perfluorooctane amide related compounds (Dasu et al., 2012; Mejia-Avendaño et al., 2016).

Growing evidence suggests toxicological effects of PFOS and PFOA on a variety of organisms (Hagenaars et al., 2008; Xia et al., 2014; Zhang et al., 2013). For example, it is suggested that PFOS exposure (depending on exposure time and concentration levels) can lead to epigenetic changes in sea urchins and affect the cardiac development in fish (Ding et al., 2015; Huang et al., 2011). Annual average Environmental Quality Standards (EQS) have thus been derived for biota (9.1 µg kg^{-1} biota wet weight), freshwater (0.00065 µg L^{-1}) and marine waters (0.00013 µg L^{-1}) in the European Union (Directive 2013/39/EU).

The Bay of Marseille in the NW Mediterranean Sea is subject to different anthropogenic pressures including touristic activity on the coastline, (especially during high season in summer) recreational and commercial activities in the Old Harbor ("Vieux Port"), as well as ferry, leisure and commercial harbors (e.g., at L'Estaque). Additionally, the local wastewater treatment plant

rejects from 0.4 to 3.8 $m^3 s^{-1}$ wastewater (Oursel et al., 2013) into the sea at its outlet (Cortiou) eastwards of the city in the Calanques National Park. At Cortiou, the small rivers Huveaune and Jarret (1-5 $m^3 s^{-1}$ and 0.5-3 $m^3 s^{-1}$, respectively, Oursel et al., 2013) also enter the Mediterranean Sea, except during strong rain events, when the river water is deviated. The Bay of Marseille, and more generally the Gulf of Lions, is also subject to high solar radiation (Sempéré et al., 2015) and strong wind regimes, which often make plant and plastic debris accumulate on the coast. Depending on wind forcing (among other factors), the Bay of Marseille can also be influenced by the Rhône River *via* freshwater intrusions (Fraysse et al., 2014; Gatti et al., 2006; Para et al., 2010).

The Rhône River is the main freshwater source of the Mediterranean Sea since the damming of the Nile River and a major carbon source (Sempéré et al., 2000). It is 816 km long and has an average annual water discharge of 53×10^9 m^3. The Rhône River has been strongly modified by human activities (e.g., dams, wastewater treatment plant inputs, hydro-electrical facilities) and has a history of polychlorinated biphenyls (PCB) contamination (Mourier et al., 2014). Recent studies also detected organic contaminants of emerging concern in its waters, such as phthalates and organophosphate esters (Paluselli et al., 2018; Schmidt et al., submitted), along with micro- and macroplastics (Castro-Jiménez et al., 2019; Schmidt et al., 2018). Furthermore, various PFAS have been found in aquatic plants, benthic invertebrates and different fish species from the Rhône River (Babut et al., 2017), and Miège et al. (2012) showed that more than two-thirds of fishes analyzed had PFOS concentrations above the EQS.

The objectives of this study were: (1) to investigate the waterborne occurrence of PFOS and three other PFAS (perfluorohexanoic acid -PFHxA-, perfluorohexane sulfonic acid -PFHxS- and perfluorooctanoic acid -PFOA-) in the Rhône River and Marseille Bay; (2) to perform a local risk assessment by comparing the measured concentrations with the annual

average EQS values for water and; (3) to investigate the PFOS inputs into the Gulf of Lions and the Bay of Marseille associated to freshwater intrusion from the Rhône River by using a modelling approach.

2. Materials & Methods

2.1. Study area and sampling

Surface water samples (1 L) were collected from April 2017 to April 2018 in duplicate in the Rhône River at Arles city (n = 2 × 13) and at three sampling stations in Marseille Bay: L'Estaque harbor (n = 2 × 6), Frioul island (n = 2 × 6) and WWTP-Cortiou (n = 2 × 6) (Fig. 1) using a stainless steel collector, poured into corresponding 1 L glass bottles and filtered (GF/F, 0.7 µm retention size; Whatman, Maidstone, UK) within three hours after collection and either stored at 4 °C in the dark and extracted within 24 h or otherwise stored at -25 °C until sample processing. River water temperature was measured using a handheld electronic thermometer whereas river flow data were extracted from "Banque Hydro" (http://www.hydro.eaufrance.fr/). The river flow data used originates from a measuring station in Tarascon, about 16 km upstream of Arles. Since the Rhône River divides into two branches downstream of the flow-measuring station, but upstream of the water sampling station, it was considered that the river flow at the water sampling station corresponds to about 90 percent (Sempéré et al., 2000) of the flow measured in Tarascon.

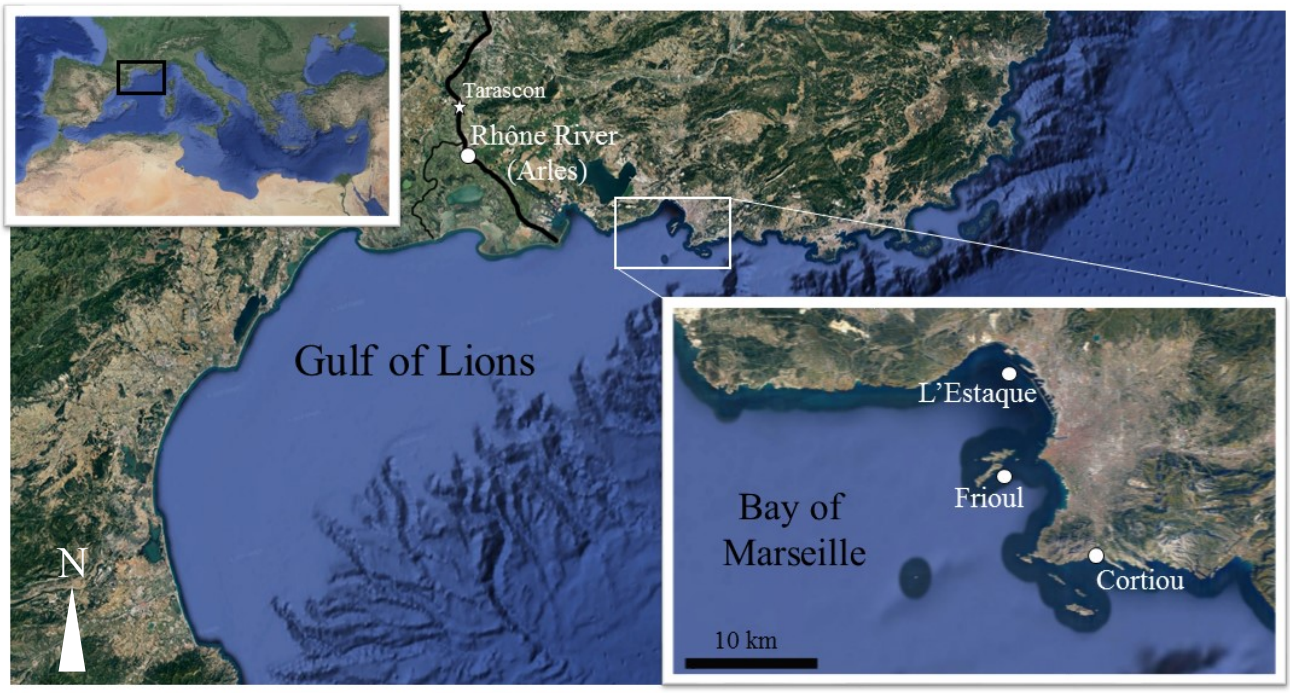

Figure 1: Google Earth map of the study area in the Gulf of Lions (northwestern Mediterranean Sea, see upper left corner). The position of the river flow measuring station in the commune of Tarascon is indicated as well as the trace of the Rhône River and the sampling station in Arles city. A zoom of the Bay of Marseille (lower right corner) indicates the three marine sampling stations including L'Estaque harbor, Frioul island and WWTP-Cortiou.

2.2. Chemicals and standards

Hexane, dichloromethane and acetone (used to pre-clean the SPE cartridges) were purchased from Promochem (Picograde, LGC standard) together with ethyl acetate. Methanol was provided by Biosolve (ULC-MS grade), whereas ultrapure water was obtained from a Millipore (resistivity > 18.2 MΩ) Milli-Q system. Native PFAS were obtained from AccuStandard (USA) and isotope labeled PFAS (internal standards) from Wellington Laboratories (Canada). SPE glass cartridges were prepared in the laboratory using 250 mg hydrophilic-lipophilic balance (HLB) Oasis ® (30 µm) bulk sorbent (Waters, Milford, USA).

2.3. Chemical analysis

Dissolved water phase samples were processed by solid phase extraction (SPE), using a method modified after Fauvelle et al. (2018) and analyzed for four PFAS (Fig. S1). Briefly, the filtrated water samples were vigorously shaken and passed through pre-cleaned glass cartridges using pre-cleaned polytetrafluoroethylene (PTFE) liners. Afterwards, 10 mL of ultrapure water were passed through the cartridges, which were then vacuum dried for two hours. PFAS were eluted by using 5 mL of ethyl acetate followed by 5 mL of methanol. The extracts were then evaporated with pure N_2 gas until dryness and reconstituted using 990 µL methanol. Twenty ng sample^{-1} of PFHxA-$^{13}C_5$ and PFOS-$^{13}C_8$ were added as internal standards. PFAS were quantified using a LC-QTOF (Agilent 1290 Infinity LC system coupled with Agilent 6530 Accurate-Mass Q-TOF, Agilent Technologies, Les Ulis, France). Separation was achieved using an Agilent Zorbax Eclipse XDB reversed phase column (50 mm x 2.1 mm, 1.8 µm), with temperature set at 30 °C. Quantification was performed using the isotope dilution method, considering the native analyte to internal standard area ratio and solvent-based calibration curves. Instrumental details are available in the Supplementary Material (Text S1, Table S2).

Dissolved organic carbon (DOC) was measured from filtered (GF/F, 0.7 µm), acidified (by 20 µL of 85% H_3PO_4 acid) subsamples using a Shimadzu TOC-5000 carbon analyzer (Sempéré et al., 2008). The instrument blank (≤ 5 µM) was subtracted from all measured results. All organic contaminant and DOC analysis were conducted in duplicate. The GF/F filters used for particulate organic carbon (POC) and nitrogen (PON) analysis were acidified with 50 µL H_2SO_4 (0.5 N) to remove inorganic carbon. POC and PON measurements were obtained using high combustion (1000 °C) on a CN Integra mass spectrometer (SERCON), calibrated using glycine references for every batch of 10–15 samples (Raimbault et al., 2008).

2.4. Quality Assurance / Quality Control (QA/QC)

The whole procedure was conducted in an International Standards Organization (ISO) 6 cleanroom and strict QA/QC procedures were implemented. All glass materials and the GF/F filters were baked (450 °C, 6 h) prior to use. Given that PTFE might be a source of PFAS (at least at high temperatures; Schlummer et al. (2015)), its use was limited to SPE sample loading lines and each PFTE line was cleaned thoroughly with MeOH prior to use in order to avoid sample contamination. Replicate blanks were made during each extraction and no contamination was detected in any of the blanks. Method recoveries obtained during a previous method validation ranged from 73 ± 14 (PFHxS) to 124 ± 5 (PFOA) percent (Fauvelle et al., 2018). Method limits of quantification ranged from 0.10 (PFOS) to 8.00 (PFHxA) ng L^{-1}. Concerning the linearity performance of the quantitative method, the linearity range was 0.5-200 ng mL^{-1} for the calibration curve, the R^2 varied from 0.997 (PFHxS) to 0.999 (PFOS) and the slope RSD ranged from 2.3% (PFOS) to 5.1% (PFHxS). Samples were collected in duplicates and the concentrations of duplicates were averaged.

2.5. Hydrodynamic model (MARS3D)

The hydrodynamic model used to study the PFAS inputs from the Rhône River into the eastern Gulf of Lions was the three-dimensional MARS3D model (3D hydrodynamic Model for Applications at Regional Scale, IFREMER) as described in detail by Lazure and Dumas (2008). The high resolution MARS3D-RHOMA configuration was applied and validated for the simulation of oceanic circulation (Pairaud et al., 2011) and the biogeochemical processes of the Bay of Marseille by Fraysse et al. (2013) and was then used to reproduce realistic, observed conditions (Fraysse et al., 2014; Ross et al., 2016). The model domain covered an area of 100 km x 48 km between the mouth of the Rhône River and Cape Sicié (Figure S2), with a

horizontal resolution of 400 m and 30 sigma vertical levels. The model takes into account the forcing through the NW Mediterranean general circulation, on the basis of a nesting strategy with the large scale MARS3D-MENOR configuration (1.2 km resolution) (Nicolle et al., 2009). It is forced by the Rhône River discharge, and by atmospheric conditions of the year 2017, with a spatially homogenous wind reproducing the temporal evolution simulated at the SOLEMIO station in Marseille Bay (Figure S2) thanks to the meteorological WRF-ARW model, which was described in detail by Klemp et al. (2007). The high resolution of the WRF-ARW configuration was applied for the atmospheric circulation and reproduced realistic conditions (Yohia, 2017). The model covers an area of 864 km by 1400 km with a resolution of 2 km and is forced by the GFS model (NCEP/NOAA).

The simulation was run for the year 2017 using inputs of PFAS concentrations measured in the Rhône River during field campaigns in between April 12th and December 12th (data from Table 1).

3. Results and discussion

3.1. Σ_4 PFAS concentrations and estimated flux to the Mediterranean Sea

Total PFAS concentrations were higher in the Rhône River (ranging from 13 to 200 ng L^{-1}) than in Marseille Bay (0.11-9 ng L^{-1}); the lowest concentration (0.11 ng L^{-1}) being detected in the Bay of Marseille (L'Estaque and Frioul stations; Table 1). Although the highest Σ_4 PFAS concentration observed in Marseille Bay was 9 ng L^{-1} near the Marseille-Cortiou-WWTP outlet, the concentrations were lower than those detected in the Rhône River. This could indicate that riverine sources are generally more important than coastal sources, that relatively low amounts of PFAS enter the WWTP, that an important dilution effect occurs after the wastewater enters the sea, or that the applied treatments efficiently remove important quantities of PFAS from the

wastewater before releasing it into the sea. While it is difficult to clearly name the source of the high PFAS concentrations detected in the Rhône River, one possible explanation could be the textile industry. PFAS are commonly used for technical and outdoor clothing, and the Rhône-Alpes region is leading the French textile industry with 712 companies and more than 15 000 workers (UNITEX, http://medef-aura.fr/rhone-alpes-premiere-region-textile-francaise.html).

Table 1: PFAS concentrations (in ng L^{-1}) measured in surface waters of the Rhône River and Marseille Bay. Asterisks indicate that the measured PFOS concentration exceeded the fresh- and seawater EQSs of 0.65 ng L^{-1} (Rhône River) or 0.13 ng L^{-1} (Cortiou, L'Estaque and Frioul).

Station	*Date*	*PFOS*	*PFHxA*	*PFHxS*	*PFOA*	*Σ*
Rhône River	12/04/2017	2.97 *	191	1.23	2.27	**198**
Rhône River	23/05/2017	3.68 *	27	1.01	n.d.	**32**
Rhône River	22/06/2017	4.57 *	104	1.60	2.32	**112**
Rhône River	12/07/2017	3.13 *	69	1.58	2.68	**76**
Rhône River	24/08/2017	3.39 *	76	1.67	2.92	**84**
Rhône River	19/09/2017	4.53 *	154	2.23	3.10	**164**
Rhône River	03/11/2017	3.48 *	11	1.33	2.06	**18**
Rhône River	30/11/2017	3.72 *	108	1.54	2.81	**116**
Rhône River	12/12/2017	2.53 *	87	1.41	2.35	**93**
Rhône River	05/01/2018	1.80 *	8	0.47	2.58	**13**
Rhône River	13/02/2018	2.60 *	14	1.14	2.19	**20**
Rhône River	01/03/2018	3.29 *	193	0.63	3.21	**200**
Rhône River	09/04/2018	2.27 *	17	0.63	1.87	**22**
Cortiou (WWTP outlet)	09/05/2017	3.44 *	n.d.	2.93	2.38	**9**
Cortiou (WWTP outlet)	06/07/2017	1.79 *	n.d.	2.80	n.d.	**4.6**
Cortiou (WWTP outlet)	08/09/2017	1.26 *	n.d.	1.59	n.d.	**2.9**
Cortiou (WWTP outlet)	15/11/2017	1.68 *	n.d.	2.10	n.d.	**3.8**
Cortiou (WWTP outlet)	24/01/2018	1.52 *	n.d.	1.53	2.46	**5.5**
Cortiou (WWTP outlet)	20/03/2018	1.02 *	<LOQ	0.86	n.d.	**1.9**
L'Estaque harbor	09/05/2017	0.25 *	n.d.	0.18	n.d.	**0.43**
L'Estaque harbor	06/07/2017	0.12	n.d.	n.d.	n.d.	**0.12**
L'Estaque harbor	08/09/2017	0.16 *	n.d.	0.15	n.d.	**0.31**
L'Estaque harbor	15/11/2017	0.11	n.d.	n.d.	n.d.	**0.11**
L'Estaque harbor	24/01/2018	0.17 *	n.d.	0.14	n.d.	**0.31**
L'Estaque harbor	20/03/2018	0.15 *	n.d.	n.d.	0.18	**0.33**
Frioul island	09/05/2017	0.16 *	n.d.	0.15	n.d.	**0.31**
Frioul island	06/07/2017	0.11	n.d.	n.d.	n.d.	**0.11**
Frioul island	08/09/2017	0.45 *	n.d.	0.14	n.d.	**0.59**
Frioul island	15/11/2017	0.12	n.d.	n.d.	n.d.	**0.12**
Frioul island	24/01/2018	0.12	n.d.	n.d.	n.d.	**0.12**
Frioul island	20/03/2018	0.35 *	n.d.	n.d.	n.d.	**0.35**

To roughly estimate the flux of PFAS into the NW Mediterranean Sea, the measured concentrations of each sampling event were multiplied with the corresponding daily river discharge. The estimated daily dissolved water phase Σ_4 PFAS flux from the Rhône River into the Mediterranean Sea varies thus between 0.72 and 27 kg day^{-1} (Fig. 2). The high variability results hereby from the high variability in measured PFAS concentrations and the high temporal fluctuations of the river discharge (between 460 and 3960 m^3 s^{-1} on sampling events). While the river discharge had important temporal fluctuations, we counted six sampling events with a discharge < 1000 m^3 s^{-1} and seven sampling events with a discharge > 1000 m^3 s^{-1} (three of which were > 2000 m^3 s^{-1}), indicating a relatively good equilibrium of samples taken in situations of low and high water discharge. Still, the calculated flux can only be considered as a limited, rough estimation, but it gives a first idea of PFAS inputs from the dissolved phase of the Rhône River to the Mediterranean Sea. For individual compounds we calculated fluxes of 4.13-18 kg $month^{-1}$ (PFOS), 2.45-27 kg $month^{-1}$ (PFOA; not taking into account the one sampling date when PFOA was not detected), 13-783 kg $month^{-1}$ (PFHxA) and 1.59-10 kg $month^{-1}$ (PFHxS) when considering one month as equal to 30 days.

3.2. Relative abundances of individual compounds

In the Rhône River, the predominant compound was PFHxA, with its relative abundance varying between 62-97%, while PFHxS was the least abundant compound with <1-7%. PFOS made up for 2-19% of the sample composition in the Rhône River. Interestingly, Miège et al. (2012) did not detect any PFHxA in their fish samples from the Rhône River (PFOS was most abundant in their samples), indicating that the relative abundances of PFAS in biota and water samples can be very different, possibly due to the different bioaccumulation potential of individual PFAS, in relation to their different perfluoroalkyl chain length (Simmonet-Laprade

et al., 2019). In contrast, in Marseille Bay PFOS was generally dominating the PFAS composition with 16-54% (WWTP-Cortiou), 45-100% (L'Estaque harbor) and 52-100% (Frioul island). Furthermore, PFHxS had sometimes a relatively high relative abundance with 14-61% in WWTP-Cortiou and 0-48% in L'Estaque and Frioul stations. PFOA was never detected in Frioul, once in L'Estaque station (with 55% relative abundance) and twice in WWTP-Cortiou (27% and 45% relative abundance). In the Rhône River PFOA abundance varied between 0-20% (Fig. 2). These results clearly indicate net differences in the relative abundance of PFAS in waters from Marseille Bay and the Rhône River, suggesting different sources and/or environmental processes. Moreover, WWTP-Cortiou exhibits a different pattern than the other two marine stations, with higher Σ_4 PFAS concentrations and differing relative abundances (lower PFOS abundance; PFHxS abundance always > 0). This is probably due to specific WWTP related PFAS inputs at the WWTP outlet, but it also indicates that Σ_4 PFAS compound composition can be variable at a small spatial scale and that the WWTP outlet does not necessarily have an influence on PFAS occurrence and abundance in the inner Bay of Marseille, even though this needs further investigations.

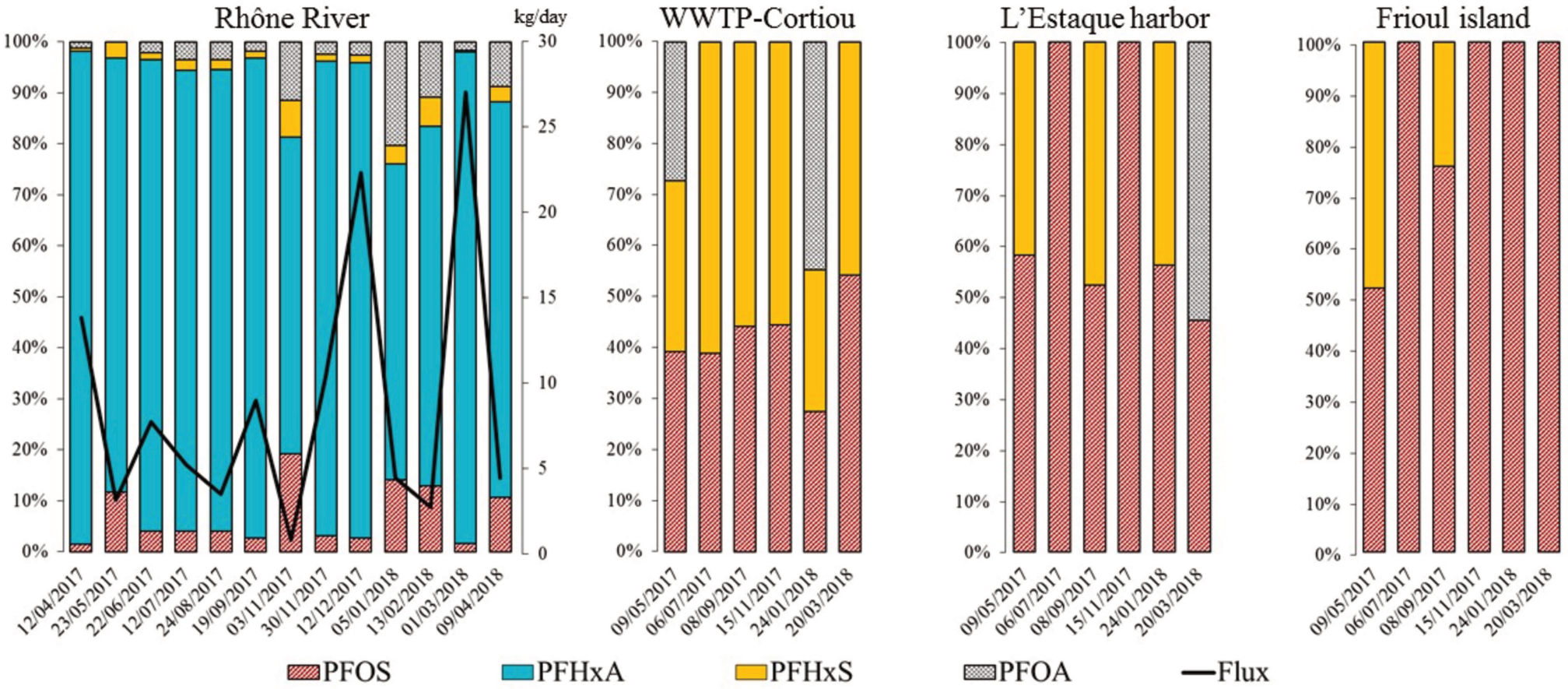

Figure 2: Relative abundances (in %) of the four PFAS at each sampling date at the four sites. For the Rhône River, the black line indicates the estimated daily flux (in kg day^{-1}) of Σ_4 PFAS into the Mediterranean Sea.

In the riverine samples, PFHxA was found at concentrations of 8-193 ng L^{-1} (Table 1). Our maximum PFHxA concentration detected is about 20 times higher than the one observed in the Danube River by Loos et al. (2017) (max. 8.5 ng L^{-1}) and more than two-fold the highest amount measured by Munoz et al. (2015) during a French nationwide survey comprising 333 freshwater samples (max. 86 ng L^{-1}). However, in accordance with our results, Munoz et al. (2015) observed that PFHxA concentrations in the Rhône River were very variable and could reach higher relative abundances than in other watersheds. The authors suggested that the high PFHxA amounts could hereby originate from a fluorochemical plant producing polyvinylidene fluoride. This factory is located over 250 km upstream of our sampling station, but given the persistence of PFAS (Kunacheva et al., 2011; Stahl et al., 2011) and the high mobility of short-chain perfluorocarboxylates (Ateia et al., 2019), it could still be a possible explanation for the high PFHxA concentrations measured in this study. In a Mediterranean wetland area, up to 18.7 ng L^{-1} of PFHxA have been detected (Lorenzo et al., 2019). In Marseille Bay, PFHxA was only detected once (at a concentration <LOQ) at WWTP-Cortiou station, where some freshwater inputs occur *via* the rivers Huveaune and Jarret. We thus suggest that high PFHxA concentrations could possibly be considered as a tracer of a riverine signature. This is in accordance with previous observations in the Atlantic Ocean where PFHxA was only detected in samples closest to the Amazon River mouth (Schmidt et al., 2019).

3.3. PFOS occurrence, estimated flux and modelled inputs to Marseille Bay via freshwater intrusions

PFOS was detected in all seawater and freshwater samples. In the Bay of Marseille, PFOS and DOC concentrations were positively correlated (p-value < 0.001), as has been observed before in seawater of the North Sea (Ahrens et al., 2009). In the Rhône River, PFOS concentrations seem mainly driven by the magnitude of river discharge (p-value = 0.002).

However, DOC and POC concentrations are well correlated with river discharge (see Table S1 for all DOC, POC, PON and river discharge data), PFOS is also correlated with DOC in the Rhône River (p-value = 0.007). Hereby, the correlation is negative (i.e., an increase in DOC entrains a decrease in PFOS concentrations), in contrast to the correlation observed between DOC and PFOS in seawater samples from Marseille Bay (Fig. 3). The negative correlation between PFOS and river flowrate might indicate that the PFOS sources in the Rhône River are rather constant and the PFOS amounts are more or less diluted depending on the river discharge. Another explanation could be that the increased amount of suspended particulate matter (such as POC) during high river discharge might enhance the sequestration of long-chain PFAS and thus reduce the dissolved PFOS concentration.

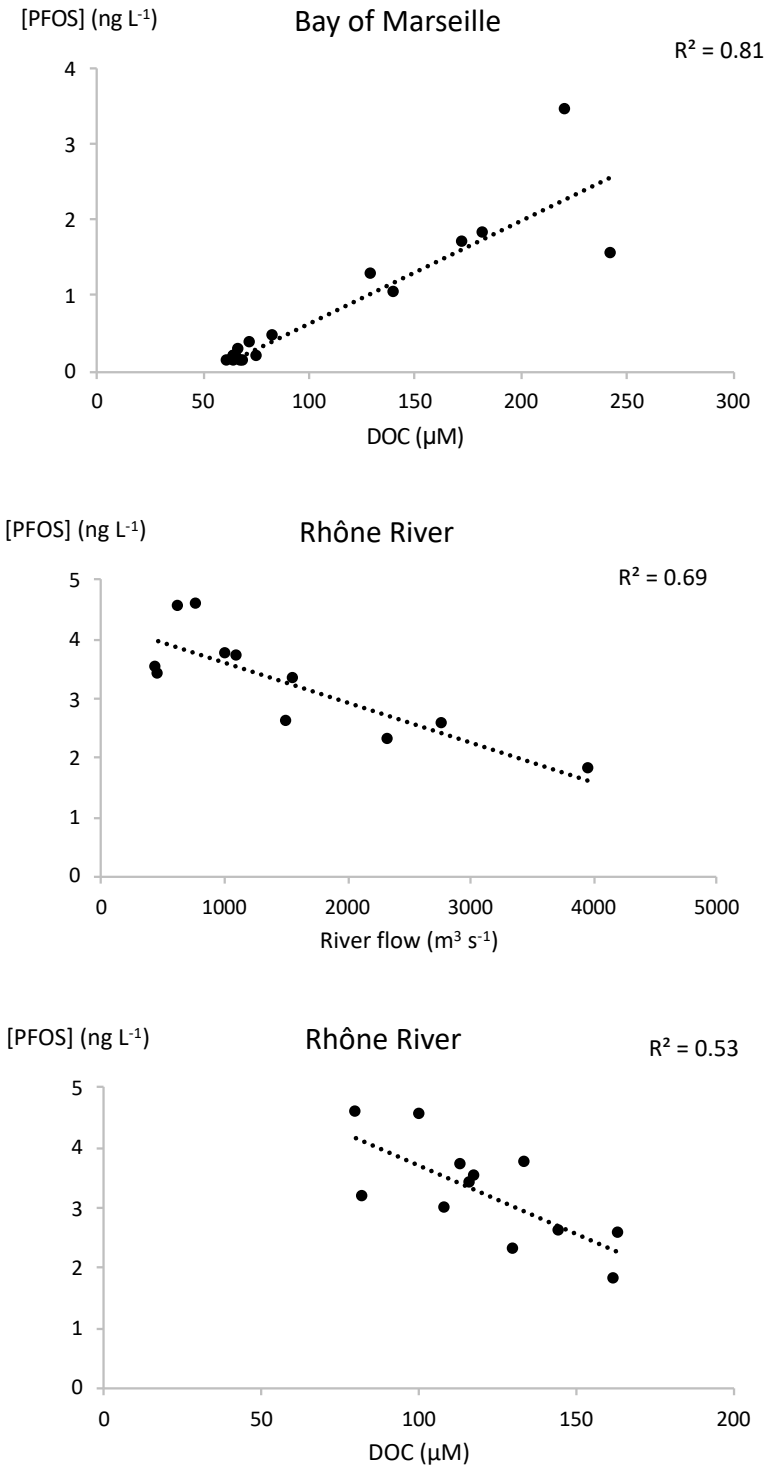

Figure 3: Relationships between PFOS concentrations and DOC (Bay of Marseille, Rhône River) or river discharge (Rhône River).

In this study, 84% of samples had PFOS concentrations higher than the respective annual average (AA) EQS (i.e., 0.65 ng L^{-1} for freshwater and 0.13 ng L^{-1} for marine waters). All samples from the Rhône River and Cortiou station showed concentrations ~ 3-7 or ~ 8-26 times higher than the corresponding AA EQS, respectively. At L'Estaque station, 67% of samples had exceeding PFOS concentrations, whereas this was the case for only 50% of samples from Frioul station (Table 1). The Maximum Allowable Concentration (MAC) EQS for PFOS (36 000 ng L^{-1} in freshwater and 7 200 ng L^{-1} in marine waters) was never exceeded in our study. A recent study showed that some invertebrates (Oligochaetes and Dytiscidae) and fish samples from the Rhône River also exhibited PFOS concentrations exceeding the EQS (EQS_{biota} of 9.1 µg kg^{-1}), with up to 27 µg kg^{-1} detected (Babut et al., 2017). It thus seems as if the Rhône River food web could be affected by the environmental PFOS contamination and potentially negative impacts on human health through fish consumption should be investigated. The highest PFOS concentration measured in this study was on 22/06/2017 in the Rhône River (4.6 ng L^{-1}), where 1.8 ng L^{-1} was the lowest concentration observed (on 05/01/2018). These values are comparable to those of the River Rhine upstream of Leverkusen in Germany (1.41-6.38 ng L^{-1}, Möller et al., 2010) and Swedish Rivers (0.04-6.90 ng L^{-1}, Nguyen et al., 2017) as well as those of three samples collected in the Rhône River in 2012 (1.5-4.9 ng L^{-1}, Munoz et al., 2015). Significantly higher PFOS concentrations of 36.3-703.3 ng L^{-1} were measured in the Yangtze River Estuary in China (Pan and You, 2010).

Using the PFOS concentrations measured and the corresponding daily river discharge, a PFOS input from the Rhône River into the Mediterranean Sea of 138-616 (mean 338, median 330) g day^{-1} was estimated. For comparison, we made the same calculation using data from Lorenzo et al. (2016) and Loos et al. (2008) (mean PFOS concentrations 2.2 ng L^{-1} and 5.55 ng L^{-1}, respectively) together with the average water discharges of the Ebro and Po Rivers (426 m^3

s^{-1} and 1540 m^3 s^{-1}, respectively) and obtained a daily PFOS input into the Mediterranean Sea of 81 g from the Ebro River and 738 g from the Po River. However, the comparison with the Po River has restrictions, since the authors did not filter their water samples prior to analysis, in contrast to this study and the one from Lorenzo et al. (2016). The Ebro River is, by drainage basin, the third largest river flowing into the Mediterranean Sea, but its discharge is restrained due to high water demands (Lorenzo et al., 2016; Struglia et al., 2004). For comparison, the Nile River has an average discharge of approximately 1200 m^3 s^{-1} (Struglia et al., 2004), but its drainage basin is by far the largest of all the rivers draining into the Mediterranean Sea (2.988 $\times$ 10^6 km^2, compared to 0.098 $\times$ 10^6 km^2 for the Rhône River) (Montreuil and Ludwig, 2013). To get a better idea concerning global riverine PFOS inputs into the Mediterranean Sea, it would thus be important to obtain measurement data from the Nile River, as well.

The numerical approach chosen to investigate the PFOS inputs from the Rhône River into the eastern part of the Gulf of Lions allowed us to examine whether the Bay of Marseille is influenced by these inputs or not. Hereby, the simulation started on 01/01/2017 and the contaminants were injected continually with concentrations punctually updated at the dates for which measurement data was available, and with an interpolation between two dates. The temporal series (Figure S3) indicate that in the Bay of Marseille, the first PFAS inputs originating from the Rhône River were perceivable at the beginning of October 2017 in L'Estaque and Frioul stations and approximately one month later - at much lower concentrations - in WWTP-Cortiou, which is farther away from the source and is rather protected from currents through the neighboring cliffs. In the vicinity of the Rhône River mouth, the modelled PFOS concentrations were quite high ($\geq$ 1 ng L^{-1}); negative effects on the aquatic food web in and near the estuary can thus not be excluded and require further investigations. Furthermore, even in the northern part of the Bay of Marseille (e.g., in L'Estaque), the PFOS

input from the Rhône River is sometimes enough to exceed the EQS value (EQS of 0.13 ng L^{-1}; see black isoline in Fig. 4) in these marine waters (Fig. 4). The maximum value simulated at l'Estaque on November 16th occurred during south-south-easterly winds, associated with the anticyclonic Marseille eddy, which is necessary to advect the diluted Rhône River waters toward the northern part of the Bay (Fraysse et al., 2014). In contrast the south-westerly winds that occurred for example on October 31st moved the panache eastwards without generating the eddy necessary to reach the Bay of Marseille. Maps of the barotropic currents for the four selected dates from Figure 4 can be found in the Supplementary Material (Figure S4).

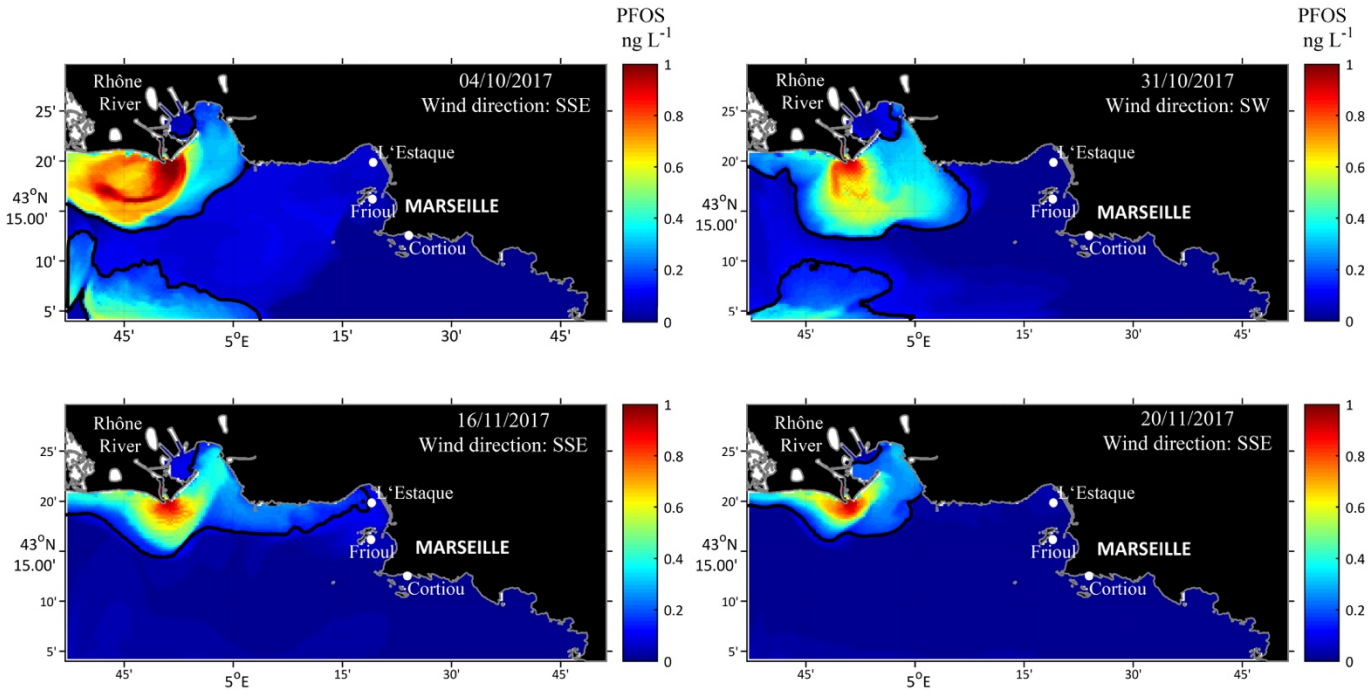

Figure 4: Simulated PFOS distribution (with concentrations in ng L^{-1}) in the eastern part of the Gulf of Lions, including the Rhône River mouth and the Bay of Marseille. The black isoline indicates a PFOS concentration of 0.13 ng L^{-1}, the EQS for marine waters. Four dates were chosen to represent different directions and extensions of the river plume. The color bar is limited between 0-1 ng L^{-1} to better represent low concentrations (including the EQS value of 0.13 ng L^{-1}); note that dark red values can also represent concentrations > 1 ng L^{-1}.

4. Conclusion

Highest PFAS concentrations were detected in the Rhône River, followed by WWTP-Cortiou and the two other marine sampling stations. Relative abundances of individual compounds between samples from the Rhône River and Marseille Bay were strongly different, probably indicating different PFAS sources. PFOS concentrations were exceeding the annual average EU EQS values in over 80% of samples. As shown by our results and comparison with literature, PFOS concentrations exceeding the EQS seems to be a frequent situation and should encourage decision makers to enforce stricter measures to avoid and reduce the contamination of water bodies. While at Cortiou station the local WWTP and/or riverine inputs through the Huveaune and Jarret rivers are the most likely PFOS sources, the model simulation indicated that in L'Estaque station the exceeding PFOS concentrations could – at least partly – result from inputs from the Rhône River. Our data furthermore suggest that up to 27 kg of dissolved water phase Σ_4 PFAS could enter the Gulf of Lion area in the Mediterranean Sea each day through freshwater inputs from the Rhône River. This points to the Rhône River as a possible major source of PFAS to the Mediterranean Sea and a monitoring with higher spatial and temporal resolution is needed to validate our observations. Model results could be improved by considering heterogeneous atmospheric conditions to better represent upwelling and river intrusion events.

Acknowledgements

The project leading to this publication has received funding from the Agence de l'eau Rhône Méditerranée Corse Blue-POLUT project and the JPI Oceans PLASTOX project. The project has also received funding from European FEDER Fund under project 1166-39417. Thanks also

to Michel Fornier, Dorian Guillemain and Deny Malengros for their help during sampling and to Patrick Raimbault and the PACEM-MIO platform for POC and PON measurements.

References

Ahrens, L., Felizeter, S., Ebinghaus, R., 2009. Spatial distribution of polyfluoroalkyl compounds in seawater of the German Bight. Chemosphere 76, 179–184. https://doi.org/10.1016/j.chemosphere.2009.03.052

Asher, B.J., Wang, Y., De Silva, A.O., Backus, S., Muir, D.C.G., Wong, C.S., Martin, J.W., 2012. Enantiospecific perfluorooctane sulfonate (PFOS) analysis reveals evidence for the source contribution of PFOS-precursors to the Lake Ontario foodweb. Environ. Sci. Technol. 46, 7653–7660. https://doi.org/10.1021/es301160r

Ateia, M., Maroli, A., Tharayil, N., Karanfil, T., 2019. The overlooked short- and ultrashort-chain poly- and perfluorinated substances: A review. Chemosphere 220, 866–882. https://doi.org/10.1016/j.chemosphere.2018.12.186

Babut, M., Labadie, P., Simonnet-Laprade, C., Munoz, G., Roger, M.C., Ferrari, B.J.D., Budzinski, H., Sivade, E., 2017. Per- and poly-fluoroalkyl compounds in freshwater fish from the Rhône River: Influence of fish size, diet, prey contamination and biotransformation. Sci. Total Environ. 605–606, 38–47. https://doi.org/10.1016/j.scitotenv.2017.06.111

Castro-Jiménez, J., González-Fernández, D., Fornier, M., Schmidt, N., Sempéré, R., 2019. Macro-litter in surface waters from the Rhone River: Plastic pollution and flows to the NW Mediterranean Sea. Mar. Pollut. Bull. 146, 60–66. https://doi.org/10.1016/j.marpolbul.2019.05.067

Dasu, K., Liu, J., Lee, L.S., 2012. Aerobic soil biodegradation of 8:2 fluorotelomer stearate monoester. Environ. Sci. Technol. 46, 3831–3836. https://doi.org/10.1021/es203978g

Ding, G., Wang, L., Zhang, J., Wei, Y., Wei, L., Li, Y., Shao, M., Xiong, D., 2015. Toxicity and DNA methylation changes induced by perfluorooctane sulfonate (PFOS) in sea urchin Glyptocidaris crenularis. Chemosphere 128, 225–230. https://doi.org/10.1016/j.chemosphere.2015.01.045

Earnshaw, M.R., Paul, A.G., Loos, R., Tavazzi, S., Paracchini, B., Scheringer, M., Hungerbühler, K., Jones, K.C., Sweetman, A.J., 2014. Comparing measured and modelled PFOS concentrations in a UK freshwater catchment and estimating emission rates. Environ. Int. 70, 25–31. https://doi.org/10.1016/j.envint.2014.05.004

Fauvelle, V., Castro-Jiménez, J., Schmidt, N., Carlez, B., Panagiotopoulos, C., Sempéré, R., 2018. One-Single Extraction Procedure for the Simultaneous Determination of a Wide Range of Polar and Nonpolar Organic Contaminants in Seawater. Front. Mar. Sci. 5, 1–10. https://doi.org/10.3389/fmars.2018.00295

Fraysse, M., Pairaud, I., Ross, O.N., Faure, V.M., Pinazo, C., 2014. Intrusion of Rhone River diluted water into the Bay of Marseille: Generation processes and impacts on ecosystem functioning. J. Geophys. Res. Ocean. 119, 6535–6556. https://doi.org/10.1002/2014JC010022.Received

Fraysse, M., Pinazo, C., Faure, V.M., Fuchs, R., Lazzari, P., Raimbault, P., Pairaud, I., 2013. Development of a 3D coupled physical-biogeochemical model for the Marseille Coastal Area (NW Mediterranean Sea): What complexity is required in the coastal zone? PLoS One 8. https://doi.org/10.1371/journal.pone.0080012

Gatti, J., Petrenko, A., Devenon, J.L., Leredde, Y., Ulses, C., 2006. The Rhone river dilution zone present in the northeastern shelf of the Gulf of Lion in December 2003. Cont. Shelf Res. 26, 1794–1805. https://doi.org/10.1016/j.csr.2006.05.012

Hagenaars, A., Knapen, D., Meyer, I.J., van der Ven, K., Hoff, P., De Coen, W., 2008. Toxicity evaluation of perfluorooctane sulfonate (PFOS) in the liver of common carp (Cyprinus carpio). Aquat. Toxicol. 88, 155–163. https://doi.org/10.1016/j.aquatox.2008.04.002

Huang, Q., Fang, C., Wu, X., Fan, J., Dong, S., 2011. Perfluorooctane sulfonate impairs the cardiac development of a marine medaka (Oryzias melastigma). Aquat. Toxicol. 105, 71–77. https://doi.org/10.1016/j.aquatox.2011.05.012

Kärrman, A., Langlois, I., Bavel, B. van, Lindström, G., Oehme, M., 2007. Identification and pattern of perfluorooctane sulfonate (PFOS) isomers in human serum and plasma. Environ. Int. 33, 782–788. https://doi.org/10.1016/j.envint.2007.02.015

Klemp, J.B., Skamarock, W.C., Dudhia, J., 2007. Conservative Split-Explicit Time Integration Methods for the Compressible Nonhydrostatic Equations. Mon. Weather Rev. 135, 2897–2913. https://doi.org/10.1175/MWR3440.1

Kunacheva, C., Senevirathna, S.T.M.L.D., Tanaka, S., Fujii, S., Lien, N.P.H., Nozoe, M., Shivakoti, B.R., 2011. The emergence of persistent organic pollutants in the environment : the occurrence and treatment of perfluorinated compounds. SANSAI An Environ. J. Glob. Community 5, 37–50.

Lazure, P., Dumas, F., 2008. An external-internal mode coupling for a 3D hydrodynamical model for applications at regional scale (MARS). Adv. Water Resour. 31, 233–250. https://doi.org/10.1016/j.advwatres.2007.06.010

Lim, T.C., Wang, B., Huang, J., Deng, S., Yu, G., 2011. Emission inventory for PFOS in China: Review of past methodologies and suggestions. ScientificWorldJournal. 11, 1963–1980. https://doi.org/10.1100/2011/868156

Loos, R., Locoro, G., Huber, T., Wollgast, J., Christoph, E.H., de Jager, A., Manfred Gawlik, B., Hanke, G., Umlauf, G., Zaldívar, J.M., 2008. Analysis of perfluorooctanoate (PFOA) and other perfluorinated compounds (PFCs) in the River Po watershed in N-Italy. Chemosphere 71, 306–313. https://doi.org/10.1016/j.chemosphere.2007.09.022

Loos, R., Tavazzi, S., Mariani, G., Suurkuusk, G., Paracchini, B., Umlauf, G., 2017. Analysis of emerging organic contaminants in water, fish and suspended particulate matter (SPM) in the Joint Danube Survey using solid-phase extraction followed by UHPLC-MS-MS and GC–MS analysis. Sci. Total Environ. 607–608, 1201–1212. https://doi.org/10.1016/j.scitotenv.2017.07.039

Lorenzo, M., Campo, J., Farré, M., Pérez, F., Picó, Y., Barceló, D., 2016. Perfluoroalkyl substances in the Ebro and Guadalquivir river basins (Spain). Sci. Total Environ. 540, 191–199. https://doi.org/10.1016/j.scitotenv.2015.07.045

Lorenzo, M., Campo, J., Morales Suárez-Varela, M., Picó, Y., 2019. Occurrence, distribution and behavior of emerging persistent organic pollutants (POPs) in a Mediterranean wetland protected area. Sci. Total Environ. 646, 1009–1020. https://doi.org/10.1016/j.scitotenv.2018.07.304

Mejia-Avendaño, S., Duy, S.V., Sauvé, S., Liu, J., 2016. Generation of Perfluoroalkyl Acids

from Aerobic Biotransformation of Quaternary Ammonium Polyfluoroalkyl Surfactants. Environ. Sci. Technol. 50, 9923–9932. https://doi.org/10.1021/acs.est.6b00140

Miège, C., Peretti, A., Labadie, P., Budzinski, H., Le Bizec, B., Vorkamp, K., Tronczynski, J., Persat, H., Coquery, M., Babut, M., 2012. Occurrence of priority and emerging organic compounds in fishes from the Rhone River (France). Anal. Bioanal. Chem. 404, 2721–2735. https://doi.org/10.1007/s00216-012-6187-0

Möller, A., Ahrens, L., Surm, R., Westerveld, J., Van Der Wielen, F., Ebinghaus, R., De Voogt, P., 2010. Distribution and sources of polyfluoroalkyl substances (PFAS) in the River Rhine watershed. Environ. Pollut. 158, 3243–3250. https://doi.org/10.1016/j.envpol.2010.07.019

Montreuil, O., Ludwig, W., 2013. Rivers of the Mediterrenean Sea: Water discharge and nutrient fluxes. UNEP MED POL, 1–126.

Mourier, B., Desmet, M., Van Metre, P.C., Mahler, B.J., Perrodin, Y., Roux, G., Bedell, J.P., Lefèvre, I., Babut, M., 2014. Historical records, sources, and spatial trends of PCBs along the RhÔne River (France). Sci. Total Environ. 476–477, 568–576. https://doi.org/10.1016/j.scitotenv.2014.01.026

Munoz, G., Giraudel, J.L., Botta, F., Lestremau, F., Dévier, M.H., Budzinski, H., Labadie, P., 2015. Spatial distribution and partitioning behavior of selected poly- and perfluoroalkyl substances in freshwater ecosystems: A French nationwide survey. Sci. Total Environ. 517, 48–56. https://doi.org/10.1016/j.scitotenv.2015.02.043

Naile, J.E., Khim, J.S., Wang, T., Chen, C., Luo, W., Kwon, B.O., Park, J., Koh, C.H., Jones, P.D., Lu, Y., Giesy, J.P., 2010. Perfluorinated compounds in water, sediment, soil and biota from estuarine and coastal areas of Korea. Environ. Pollut. 158, 1237–1244. https://doi.org/10.1016/j.envpol.2010.01.023

Nguyen, M.A., Wiberg, K., Ribeli, E., Josefsson, S., Futter, M., Gustavsson, J., Ahrens, L., 2017. Spatial distribution and source tracing of per- and polyfluoroalkyl substances (PFASs) in surface water in Northern Europe. Environ. Pollut. 220, 1438–1446. https://doi.org/10.1016/j.envpol.2016.10.089

Nicolle, A., Garreau, P., Liorzou, B., 2009. Modelling for anchovy recruitment studies in the Gulf of Lions (Western Mediterranean Sea). Ocean Dyn. 59, 953–968. https://doi.org/10.1007/s10236-009-0221-6

Oursel, B., Garnier, C., Durrieu, G., Mounier, S., Omanović, D., Lucas, Y., 2013. Dynamics and fates of trace metals chronically input in a Mediterranean coastal zone impacted by a large urban area. Mar. Pollut. Bull. 69, 137–149. https://doi.org/10.1016/j.marpolbul.2013.01.023

Pairaud, I.L., Gatti, J., Bensoussan, N., Verney, R., Garreau, P., 2011. Hydrology and circulation in a coastal area off Marseille: Validation of a nested 3D model with observations. J. Mar. Syst. 88, 20–33. https://doi.org/10.1016/j.jmarsys.2011.02.010

Paluselli, A., Aminot, Y., Galgani, F., Net, S., Sempéré, R., 2018. Occurrence of phthalate acid esters (PAEs) in the northwestern Mediterranean Sea and the Rhone River. Prog. Oceanogr. 163, 221–231. https://doi.org/10.1016/j.pocean.2017.06.002

Pan, G., You, C., 2010. Sediment-water distribution of perfluorooctane sulfonate (PFOS) in Yangtze River Estuary. Environ. Pollut. 158, 1363–1367.

https://doi.org/10.1016/j.envpol.2010.01.011

Para, J., Coble, P.G., Charrière, B., Tedetti, M., Fontana, C., Sempéré, R., 2010. Fluorescence and absorption properties of chromophoric dissolved organic matter (CDOM) in coastal surface waters of the northwestern Mediterranean Sea, influence of the Rhône River. Biogeosciences 7, 4083–4103. https://doi.org/10.5194/bg-7-4083-2010

Raimbault, P., Garcia, N., Cerutti, F., 2008. Distribution of inorganic and organic nutrients in the South Pacific Ocean − evidence for long-term accumulation of organic matter in nitrogen-depleted waters. Biogeosciences 5, 281–298. https://doi.org/10.5194/bg-5-281-2008

Ross, O.N., Fraysse, M., Pinazo, C., Pairaud, I., 2016. Impact of an intrusion by the Northern Current on the biogeochemistry in the eastern Gulf of Lion, NW Mediterranean. Estuar. Coast. Shelf Sci. 170, 1–9. https://doi.org/10.1016/j.ecss.2015.12.022

Sánchez-Avila, J., Meyer, J., Lacorte, S., 2010. Spatial distribution and sources of perfluorochemicals in the NW Mediterranean coastal waters (Catalonia, Spain). Environ. Pollut. 158, 2833–2840. https://doi.org/10.1016/j.envpol.2010.06.022

Schlummer, M., Sölch, C., Meisel, T., Still, M., Gruber, L., Wolz, G., 2015. Emission of perfluoroalkyl carboxylic acids (PFCA) from heated surfaces made of polytetrafluoroethylene (PTFE) applied in food contact materials and consumer products. Chemosphere 129, 46–53. https://doi.org/10.1016/j.chemosphere.2014.11.036

Schmidt, N., Castro-Jiménez, J., Fauvelle, V., Ourgaud, M., Sempéré, R., n.d. Occurrence of organic plastic additives in surface waters of the Rhône River (France). Environ. Pollut. submitted.

Schmidt, N., Fauvelle, V., Ody, A., Castro-Jiménez, J., Jouanno, J., Changeux, T., Thibaut, T., Sempéré, R., 2019. The Amazon River – a major source of organic plastic additives to the tropical North Atlantic? Environ. Sci. Technol. https://doi.org/10.1021/acs.est.9b01585

Schmidt, N., Thibault, D., Galgani, F., Paluselli, A., Sempéré, R., 2018. Occurrence of microplastics in surface waters of the Gulf of Lion (NW Mediterranean Sea). Prog. Oceanogr. 163, 214–220. https://doi.org/10.1016/j.pocean.2017.11.010

Sempéré, R., Charrière, B., Van Wambeke, F., Cauwet, G., 2000. Carbon inputs of the Rhône River to the Mediterranean Sea: Biogeochemical implications. Global Biogeochem. Cycles 14, 669–681. https://doi.org/10.1029/1999GB900069

Sempéré, R., Para, J., Tedetti, M., Charrière, B., Mallet, M., 2015. Variability of Solar Radiation and CDOM in Surface Coastal Waters of the Northwestern Mediterranean Sea. Photochem. Photobiol. 91, 851–861. https://doi.org/10.1111/php.12434

Simmonet-Laprade, C., Budzinski, H., Babut, M., Le Menach, K., Munoz, G., Lauzent, M., Ferrari, B.J.D., Labadie, P., 2019. Investigation of the spatial variability of poly- and perfluoroalkyl substance trophic magnification in selected riverine ecosystems. Sci. Total Environ. 686, 393–401. https://doi.org/10.1016/j.scitotenv.2019.05.461

Stahl, T., Mattern, D., Brunn, H., 2011. Toxicology of perfluorinated compounds. Environ. Sci. Eur. 23, 1–52. https://doi.org/10.1186/2190-4715-23-38

Struglia, M.V., Mariotti, A., Filograsso, A., 2004. River discharge into the Mediterranean sea: Climatology and aspects of the observed variability. J. Clim. 17, 4740–4751.

https://doi.org/10.1175/JCLI-3225.1

Xia, J., Cao, Z., Peng, J., Fu, S., Fu, C., 2014. The use of spontaneous behavior, swimming performances and metabolic rate to evaluate toxicity of PFOS on topmouth gudgeon Pseudorasbora parva. Acta Ecol. Sin. 34, 284–289. https://doi.org/10.1016/J.CHNAES.2014.07.006

Yohia, C., 2017. Genèse du mistral par interaction barocline et advection du tourbillon potentiel. Climatologie. https://doi.org/10.4267/climatologie.1182

Zhang, L., Niu, J., Li, Y., Wang, Y., Sun, D., 2013. Evaluating the sub-lethal toxicity of PFOS and PFOA using rotifer Brachionus calyciflorus. Environ. Pollut. 180, 34–40. https://doi.org/10.1016/j.envpol.2013.04.031

CHAPTER IV: Plastic additives in the Bay of Marseille

Phthalates and organophosphate esters in the NW Mediterranean Sea (Bay of Marseille): occurrence and possible implications for the marine food web.

Natascha Schmidt [a], Javier Castro-Jiménez [a], Richard Sempéré [a]

[a] *Aix-Marseille Univ., Toulon Univ., CNRS, IRD, Mediterranean Institute of Oceanography (M I O), UM 110, Marseille, France*

Keywords: Plasticizers, flame retardants, zooplankton, environmental pollution, Mediterranean Sea

In preparation

Abstract

Phthalates (PAEs) and organophosphate esters (OPEs) are common organic plastic additives and flame retardants, frequently detected in the environment due to their increasing use. In this study, seven PAEs and nine OPEs were analyzed in surface water, sediment and zooplankton samples from three different sampling stations in Marseille Bay (NW Mediterranean Sea), on six sampling events. PAE concentrations ranged from 100-527 ng L^{-1} in water, 12-610 ng g^{-1} in sediment and 0.9-47 µg g^{-1} dw in zooplankton samples. OPE concentrations varied between 8.9-1013 ng L^{-1} in water, 13-49 ng g^{-1} in sediment and 0.4-4.6 µg g^{-1} dw in zooplankton samples. Microplastic counts ranged from 0 to 0.3 items m^{-3} (mean 0.05±0.05 items m^{-3}). PAEs were generally more abundant in all matrixes than OPEs. Especially in zooplankton samples high fluctuations in concentrations between different sampling events were observed. Samples collected near the municipal wastewater treatment plant outlet exhibited highest PAE and OPE concentrations, but lowest microplastic counts.

1. **Introduction**

The chemical pollution of watercourses and the oceans is one of the main man-made threats to aquatic biodiversity (Young et al., 2016). The number of pollutants present in the aquatic environment is constantly increasing, with "modern" persistent organic pollutants (POPs) like perfluorinated compounds (PFCs) joining legacy POPs, such as polychlorinated biphenyls (PCBs). Two chemical families of plastic additives and/or flame retardants are phthalate esters (PAEs) and organophosphate esters (OPEs). PAEs are widely used in the manufacturing of PVC and other plastics, but also as solvents in cosmetics and paints, among others (Net et al., 2015), while OPEs are commonly incorporated in polyurethane foams and electronic devices (Marklund, 2005; van der Veen and de Boer, 2012; Yang et al., 2019). These additives are not covalently bound to the polymeric matrix and are thus prone to leach from the

materials, especially if exposed to UV radiation or heat (Paluselli et al., 2019), though direct inputs from manufacturing processes or wastewater treatment plants (WWTP) might be predominant. In the last decades, the presence of PAEs and OPEs in the environment has been reported by numerous studies (Castro-Jiménez et al., 2016, 2014; Ma et al., 2017; Pantelaki and Voutsa, 2019; Peijnenburg and Struijs, 2006; Reemtsma et al., 2008; Sánchez-Avila et al., 2012; Sousa et al., 2018; Wang et al., 2015; Wolschke et al., 2015). In surface waters of the Bay of Marseille, PAEs have previously been reported at concentrations of 130-1330 ng L^{-1} ($\sum_6$ PAEs) (Paluselli et al., 2018b). For biota, fewer data exists, especially regarding zooplankton, in spite of its important role in the aquatic food web. Wang et al. (2019) measured OPEs in zooplankton from Taihu Lake, China, and concluded that relative abundances of individual OPEs between water and zooplankton samples were significantly different. To our knowledge, no comprehensive studies on OPE occurrence in waters of (or near) Marseille Bay have been published so far, neither concerning PAEs and OPEs in sediments or zooplankton from Marseille Bay.

Another threat to the environment are microplastics (i.e., plastics ≤ 5 mm), especially to the marine environment, which receives important microplastic loads from rivers (Horton et al., 2017; Lebreton et al., 2017; van Wijnen et al., 2019), coastal cities (Liubartseva et al., 2018; Schmidt et al., 2018) and through maritime traffic and fishing activities (Liubartseva et al., 2018). Microplastics have recently received much attention from the media and scientists, given their omnipresence and their potential deleterious effects, such as ingestion by a wide variety of aquatic species (Cole et al., 2013; Duncan et al., 2019; Silva-Cavalcanti et al., 2017; Zhu et al., 2019). Hotspots and accumulation zones have been identified, including the East Asian Seas, with concentrations of up to 491items m^{-3} (Isobe et al., 2015) and the Mediterranean Sea (Suaria et al., 2016). In Marseille Bay, highly variable microplastic concentrations have so far

been reported (0.01 items m^{-2}, Collignon et al., 2012; $6 \cdot 10^3$ to $1 \cdot 10^6$ items km^{-2}, Schmidt et al., 2018).

The objectives of this work were i) to investigate PAE and OPE occurrence and spatial and temporal variability in water, sediment and zooplankton samples in the Bay of Marseille during one year, ii) to examine their potential to bioconcentrate at the base of the Mediterranean food web and iii) to provide data on microplastic abundance and size in order to iv) examine whether organic plastic additive concentrations are linked with microplastic abundances.

2. Material & Methods

2.1. Study area

The Bay of Marseille is located at the eastern edge of the Gulf of Lion (northwestern Mediterranean Sea). It is influenced by strong wind regimes (mainly the northwestern Mistral wind) and intrusions from the Rhone River can occur several times per year (Fraysse et al., 2014). The three sampling stations chosen for this study are characterized by harbor activity (L'Estaque), tourism and fish-farming (Frioul) and the outlet of treated effluents from the municipal wastewater treatment plant (WWTP; Cortiou) (Fig. 1). After Paris, Marseille is the second largest city of France and the WWTP treats the effluents of 1.7 million inhabitant equivalents (Oursel et al., 2013). Marine resources play an important role in the local economy as well as for traditional values.



Figure 1: Map of the Bay of Marseille showing the three sampling stations L'Estaque, Frioul island and Cortiou. A map of the Mediterranean Sea (right corner) indicates the position of the sampling area.

2.2. Sampling and sample processing

1 L water samples were collected in duplicate using a stainless-steel collector and poured into pre-combusted (450 °C, 6 h) 1 L glass bottles. They were filtered (GF/F, 0.7 µm) within three hours after collection and were either stored at 4 °C and extracted within 24 h or otherwise stored at -25 °C until extraction. Sediments were sampled using a Van Veen grab. Approximately the upper 5 cm of the samples were collected and put into pre-combusted glass bottles. Once in the laboratory, the sediments were stored in the freezer (-20 °C) and afterwards lyophilized. Next, they were sieved to a size class ≤ 500 µm using a metal sieve.

Zooplankton and microplastic samples were collected using a manta net (opening area 40 x 70 cm, mesh size 150 µm), which was towed horizontally at a speed of 2-3 knots for 20 minutes. Due to a floater on each side of the net, usually only half of the net height was

submerged in the water, therefore an opening area of 20 x 70 cm was used for the calculation of microplastic concentrations. The samples were poured into glass bottles and kept under cool and dark conditions until reaching the laboratory. They were left for 24 h to enable the zooplankton to defecate, to avoid a falsification of or interference with the chemical analysis. Next, three zooplankton size classes were established using metal sieves: 150-500 µm, 500-1000 µm and > 1000 µm. The advantage of analyzing different size classes as opposed to pooled samples is that size-specific differences in contaminant uptake (due to different surface area : volume ratios, feeding behaviors or developmental stages) can be investigated. The samples were thoroughly rinsed using ultrapure water. Next, microplastics were sorted out using a dissecting microscope and tweezers. They were counted and their size was measured using a ZooScan (HYDROPTIC SARL). To do so, each item was placed on the screen of the ZooScan without water. Surface area measurements in pixels were obtained with the ImageJ software and then converted into mm^2. Other debris (e.g., plant debris) was also removed from the samples and a rough taxonomical identification was made. The plankton samples were then frozen (-20 °C), lyophilized and ground using an agate mortar and pestle. Details on sampling dates, temperature, salinity and depth are given in Table S1 (Supplementary Material).

2.3. Contaminant extraction

2.3.1. Water samples

Contaminants were extracted from water samples using Solid Phase Extraction (SPE) as previously reported by Fauvelle et al. (2018). Hereby, the filtered samples were spiked with labeled surrogate standards (100 ng $sample^{-1}$ of D_{27}-TBP, D_{18}-TCPP, D_{15}-TDCP and D_4-DnBP) and thoroughly shaken. Then, the samples were passed through pre-cleaned and conditioned glass cartridges containing 250 mg Oasis HLB sorbent by using polytetrafluoroethylene liners. Following a washing (ultrapure water) and vacuum-drying step, the compounds were eluted

using 5 mL hexane and 5 mL hexane/dichloromethane (50/50, v/v) and collected in pre-combusted glass tubes. The extract volume was reduced to approximately 100 µL using pure N_2.

2.3.2. Sediment and zooplankton samples

3 g and 100 mg of freeze-dried sediments and zooplankton samples (dry weight), respectively, were used for the extraction. They were filled into glass tubes, spiked with surrogate standards (100 ng sample^{-1} of D_{27}-TBP, D_{18}-TCPP, D_{15}-TDCP and D_4-DnBP), vortexed and left to equilibrate for about 30 min. A small spatula of activated copper was then added to sediment samples, while for zooplankton samples the activated copper was added to the final extract. Next, 5 mL of hexane were added and an ultrasound extraction (Elmasonic X-tra TT 120 H, extraction power 800 W) was performed during 15 min without heating. Afterwards, the extracts were collected with a Pasteur pipette and filled into glass cartridges containing 250 mg of Oasis MAX sorbent used for the clean-up of the extracts, which were previously cleaned three times by a sequence of solvents (3 × 5 mL each of acetone, ethyl acetate and dichloromethane). The processed extracts were collected in glass tubes. The extraction and following procedure were repeated one more time with 5 mL of hexane and two more times with 5 mL hexane/dichloromethane (50/50, v/v). The volume of the extracts was then reduced using subsequent N_2 evaporation until a final volume of approximately 100 µL.

2.4. GC/MS analysis

Water, sediment and zooplankton samples were spiked with internal standards (100 ng sample^{-1} of D_4-DEP, D_4-DEHP, D_{21}-TPrP, D_{12}-TCEP and D_{15}-TPhP) and injected into GC/MS in Selected Ion Monitoring (SIM) mode. Injection details were the same for all matrices and have already been reported elsewhere (Fauvelle et al., 2018). Sven PAEs (dimethyl phthalate -

DMP-, diethyl phthalate -DEP-, di-n-butyl phthalate -DnBP-, diisobutyl phthalate -DiBP-, benzylbutyl phthalate -BzBP-, diethylhexyl phthalate -DEHP- and di-n-octyl phthalate -DnOP-) and nine OPEs (tripropyl phosphate -TPP-, tri-iso-buthyl phosphate -TiBP-, tri-n-butyl phosphate -TnBP-, tris-(2-chloroethyl) phosphate -TCEP-, tris-(2-chloro, 1-methylethyl) phosphate -TCPP-, tris-(2-chloro-, 1-chloromethylethyl) phosphate -TDCP-, triphenyl phosphate -TPhP-, 2- ethylhexyl-diphenyl phosphate -EHDPP- and tris(2-ethylhexyl) phosphate -TEHP-) were quantified.

2.5. Quality Assurance / Quality Control

Ultrasound extraction recovery experiments were performed by spiking 3 g of freeze-dried sediment and 100 mg zooplankton with a PAE and OPE analytical standard mixture (50 ng sample^{-1}). Recoveries were calculated by subtracting the measured concentrations in the spiked samples from those in the non-spiked samples (Table S2). Information on recovery rates in water samples has been published elsewhere (Fauvelle et al., 2018). Furthermore, surrogates were added to each sample prior to extraction and their recovery rates were monitored. Mean surrogate recoveries in water, sediment and zooplankton samples, respectively, were as follows: 94%, 90% and 90% (D_4-DnBP), 87%, 86% and 96% (D_{27}-TBP), 80%, 40% and 53% (D_{18}-TCPP) and 88%, 73% and 68% (D_{15}-TDCP). Extraction blanks were made for all sample batches to monitor possible contamination. All blank values can be found in Table S3. The results presented here are blank-corrected, but not recovery-corrected. Instrumental limits of quantification (LOQ) ranged from 1 pg to 10 pg (Fauvelle et al., 2018).

The middle-sized zooplankton samples (< 1mm, > 500 µm) collected on S5 in L'Estaque and Frioul stations were contaminated through dissolving rubber boot fragments, which got washed from the boat into the sampling net. These samples exhibited very high DnBP and DiBP concentrations (11,480-13,310 ng g^{-1} dw and 810-973 ng g^{-1} dw, respectively) and were thus

excluded from the calculation of means. Furthermore, certain zooplankton samples (especially in the size class > 1 mm) did not contain enough biomass to perform an extraction and in other samples (particularly those from Frioul station) matrix interferences inhibited the quantification of TCPP and TDCP.

3. Results & Discussion

3.1. Surface waters

Total PAE and OPE concentrations varied in water samples between 100-527 ng L^{-1} and 8.9-1013 ng L^{-1}, respectively (Fig. 2 A-C). TPP was never detected, TEHP was detected in 28% of samples, followed by DnOP (39%), TDCP (56%), BzBP (67%), DEP (72%), TnBP and TCEP (89%) and TPhP (94%). DMP, DnBP, DiBP, DEHP, TiBP, TCPP and EHDPP were found in 100% of water samples. Of all PAEs, DEHP was predominant with 62-454 ng L^{-1} (50-90% relative abundance), while TCPP was the dominant OPE with 6.2-876 ng L^{-1} (28-91% relative abundance). In L'Estaque, highest OPE concentrations were observed in September 2017 (S3), where a surprisingly high TPhP peak (24 ng L^{-1}) was detected. Another interesting observation is the high amount of TCEP detected in March 2018 (S6) in L'Estaque (19 ng L^{-1}) and Frioul (26 ng L^{-1}) stations (Fig. 2 A-B). In contrast to the highest OPE concentrations, the highest PAE concentration detected in L'Estaque was in November 2017 (S4). PAE and OPE concentrations in water samples from all stations were not correlated (p-value = 0.11).

First data on OPE occurrence in the dissolved water phase of seawater from the Mediterranean Sea (~60 km north-east of Barcelona, Spain) was recently published (Vila-Costa et al., 2019). The authors detected a total of 10.5±1.0 ng L^{-1} (Σ_5 OPEs), with TiBP being the dominant compound (3.7±1.3 ng L^{-1}). Unfortunately, TCPP was not analyzed in this study, but their mean TiBP concentration is comparable with ours (8.3±10.1 ng L^{-1}). The higher standard

deviation in our case can be explained by the differences between sampling stations, with Cortiou having 4-times or more the concentrations found at Frioul and L'Estaque. Concerning PAEs, Paluselli et al. (2018a) found 212.6 ng L^{-1} of Σ_7 PAE at Cortiou station in 2014, i.e., a value close to our mean Σ_7 PAE concentration at this station (263.6 ng L^{-1}). Furthermore, the authors found higher PAE concentrations (424.2 ng L^{-1} in surface waters and 1207.1 ng L^{-1} at 30 m depth) at a station where previously high microplastic counts have been reported ($1 \cdot 10^6$ items km^{-2}; Schmidt et al., 2018), raising the question whether there is a correlation between dissolved PAE concentrations and waterborne microplastic abundances.

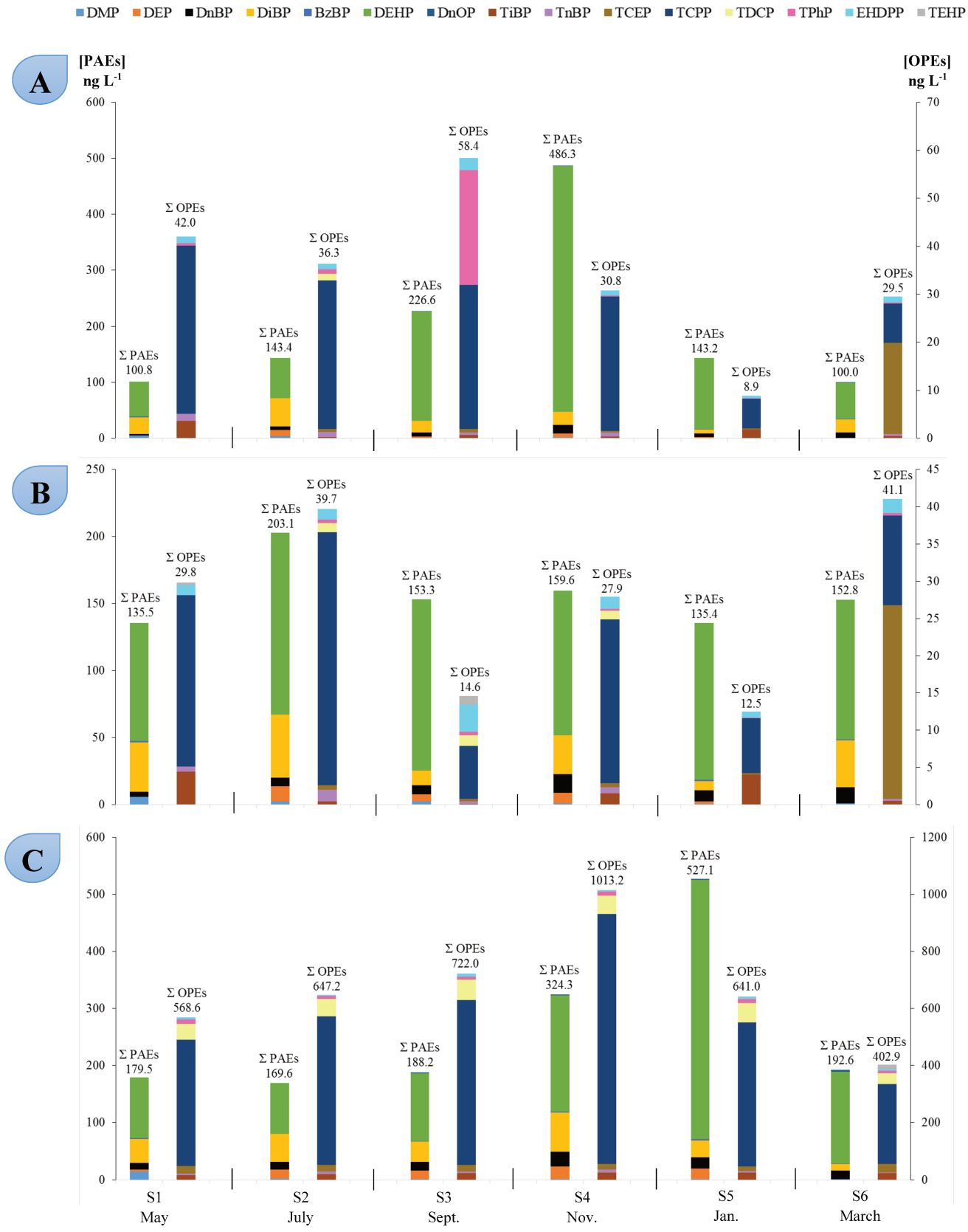

Fig. 2: PAE and OPE concentrations measured in filtered water samples during six sampling events (S1-S6) in L'Estaque (A), Frioul (B) and Cortiou (C) stations in the Bay of Marseille. Note the different scales for PAE (left) and OPE (right) concentrations.

3.2. Sediments

In sediment samples, PAEs (12-610 ng g^{-1} dw) were generally observed at higher concentrations than OPEs (13-49 ng g^{-1} dw) (Fig. 3 A-C). TPP and TDCP were not detected in any samples, DnOP was found in 11% of samples, followed by BzBP (28%), TiBP (67%), TPhP (72%), EHDPP (78%), TEHP (89%) and TCPP (94%). DMP, DEP, DnBP, DiBP, DEHP, TnBP and TCEP had a detection frequency of 100%. TnBP was usually the most abundant OPE, with concentrations ranging from 2.2 to 32 ng g^{-1} dw, followed by TCPP (1.0-20 ng g^{-1} dw) and TEHP (0.3-9.5 ng g^{-1} dw). These concentrations are slightly higher than the ones reported for sediment samples from the Bohai and Yellow Seas (China), where TCPP was detected at 0.029-1.521 ng g^{-1} dw and TEHP at 0.008-3.445 ng g^{-1} dw (Zhong et al., 2018). Hereby, the authors noted that halogenated OPEs were more abundant than non-halogenated OPEs, which was not the case in our study. Another study in the Bohai Sea found TnBP to be dominant in surface (0-20 cm) sediments, with a relative abundance of 34-60% (Wang et al., 2017). The authors pointed out that TnBP is commonly used in hydraulic fluids and lubricating oils (van der Veen and de Boer, 2012), which could also explain the important abundance of TnBP in our sediment samples, given that the Bay of Marseille is influenced by maritime traffic of all kinds. Sediments from the North Pacific and Arctic Oceans yielded lower OPE loads (<1-460 pg g^{-1} dw TCPP and 19-209 pg g^{-1} dw TnBP) and TCEP and TiBP were the dominant compounds in these samples (Ma et al., 2017).

When comparing sampling stations, Cortiou station had the highest mean PAE and OPE concentrations (404 and 33 ng g^{-1}, respectively), followed by L'Estaque (140 and 24 ng g^{-1}) and, finally, Frioul (37 and 20 ng g^{-1}). In contrast to water samples, PAE and OPE concentrations in sediment samples were positively correlated (p-value = 0.01).

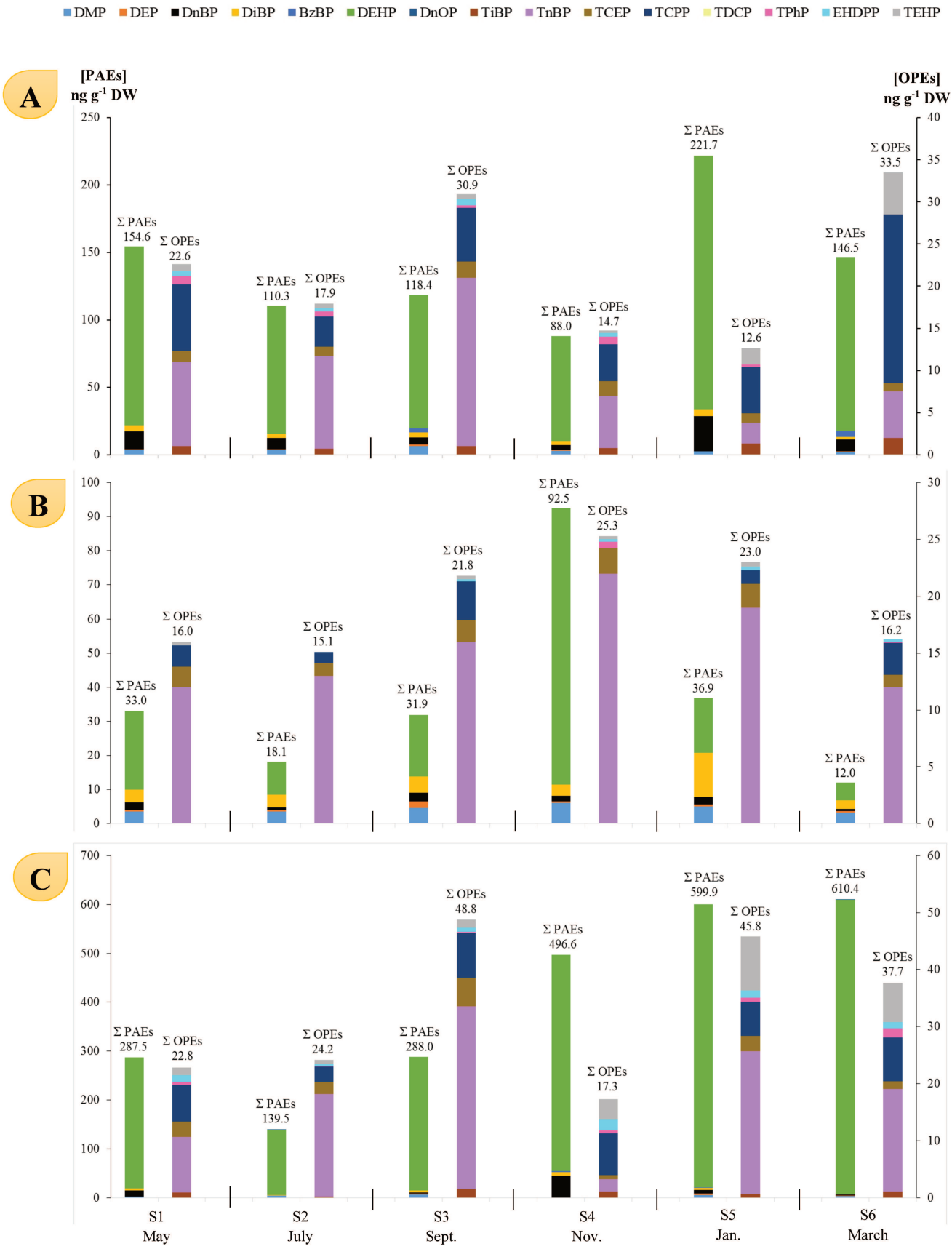
DMP DEP DnBP DiBP BzBP DEHP DnOP TiBP TnBP TCEP TCPP TDCP TPhP EHDPP TEHP
A
[PAEs] ng g-1 DW
[OPEs] ng g-1 DW
Σ PAEs 154.6
Σ OPEs 22.6
Σ PAEs 110.3
Σ OPEs 17.9
Σ PAEs 118.4
Σ OPEs 30.9
Σ PAEs 88.0
Σ OPEs 14.7
Σ PAEs 221.7
Σ OPEs 12.6
Σ PAEs 146.5
Σ OPEs 33.5
B
Σ PAEs 33.0
Σ OPEs 16.0
Σ PAEs 18.1
Σ OPEs 15.1
Σ PAEs 31.9
Σ OPEs 21.8
Σ PAEs 92.5
Σ OPEs 25.3
Σ PAEs 36.9
Σ OPEs 23.0
Σ PAEs 12.0
Σ OPEs 16.2
C
Σ PAEs 287.5
Σ OPEs 22.8
Σ PAEs 139.5
Σ OPEs 24.2
Σ PAEs 288.0
Σ OPEs 48.8
Σ PAEs 496.6
Σ OPEs 17.3
Σ PAEs 599.9
Σ OPEs 45.8
Σ PAEs 610.4
Σ OPEs 37.7
S1 May
S2 July
S3 Sept.
S4 Nov.
S5 Jan.
S6 March

Fig. 3: PAE and OPE concentrations measured in sediment samples during six sampling events (S1-S6) in L'Estaque (A), Frioul (B) and Cortiou (C) stations in the Bay of Marseille. Note the different scales for PAE (left) and OPE (right) concentrations.

3.3. Zooplankton samples

As in sediment samples, OPEs were generally observed at lower concentrations in zooplankton than PAEs. Considering average concentrations, the smallest size class (< 500 µm, > 150 µm) had highest Σ_7 PAE and Σ_9 OPE concentrations (9,670±13,837 and 1,863±1,115 ng g^{-1} dw, respectively), followed by the biggest size class (> 1 mm; 6,577±5,794 and 1,492±1,222 ng g^{-1} dw), while zooplankton < 1 mm, > 500 µm exhibited lowest mean PAE (4,562±4,977 ng g^{-1} dw) and OPE (1,342±674 ng g^{-1} dw) concentrations (Table 2 & 3). The high concentrations observed in small sized plankton is probably due to their higher surface area : volume ratio which can lead to a fast uptake of contaminants from the surrounding media (DeLorenzo et al., 2002; Hargrave et al., 2000). However, this does not explain why the middle-sized class is generally the least contaminated. Moreover, the high standard deviation values point out an important variability between sampling events, possibly linked to the planktonic life cycle. Indeed, a seasonality of bioaccumulation in zooplankton has already been observed for certain organochlorine chemicals, such as PCBs and the authors suggested that a varying lipid content in zooplankton due to reproduction and growth could be an explanation (Hargrave et al., 2000).

Table 2: PAE concentrations in zooplankton samples (sized > 1 mm; < 1 mm, > 500 µm; < 500 µm, > 150 µm) collected on six sampling days (S1-S6) in the Bay of Marseille (L'Estaque, Frioul and Cortiou station). "*" indicates the samples exhibiting very high DnBP and DiBP concentrations due to contamination through rubber boot fragments.

	L'Estaque						Frioul						Cortiou					
Zooplankton > 1 mm	*S1*	*S2*	*S3*	*S4*	*S5*	*S6*	*S1*	*S2*	*S3*	*S4*	*S5*	*S6*	*S1*	*S2*	*S3*	*S4*	*S5*	*S6*
DMP	-	-	642	39	-	29	-	-	27	56	-	30	-	-	32	501	12	41
DEP	-	-	19	11	-	8.9	-	-	16	16	-	19	-	-	32	19	21	14
DnBP	-	-	305	386	-	67	-	-	349	178	-	47	-	-	93	527	1601	218
DiBP	-	-	120	118	-	41	-	-	90	92	-	127	-	-	56	224	64	172
BzBP	-	-	35	75	-	91	-	-	n.d.	37	-	184	-	-	98	n.d.	166	125
DEHP	-	-	3553	3803	-	1090	-	-	4062	1885	-	1057	-	-	8285	7838	3721	20573
DnOP	-	-	180	n.d.	-	n.d.	-	-	n.d.	149	-	113	-	-	398	544	197	1048
Σ PAEs	-	-	**4 854**	**4 432**	-	**1 327**	-	-	**4 544**	**2 413**	-	**1 577**	-	-	**8 994**	**9 653**	**5 782**	**22 191**
< 1 mm, > 500 µm	*S1*	*S2*	*S3*	*S4*	*S5*	*S6*	*S1*	*S2*	*S3*	*S4*	*S5*	*S6*	*S1*	*S2*	*S3*	*S4*	*S5*	*S6*
DMP	n.d.	-	456	5.9	n.d.	17	n.d.	150	n.d.	16	2.8	n.d.	9.1	2.1	n.d.	6.1	-	9.6
DEP	21	-	14	13	33	9.8	24	23	12	14	26	17	25	16	25	20	-	12
DnBP	258	-	113	42	*13310**	177	159	150	38	80	*11480**	189	217	151	69	50	-	69
DiBP	88	-	25	10	*973**	50	62	48	8.2	42	*810**	56	82	38	26	26	-	26
BzBP	204	-	25	n.d.	n.d.	203	175	67	n.d.	n.d.	n.d.	158	72	33	78	57	-	109
DEHP	309	-	2192	658	1434	865	601	3846	778	811	2703	545	8040	5681	4019	12247	-	15642
DnOP	66	-	168	12	62	88	79	252	27	20	132	74	353	138	134	1003	-	767
Σ PAEs	**946**	-	**2 993**	**741**	***15 812****	**1 410**	**1 100**	**4 536**	**863**	**983**	***15 154****	**1 039**	**8 798**	**6 059**	**4 351**	**13 409**	-	**16 635**
< 500 µm, > 150 µm	*S1*	*S2*	*S3*	*S4*	*S5*	*S6*	*S1*	*S2*	*S3*	*S4*	*S5*	*S6*	*S1*	*S2*	*S3*	*S4*	*S5*	*S6*
DMP	3.1	7.1	197	21	n.d.	n.d.	n.d.	117	n.d.	14	5.7	n.d.	9.0	24	6.2	43	n.d.	19
DEP	17	29	7.0	20	23	47	162	38	14	19	11	39	27	17	9.9	26	17	108
DnBP	163	288	104	133	66	64	537	815	197	60	194	103	27	74	40	51	206	98
DiBP	68	110	31	40	55	36	65	224	75	9.4	47	19	60	44	45	34	230	138
BzBP	49	340	35	74	95	173	54	88	n.d.	n.d.	40	127	n.d.	n.d.	n.d.	n.d.	n.d.	n.d.
DEHP	2521	1257	2930	2737	1245	1991	869	6341	3506	1653	2126	951	33568	14346	5032	30736	1397	43228
DnOP	87	96	125	235	73	152	21	570	1361	27	133	7.6	1203	901	182	2166	182	3377
Σ PAEs	**2 908**	**2 127**	**3 429**	**3 260**	**1 557**	**2 463**	**1 708**	**8 193**	**5 153**	**1 782**	**2 557**	**1 247**	**34 894**	**15 406**	**5 315**	**33 056**	**2 032**	**46 968**

As in water and sediment samples, the most abundant PAE in all zooplankton samples was DEHP, with a maximum concentration of ~43,000 ng g^{-1} dw. A previous study analyzing PAEs in zooplankton samples from the NW Mediterranean Sea detected Σ_7 PAEs at concentrations of 16.8-4576 ng g^{-1} dw, with DEHP concentrations of up to 2699 ng g^{-1} dw (mean 679±739) (Baini et al., 2017). This mean DEHP concentration is clearly lower than our mean DEHP concentration in zooplankton samples, even if we exclude the highly contaminated WWTP outlet Cortiou station (i.e., 2011±1405 ng g^{-1} dw without Cortiou station), indicating that the Bay of Marseille could be a contamination hotspot. Since zooplankton is at the base of the marine food web, negative implications for organisms of higher trophic levels cannot be excluded and the consequences for the local marine resources should be investigated. More data from other parts of the Mediterranean Sea, and elsewhere, are urgently needed for comparison. Concerning OPEs in zooplankton, to our knowledge, only one study reported concentrations detected in freshwater samples so far (10.8±0.5 ng g^{-1} ww of Σ_{11} OPEs; Wang et al., 2019). Zooplankton is also impacted by other organic contaminants, such as PCBs (14.2-88.1 ng g^{-1} dw Σ_7 PCBs in Marseille Bay; Tiano et al., 2014) and perfluorooctane sulfonate (PFOS) (4.18 ng g^{-1} ww in Gaobeidian Lake, China; Li et al., 2008).

Table 3: OPE concentrations in zooplankton samples (sized > 1 mm; < 1 mm, > 500 µm; < 500 µm, > 150 µm) collected on six sampling days (S1-S6) in the Bay of Marseille (L'Estaque, Frioul and Cortiou station). "-" indicate that not enough biomass was available for extraction or that TCPP and/or TDCP could not be quantified due to matrix effects.

	L'Estaque						Frioul						Cortiou					
Zooplankton > 1 mm	*S1*	*S2*	*S3*	*S4*	*S5*	*S6*	*S1*	*S2*	*S3*	*S4*	*S5*	*S6*	*S1*	*S2*	*S3*	*S4*	*S5*	*S6*
TPP	-	-	n.d.	n.d.	-	n.d.	-	-	n.d.	n.d.	-	n.d.	-	-	n.d.	n.d.	n.d.	n.d.
TiBP	-	-	183	301	-	85	-	-	766	218	-	68	-	-	188	155	79	309
TnBP	-	-	8.3	4.6	-	n.d.	-	-	32	8.4	-	4.4	-	-	21	25	9.8	74
TCEP	-	-	88	92	-	44	-	-	217	145	-	92	-	-	162	123	197	107
TCPP	-	-	367	477	-	128	-	-	-	287	-	-	-	-	548	646	261	1487
TDCP	-	-	217	221	-	129	-	-	n.d.	n.d.	-	80	-	-	707	n.d.	1606	2267
TPhP	-	-	15	16	-	n.d.	-	-	19	18	-	5.3	-	-	38	12	16	64
EHDPP	-	-	114	83	-	6.6	-	-	148	162	-	50	-	-	124	139	69	149
TEHP	-	-	92	n.d.	-	n.d.	-	-	n.d.	n.d.	-	n.d.	-	-	80	94	n.d.	175
Σ OPEs	**-**	**-**	**1 084**	**1 195**	**-**	**393**	**-**	**-**	**1 182**	**838**	**-**	**300**	**-**	**-**	**1 868**	**1 194**	**2 238**	**4 632**
< 1 mm, > 500 µm	*S1*	*S2*	*S3*	*S4*	*S5*	*S6*	*S1*	*S2*	*S3*	*S4*	*S5*	*S6*	*S1*	*S2*	*S3*	*S4*	*S5*	*S6*
TPP	n.d.	-	n.d.	n.d.	n.d.	n.d.	n.d.	n.d.	n.d.	n.d.	n.d.	n.d.	n.d.	n.d.	n.d.	n.d.	-	n.d.
TiBP	49	-	286	51	261	112	55	140	64	74	144	76	97	81	54	87	-	131
TnBP	50	-	4.7	3.5	25	n.d.	5.3	13	21	4.0	12	n.d.	9.2	4.7	23	15	-	53
TCEP	209	-	95	132	507	160	167	171	162	141	299	186	121	149	100	126	-	120
TCPP	-	-	180	67	497	-	-	352	137	131	302	-	459	416	207	386	-	764
TDCP	1269	-	566	57	n.d.	1024	2200	517	500	-	53	1099	1175	n.d.	403	786	-	484
TPhP	n.d.	-	12	7.3	16	n.d.	n.d.	48	22	12	18	n.d.	19	25	16	23	-	21
EHDPP	42	-	74	82	55	21	37	314	104	215	72	40	149	171	100	160	-	188
TEHP	n.d.	-	9.5	6.5	7.8	39	n.d.	n.d.	67	n.d.	n.d.	n.d.	87	n.d.	80	113	-	120
Σ OPEs	**1 619**	**-**	**1 227**	**406**	**1 369**	**1 356**	**2 464**	**1 555**	**1 077**	**577**	**900**	**1 401**	**2 116**	**847**	**983**	**1 696**	**-**	**1 881**
< 500 µm, > 150 µm	*S1*	*S2*	*S3*	*S4*	*S5*	*S6*	*S1*	*S2*	*S3*	*S4*	*S5*	*S6*	*S1*	*S2*	*S3*	*S4*	*S5*	*S6*
TPP	n.d.	n.d.	n.d.	n.d.	n.d.	n.d.	n.d.	n.d.	n.d.	n.d.	n.d.	n.d.	n.d.	n.d.	n.d.	n.d.	n.d.	n.d.
TiBP	70	88	169	263	359	152	53	276	929	79	53	251	121	193	48	128	103	120
TnBP	42	14	5.0	8.6	27	n.d.	14	19	79	40	5.6	n.d.	11	68	13	66	68	38
TCEP	171	206	158	99	205	235	206	583	207	129	72	219	228	162	121	130	177	218
TCPP	-	269	240	229	716	-	-	933	-	210	111	-	1532	906	483	970	-	644
TDCP	1558	2610	40	643	-	891	-	985	-	523	460	583	192	2038	591	1030	-	931
TPhP	3.8	69	20	16	n.d.	n.d.	n.d.	70	n.d.	21	5.9	n.d.	29	31	15	27	n.d.	38
EHDPP	68	310	89	227	53	48	-	572	-	697	66	79	405	178	98	311	53	398
TEHP	n.d.	n.d.	n.d.	21	n.d.	146	-	121	n.d.	77	9.6	91	271	288	103	229	n.d.	365
Σ OPEs	**1 913**	**3 566**	**721**	**1 507**	**1 360**	**1 472**	**273**	**3 559**	**1 215**	**1 776**	**783**	**1 223**	**2 789**	**3 864**	**1 472**	**2 891**	**401**	**2 752**

To get an idea of the bioconcentration potential of the studied compounds, the average and median bioconcentration factors (BCF) of PAEs and OPEs were calculated for the three zooplankton size classes by using the following equation:

$$\text{BCF} = \frac{[zooplankton](mg\ kg^{-1})}{[water](mg\ L^{-1})}$$

Since the wet weight is used for the BCF calculation, zooplankton concentrations were converted from ng g^{-1} dw to ng g^{-1} ww by using a conversion factor of 0.2, based on literature (Håkanson and Boulion, 2003; Pagano and Saint-Jean, 1994). The BCF does not take diet into account. Instead, it is a quantity that represents the proportion of concentrations in the organism compared to concentrations in water. However, zooplankton is thought to accumulate a significant fraction of organic contaminants from the dissolved water phase (Borgå et al., 2005), justifying the use of the BCF as a basic risk assessment tool. In Annex D of the Stockholm Convention on Persistent Organic Pollutants, a BCF $\geq$ 5000 L kg^{-1} is listed as a criterion identifying a chemical as bioaccumulative. If we apply this criterion to the median BCFs, BzBP, DnOP, TiBP, TCEP, EHDPP and TEHP can be considered as bioaccumulative. Between size classes, the calculated BCFs were sometimes variable, but without clear trends (Table S3).

3.4. Microplastics

Microplastic density in surface waters varied between 0 and 0.308 items per cubic meter (mean 0.051 items m^{-3}). Surprisingly, the highest mean MP abundance was found at Frioul island (0.081 items m^{-3}), the station where generally lower contaminant concentrations were measured, compared to the other two stations and more specifically compared to Cortiou station. In contrast, at Cortiou station the lowest mean MP density (0.025 items m^{-3}) was observed (Fig. 4). This could suggest that the water near the outfall is well mixed and the

microplastics are therefore distributed in the whole water column, leading to lower MP concentrations at the surface, or that the contaminants probably originate from various sources, such as household greywater, leaching from PVC pipes (e.g., from the sewage system) or industrial inputs and not solely from plastic litter. A regression analysis confirmed that PAE and OPE concentrations at the three sampling stations were not correlated with the corresponding microplastic abundances (p-value = 0.7). This indicates, that in coastal systems microplastic abundances cannot be taken as a proxy of contamination by organic plastic additives and *vice versa*. When compared to literature, our MP density observed is at the lower limit of previous studies. For example, a mean abundance of 0.15 items m^{-3} was measured in the Central-Western Mediterranean Sea (de Lucia et al., 2014). Hereby, the authors observed lower MP concentrations close to the shore (0.01±0.00 - 0.18±0.03 items m^{-3}) than in off-shore waters (up to 0.35±0.11 items m^{-3}). In the Atlantic Ocean (Portuguese coast) mean MP concentrations ranging from 0.002±0.001 to 0.036±0.027 items m^{-3} have been reported (Frias et al., 2014).

In L'Estaque, small MPs (surface area < 1 mm^2) were predominant with 90.1% relative abundance, followed by MPs with a surface area between 1-5 mm^2 (8.5%) and between 5-10 mm^2 (1.4%). In Cortiou, the percentage of particles sized 1-5 mm^2 (35.5%) and 5-10 mm^2 (3.2%) was higher, but the small-sized items < 1 mm^2 remained dominant (61.3%). Finally, in Frioul items sized < 1 mm^2 and 1-5 mm^2 had similar relative abundances (40.5% and 44.0%, respectively), as well as MPs with a surface area of 5-10 mm^2 and > 10 mm^2 (6.7% and 8.6%, respectively) (Fig. 4). This indicates, that the size distribution in samples can differ even at a small spatial scale. In a previous study analyzing MPs at three sampling stations in the Bay of Marseille (all close to Frioul island), a similar size distribution like in this study (at Frioul station) was observed, but with an even higher percentage of items sized 1-5 mm^2 (55%; compared to 27% of items < 1 mm^2) (Schmidt et al., 2018).

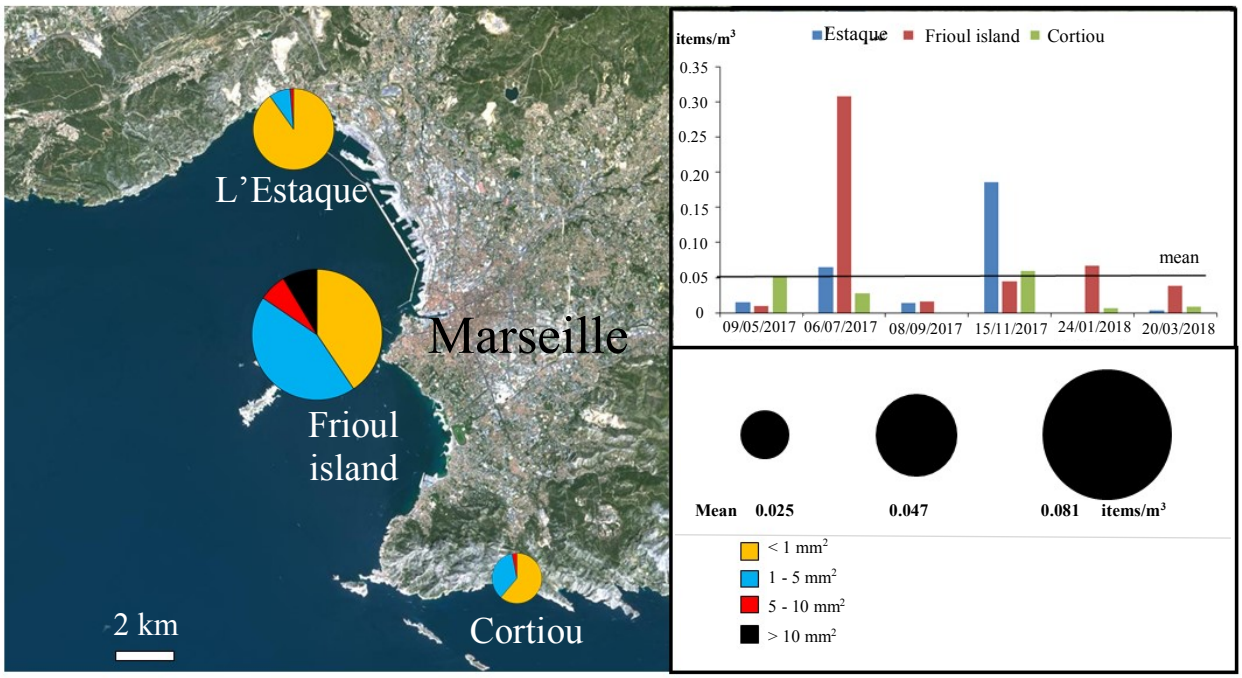

Fig. 4: Microplastic density (items/m^3) observed on each of the six sampling dates at the three stations (upper right corner) and distribution of microplastic surface area (mm^2) along stations (left).

4. Conclusion

PAEs and OPEs were detected at high (zooplankton), moderate (water) and low (sediment) concentrations in Marseille Bay. PAEs were generally more abundant than OPEs, with DEHP being the predominant PAE in all matrixes. Especially zooplankton samples collected near the municipal WWTP outlet exhibited disturbingly high DEHP concentrations, raising questions about potential toxicity and impacts on the local marine food web. Variability in contaminant concentrations within the same size class and sampling station are possibly due to the life cycle of zooplanktonic organisms, though this needs further investigations. The smallest zooplankton size class exhibited highest PAE and OPE concentrations. These differences in contaminant concentrations between size classes also need further investigations and it would be interesting to study this aspect in laboratory experiments. Certain compounds

had median bioconcentration factors > 5000 L kg^{-1}, suggesting a potential for bioaccumulation. This was, however, not the case for DEHP and TCPP, generally the most abundant PAE/OPE in environmental samples. The amounts of dissolved organic plastic additives in surface waters and the abundance of microplastic were not correlated. This is the first comprehensive study on PAE and OPE occurrence and temporal variability in water, sediment and differently sized zooplankton.

Acknowledgements

We thank the captain and crew of the R/V Antedon II and Dorian Guillemain, Michel Lafont, Deny Malengros and the MIO SAM platform for help during sampling. Thanks to Benjamin Oursel for help with ultrasound extractions. Sediment sampling at Cortiou station was permitted by the Calanques National Park through the individual decision N° 2016-333.

References

Baini, M., Martellini, T., Cincinelli, A., Campani, T., Minutoli, R., Panti, C., Finoia, M.G., Fossi, M.C., 2017. First detection of seven phthalate esters (PAEs) as plastic tracers in superficial neustonic/planktonic samples and cetacean blubber. Anal. Methods 9, 1512–1520. https://doi.org/10.1039/c6ay02674e

Borgå, K., Fisk, A.T., Hargrave, B., Hoekstra, P.F., Swackhamer, D., Muir, D.C.G., 2005. Bioaccumulation factors for PCBs revisited. Environ. Sci. Technol. 39, 4523–4532. https://doi.org/10.1021/es050376i

Castro-Jiménez, J., Berrojalbiz, N., Pizarro, M., Dachs, J., 2014. Organophosphate ester (OPE) flame retardants and plasticizers in the open mediterranean and black seas atmosphere. Environ. Sci. Technol. 48, 3203–3209. https://doi.org/10.1021/es405337g

Castro-Jiménez, J., Casal, P., González-Gaya, B., Pizarro, M., Dachs, J., 2016. Organophosphate ester flame retardants and plasticizers in the global oceanic atmosphere. Environ. Sci. Technol 50, 12831–12839.

Cole, M., Lindeque, P., Fileman, E., Halsband, C., Goodhead, R., Moger, J., Galloway, T.S., 2013. Microplastic Ingestion by Zooplankton. Environ. Sci. Technol 47, 6646–6655. https://doi.org/10.1021/es400663f

Collignon, A., Hecq, J.H., Glagani, F., Voisin, P., Collard, F., Goffart, A., 2012. Neustonic microplastic and zooplankton in the North Western Mediterranean Sea. Mar. Pollut. Bull. 64, 861–864. https://doi.org/10.1016/j.marpolbul.2012.01.011

de Lucia, G.A., Caliani, I., Marra, S., Camedda, A., Coppa, S., Alcaro, L., Campani, T., Giannetti, M., Coppola, D., Cicero, A.M., Panti, C., Baini, M., Guerranti, C., Marsili, L., Massaro, G., Fossi, M.C., Matiddi, M., 2014. Amount and distribution of neustonic micro-plastic off the western Sardinian coast (Central-Western Mediterranean Sea). Mar. Environ. Res. 100, 10–16. https://doi.org/10.1016/j.marenvres.2014.03.017

DeLorenzo, M.E., Taylor, L.A., Lund, S.A., Pennington, P.L., Strozier, E.D., Fulton, M.H., 2002. Toxicity and bioconcentration potential of the agricultural pesticide endosulfan in phytoplankton and zooplankton. Arch. Environ. Contam. Toxicol. 42, 173–181. https://doi.org/10.1007/s00244-001-0008-3

Duncan, E.M., Broderick, A.C., Fuller, W.J., Galloway, T.S., Godfrey, M.H., Hamann, M., Limpus, C.J., Lindeque, P.K., Mayes, A.G., Omeyer, L.C.M., Santillo, D., Snape, R.T.E., Godley, B.J., 2019. Microplastic ingestion ubiquitous in marine turtles. Glob. Chang. Biol. 25, 744–752. https://doi.org/10.1111/gcb.14519

Fauvelle, V., Castro-Jiménez, J., Schmidt, N., Carlez, B., Panagiotopoulos, C., Sempéré, R., 2018. One-Single Extraction Procedure for the Simultaneous Determination of a Wide Range of Polar and Nonpolar Organic Contaminants in Seawater. Front. Mar. Sci. 5, 1–10. https://doi.org/10.3389/fmars.2018.00295

Fraysse, M., Pairaud, I., Ross, O.N., Faure, V.M., Pinazo, C., 2014. Intrusion of Rhone River diluted water into the Bay of Marseille: Generation processes and impacts on ecosystem functioning. J. Geophys. Res. Ocean. 119, 6535–6556. https://doi.org/10.1002/2014JC010022.Received

Frias, J.P.G.L., Otero, V., Sobral, P., 2014. Evidence of microplastics in samples of zooplankton from Portuguese coastal waters. Mar. Environ. Res. 95, 89–95.

https://doi.org/10.1016/j.marenvres.2014.01.001

Håkanson, L., Boulion, V. V., 2003. A general dynamic model to predict biomass and production of phytoplankton in lakes. Ecol. Modell. 165, 285–301. https://doi.org/10.1016/S0304-3800(03)00096-6

Hargrave, B.T., Phillips, G.A., Vass, W.P., Bruecker, P., Welch, H.E., Siferd, T.D., 2000. Seasonality in bioaccumulation of organochlorines in lower trophic level arctic marine biota. Environ. Sci. Technol. 34, 980–987. https://doi.org/10.1021/es990871c

Horton, A.A., Walton, A., Spurgeon, D.J., Lahive, E., Svendsen, C., 2017. Microplastics in freshwater and terrestrial environments: Evaluating the current understanding to identify the knowledge gaps and future research priorities. Sci. Total Environ. 586, 127–141. https://doi.org/10.1016/j.scitotenv.2017.01.190

Isobe, A., Uchida, K., Tokai, T., Iwasaki, S., 2015. East Asian seas: A hot spot of pelagic microplastics. Mar. Pollut. Bull. 101, 618–623. https://doi.org/10.1016/j.marpolbul.2015.10.042

Lebreton, L.C.M., Van Der Zwet, J., Damsteeg, J.W., Slat, B., Andrady, A., Reisser, J., 2017. River plastic emissions to the world's oceans. Nat. Commun. 8, 1–10. https://doi.org/10.1038/ncomms15611

Li, X., Yin Yeung, L.W., Xu, M., Taniyasu, S., Lam, P.K.S., Yamashita, N., Dai, J., 2008. Perfluorooctane sulfonate (PFOS) and other fluorochemicals in fish blood collected near the outfall of wastewater treatment plant (WWTP) in Beijing. Environ. Pollut. 156, 1298–1303. https://doi.org/10.1016/j.envpol.2008.03.008

Liubartseva, S., Coppini, G., Lecci, R., Clementi, E., 2018. Tracking plastics in the Mediterranean: 2D Lagrangian model. Mar. Pollut. Bull. 129, 151–162. https://doi.org/10.1016/j.marpolbul.2018.02.019

Ma, Y., Xie, Z., Lohmann, R., Mi, W., Gao, G., 2017. Organophosphate Ester Flame Retardants and Plasticizers in Ocean Sediments from the North Pacific to the Arctic Ocean. Environ. Sci. Technol. 51, 3809–3815. https://doi.org/10.1021/acs.est.7b00755

Marklund, A., 2005. Levels and Sources of Organophosphorus Flame Retardants and Plasticizers in.

Net, S., Sempéré, R., Delmont, A., Paluselli, A., Ouddane, B., 2015. Occurrence, fate, behavior and ecotoxicological state of phthalates in different environmental matrices. Environ. Sci. Technol. 49, 4019–4035. https://doi.org/10.1021/es505233b

Oursel, B., Garnier, C., Durrieu, G., Mounier, S., Omanović, D., Lucas, Y., 2013. Dynamics and fates of trace metals chronically input in a Mediterranean coastal zone impacted by a large urban area. Mar. Pollut. Bull. 69, 137–149. https://doi.org/10.1016/j.marpolbul.2013.01.023

Pagano, M., Saint-Jean, L., 1994. In situ metabolic budget for the calanoid copepod Acartia clausi in a tropical brackish water lagoon (Ebrié Lagoon, Ivory Coast). Hydrobiologia 272, 147–161. https://doi.org/10.1007/BF00006518

Paluselli, A., Aminot, Y., Galgani, F., Net, S., Sempéré, R., 2018a. Occurrence of phthalate acid esters (PAEs) in the northwestern Mediterranean Sea and the Rhone River. Prog. Oceanogr. 163, 221–231. https://doi.org/10.1016/j.pocean.2017.06.002

Paluselli, A., Fauvelle, V., Galgani, F., Sempéré, R., 2019. Phthalate release from plastic fragments and degradation in seawater. Environ. Sci. Technol. 53, 166–175. https://doi.org/10.1021/acs.est.8b05083

Paluselli, A., Fauvelle, V., Schmidt, N., Galgani, F., Net, S., Sempéré, R., 2018b. Distribution of phthalates in Marseille Bay (NW Mediterranean Sea). Sci. Total Environ. 621, 578–587. https://doi.org/10.1016/j.scitotenv.2017.11.306

Pantelaki, I., Voutsa, D., 2019. Organophosphate flame retardants (OPFRs): A review on analytical methods and occurrence in wastewater and aquatic environment. Sci. Total Environ. 649, 247–263. https://doi.org/10.1016/j.scitotenv.2018.08.286

Peijnenburg, W.J.G.M., Struijs, J., 2006. Occurrence of phthalate esters in the environment of the Netherlands. Ecotoxicol. Environ. Saf. 63, 204–215. https://doi.org/10.1016/j.ecoenv.2005.07.023

Reemtsma, T., Quintana, J.B., Rodil, R., García-López, M., Rodríguez, I., 2008. Organophosphorus flame retardants and plasticizers in water and air I. Occurrence and fate. Trends Anal. Chem. 27, 727–737. https://doi.org/10.1016/j.trac.2008.07.002

Sánchez-Avila, J., Tauler, R., Lacorte, S., 2012. Organic micropollutants in coastal waters from NW Mediterranean Sea: Sources distribution and potential risk. Environ. Int. 46, 50–62. https://doi.org/10.1016/j.envint.2012.04.013

Schmidt, N., Thibault, D., Galgani, F., Paluselli, A., Sempéré, R., 2018. Occurrence of microplastics in surface waters of the Gulf of Lion (NW Mediterranean Sea). Prog. Oceanogr. 163, 214–220. https://doi.org/10.1016/j.pocean.2017.11.010

Silva-Cavalcanti, J.S., Silva, J.D.B., França, E.J. de, Araújo, M.C.B. de, Gusmão, F., 2017. Microplastics ingestion by a common tropical freshwater fishing resource. Environ. Pollut. 221, 218–226. https://doi.org/10.1016/j.envpol.2016.11.068

Sousa, J.C.G., Ribeiro, A.R., Barbosa, M.O., Pereira, M.F.R., Silva, A.M.T., 2018. A review on environmental monitoring of water organic pollutants identified by EU guidelines. J. Hazard. Mater. 344, 146–162. https://doi.org/10.1016/j.jhazmat.2017.09.058

Suaria, G., Avio, C.G., Mineo, A., Lattin, G.L., Magaldi, M.G., Belmonte, G., Moore, C.J., Regoli, F., Aliani, S., 2016. The Mediterranean Plastic Soup: Synthetic polymers in Mediterranean surface waters. Sci. Rep. 6, 1–10. https://doi.org/10.1038/srep37551

Tiano, M., Tronczyński, J., Harmelin-Vivien, M., Tixier, C., Carlotti, F., 2014. PCB concentrations in plankton size classes, a temporal study in Marseille Bay, Western Mediterranean Sea. Mar. Pollut. Bull. 89, 331–339. https://doi.org/10.1016/j.marpolbul.2014.09.040

van der Veen, I., de Boer, J., 2012. Phosphorus flame retardants: properties, production, environmental occurrence, toxicity and analysis. Chemosphere 88, 1119–1153. https://doi.org/10.1016/j.chemosphere.2012.03.067

van Wijnen, J., Ragas, A.M.J., Kroeze, C., 2019. Modelling global river export of microplastics to the marine environment: Sources and future trends. Sci. Total Environ. 673, 392–401. https://doi.org/10.1016/j.scitotenv.2019.04.078

Vila-Costa, M., Sebastián, M., Pizarro, M., Cerro-Gálvez, E., Lundin, D., Gasol, J.M., Dachs, J., 2019. Microbial consumption of organophosphate esters in seawater under phosphorus limited conditions. Sci. Rep. 9, 1–11. https://doi.org/10.1038/s41598-018-

36635-2

Wang, R., Tang, J., Xie, Z., Mi, W., Chen, Y., Wolschke, H., Tian, C., Pan, X., Luo, Y., Ebinghaus, R., 2015. Occurrence and spatial distribution of organophosphate ester flame retardants and plasticizers in 40 rivers draining into the Bohai Sea, north China. Environ. Pollut. 198, 172–178. https://doi.org/10.1016/j.envpol.2014.12.037

Wang, X., Zhong, W., Xiao, B., Liu, Q., Yang, L., Covaci, A., Zhu, L., 2019. Bioavailability and biomagnification of organophosphate esters in the food web of Taihu Lake, China: Impacts of chemical properties and metabolism. Environ. Int. 125, 25–32. https://doi.org/10.1016/j.envint.2019.01.018

Wang, Y., Wu, X., Zhang, Q., Hou, M., Zhao, H., Xie, Q., Du, J., Chen, J., 2017. Organophosphate esters in sediment cores from coastal Laizhou Bay of the Bohai Sea, China. Sci. Total Environ. 607–608, 103–108. https://doi.org/10.1016/j.scitotenv.2017.06.259

Wolschke, H., Sühring, R., Xie, Z., Ebinghaus, R., 2015. Organophosphorus flame retardants and plasticizers in the aquatic environment: A case study of the Elbe River, Germany. Environ. Pollut. 206, 488–493. https://doi.org/10.1016/j.envpol.2015.08.002

Yang, C., Harris, S.A., Jantunen, L.M., Siddique, S., Kubwabo, C., Tsirlin, D., Latifovic, L., Fraser, B., St-Jean, M., De La Campa, R., You, H., Kulka, R., Diamond, M.L., 2019. Are cell phones an indicator of personal exposure to organophosphate flame retardants and plasticizers? Environ. Int. 122, 104–116. https://doi.org/10.1016/j.envint.2018.10.021

Young, H.S., McCauley, D.J., Galetti, M., Dirzo, R., 2016. Patterns, Causes, and Consequences of Anthropocene Defaunation. Annu. Rev. Ecol. Evol. Syst. 47, 333–358. https://doi.org/10.1146/annurev-ecolsys-112414-054142

Zhong, M., Wu, H., Mi, W., Li, F., Ji, C., Ebinghaus, R., Tang, J., Xie, Z., 2018. Occurrences and distribution characteristics of organophosphate ester flame retardants and plasticizers in the sediments of the Bohai and Yellow Seas, China. Sci. Total Environ. 615, 1305–1311. https://doi.org/10.1016/j.scitotenv.2017.09.272

Zhu, J., Yu, X., Zhang, Q., Li, Y., Tan, S., Li, D., Yang, Z., Wang, J., 2019. Cetaceans and microplastics: First report of microplastic ingestion by a coastal delphinid, Sousa chinensis. Sci. Total Environ. 659, 649–654. https://doi.org/10.1016/j.scitotenv.2018.12.389

CHAPTER V:
Organic contaminants in the tropical North Atlantic

Environmental Science & Technology

Article

Cite This: Environ. Sci. Technol. 2019, 53, 7513−7521

pubs.acs.org/est

The Amazon River: A Major Source of Organic Plastic Additives to the Tropical North Atlantic?

Natascha Schmidt,[†] Vincent Fauvelle,[†] Anouck Ody,[†] Javier Castro-Jiménez,[†] Julien Jouanno,[‡] Thomas Changeux,[†] Thierry Thibaut,[†] and Richard Sempéré*[,†]

[†]Aix-Marseille Univ., Toulon Univ., CNRS, IRD, Mediterranean Institute of Oceanography (MIO), Marseille 13288, France

[‡]LEGOS, Université de Toulouse, IRD, CNRS, CNES, UPS, Toulouse 31400, France

Supporting Information

ABSTRACT: The release of emerging organic contaminants is identified among the most critical hazards to the marine environment, and plastic additives have received growing attention due to their worldwide distribution and potential deleterious effects. Here, we report dissolved surface water concentrations of two important families of plastic additives (organophosphate esters (OPEs) and bisphenols) and other related organic compounds (perfluorinated chemicals) measured in the North Atlantic from Cape Verde to the West Indies. We found that OPEs were the most abundant contaminants, reaching remarkably high concentrations in open ocean waters (1200 km offshore of the American Coast, at the location of the Amazon river plume during the sampling period), with up to 1.3 μg L^{-1} (Σ_9OPEs). A Lagrangian analysis confirmed that these high concentrations of contaminants originated from the Amazon River plume and were transported more than 3000 km by the North Brazil Current and its retroflection. We thus consider the Amazon River as a major source of organic contaminants of emerging concern to the tropical North Atlantic Ocean and suggest that medium-/long-range contaminant transport occurs, most certainly facilitated by the highly stratified conditions offered by the river plume.

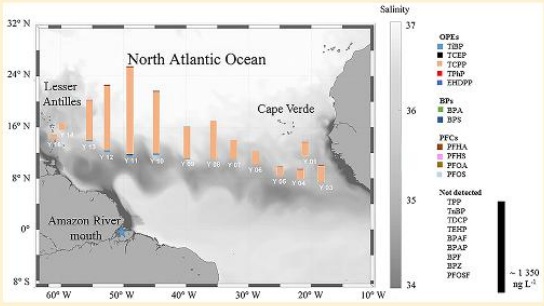

INTRODUCTION

Over the past few decades, the dramatic increase in plastic and, more generally, chemical production volumes has led to the widespread occurrence of organic contaminants in all water bodies, including marine environments and numerous living organisms.[1] Organophosphate ester (OPE) flame retardants and plasticizers are among the most common organic plastic additives, representing up to 7% by mass of global plastic production.[2] The most important OPE by production volume is tris(2-chloro, 1-methylethyl) phosphate (TCPP).[3] Although the occurrence of OPEs in indoor and outdoor air, freshwater environments, sediments, and soils is relatively well-documented,[4−7] there are still many open questions concerning the distribution and fate of OPEs in the marine environment. OPEs have been reported as persistent, bioaccumulative, and toxic.[5] While most research focuses on Asia (mainly China),[8−10] and Europe[11−13] and some focuses on North America,[14−16] no data for South American rivers, lakes or coastal areas are available to date to the best of our knowledge.

Bisphenols (BPs), known for their endocrine-disrupting properties, which have led to various national and international bans and regulations, are still used in the production of thermal paper, plastic bottles and food can linings, among other items.[17,18] Bisphenols have been detected in sediment and seawater samples[19,20] as well as in the atmosphere, where the presence of bisphenol A (BPA) has been linked to plastic burning.[21] Perfluorinated compounds (PFCs) have water- and oil-resistant properties and therefore are used in outdoor textiles and food packaging as well as in fire-fighting foams.[22,23] PFCs are very resistant to heat and chemicals, which qualifies them as persistent pollutants in the environment. Perfluorooctanesulfonic acid (PFOS) and PFOS precursors have therefore been listed as persistent organic pollutants (POPs) under the Stockholm Convention.[24] PFCs have been detected in remote regions, such as the Central Arctic Ocean,[25] and the most oligotrophic areas of the subtropical Atlantic, Pacific, and Indian oceans[26] as well as in coastal waters.[27] The main source of PFCs in the marine environment is river inputs.[28]

To study their waterborne occurrence and possible sources in the tropical North Atlantic Ocean, surface seawater samples were collected in October 2017 at 14 coastal and open ocean stations (Table S1) during the Transatlantic Sargassum expedition (https://doi.org/10.17600/17016900) on the M/V Yersin from Cape Verde to Martinique Island (Lesser Antilles) along 6000 km. Seawater samples were analyzed for

Received: March 26, 2019
Revised: June 4, 2019
Accepted: June 4, 2019
Published: June 4, 2019

ACS Publications © 2019 American Chemical Society

DOI: 10.1021/acs.est.9b01585
Environ. Sci. Technol. 2019, 53, 7513−7521

Downloaded via Natascha Schmidt on July 10, 2019 at 09:01:51 (UTC).
See https://pubs.acs.org/sharingguidelines for options on how to legitimately share published articles.

The Amazon River – a major source of organic plastic additives to the tropical North Atlantic?

Natascha Schmidt [1], Vincent Fauvelle [1], Anouck Ody [1], Javier Castro-Jiménez [1], Julien Jouanno [2], Thomas Changeux [1], Thierry Thibaut [1], Richard Sempéré [1,*]

[1] *Aix-Marseille Univ., Toulon Univ., CNRS, IRD, Mediterranean Institute of Oceanography (M I O), Marseille, France*

[2] *LEGOS, Université de Toulouse, IRD, CNRS, CNES, UPS, Toulouse, France*

* *corresponding author*

Mail: richard.sempere@mio.osupytheas.fr

Declarations of interest: none

Abstract

The release of emerging organic contaminants is identified among the most critical hazards to the marine environment, and plastic additives have received growing attention due to their worldwide distribution and potential deleterious effects. Here we report dissolved surface water concentrations of two important families of plastic additives (organophosphate esters -OPEs-, bisphenols) and other related organic compounds (perfluorinated chemicals) measured in the North Atlantic from Cape Verde to the West Indies. We found that OPEs were the most abundant contaminants, reaching remarkably high concentrations in open ocean waters (1,200 km offshore of the American Coast, at the location of the Amazon river plume during the sampling period), with up to 1.3 μg L^{-1} (Σ_9 OPEs). A Lagrangian analysis confirmed that these high concentrations of contaminants originated from the Amazon River plume, and have been transported for more than 3,000 km by the North Brazil Current and its retroflection. We thus consider the Amazon River as a major source of organic contaminants of emerging concern to the tropical North Atlantic Ocean and suggest that medium/long-range contaminant transport occurs, most certainly facilitated by the highly stratified conditions offered by the river plume.

Keywords: Organophosphate esters, plasticizers, marine pollution, tropical Atlantic Ocean, Amazon River

Introduction

Over the past few decades, the dramatic increase in plastic and, more generally, chemical production volumes has led to the widespread occurrence of organic contaminants in all waterbodies, including marine environments and numerous living organisms[1]. Organophosphate ester (OPE) flame retardants and plasticizers are among the most common organic plastic additives, representing up to 7% by mass of global plastic production[2]. The most important OPE by production volume is tris-(2-chloro, 1-methylethyl) phosphate (TCPP)[3].Although the occurrence of OPEs in indoor and outdoor air, freshwater environments, sediments and soils is relatively well-documented[4-7], there are still many open questions concerning the distribution and fate of OPEs in the marine environment. OPEs have been reported as persistent, bioaccumulative and toxic[5]. While most research focuses on Asia (mainly China)[8-10], and Europe[11-13] and some focuses on North America[14-16], no data for South American rivers, lakes or coastal areas are available to date to the best of our knowledge.

Bisphenols (BPs), known for their endocrine disrupting properties, which have led to various national and international bans and regulations, are still used in the production of thermal paper, plastic bottles and food can linings, among others[17,18]. Bisphenols have been detected in sediment and seawater samples[19,20], as well as in the atmosphere, where the presence of bisphenol A (BPA) has been linked to plastic burning[21]. Perfluorinated compounds (PFCs) have water and oil resistant properties and therefore are used in outdoor textiles and food packaging, as well as in fire-fighting foams[22,23]. PFCs are very resistant to heat and chemicals, which qualifies them as persistent pollutants in the environment. Perfluorooctane sulfonic acid (PFOS) and PFOS precursors have therefore been listed as persistent organic pollutants (POPs) under the Stockholm Convention[24]. PFCs have been detected in remote regions, such as the Central Arctic Ocean[25] and the most oligotrophic areas of the subtropical Atlantic, Pacific and

Indian oceans[26] as well as in coastal waters[27]. The main source of PFCs in the marine environment is river inputs[28].

To study their waterborne occurrence and possible sources in the tropical North Atlantic Ocean, surface seawater samples were collected in October 2017 at 14 coastal and open ocean stations (Table S1) during the Transatlantic Sargassum expedition (https://doi.org/10.17600/17016900) on the M/V Yersin from Cape Verde to Martinique Island (Lesser Antilles) along 6,000 km. Seawater samples were analyzed for 20 organic contaminants of emerging concern, including OPEs, BPs and PFCs, by applying a multi-contaminant extraction protocol. A Lagrangian analysis was used to investigate the origin of the sampled surface waters.

Methods

Contaminant analysis

One-liter seawater samples were collected in duplicates at 14 sampling stations (Table S1, Fig. 1), amounting thus to a total of 28 samples. They were collected using an inox collector, poured into corresponding pre-combusted (450 °C, 6 h) glass bottles, GF/F-filtered (0.7 μm) and stored in a fridge for a maximum of 72 h before sample processing. Samples were analyzed for nine organophosphate esters (tripropyl phosphate -TPP-, tri-iso-buthyl phosphate -TiBP-, tri-n-butyl phosphate -TnBP-, tris-(2-chloroethyl) phosphate -TCEP-, tris-(2-chloro, 1-methylethyl) phosphate -TCPP-, tris-(2-chloro-, 1-chloromethylethyl) phosphate -TDCP-, triphenyl phosphate -TPhP-, 2-ethylhexyl-diphenyl phosphate -EHDPP- and tris(2-ethylhexyl) phosphate -TEHP-), five perfluorinated compounds (perfluorohexanoic acid -PFHA-, perfluorohexane sulfonic acid -PFHS-, perfluorooctanoic acid -PFOA-, perfluorooctane sulfonic acid -PFOS- and perfluorooctane sulfonyl fluoride -PFOSF-) and six bisphenols (bisphenol A -BPA-, bisphenol AF -BPAF-, bisphenol AP -BPAP-, bisphenol F -BPF-,

bisphenol S -BPS- and bisphenol Z -BPZ-). To do so, organic contaminants were extracted from batches of two replicates from three stations on-board using solid phase extraction (SPE)[29]. Briefly, glass cartridges containing 250 mg of HLB Oasis sorbent (Waters, Milford, USA) were mounted on a manifold (Supelco Visiprep®) and rinsed three times sequentially with 10 mL of ethyl acetate and 10 mL of methanol. Next, 10 mL of ultrapure water were passed through the cartridges. The seawater samples were spiked with surrogate standards (100 ng sample^{-1} of D_{27}-TBP, D_{18}-TCPP, D_{15}-TDCP and D_{15}-TPhP), vigorously shaken and passed through the cartridges using polytetrafluoroethylene (PTFE) liners, which were previously cleaned thoroughly with methanol.

Afterwards, 10 mL of ultrapure water were again passed through the cartridges. The cartridges were then vacuum dried for approximately an hour, wrapped in burnt aluminum foil and stored in the freezer (-25 °C). Upon arrival in the ISO 6 laboratory equipped for trace-clean analysis of organic compounds, a sequential elution was performed as follows: 5 mL of hexane followed by 5 mL of hexane/dichloromethane 50:50 (v/v) (F1) and 5 mL of ethyl acetate followed by 5 mL of methanol (F2). The two fractions were then evaporated with pure N_2 gas until a final volume of approximately 50 µL was left (F1) or until dryness (F2), in which case the extract was then reconstituted using 990 µL methanol. Internal standards were added as follows: 100 ng sample^{-1} of D_{21}-TPrP, D_{12}-TCEP and D_7- Malathion (F1) and 20 ng sample^{-1} of BPA-D_{16}, PFHA-$^{13}C_5$, PFBS-$^{13}C_3$, PFHS-$^{13}C_3$ and PFOS-$^{13}C_8$ (F2). OPEs were quantified by GC/MS (Agilent Technology 7820A-5977E) in the splitless selected ion monitoring (SIM) mode. The separation was achieved using a 30 m x 0.25 mm i.d. x 0.25 µm HP-5MS capillary column (Agilent J&W). PFCs and BPs were quantified using LC-QTOF (Agilent 1290 Infinity LC system coupled with Agilent 6530 Accurate-Mass Q-TOF, Agilent Technologies, Les Ulis, France). Separation was achieved using an Agilent Zorbax Eclipse XDB reversed phase column (50 mm x 2.1 mm, 1.8 µm), with the temperature set at 30 °C. GC/MS and LC-QTOF method

details are given in Supplementary Material (Text S1, Tables S2 & S3). CAS numbers of each compound are given in Table S4.

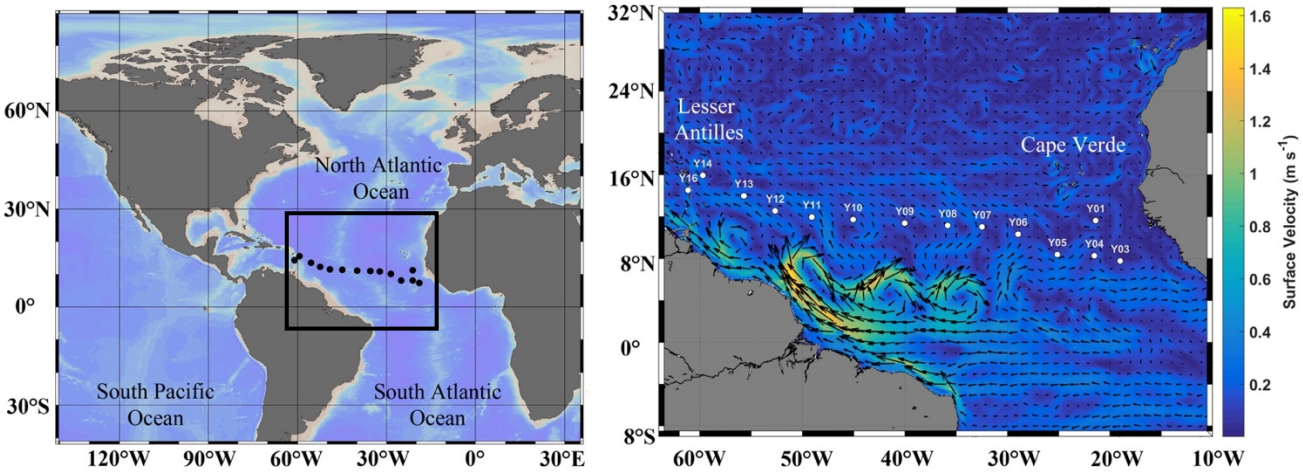

Fig. 1: Map showing the position of the sampling area in the North Atlantic Ocean as well as a zoom showing the individual sampling stations and the mean water surface velocity (in m s^{-1}) observed during the sampling period (October 2017).

Quality assurance/quality control (QA/QC)

Strict QA/QC measurements were implemented. Extraction, transport and laboratory blanks were made and analyzed concurrently with the samples to detect possible contaminations. Blank levels and compound concentrations of samples are presented in Table S5. No contamination was found, except in the case of TCPP, where mean blank levels (n = 5) of ~16 ng were detected, and for some PFCs and BPs, where trace levels were detected in the blanks (PFHA <LOQ, PFOA n.d.-<LOQ, PFOS n.d.-<LOQ, BPA n.d.-1.0 ng L^{-1} and BPS n.d.-<LOQ). The transport blank showed similar blank levels that field blanks, excluding sample contamination during transport and storing. The results presented here are blank-corrected.

Limits of quantification (LOQs) ranged from 0.03 to 8 ng L^{-1} (all LOQs are given in Table S4). If compounds were detected at concentrations <LOQ, they were considered as zero (i.e., not detected) for the calculation of detection frequencies and sums. Mean surrogate recovery rates were as follows: D_{27}-TBP 74%, D_{18}-TCPP 70%, D_{15}-TDCP 76% and D_{15}-TPhP 71% (see Table S6 for all recovery rates). The results presented here are not recovery corrected. The variability between duplicate samples ranged between 6-27%.

Solvents and reagents

Solvents were purchased from Promochem (hexane, ethyl acetate and dichloromethane, Picograde, LGC standard) and Biosolve (methanol, ULC-MS grade). Isotope-labeled PFCs were purchased from Wellington Laboratories (Canada), labeled OPEs from C/D/N Isotopes Inc. (Canada) (D_{27}-TBP, D_{15}-TPhP, D_{21}-TPrP and D_7-Malathion) and from Cambridge Isotope Laboratories, Inc. (USA) (D_{18}-TCPP, D_{15}-TDCP and D_{12}-TCEP). Isotope-labeled bisphenols were obtained from AccuStandard (USA).

Salinity and velocity maps

Daily surface salinity and velocity fields at 1/12° (~ 8 km) were computed by the Operational Mercator global ocean analysis and forecast system PSY4V3R1 from MERCATOR-OCEAN[30]. This system used version 3.1 of the NEMO ocean model, which solves the three-dimensional primitive hydrodynamic equations in spherical coordinates discretized on a C-grid and 50 vertical levels, under the hypothesis of boussinesq, hydrostatics and incompressibility[31]. This model is forced by realistic surface fluxes from ECMWF and jointly assimilates altimeter data, vertical *in situ* temperature and salinity profiles and satellite sea surface temperature. Data were downloaded for the surface layer (<1 m depth) of the whole

North Atlantic Ocean from the Marine Copernicus Portal (GLOBAL_ANALYSIS_FORECAST_PHY_001_024; http://marine.copernicus.eu/services-portfolio/access-to-products/).

Backwards trajectories

Backward Lagrangian particles trajectories were computed using the Lagrangian transport model Ichthyop[32], which simulates horizontal and vertical advection and dispersion. In our study, we considered our particles as passive surface tracers and only used horizontal advection in the movement equation. The Ichthyop model was run using the MERCATOR-OCEAN daily surface velocity fields at 1/12° described above. These fields were interpolated in space and time using a fourth order Runge–Kutta integration scheme with a constant time step of 1800 s that respected the Courant–Friedrichs–Lewy (CFL) criterion on the entire domain. Each sampled surface water mass was modeled by a circular patch with a radius of 10 km and seeded at the surface with 400 randomly released particles (i.e., approximately 1.3 particles km^{-2}) at the station times and geographic coordinates. Horizontal particle advection was carried out for 180 days with an output time step of 12 hours. At the end of each simulation, the percentage of seeded particles that passed in the Amazon Estuary area was computed, as well as the number of days between the day that they left the Amazon estuary area and the sampling day of the water masses. The Amazon Estuary area is hereby represented by a box, including longitude between -52°E and -46°E and latitude between -2°N and 3°N. Simulation was not run for station Y16 because of its high proximity to the coast (4 km; lower than the current model resolution).

The choice of a particle patch radius of 10 km for the backward trajectory simulations was motivated by two arguments: the radius needed (i) to be small enough to be representative

of the sampled water mass and (ii) to be large enough to include at least two meshes of the velocity field in diameter to take into account possible shifts between modeled and actual velocity fields. Comparison between daily salinity maps and seeded patch areas shows that a 10-km patch size allows for representation of a water mass with a salinity variability lower than +/-0.2, in comparison with the overall salinity varying between ~34 inside the Amazon River plume to 37 in the surrounding seawater (Fig. S1). In addition, sensitivity tests for radii from 5 to 25 km and densities from 0.5 to 2.5 particles km^{-2} were performed to test the robustness of our results (Table S7). The upper limit of 25 km was chosen because higher radii showed too much salinity variability inside patch areas to be consistent with the sampled water mass. These tests showed that the sensitivity of our results to the seeded patch radius and the particle density was very low, with a maximum difference in particle percentage that passed through the Amazon estuary area (Amazon box) lower than 10%, except at stations Y04 (40%) and Y14 (26%).

Results and discussion

OPEs were detected in all samples, while BPs and PFCs were only detected in 3 of 14 samples, each. From the nine OPEs analyzed, TPP, TnBP, TEHP and TDCP were not detected, while TCEP was found only at trace levels < 2 ng L^{-1} in 36% of samples. TCPP was detected in all samples, followed by TiBP and TPhP (93 and 57% detection frequency, respectively, Fig. S2). Concerning bisphenols, BPA was detected at stations Y01, Y09 and Y10 and BPS was found at station Y10, while the remaining four bisphenols were not detected in any samples. Of the five PFCs studied, only PFOSF was not detected at all. PFHS, PFOA and PFOS were found at one sampling station (Y11), while PFHA was detected in 21% of samples.

OPEs were the most abundant compound class with a relative abundance of 98-100%, followed by PFCs (0-1.9%) and finally, bisphenols (0-0.6%). The highest amounts of Σ_9 OPEs were measured at stations Y11, Y12 and Y10 (1340, 1000 and 955 ng L^{-1}, respectively), hence in offshore waters (Fig, 2A). In contrast, the two stations showing the lowest Σ_9 OPEs concentrations (Y16 and Y14, 74 and 106 ng L^{-1}, respectively) are in the most western coastal area. TCPP was hereby the most abundant OPE, with concentrations ranging from 74 (station Y16) to ~1300 ng L^{-1} (station Y11) and a relative abundance ranging from 92 to 100%. TiBP concentrations ranged from < 1 (station Y16) to 38 ng L^{-1} (station Y11). In contrast, the maximum TPhP and EHDPP concentrations were measured at station Y03 (7 ng L^{-1} and 5 ng L^{-1}, respectively), closer to the NW African coast (Fig. 2B). These two compounds exhibit thus a different distribution pattern than Σ_9 OPEs, possibly due to different sources and/or degradation rates. TPhP and EHDPP are used in hydraulic fluids[3], among others, and the fact that they exhibited highest concentrations at stations closest to the NW African coast could possibly be due to the high fishing activities in this area and other maritime traffic. This is in agreement with another study[33] reporting that EHDPP concentrations seem to derive mainly from local sources (airports, harbors and naval bases, urbanized and industrial areas) instead of from waterborne transport.

Station Y11, which was characterized by the highest Σ_9 OPEs concentrations, is the station closest to the Amazon River estuary, with a distance of approximately 1,200 km. Despite the large distance involved, diluted water from the Amazon River has already been found in the Caribbean Sea and has been shown to influence the tropical Atlantic Ocean more than 3,500 km away from the river mouth[34]. The freshwater is hereby transported by the North Brazil Current (NBC) and the North Equatorial Counter Current (NECC). Our results indicate, that medium-/long-range transport of OPEs *via* the water phase is occurring, further challenging the consideration of OPEs as being environmentally friendly alternatives for brominated flame

retardants. This observation seems to be especially true for chlorinated OPEs, such as TCPP, since they are more persistent than non-chlorinated OPEs[35]. Furthermore, it has been suggested that chlorinated OPEs have a longer characteristic travel distance in water than in air[33], supporting the hypothesis of water-borne medium-/long-range transport. This could be a particular reason of concern, since especially chlorinated OPEs are considered to have negative impacts on human health and the environment[3].

Generally, OPE levels in rivers and their estuaries can be very variable and can depend on the season[36]. TCPP concentrations ranging from 4.6 to 921 ng L^{-1} were measured in rivers in northern China[37], concentrations of 126 ± 14 ng L^{-1} were found in the Elbe River in Germany[38], and concentrations of 1.1-4.4 µg L^{-1} were measured in streams in Toronto, Canada[39]. These ranges are comparable with our results (74-1,300 ng L^{-1} of TCPP).

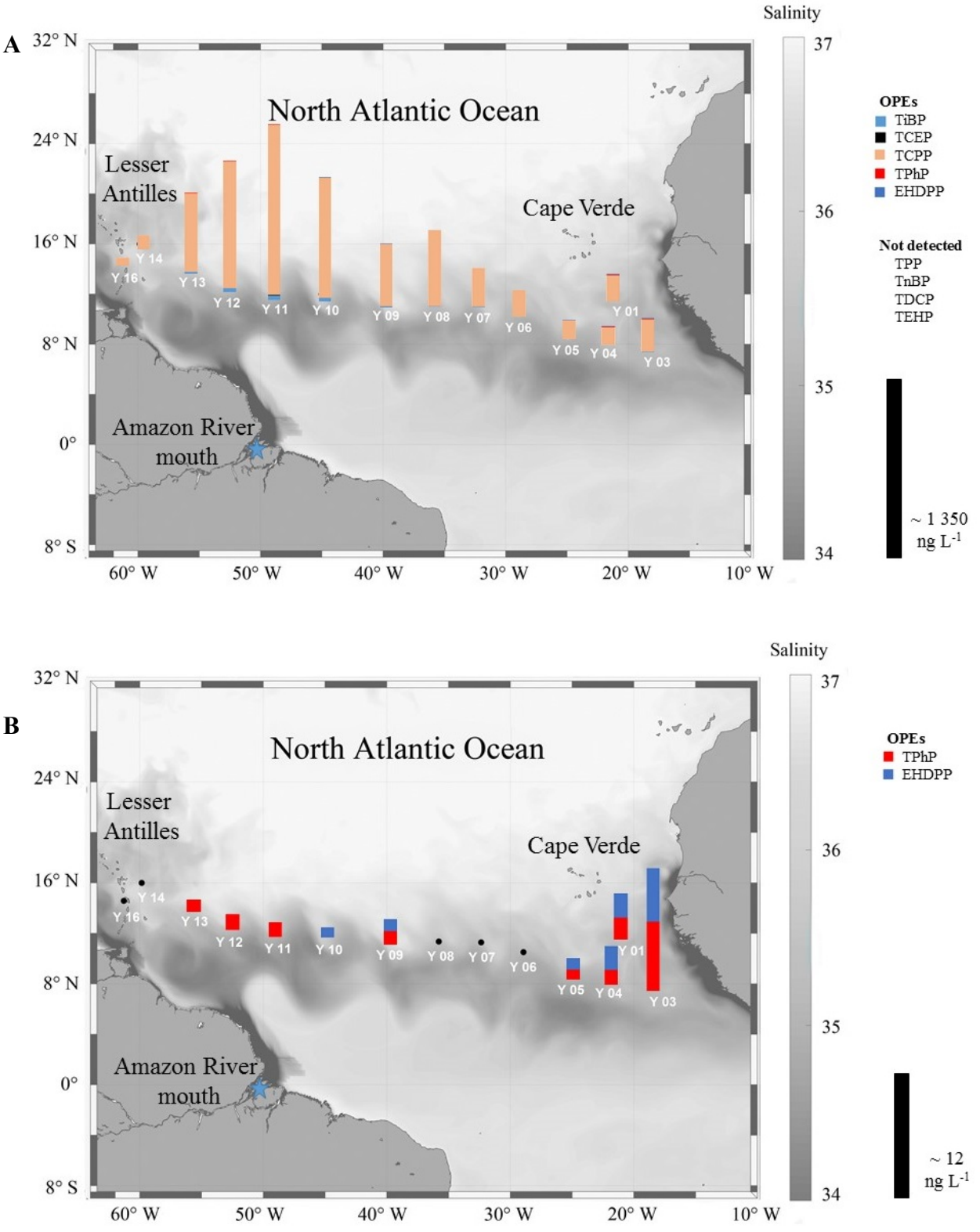

Fig. 2: Concentrations (in ng L^{-1}) of the individual OPEs (A) and the two compounds TPhP and EHDPP (B) which do not completely follow the same dynamics as ΣOPEs. Monthly average salinity distribution in the surface waters of the tropical North Atlantic in October 2017 is

indicated as well as the Amazon River mouth (blue star). Lower salinity areas are colored in dark grey. In the west, areas showing lower salinity are mainly influenced by freshwater inputs from the Amazon River, while in the east Intertropical Convergence Zone (ITCZ) rainfall is presumably at the origin of lower salinity waters.

Bisphenols and perfluorinated compounds were present at lower concentrations than OPEs (Table S5). BPA concentrations ranged between 1.2 ng L^{-1} (station Y01) and 1.8 ng L^{-1} (Y09 and Y10), while BPS was found at 1.1 ng L^{-1} (Y10) (Fig. 3A). While BPS is used as a substitute for BPA in certain products (e.g., in thermal paper or polycarbonate plastics), BPA is still dominating these sectors[18,40], probably explaining why BPA was more abundant in our samples than BPS. The finding that bisphenols were only found at concentrations lower than 2 ng L^{-1} or not detected at all could be due to rapid degradation rates. According to the simulation of the backwards trajectories (see below), the surface waters needed at least two months after leaving the Amazon River estuary before they reached the sampling stations. It was observed that complete biodegradation of BPA in river water was achieved within a few days, even at high initial concentrations (up to 5,500 µg L^{-1})[41]. The presence of bisphenols at stations Y09 and Y10, and especially at Y01, is thus probably not necessarily linked to the Amazon River, but could for example originate from ships that recently passed through or near the sampling area. Similar to the OPE results, Y11 was the station that exhibited the highest Σ_5 PFCs concentration (26 ng L^{-1}) - and in particular the highest PFHA concentration (16 ng L^{-1}) - , followed in this case by the adjacent stations Y12 and Y10 (11 and 9.7 ng L^{-1}, respectively). At station Y11, PFHS was found at 4.4 ng L^{-1}, PFOA at 2.9 ng L^{-1} and PFOS at 2.3 ng L^{-1} (Fig. 3B). This PFOS concentration is quite high, especially for open-ocean waters. As a reference, it clearly exceeded the European Environmental Quality Standard (EQS) for PFOS (0.13 ng L^{-1} for marine waters; Directive 2013/39/EU). PFHA concentrations in seawater generally tend

to be very low, with 0.02-0.19 ng L^{-1} of PFHA measured in Western Mediterranean waters[23] and <0.003-0.12 ng L^{-1} detected in seawater samples from Northern Europe, the Atlantic Ocean and the Southern Ocean[22]. A study analyzing PFHA in surface seawater samples close (at a distance of 140 – 370 km) to our sampling stations Y16, Y14 and Y05 found concentrations between n.d. and 0.0187 ng L^{-1}, values that were comparable with ours (n.d. or <LOQ) at the three stations mentioned above.[26] In contrast, PFHA concentrations in rivers have been found to vary between 0.50-5.3 ng L^{-1} (Elbe and Weser Rivers in Germany)[42] and between <0.10 and 38 ng L^{-1} (data from 29 Chinese rivers)[43] or reach peak concentrations of up to 16,000 ng L^{-1} downstream of a PFC production facility (Samondogawa River in Japan)[44]. Our PFHA concentrations at stations Y11, Y12 and Y10 (16, 11 and 9.7 ng L^{-1}, respectively) thus seem quite high for seawater samples and indicate once again a riverine source, i.e., the Amazon River.

A recent study proposed fire-fighting foams used at offshore oil and gas platforms to be a potentially important PFC source to the marine environment[45]. Important oil and gas drilling close to our study area mainly occurs in the Campos and Santos basins off the coasts of Rio de Janeiro and Sao Paulo, Brazil. Given the direction of the oceanic currents there (from north to south; not towards our sampling stations), these offshore platforms do not seem to be a plausible explanation for the high PFC concentrations detected at stations Y10-Y12. However, multiple studies[46-48] have investigated the magnitude of oil and gas extractions in the Amazon basin and the far-reaching environmental impacts. These inland oil and gas extraction activities and the associated use of fire-fighting foams, could thus be a possible explanation of the PFC concentrations observed. Another potential source of PFCs, OPEs and BPs in the Amazon basin could be the city of Manaus, which houses an important industry producing chemicals and electronic equipment, among others. Furthermore, more than two million people live in Manaus, but less than 20% of households are connected to the sewage system[49].

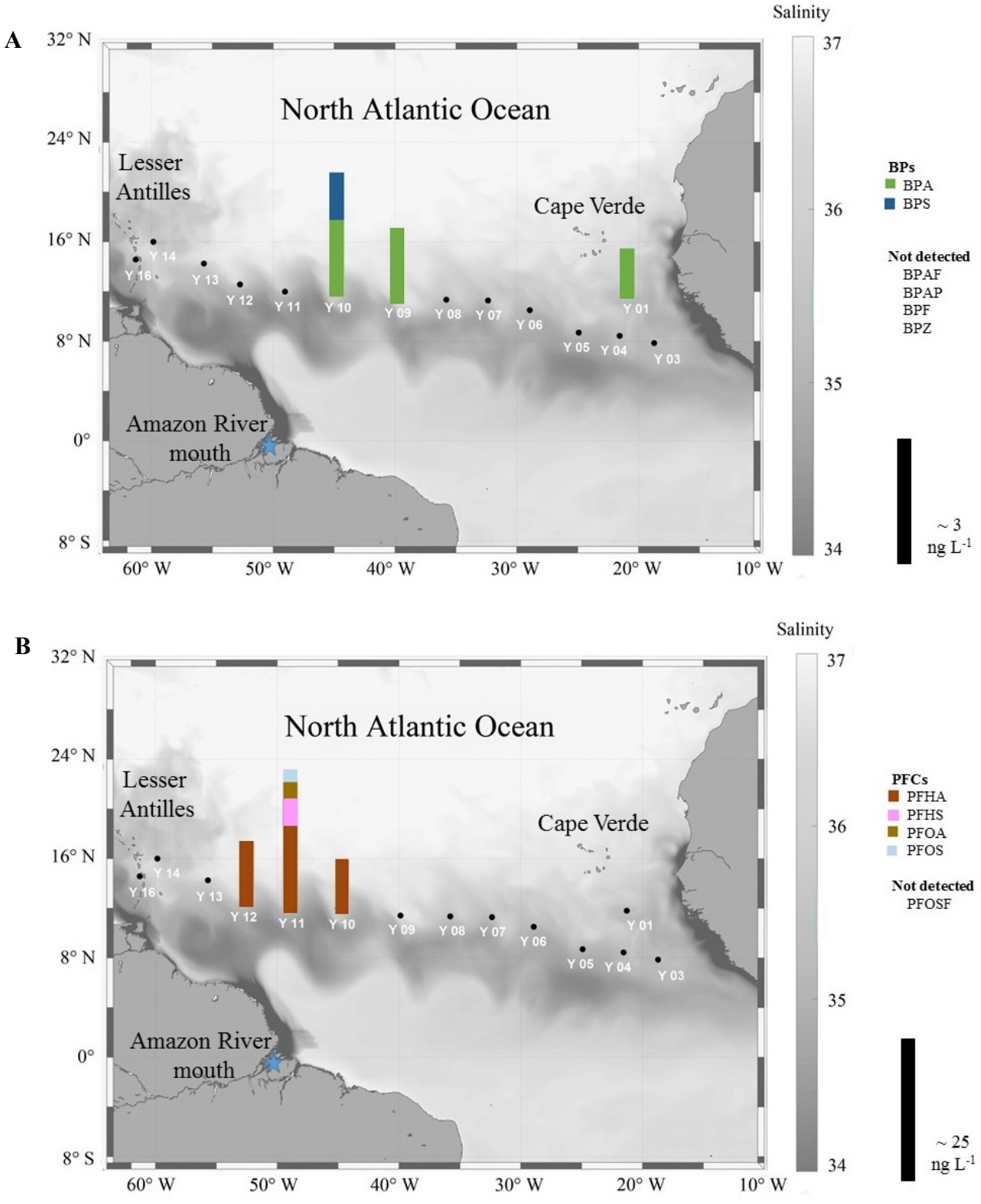

Fig. 3: Concentrations (in ng L^{-1}) of the individual BPs (A) and PFCs (B) detected at sampling stations Y 01 - Y 16. Monthly average salinity distribution in the surface waters of the tropical North Atlantic in October 2017 is indicated as well as the Amazon River mouth (blue star).

Low surface salinity (between 33 and 35; Table S1 & Fig. S3) was measured at all stations. In the west, this freshening is thought to be primarily due to transport of freshwater from the Amazon, while to the east it mainly emanates from Intertropical Convergence Zone (ITCZ) rainfall[50]. These trends were also observed for the chlorophyll a spatial concentration distribution, represented by Kd490 (Fig. S4). To confirm the origin of the sampled surface waters, a Lagrangian analysis was performed. Simulations using MERCATOR daily surface velocity fields indicated that 98-100% of the surface waters encountered at stations Y06 - Y08 and Y10 - Y13 passed near or originated from the Amazon River mouth. While the model cannot distinguish whether the surface waters passed by the Amazon River estuary or originated from the river itself, the term "originated from" will be used hereafter in accordance with our hypothesis. According to the simulation, the farthest east where an influence of the Amazon can be observed is at station Y04, where 82% of surface waters originated from the far east corner of the black box enclosing the river estuary (Fig. 4; backwards trajectories for all stations are provided in Fig. S5). These results indicate that the influence of the Amazon River is reaching far into the North Atlantic since even water masses and contaminant concentrations from sampling stations close to the African continent were partially linked to the Amazon River. Hereby, the surface waters of station Y04 (8 °N, 21 °W) had a calculated travel time of ~125 days, which is in good agreement with the results obtained by Coles et al. (2013), who found that drifters released in the Amazon River estuary reached this zone after approximately 120-150 days[51]. Stations with high contaminant levels seem generally characterized by i) a high percentage of surface waters that originated in the Amazon River plume, ii) a short travel time and/or a short travel distance and iii) an origin close to the river mouth where contamination is probably highest. However, we would like to point out that the Lagrangian approach used to simulate the backwards trajectories does not take vertical mixing into account which can complexify (or partly explain some discrepancies in) the relationship between contaminant

concentration and percentage, origin and travel time of surface water masses. Similarly, for station Y09 the simulation suggests that 0% of surface waters originated from the Amazon River mouth, even though the total contaminant level is relatively high (~480 ng L^{-1}).

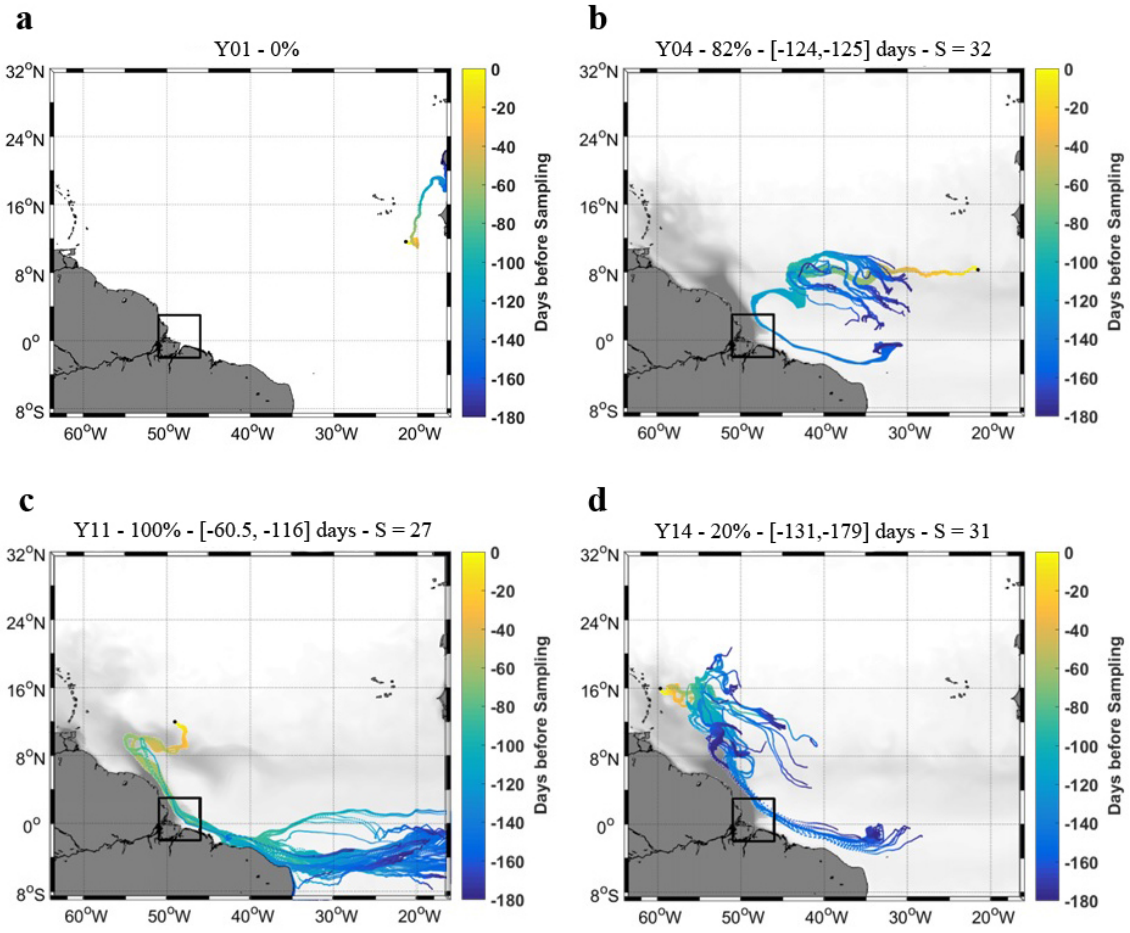

Fig. 4: Water mass backwards trajectories for the stations Y01 (a), Y04 (b), Y11 (c) and Y14 (d). Each map has a caption indicating the station ID, the date, the percentage of water masses that were in the black box (indicating the Amazon Estuary) and the number of days that passed between the sampling of the water masses and their journey in the area of the black box (in brackets). The minimum salinity (S) reached by particles during their journey in the black box is indicated as well as the river plume (with a dark to light grey scale; S = 27-37).

Another explanation for the contamination pattern observed could be that not the Amazon River itself is the source, but that the contaminants originate from coastal areas near the river mouth. In this case, a potential source could for example be the metropolis of Belém, including its two airports and the naval base. Furthermore, a phenomenon that could explain the high contaminant concentrations measured in this study could be the transfer of contaminants from the atmosphere to surface waters of the tropical North Atlantic *via* atmospheric deposition. A recent study (based on cruise measurements) estimated that between 0.2 and 2.5 Kt y^{-1} of OPEs (Σ_{14} OPEs) associated with atmospheric dry deposition fluxes could be loaded to the entire Atlantic Ocean (surface of 8.2×10^{13} m^2).[52] To investigate this possibility, NOAA's HYSPLIT model[53,54] was used to simulate air mass backward trajectories. However, while a background atmospheric deposition of OPEs cannot be excluded, the simulation results suggest that potential atmospheric inputs were not related to the Amazon area. Air masses from most stations originated from a northeastern direction (Figure S6), close to the NW African and European coasts, and could thus not convincingly explain why highest contaminant concentrations were measured at stations far away from the African and European coasts.

The Amazon drainage basin represents approximately 7,500,000 km^2, and each second it discharges an average of 209,000 m^3 of freshwater into the Atlantic Ocean, representing up to 20% of the freshwater input to the global ocean[55]. It also exports considerable amounts of DOC and dissolved organic matter (DOM) to the tropical Atlantic Ocean[55,56]. Furthermore, recent research suggests that the Amazon River is a significant source of plastic pollution, with an estimated input into the Atlantic Ocean of 32,000-64,000 metric tons per year[57]. However, little is known about the presence of organic contaminants of emerging concern in the watershed, such as OPEs, PFCs and bisphenols, which are common plastic additives. The high discharge rate of the river and the high contaminant levels observed in our study strongly

suggest that the Amazon River could be a major source of contaminants to the Atlantic Ocean, as well. The surface water backward trajectory simulations further strengthen this hypothesis. Analyzing samples originating from the river itself and monitoring contaminant concentrations during wet and dry seasons will be crucial tasks for the future and will be necessary to fully understand the extent of organic plastic additive occurrence in the Amazon River and their transport to the Atlantic Ocean.

Attention must be focused on the potential effects for freshwater and marine ecosystems, but should also be given to the consequences for local communities that use river water for agriculture or household activities. New evidence suggests that long-term exposure to high OPE concentrations could significantly affect marine organisms and human health by influencing the immune system or disturbing cell growth, among others[58,59]. While these effects need to be studied further, findings such as those presented here help to identify geographical zones of scientific interest and to note the current magnitude of environmental pollution that calls for changes in uses and practices at the scale of the Amazon watershed. The importance of the situation is highlighted when we consider that future climate scenarios predict an increase in the discharge of the Amazon River[60] and that plastic litter in the Amazon watershed is expected to double between 2010 and 2025.[61]

Acknowledgments

We deeply thank the crew and captain of the M/V Yersin as well as HSH Prince Albert II of Monaco, and Monaco Explorations. Thanks to Laurent Vassalo from Laboratoire de Chimie de l'Environnement Aix-Marseille University for salinity measurements. Thanks also to Cristèle Chevalier and Vincent Rossi from the Mediterranean Institute of Oceanography (MIO) for their helpful advices on backwards trajectories computation. Thanks to IRD for

financial and logistical support and for the funding of A. Ody's postdoctoral fellowship. Thanks to the Ministere de l'Ecologie et du Développement Durable for financial support. The project leading to this publication has received funding from European FEDER Fund under project 1166-39417. The project has also received funding from the JPI Oceans PLASTOX project and the Agence de l'Eau Rhône Méditerranée Corse Blue-POLUT and CAREMED projects.

References

(1) Sousa, J.C.G.; Ribeiro, A.R.; Barbosa, M.O.; Pereira, M.F.R.; Silva, A.M.R. A review on environmental monitoring of water organic pollutants identified by EU guidelines. *J. Hazard. Mater.* **2018**, 344:146–162.

(2) Geyer, R.; Jambeck, J.R.; Law, K.L. Production, use, and fate of all plastics ever made. *Science Advances* **2017**, 3**:**e1700782.

(3) van der Veen, I.; de Boer, J. Phosphorus flame retardants: Properties, production, environmental occurrence, toxicity and analysis. *Chemosphere* **2012**, 1119–1153.

(4) Marklund, A.; Andersson, B.; Haglund, P. Organophosphorus flame retardants and plasticizers in air from various indoor environments. *J. Environ. Monit.* **2005**, 7:814–819.

(5) Wei, G.-L.; Li, D.-Q.; Zhuo, M.-N.; Liao, Y.-S.; Xie, Z.-Y.; Guo, T.-L.; Li, J.-J.; Zhang, S.-Y.; Liang, Z.-Q. Organophosphorus flame retardants and plasticizers: Sources, occurrence, toxicity and human exposure. *Environ. Pollut.* **2015**, 196:29–46.

(6) Greaves, A.K.; Letcher, R.J. A Review of Organophosphate Esters in the Environment from Biological Effects to Distribution and Fate. *Bull. Environ. Contam. Toxicol.* **2017**, 98:2−7.

(7) Zha, D.; Li, Y.; Yang, C.; Yao, C. Assessment of organophosphate flame retardants in surface water and sediment from a freshwater environment (Yangtze River, China). *Environ. Monit. Assess.* **2018**, 190:222.

(8) Hu, M.; Li, J.; Zhang, B.; Cui, Q.; Wei, S.; Yu, H. Regional distribution of halogenated organophosphate flame retardants in seawater samples from three coastal cities in China. *Mar. Pollut. Bull.* **2014**, 86:569–574.

(9) Lai, S.; Xie, Z.; Song, T.; Tang, J.; Zhang, Y.; Mi, W.; Peng, J.; Zhao, Y.; Zou, S.; Ebinghaus, R. Occurrence and dry deposition of organophosphate esters in atmospheric particles over the northern South China Sea. *Chemosphere* **2015**, 127:195–200.

(10) Zhong, M.; Wu, H.; Mi, W.; Li, F.; Ji, C.; Ebinghaus, R.; Tang, J.; Xie, Z. Occurrences and distribution characteristics of organophosphate ester flame retardants and plasticizers in the sediments of the Bohai and Yellow Seas, China. *Sci. Total Environ.* **2018**, 615:1305–1311.

(11) Martínez-Carballo, E.; González-Barreiro, C.; Sitka, A.; Scharf, S.; Gans, O. Determination of selected organophosphate esters in the aquatic environment of Austria. *Sci. Total Environ.* **2007**, 388:290–299.

(12) Cristale, J.; Vázquez, A.G.; Barata, C.; Lacorte, S. Priority and emerging flame retardants in rivers: Occurrence in water and sediment, Daphnia magna toxicity and risk assessment. *Environ. Int.* **2013**, 59:232–243.

(13) Castro-Jiménez, J.; Berrojalbiz, N.; Pizarro, M.; Dachs, J. Organophosphate ester (OPE) flame retardants and plasticizers in the open Mediterranean and Black Seas atmosphere. *Environ. Sci. Technol.* **2014**, 48:3203−3209.

(14) Peverly, A.A.; O'Sullivan, C.; Liu, L.-Y.; Venier, M.; Martinez, A.; Hornbuckle, K.C.; Hites, R.A. Chicago's Sanitary and Ship Canal sediment: Polycyclic aromatic

hydrocarbons, polychlorinated biphenyls, brominated flame retardants, and organophosphate esters. *Chemosphere* **2015**, 134:380–386.

(15) Cao, D.; Guo, J.; Wang, Y.; Li, Z.; Liang, K.; Corcoran, M.B.; Hosseini, S.; Bonina, S.M.C.; Rockne, K.J.; Sturchio, N.C.; Giesy, J.P.; Liu, J.; Li, A.; Jiang, G. Organophosphate esters in sediment of the Great Lakes. *Environ. Sci. Technol.* **2017**, 51:1441−1449.

(16) Guo, J.; Venier, M.; Salamova, A.; Hites, R.A. Bioaccumulation of dechloranes, organophosphate esters, and other flame retardants in Great Lakes fish. *Sci. Total Environ.* **2017**, 583:1–9.

(17) Danzl, E.; Sei, K.; Soda, S.; Ike, M.; Fujita, M. Biodegradation of bisphenol A, bisphenol F and bisphenol S in seawater. *Int. J. Environ. Res. Public Health* **2009**, 6(4):1472-1484.

(18) Björnsdotter, M.K.; Jonker, W.; Legradi, J.; Kool, J.; Ballesteros-Gómez, A. Bisphenol A alternatives in thermal paper from the Netherlands, Spain, Sweden and Norway. Screening and potential toxicity. *Sci. Total Environ.* **2017**, 601–602:210–221.

(19) Pojana, G.; Gomiero, A.; Jonkers, N.; Marcomini, A. Natural and synthetic endocrine disrupting compounds (EDCs) in water, sediment and biota of a coastal lagoon. *Environ. Int.* **2007**, 33:929–936.

(20) Xie, H.; Chen, Q.; Chen, J.; Chen, C.-E.L.; Du, J. Investigation and application of diffusive gradients in thin-films technique for measuring endocrine disrupting chemicals in seawaters. *Chemosphere* **2018**, 200:351–357.

(21) Fu, P.; Kawamura, K. Ubiquity of bisphenol A in the atmosphere. *Environ. Pollut.* **2010**, 158: 3138–3143.

(22) Ahrens, L.; Xie, Z.; Ebinghaus, R. Distribution of perfluoroalkyl compounds in seawater from Northern Europe, Atlantic Ocean, and Southern Ocean. *Chemosphere* **2010**, 78:1011–1016.

(23) Brumovský, M.; Karásková, V.; Borghini, M.; Nizzetto, L. Per- and polyfluoroalkyl substances in the Western Mediterranean Sea waters. *Chemosphere* **2016**, 159:308-316.

(24) Stockholm Convention, Reference: C.N.524.2009.TREATIES-4 (Depositary Notification), **2009**. http://chm.pops.int/.

(25) Yeung, L.W.Y.; Dassuncao, C.; Mabury, S.; Sunderland, E.M.; Zhang, X.; Lohmann, R. Vertical profiles, sources, and transport of PFASs in the Arctic Ocean. *Environ. Sci. Technol.* **2017**, 51:6735−6744.

(26) González-Gaya, B.; Dachs, J.; Roscales, J.L.; Caballero, G.; Jiménez, B. Perfluoroalkylated substances in the global tropical and subtropical surface oceans. *Environ. Sci. Technol.* **2014**, 48:13076−13084.

(27) Cai, M.; Zhao, Z.; Yang, H.; Yin, Z.; Hong, Q.; Sturm, R.; Ebinghaus, R.; Ahrens, L.; Cai, M.; He, J.; Xie, Z. Spatial distribution of per- and polyfluoroalkyl compounds in coastal waters from the East to South China Sea. *Environ. Pollut.* **2012**, 161:162–169.

(28) Zhou, Y.; Wang, T.; Li, Q.; Wang, P.; Li, L.; Chen, S.; Zhang, Y.; Khan, K.; Meng, J. Spatial and vertical variations of perfluoroalkyl acids (PFAAs) in the Bohai and Yellow Seas: Bridging the gap between riverine sources and marine sinks. *Environ. Pollut.* **2018**, 238:111–120.

(29) Fauvelle, V.; Castro-Jimenez, J.; Schmidt, N.; Carlez, B.; Panagiotopoulos, C.; Sempere, R. One-single extraction procedure for the simultaneous determination of a wide range of polar and non-polar organic contaminants in marine surface water. *Front. Mar. Sci.* **2018**, 5:295.

(30) Lellouche, J.-M.; Le Galloudec, O.; Drévillon, M.; Régnier, C.; Greiner, E.; Garric, G.; Ferry, N.; Desportes, C.; Testut, C.-E.; Bricaud, C.; Bourdallé-Badie, R.; Tranchant, B.; Benkiran, M.; Drillet, Y.; Daudin, A.; De Nicola, C. Evaluation of global monitoring and forecasting systems at Mercator Océan. *Ocean Sci.* **2013**, 9(1):57.

(31) Madec, G.; and the NEMO team. NEMO ocean engine. *Note du Pôle de modélisation*, Institut Pierre-Simon Laplace (IPSL), France, **2008**, 27:1288-1619 (https://www.nemo-ocean.eu/wp-content/uploads/NEMO_book.pdf).

(32) Lett, C.; Verley, P.; Mullon, C.; Parada, C.; Brochier, T.; Penven, P.; Blanke, B. A Lagrangian tool for modelling ichthyoplankton dynamics. *Environ. Model. Softw.* **2008**, 29(9):1210–1214.

(33) Sühring, R.; Diamond, M.L.; Scheringer, M.; Wong, F.; Pućko, M.; Stern, G.; Burt, A.; Hung, H.; Fellin, P.; Li, H.; Jantunen, L.M. Organophosphate Esters in Canadian Arctic Air: Occurrence, Levels and Trends. *Environ. Sci. Technol.* **2016**, 50:7409−7415.

(34) Korosov, A.; Counillon, F.; Johannessen, J.A. Monitoring the spreading of the Amazon freshwater plume by MODIS, SMOS, Aquarius, and TOPAZ. *J. Geophys. Res. Oceans* **2015**, 120:268–283.

(35) McDonough, C.A.; De Silva, A.O.; Sun, C.; Cabrerizo, A.; Adelman, D.; Soltwedel, T.; Bauerfeind, E.; Muir, D.C.G.; Lohmann, R. Dissolved Organophosphate Esters and Polybrominated Diphenyl Ethers in Remote Marine Environments: Arctic Surface Water Distributions and Net Transport through Fram Strait. *Environ. Sci. Technol.* **2018**, 52:6208−6216.

(36) Wang, X.; He, Y.; Lin, L.; Zeng, F.; Luan, T. Application of fully automatic hollow fiber liquid phase microextraction to assess the distribution of organophosphate esters in the Pearl River Estuaries. *Sci. Total Environ.* **2014**, 470–471:263–269.

(37) Wang, R.; Tang, J.; Xie, Z.; Mi, W.; Chen, Y.; Wolschke, H.; Tian, C.; Pan, X.; Luo, Y.; Ebinghaus, R. Occurrence and spatial distribution of organophosphate ester flame retardants and plasticizers in 40 rivers draining into the Bohai Sea, north China. *Environ. Pollut.* **2015**, 198: 172-178.

(38) Wolschke, H.; Sühring, R.; Xie, Z.; Ebinghaus, R. Organophosphorus flame retardants and plasticizers in the aquatic environment: A case study of the Elbe River, Germany. *Environ. Pollut.* **2015**, 206:488–493.

(39) Truong, J.W.; Diamond, M.L.; Helm, P.A.; Jantunen, L.M. Isomers of tris(chloropropyl) phosphate (TCPP) in technical mixtures and environmental samples. *Anal. Bioanal. Chem.* **2017**, 409:6989–6997.

(40) Pivnenko, K.; Laner, D.; Astrup, T.F. Dynamics of bisphenol A (BPA) and bisphenol S (BPS) in the European paper cycle: Need for concern? *Resour. Conserv. Recycl.* **2018** *133*, 278–287.

(41) Klecka, G.M.; Gonsior, S.J.; West, R.J.; Goodwin, P.A.; Markham, D.A. Biodegradation of bisphenol A in aquatic environments: River die-away. *Environ. Toxicol. Chem.* **2001**, 20 (12):2725–2735.

(42) Zhao, Z.; Xie, Z.; Tang, J.; Sturm, R.; Yingjun, C.; Zhang, G.; Ebinghaus, R. Seasonal variations and spatial distributions of perfluoroalkyl substances in the rivers Elbe and lower Weser and the North Sea. *Chemosphere* **2015**, 129:118–125.

(43) Lu, Z.; Song, L.; Zhao, Z.; Ma, Y.; Wang, J.; Yang, H.; Ma, H.; Cai, M.; Codling, G.; Ebinghaus, R.; Xie, Z.; Giesy, J.P. Occurrence and trends in concentrations of perfluoroalkyl substances (PFASs) in surface waters of eastern China. *Chemosphere* **2015**, 119:820–827.

(44) Takemine, S.; Matsumura, C.; Yamamoto, K.; Suzuki, M.; Tsurukawa, M.; Imaishi, H.; Nakano, T.; Kondo, A. Discharge of perfluorinated compounds from rivers and their influence on the coastal seas of Hyogo prefecture, Japan. *Environ. Pollut.* **2014**, 184:397-404.

(45) Sühring, R.; Phillips, C.; Gioia, R.; Rowles, R.; Abdoellakhan, I. Perfluorinated compounds in offshore fire-fighting foams – a source for marine contamination? *Organohalogen Compounds* **2017**, 79:667–669.

(46) Rosell-Melé, A.; Moraleda-Cibrián, N.; Cartró-Sabaté, M.; Colomer-Ventura, F.; Mayor, P.; Orta-Martínez, M. Oil pollution in soils and sediments from the Northern Peruvian Amazon. *Sci. Total Environ.* **2018**, 610-611:1010–1019.

(47) Moquet, J.-S.; Maurice, L.; Crave, A.; Viers, J.; Arevalo, N.; Lagane, C.; Lavado-Casimiro, W.; Guyot, J.-L. Cl and Na Fluxes in an Andean Foreland Basin of the Peruvian Amazon: An Anthropogenic Impact Evidence. *Aquat. Geochem.* **2014**, 20:613–637.

(48) Finer, M.; Jenkins, C.N.; Pimm, S.L.; Keane, B.; Ross, C. Oil and Gas Projects in the Western Amazon: Threats to Wilderness, Biodiversity, and Indigenous Peoples. *PLoS ONE* **2008**, e2932.

(49) Thomas, K.V.; da Silva, F.M.A.; Langford, K.H.; de Souza, A.D.L.; Nizzeto, L.; Waichman, A.V. Screening for selected human pharmaceuticals and cocaine in the urban streams of Manaus, Amazonas, Brazil. *J. Am. Water Resour. Assoc.* **2014**, 50(2):302–308.

(50) Foltz, G.R.; Schmid, C.; Lumpkin, R. Transport of surface freshwater from the equatorial to the subtropical North Atlantic Ocean. *J. Phys. Oceanogr.* **2015**, 45(4):1086–1102.

(51) Coles, V.J.; Brooks, M.T.; Hopkins, J.; Stukel, M.R.; Yager, P.L.; Hood, R.R. The pathways and properties of the Amazon River Plume in the tropical North Atlantic Ocean. *J. Geophys. Res. Oceans.* **2013**, 118:6894–6913.

(52) Stein, A.F.; Draxler, R.R.; Rolph, G.D.; Stunder, B.J.B.; Cohen, M.D.; Ngan, F. NOAA's HYSPLIT atmospheric transport and dispersion modeling system. *Bull. Amer. Meteor. Soc.* **2015**, 96:2059–2077.

(53) Rolph, G.; Stein, A.; Stunder, B. Real-time Environmental Applications and Display sYstem: READY. *Environ. Model Softw.* **2017**, 95:210–228.

(54) Castro-Jiménez, J.; Casal, P.; González Gaya, B.; Pizarro, M.; Dachs, J. Organophosphate ester flame retardants and plasticizers in the global oceanic atmosphere. *Environ. Sci. Technol.* **2016**, 50:12831–12839.

(55) Medeiros, P.M.; Seidel, M.; Ward, N.D.; Carpenter, E.J.; Gomes, H.R.; Niggemann, J.; Krusche, A.V.; Richey, J.E.; Yager, P.L.; Dittmar, T. Fate of the Amazon River dissolved organic matter in the tropical Atlantic Ocean. *Global Biogeochem. Cy.* **2015**, 29:677–690.

(56) Moreira-Turcq, P.; Seyler, P.; Guyot, J.L.; Etcheber, H. Exportation of organic carbon from the Amazon River and its main tributaries. *Hydrol. Process.* **2003**, 17:1329–1344.

(57) Lebreton, L.C.M.; van der Zwet, J.; Damsteeg, J.-W.; Slat, B.; Andrady, A.; Reisser, J. River plastic emissions to the world's oceans. *Nat. Commun.* **2017**, 8:15611, DOI: 10.1038/ncomms15611.

(58) Li, F.; Wang, L.; Ji, C.; Wu, H.; Zhao, J.; Tang, J. Toxicological effects of tris(2-chloropropyl) phosphate in human hepatic cells. *Chemosphere* **2017**, 187:88–96.

(59) Wu, H.; Zhong, M.; Lu, Z.; Shan, X.; Li, F.; Ji, C.; Cong, M. Biological effects of tris (1-chloro-2-propyl) phosphate (TCPP) on immunity in mussel *Mytilus galloprovincialis*. *Environ. Toxicol. Pharmacol.* **2018**, 61:102–106.

(60) Nohara, D.; Kitoh, A.; Hosaka, M.; Oki, T. Impact of climate change on river discharge projected by multimodel ensemble. *J. Hydrometeorol.* **2006**, 7:1076–1089.

(61) Jambeck, J.R.; Geyer, R.; Wilcox, C.; Siegler, T.R.; Perryman, M.; Andrady, A.; Narayan, R.; Law, K.L. Plastic waste inputs from land into the ocean. *Science* **2015**, 347:768-771.

CONCLUSION & PERSPECTIVES

This thesis provides insight on the occurrence of microplastics and (associated) organic contaminants, such as PAEs, OPEs, BPs and PFAS, in coastal and remote marine areas. It focuses on the semi-enclosed Mediterranean Sea, providing first data about contaminant concentrations, fluxes from the Rhône River and distributions in the Bay of Marseille (NW Mediterranean Sea). This work also examines potential sources and allows to draw comparisons with the North Atlantic Ocean. Indeed, the generated North Atlantic data set provides unique large-scale information concerning the dynamic of organic plastic additives and related contaminants in oceanic surface waters. This study is divided into five sections. Firstly, the occurrence of microplastics in the Gulf of Lions (Northern Current, Bay of Marseille, Rhône River and its plume) was investigated. Hereby, it was confirmed that microplastics are present in surface waters of the Gulf of Lions, sometimes at very high concentrations of up to $1 \cdot 10^6$ items km^{-2}. The water residence time had an impact on microplastic particle size. The small-sized plastic items found in the Rhône River seemed to have travelled for a longer time in the watercourse and were thus more fragmented than the bigger sized microplastics collected in the Bay of Marseille, which probably originated from local inputs.

The second part of the thesis focused on the Rhône River, where a previously developed and validated multi-contaminant extraction protocol was applied to surface water samples collected on a monthly basis in order to study fluxes of organic plastic additives including phthalates, organophosphate esters and bisphenols to the Mediterranean Sea. Our results showed that PAEs were usually the most abundant compounds (97-541 ng L^{-1}), followed by OPEs (85-265 ng L^{-1}) and BPs, among which only BPS was detected (4-21 ng L^{-1}), raising questions concerning the local BPS consumption, since generally BPA still dominates most application sectors (e.g., the thermal paper industry). We also found important temporal variability of organic plastic additives in the Rhône River surface waters, which could not be satisfyingly explained with the present dataset. However, some potential sources were

identified (such as the nuclear industry, leaching from plastic litter or diffuse inputs from wastewater treatment plants). A rough estimation pointed to a flow of dissolved organic plastic additives from the Rhône River to the NW Mediterranean Sea of 15-149 kg d^{-1} (Σ OPEs + Σ PAEs + Σ BPs).

The third chapter geographically also focused on the Rhône River, along with the Bay of Marseille, and was this time specialized on a group of chemicals appreciated for their water and oil repellent qualities: perfluoroalkyl substances. In the Rhône River, PFHA reached important concentrations (8-193 ng L^{-1}), while this compound was never detected at values > LOQ in the Bay of Marseille. The EU annual average Environmental Quality Standard (EQS) for PFOS (0.65 ng L^{-1} in freshwater; 0.13 ng L^{-1} in marine waters) was exceeded in over 80% of the collected samples. Moreover, a numerical simulation showed that the PFOS input originating from the Rhône River was enough to attain PFOS concentrations higher than the EQS in certain areas of the Bay of Marseille. The consequences for the marine food web, especially in the vicinity of the Rhône River mouth need yet to be assessed.

In chapter four, PAEs and OPEs were examined in three different compartments (water, sediment and zooplankton) of three sampling stations in the Bay of Marseille (L'Estaque, Frioul and Cortiou). Except for water samples from Cortiou station, PAEs were always detected at higher concentrations than OPEs. At Cortiou, where the municipal WWTP outlet is situated and two smaller rivers (Huveaune and Jarret) enter the sea, contaminant concentrations were highest. In water samples, PAE concentrations ranged from 100 to 527 ng L^{-1} in Marseille Bay, with DEHP being the predominant compound (relative abundance 50-90%; median 67%), whereas OPE concentrations varied between 8.9 and 1013 ng L^{-1}, with TCPP generally being the most abundant (relative abundance 28-91%; median 78%). In sediment samples, the distribution changed and TnBP was usually predominant, with a relative abundance of 16-87% (median 63%). Moreover, sediment samples exhibited relatively low OPE concentrations (12.6-

48.8 ng L^{-1}), while PAEs were detected at up to 610 ng L^{-1}. Finally, zooplankton samples were characterized by very high PAE and OPE concentrations, raising questions about the consequences for the local food web and – eventually – human health (through the consumption of marine products). DEHP concentrations reached up to 43 µg g^{-1} dry weight in the smallest size class (150-500 µm) at Cortiou station. While an EQS for DEHP exists for marine waters (1.3 µg L^{-1}; this value was never exceeded in water collected during our sampling campaigns), no such standard exists for aquatic organisms, even though this would be a critical step to improve the interpretation of data on DEHP occurrence in biota, as well as for risk assessments.

Finally, the last chapter dealt with the waterborne occurrence of OPEs, BPs and PFAS in a very different environment: the tropical North Atlantic Ocean. 2 × 14 water samples collected during a transatlantic expedition from African Cape Verde, to Martinique Island in the western Atlantic were analyzed for the target contaminants. OPEs were detected at considerable concentrations (up to 1.3 µg L^{-1} for Σ_9 OPEs), with highest levels observed closest to the Amazon River mouth. A similar spatial distribution was observed for BPs and PFAS. A Lagrangian analysis revealed that the sampled water masses showing high contaminant concentrations passed by near or originated from the Amazon River mouth, confirming the hypothesis formulated that these contaminants could possibly origin from the Amazon River. Given the long travel distances involved (minimum 1,200 km from the river mouth to the closest sampling station) and the important amounts of contaminants detected, we can only suspect that the Amazon River itself must be highly contaminated.

In summary, an important global conclusion to draw from this thesis is the understanding that environmental processes at different scales and in adjacent areas are linked together. PFOS inputs from the Rhône River were high enough to generate concentrations > the EU EQS in certain areas of the Bay of Marseille and the influence of contaminated waters from the Amazon River was observed in oceanic waters thousands of kilometers away from the river

mouth (Figure 1). Thus, fighting environmental pollution at a defined scale can only be successful if adjacent areas and a maximum number of contaminant input sources are also taken into account. Comparison of PAE, OPE and BP fluxes from the Rhône River with literature and chapter one indicates that plastic litter might only partly explain the amounts of organic plastic additives detected in the Rhône River. This is in accordance with the data from Marseille Bay (chapter four) where the sampling station exhibiting highest contaminant concentrations was also the station with lowest microplastic abundance. We can conclude that especially in dynamic, urbanized environments, such as rivers and coasts, the environmental behavior of contaminants is more complex and plastic litter can thus, in such cases, not necessarily be considered as the only tracer of organic plastic additive contamination.

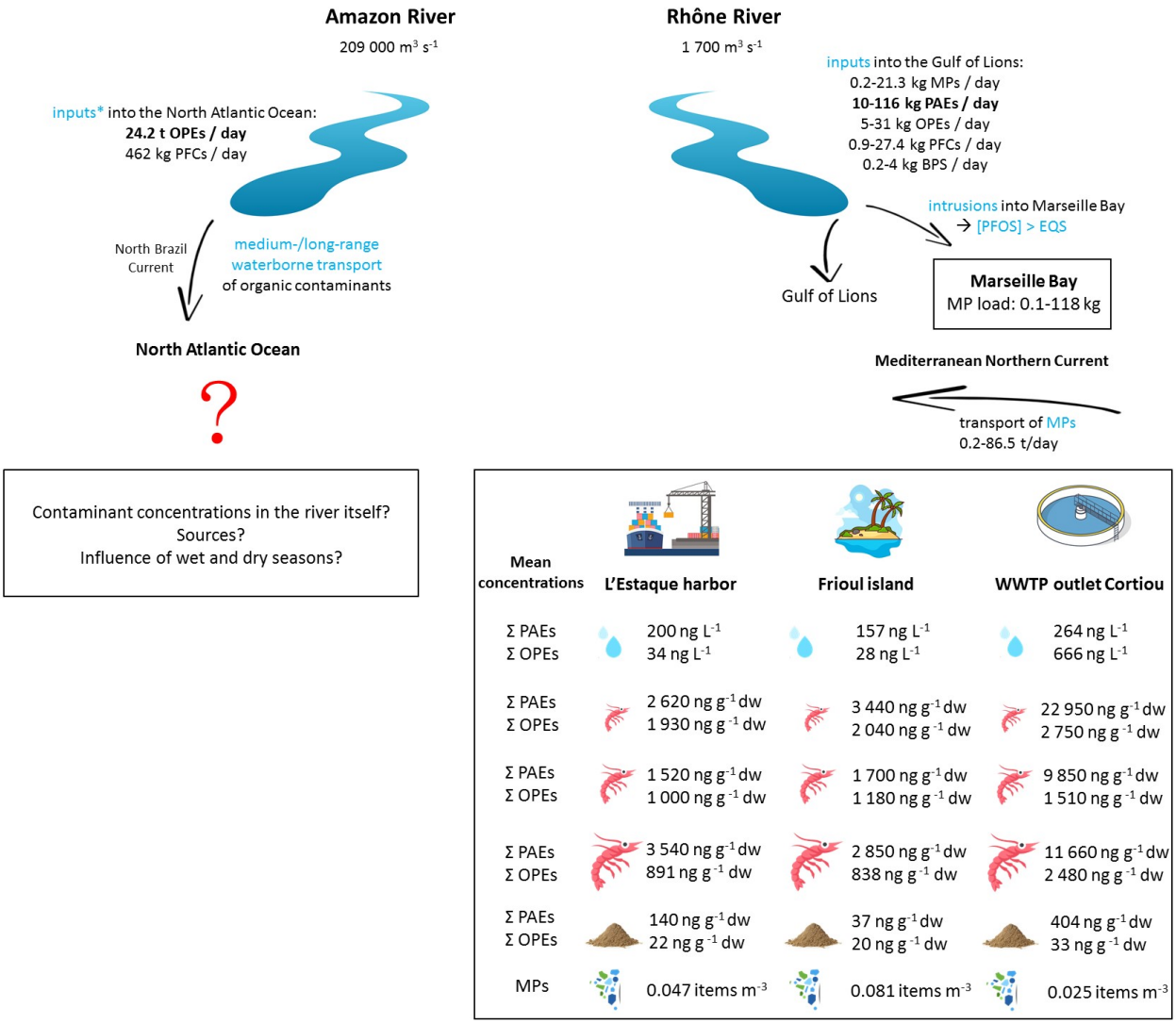

Figure 1: Schematic representation of the aspects studied in this thesis. Predominant contaminants are highlighted with bold letters. The symbol size (water, zooplankton, sediment and microplastics) represents the relative abundance of contaminants between the sampling stations (e.g., contaminant concentrations in water samples: Frioul < L'Estaque < Cortiou). * inputs from the Amazon River are very roughly estimated, since no contaminant data directly from the river exists. Therefore, the OPE and PFC (= PFAS) concentrations from the sampling station closest to the Amazon River mouth (Y11, see chapter V) were multiplied with the average river discharge (i.e., 209 000 m^3 s^{-1}).

Zooplankton seems to exhibit particularly important concentrations of organic plastic additives. Future studies should therefore investigate whether organisms from highly contaminated zooplankton samples show morphological abnormalities, such as malformations. Furthermore, on the local scale, sampling frequencies need to be intensified in order to obtain long-term series at good resolution and the number of studied species and compartments need to be increased. In water samples, the particulate water phase should also be analyzed to obtain a more complete picture of the total load present in (Marseille Bay) or exported to (Rhône River) the NW Mediterranean Sea. In the Rhône River this is particularly important, since the important number of particles in the water column could have an effect on the partitioning of the contaminants between the dissolved water phase and the particulate water phase. Concerning microplastics, a characterization of their structure should be made to explore the most abundant types as well as potential sources in the area. Measuring samples from the Amazon River, trying to distinguish potential contaminant sources and investigating the influence of wet and dry seasons, will be crucial tasks for the future as well. Globally, similar studies on the dynamics and distributions of organic contaminants of emerging interest need to be conducted in areas of particular interest, such as the Amazon River, the Nile River or the waters of the Great Pacific Garbage Patch. Other molecules used as organic plastic additives, and potentially hazardous, should also be investigated. Furthermore, atmospheric inputs of microplastics and additive compounds should be examined at the same time as waterborne occurrences.

Another aspect concerns the study of transport and degradation at a large scale in the open ocean. There is currently a lack of information dealing with the prokaryotic degradation and the transfer of contaminants within the food web during long-range transport with the general oceanic circulation. Such a study can certainly be approached in the future by coupling mesoscale transport and biogeochemical models with *in situ* data. Furthermore, there is a need

to define EQSs for prevailing organic contaminants (e.g., TCPP or DEHP for biota), in order to be able to easily make basic, local risk assessments.

While efforts remain necessary to address these subjects, this thesis joins numerous efforts made to uncover the current state of contamination of aquatic environments. We provide additional elements which could be used to better adapt regulation and remediation strategies, in order to improve the quality of polluted waterbodies. For the Bay of Marseille, some elements (occurrence of OPEs, PAEs, BPs and PFAS; spatio-temporal variability; most abundant contaminants; main sources; most affected compartment) have now been studied, identified and clarified, opening the door for further research and related, regional management actions concerning the chemical contamination of coastal waters.

PUBLICATIONS

LIST OF PUBLICATIONS

Schmidt, N., Fauvelle, V., Ody, A., Castro-Jiménez, J., Jouanno, J., Changeux, T., Thibaut, T., Sempéré, R., 2019. The Amazon River – a major source of organic plastic additives to the tropical North Atlantic? *Environmental Science & Technology*. DOI: 10.1021/acs.est.9b01585

Schmidt, N., Thibault, D., Paluselli, A., Galgani, F., Sempéré, R., 2018. Occurrence of microplastics in surface waters of the Gulf of Lion (NW Mediterranean Sea). Mermex special issue, *Progress in Oceanography* http://doi.org/10.1016/j.pocean.2017.11.010

Schmidt, N., Castro-Jiménez, J., Fauvelle, V., Ourgaud, M., Sempéré, R., (under revision) Occurrence of organic plastic additives in surface waters of the Rhône River (France). *Environmental Pollution*.

Schmidt, N., Fauvelle, V., Castro-Jiménez, J., Lajaunie-Salla, K., Pinazo, C., Yohia, C., Sempéré, R., (submitted) Occurrence of perfluorinated compounds in the Bay of Marseille (NW Mediterranean Sea) and the Rhône River. *Marine Pollution Bulletin*.

Castro-Jiménez, J., González-Fernández, D., Fornier, M., **Schmidt, N.,** Sempéré, R., 2019. Macro-litter in surface waters from the Rhone River: Plastic pollution and flows to the NW Mediterranean Sea. *Marine Pollution Bulletin* 146, 60-66. doi: 10.1016/j.marpolbul.2019.05.067

Fauvelle, V., Castro-Jiménez, J., **Schmidt, N.,** Carlez, B., Panagiotopoulos, C., Sempéré, R., 2018. One-Single Extraction Procedure for the Simultaneous Determination of a Wide Range of Polar and Nonpolar Organic Contaminants in Seawater. *Frontiers in Marine Science* 5:295. doi: 10.3389/fmars.2018.00295

Paluselli, A., Fauvelle, V., **Schmidt, N.,** Galgani, F., Net, S., Sempéré, R., 2018. Distribution of phthalates in Marseille Bay (NW Mediterranean Sea). *Science of the Total Environment* 621, 578–587.

Ody A, Thibaut T, Berline L, Changeux T, Andre´ J-M, Chevalier C, et al., 2019. From *In Situ* to satellite observations of pelagic *Sargassum* distribution and aggregation in the Tropical North Atlantic Ocean. PLoS ONE 14(9): e0222584. https://doi.org/10.1371/journal.pone.0222584

+ **Schmidt** et al. (in preparation) Phthalates and organophosphate esters in the Bay of Marseille: occurrence and possible implications for the marine food web.

Marine Pollution Bulletin 146 (2019) 60–66

Contents lists available at ScienceDirect

Marine Pollution Bulletin

journal homepage: www.elsevier.com/locate/marpolbul

Macro-litter in surface waters from the Rhone River: Plastic pollution and loading to the NW Mediterranean Sea

Javier Castro-Jiménez[a,*], Daniel González-Fernández[b], Michel Fornier[a], Natascha Schmidt[a], Richard Sempéré[a]

[a] Aix-Marseille Univ., Toulon Univ., CNRS, IRD, Mediterranean Institute of Oceanography (MIO), UM 110 Marseille, France
[b] Department of Biology, University of Cádiz. Faculty of Marine and Environmental Sciences, Puerto Real, Spain

ARTICLE INFO

Keywords:
Plastic waste
Marine pollution
Litter flow
Water quality
Large European rivers

ABSTRACT

We present here the first estimates of floating macro-litter in surface waters from the Rhone River, based on monthly visual observations during 1-year period (2016–2017). Plastic represented 77% of the identified items, confirming its predominance in riverine floating litter. Fragments (2.5–50 cm) and Single Use Plastics (i.e. bags, bottles and cover/packaging) were among the most abundant items. Frequent non-plastic floating litter were paper items such as packaging material and newspapers, and metal items (mostly cans), representing 14% and 5% of total litter, respectively. A lower-end estimate resulted in ~223,000 plastic items (~0.7 t of plastic) transported annually by the Rhone surface waters to the Gulf of Lion (NW Mediterranean Sea). Floating macro-plastics are only a fraction of the total plastic export by the Rhone. Our study highlights the current discrepancy between field observations and theoretical estimations. Improvements are needed to harmonize data collection methodologies for field studies and model validation.

1. Introduction

There is no doubt today that plastic waste generated by the world's populations is accumulating in our seas and oceans at large amounts. Numerous marine species including fishes, seabirds, marine mammals and turtles have been reported to either ingest plastic or get entangled in marine debris (Kühn et al., 2015; Gall and Thompson, 2015; Rummel et al., 2016). Coastal populations were estimated to pollute the global ocean with 4.8 to 12.7×10^6 tonnes (t) of plastic waste in 2010 (Jambeck et al., 2015). Rivers have been described as efficient "highways" playing a major role in the land-to-ocean litter transport of plastic waste, not only delivering materials generated in coastal areas, but also transporting waste generated further inland in the catchment. Recent modelling estimations point to 0.5 to 2.7×10^6 t·y^{-1} of plastic waste loaded to the seas and oceans of the world through inland water courses (Lebreton et al., 2017; Schmidt et al., 2017). These estimations are mostly based on the calculation of the amount of mismanaged plastic waste (MMPW), including a limited number of field observations and, in most cases, considering mostly the smaller plastic fragments like micro-plastics (< 5 mm). The occurrence of larger plastic fragments, called macro-plastics, in river waters and their loading to coastal areas are largely uncharacterized. This could be in part the result of a lack of consistent methodologies for sampling/monitoring larger plastic fragments, as recently pointed out (González et al., 2016; van Emmerik et al., 2018). In addition, the scientific community has paid a stronger attention to micro-plastics, even if macro-plastics are important secondary sources of micro-plastics due to degradation/fragmentation processes (Gewert et al., 2015). Moreover, the majority (87%) of the existing studies dealing with plastic pollution focused on the marine environment and freshwater ecosystems have certainly been less investigated (Blettler et al., 2018). A limited number of studies reporting on loads of macro-plastics in rivers are available, like those in the Saigon River (Vietnam) (Lahens et al., 2018; van Emmerik et al., 2018). In Europe, macro-plastic measurements have been published for the Seine (France) (Gasperi et al., 2014; Tramoy et al., 2019), Thames (UK) (Morritt et al., 2014) and Tiber (Italy) (Crosti et al., 2018) rivers. However, no previous field data on macro-plastics occurrence and loading exist for large European rivers draining into the Mediterranean Sea, a semi-enclosed marine environment reported as one of the major hotspots of plastic contamination in the World (Eriksen et al., 2014; Cózar et al., 2015).

We present here results on macro-litter occurrence, with focus on macro-plastics, in surface waters from the Rhone River (Switzerland/France). This river is the major watercourse flowing into the Western

* Corresponding author.
E-mail address: javier.castro-jimenez@mio.osupytheas.fr (J. Castro-Jiménez).

https://doi.org/10.1016/j.marpolbul.2019.05.067
Received 19 February 2019; Received in revised form 9 May 2019; Accepted 31 May 2019
Available online 07 June 2019
0025-326X/ © 2019 Elsevier Ltd. All rights reserved.

Mediterranean Sea with its 816 km encompassing a catchment area of ~95,000 km^2 (Eyrolle et al., 2012). The Rhone River delivers 2–10 Mt of sediments and ~50 × 10^9 m^3 of freshwater annually and large amounts of nutrients and inorganic/organic carbon (Sempéré et al., 2000; Eyrolle et al., 2012). It is also a known source of classical anthropogenic organic compounds like polychlorinated biphenyls (PCBs) (Mourier et al., 2014; Poulier et al., 2019), polycyclic aromatic hydrocarbons (PAHs) (Guigue et al., 2014), and dicarboxylic acids (Sempéré et al., 2018). Furthermore, the presence of the major families of organic plastic additives, like phthalates acid and organophosphate esters (PAE and OPE, respectively) and bisphenols in the Rhone surface waters have been very recently reported (Paluselli et al., 2018; Schmidt et al., n.d.). These important riverine inputs also transport unquantified amounts of plastic litter, spreading out in the entire Gulf of Lion, particularly after heavy rain events. Accumulation of plastic material has already been observed at the sea floor in the French Mediterranean coast including: (i) Marseille Bay, continental slopes and canyons from the Gulf of Lion in the NW Mediterranean Sea, with plastic bags accounting for 90% of the total debris on the floor of the continental shelf and in particular in the eastern canyons (Galgani et al., 1995, 1996, 2000); (ii) the Rhone River plume area and nearby canyons (Fabri et al., 2014). Additionally, recent reports investigated the presence of microplastics in Rhone River waters (Constant, 2018; Schmidt et al., 2018). However, no discrete data or monitoring on macro-plastics in the Rhone River is available to the best of our knowledge. The overall objective of this work was to provide the first estimate on the occurrence of floating macro-litter, with focus on plastic items, in the Rhone River and its loading to the Gulf of Lion area by applying an easy and cost-effective monitoring tool based on visual observation.

New knowledge on this topic can have an impact in the implementation of environmental regulations such as the European Marine Strategy Framework Directive (MSFD, 2008/56/EC), aimed at achieving Good Environmental Status in EU's marine waters, including the monitoring and assessment of marine litter under Descriptor 10; or the new European Strategy for Plastics in a Circular Economy (COM/2018/028 final), which has recently agreed on banning certain single use plastic (SUP) items (http://europa.eu/rapid/press-release_IP-18-3927_en.htm).

2. Materials and methods

2.1. Observation site and data collection

The Rhone Delta is divided into two flows the "Petit Rhone" and the "Grand Rhone", corresponding to around 10% and 90% of the water flow, respectively (Fig. 1A). Monthly monitoring was carried out from the Trinquetaille bridge (~13 m height) in Arles (Southern France, Fig. 1B) located on the "Grand Rhone" at around 40 km NW from the river mouth in the Gulf of Lion (NW Mediterranean Sea). Data was collected by visual observations of floating macro-plastics and documented with the European Commission-Joint Research Centre (EC-JRC) Floating Litter monitoring application (App) for mobile devices (González-Fernández and Hanke, 2017). The observations were performed within the framework of the project RIMMEL (Riverine and Marine floating macro-litter Monitoring and Modelling of Environmental Loading) from the EC-JRC. This strategy allowed the harmonized monitoring of macro-plastics, compatible with the MSFD.

The App used for the observations is aligned with the MSFD MasterList of litter categories included in the "Guidance of Monitoring of Marine Litter in European Seas" document (EC-JRC, 2013), containing the list of litter items established under the MSFD (González-Fernández and Hanke, 2017). Further, the App includes categories such as 'non litter items', 'other litter items' and also 'other plastic items' to register items that were not possible to identify or not listed in the MSFD MasterList. Non litter items were excluded for the following analysis.

A total of 16 observation sessions (generally around 30 min each) were performed from September 2016 to September 2017 (Table 1), considering an observation track width (OTW) of 65 m (i.e., the section at both sides from the observer) over a total river width of 150 m at the observation site (Fig. 1B). Although observations were aimed at monitoring litter > 2.5 cm, identification of small items (2.5–5 cm) from a 13 m height could not be assured across the whole OTW selected, expanding 32.5 m left and right from the observation site, particularly at the edges (Fig. 1B). The distance from the observer to the edges of the OTW corresponds to 35 m, and therefore we define a more realistic minimum observable size for this study ranging from 2.5 cm at the vertical of the observer to ~7 cm at the edges of the OTW. Considering this limitation, results reported herein probably include a bias in detecting large items vs. small items towards the edges of the OTW, underestimating the flux of smaller items, which also implies providing a conservative litter loading estimate. A dedicated study would be required to empirically ascertain the lower-end size of observable items across a given OTW.

In order to perform an assessment of the litter and plastic loading and their temporal variability, river flow ($m^3 \cdot s^{-1}$) time series were extracted from "Banque Hydro" (http://www.hydro.eaufrance.fr/), whereas daily precipitation measurements (mm), wind speed ($m \cdot s^{-1}$) and direction were obtained from Météo-France (https://donneespubliques.meteofrance.fr/). These data correspond to the closest measuring stations to the observation site: Tarascon, ~16 km upstream of Arles and, Tour-du-Valant, around 25 km south from the observation site, for precipitation and wind data, respectively (Fig. 1A and Table 1).

2.2. Loading estimation

The macro-litter loading was calculated for each session as number of observed anthropogenic litter items (Table S1, SI) divided by observation time, and then extrapolated from OTW (65 m) to river width at the sampling site (150 m) (Fig. 1B), obtaining items·h^{-1}. Mean and median loadings were calculated for all observation sessions (n = 16). The annual load was estimated as: median loading (items·h^{-1}) × 24 h × 365 d, providing items·y^{-1}. The median was selected against the mean, minimizing the influence of extreme litter events for a conservative estimate. This estimate was based on the assumption that floating litter is homogeneously distributed on the cross-section of the river and the datasets are representative for the litter loading variability along the year.

3. Results and discussion

3.1. Macro-litter abundance and plastic loading

Items belonging to twenty-two macro-litter categories were observed in surface waters from the Rhone River during the monitoring period, summing up a total of 181 items for 8.2 h of cumulative observation (Fig. 2).

Plastic items, including pieces, bags, sheets, bottles, and cover/packaging, represented around 77% of the floating macro-litter in Rhone River waters confirming the predominance of plastic pollution, in agreement with the top items list identified by RIMMEL across Europe (González-Fernández et al., 2018). Paper items, like packaging material and newspapers, and metal items (mostly cans), represented 14% and 5% of total floating macro-litter in Rhone Rivers waters, respectively, and were the most abundant non-plastic floating items (Fig. 2B).

Litter composition presented herein differed to a certain extent from top items lists found in the marine environment. Depending on the materials and the differential environmental conditions in rivers and marine areas, some items may get degraded and fragmented, while others may get ballasted or lose their floatability at different rates.

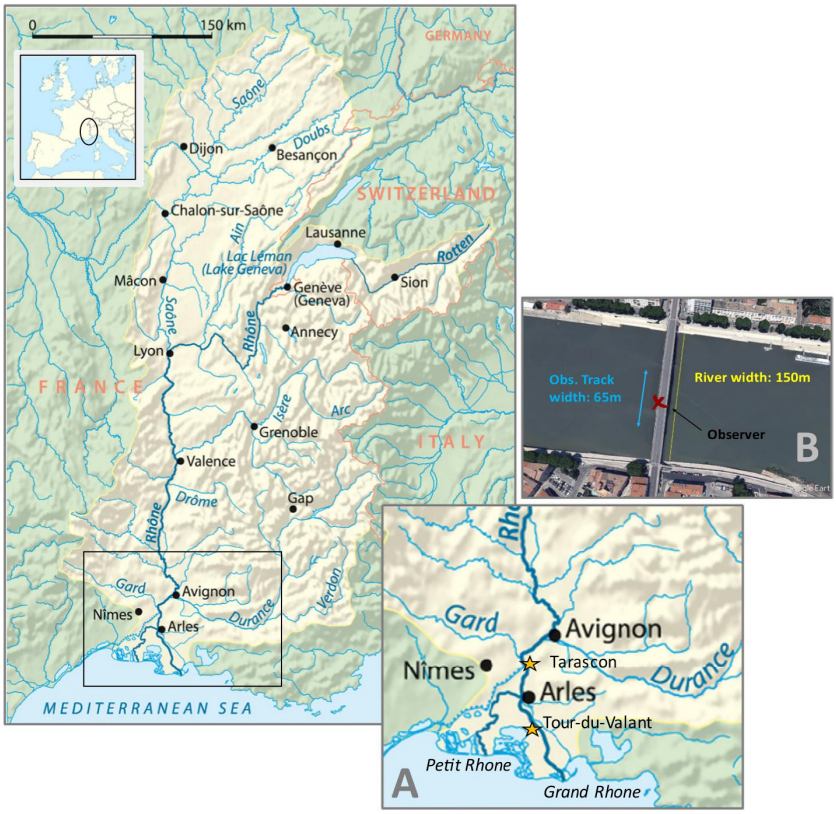

Fig. 1. Map showing the Rhone River from its source upstream Lake Geneva to its estuary in the Gulf of Lion (NW Mediterranean Sea), the position of the river flow (Tarascon) and precipitation and wind (Tour-du-Valant) measuring stations, location of Arles (A) in the "Grand Rhone", and detail of the observation site (Trinquetaille bridge) (B).

Table 1
Details of the observations performed with corresponding observation time (min) and river flow ($m^3 \cdot s^{-1}$) as registered in Tarascon; and precipitation (mm), wind speed ($m \cdot s^{-1}$) and wind direction (WD, degrees), as registered in Tour-du-Valant (Météo-France station). * 360° = N, 180° = S, 90° = E, 270° = W.

Observation	Date	Starting time	Obs time (min)	River flow ($m^3 \cdot s^{-1}$)	Precipitation (mm)	WS ($m \cdot s^{-1}$)	WD (degree)*
Obs-1	16/09/2016	11:11:50	30	868	1.0	3.7	159
Obs-2	04/10/2016	09:27:32	17	545	0.0	3.3	350
Obs-3	08/11/2016	15:10:41	34	1310	0.0	4.1	318
Obs-4	06/12/2016	11:01:16	36	1290	0.0	3.0	184
Obs-5	19/01/2017	11:48:28	33	1140	0.0	3.8	346
Obs-6	15/02/2017	10:30:21	35	1550	0.0	2.9	100
Obs-7	28/03/2017	09:14:44	34	1560	0.0	2.4	158
Obs-8	12/04/2017	13:00:00	30	894	0.0	2.8	214
Obs-9	05/05/2017	11:20:09	32	1230	0.0	3.0	173
Obs-10	06/05/2017	10:37:47	15	1130	11.3	3.7	280
Obs-11	23/05/2017	09:29:37	30	1240	0.2	3.5	268
Obs-12	22/06/2017	11:00:55	35	872	0.0	2.7	126
Obs-13	10/07/2017	09:29:16	36	671	0.0	2.6	245
Obs-14	12/07/2017	10:25:41	30	859	0.0	3.9	236
Obs-15	24/08/2017	11:52:45	33	522	0.0	3.6	125
Obs-16	25/09/2017	10:16:56	34	625	0.0	2.0	171

Therefore, the litter composition in rivers may change compared to beaches and marine waters. Additionally, the marine environment is subject to sea-based litter sources, often related to fisheries, introducing items that are not present or limited in rivers. Despite differences among floating items observed in the Rhone River and top items found in beaches and floating at sea in the Mediterranean region, there is coherence in the high percentage of plastic items composing the marine litter (Table S2, SI). Furthermore, these top items lists included SUP items such as bottles or bags within the most frequent items (Addamo et al., 2017; Arcangeli et al., 2018; Di-Meglio and Campana, 2017).

Overall, the most abundant items observed in the Rhone River were plastic pieces in the size range 2.5–50 cm, influenced by a peak in litter flux observed on 5th May 2017 (Fig. 3). No significant correlations were found with environmental variables such as river flow, rain or wind (meridional and zonal components), using Pearson correlation coefficients for $n = 16$ observations and p-level 0.05 (Table S3, SI). We acknowledge that our data set is limited and higher frequency observations may reveal some significant correlations. Predominance of plastic pieces could indicate: (i) a significant fragmentation of the larger items most commonly found such as bags, cover/packaging and other plastic materials flowing down the river; (ii) and/or the preferential direct inputs of plastic fragments in the catchment area. Additionally, small fragments are expected to have a more efficient transport in the river waters, while larger items may get trapped in the riverine banks and

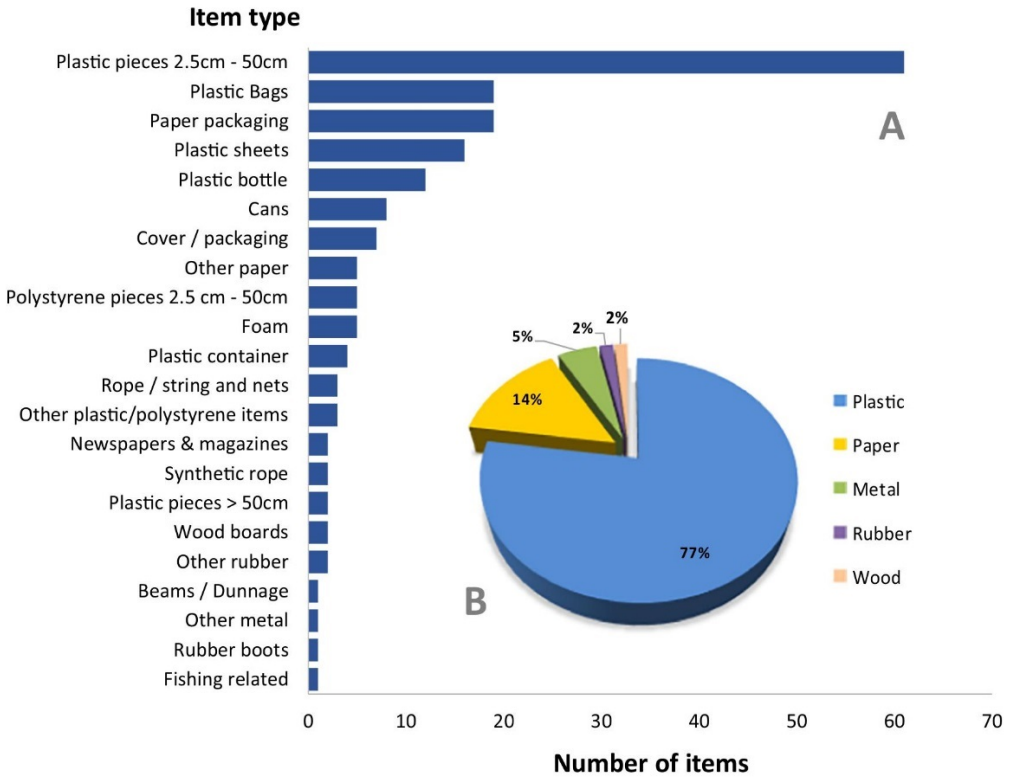

Fig. 2. Number and type of macro-litter items found in surface waters from the Rhone River (A) and relative abundance of macro-litter items grouped by material type (B).

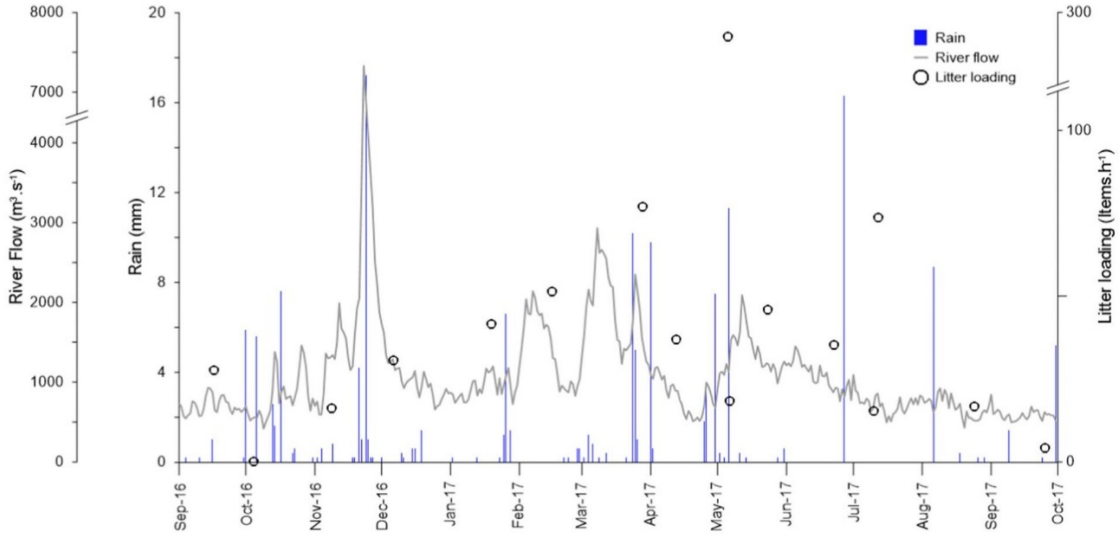

Fig. 3. Temporal variation of litter loading (items·h^{-1}), annual river flow (m^3·s^{-1}) and precipitation (mm) in the observation period from September 2016 to September 2017. These variables are separately displayed on a complementary figure presented in SI (Fig. S2).

vegetation for longer periods (Williams and Simmons, 1996).

Fig. 3 shows the estimated litter loading along with river flow and precipitation at Tarascon during the observation period. The estimated litter loading values (whole river cross-section) exhibited a high variability, ranging from none to 293 items·h^{-1}, with a mean value of ~50 ± 69 SD items·h^{-1} (~33 items·h^{-1} median value). Plastic items reached 226 items.h^{-1} with a mean macro-plastic loading of ~37 ± 61 SD items·h^{-1} (~26 items·h^{-1} median value). This large variability could have been induced by the important temporal variations in the river flow, with values ranging from around 400 to 7300 m^3·s^{-1} for the observation period (median discharge of 910 m^3·s^{-1}). However, in spite of this variability a general positive trend between river water discharge and litter loading can be observed (Fig. 3). Indeed, a linear regression analysis showed a positive

statistically significant correlation when excluding the litter peak of 5th May 2017 ($r^2 = 0.36$, $\alpha = 0.05$, p-value = 0.018) (Fig. S1). The litter peaks of 5th May, and 12th July 2017 were registered under relatively low river flow (1230 and 860 $m^3 \cdot s^{-1}$) and no precipitation (Table 1). Although these conditions cannot fully explain the high litter fluxes observed, several rain events took place before these two sampling events. First, in the period 25th–30th April 2017 and then on 27th June 2017 with ~13 mm and ~16 mm of cumulative precipitation registered, respectively (Fig. 3). These precipitation events could have facilitated new litter inputs to the watercourse and remobilized items already deposited on the river banks upstream. In addition, factors such as flow regulation by opening dams, storm overflow and runoff during rain events upstream in the basin may have an important effect, flushing litter accumulated in the basin by pulses within very short periods.

In order to gain understanding on short-term variability (e.g. after rain events), specific studies with more frequent observations are needed. No observation was performed on 23rd November 2016, when the river flow exhibited its highest value, most probably due to various consecutive days of rains in the basin, including ~22 mm of cumulative precipitation registered in Arles area for the period 21st–24th November 2016. The macro-litter observations were performed either earlier in November or almost two weeks later on 6th December 2016 (Table 1), under no rain conditions and a river flow of ~1300 $m^3 \cdot s^{-1}$, missing the flow peak.

An estimation of the total loading of the Rhone River to the NW Mediterranean Sea points to ~223,000 items of floating macro-plastics annually. Assuming an item-to-mass conversion factor of 3.2 g per item based on macro-plastic sampling in Saigon river (Vietnam) (van Emmerik et al., 2018), ~0.7 $t \cdot y^{-1}$ of macro-plastics could be transported by the Rhone surface waters into the Gulf of Lion.

We consider our plastic export from the Rhone River to the Mediterranean Sea as a lower-end estimate. First, it is based on floating macro-plastic only and the use of the median value for the calculation, which excludes the influence of extreme events. Second, the debris lying and/or flowing in the water sub-surface and the entire water column are not taken into account. River sediments, reported as final repository of marine litter (Galgani et al., 2000), have not been considered either. Given that the bottom nepheloid layer in front of the Rhone River Estuary comprises a large amount of particulate material transported and re-suspended by the Rhone (Sempéré et al., 1994), it is very likely that significant amounts of plastic debris are also exported with the sediment from the river bottom into the NW Mediterranean. In addition, an underestimation of the smallest plastic items, particularly at the observation track edges is acknowledged. Further, even if we did not observe significant accumulation areas in our site during the sampling events, an accumulation of macro-plastics could have happened upstream, and these waste deposits could be remobilized under certain circumstances, like heavy rains, leading to plastic waste pulses in surface waters punctually increasing the loading to coastal areas and having an important short-term impact. This phenomenon should be further investigated along the year.

In spite of the high uncertainties associated with this calculation, it represents the first estimate of floating macro-plastic inputs from the Rhone River to the NW Mediterranean Sea based on real observations. Thus, we cannot compare our results with other field observations of macro-plastics in this area. However, a few studies (field and modelling estimations) performed during the last years have investigated the micro-plastic export by the Rhone River (Table 2). Interestingly, our estimate is within the range of the micro-plastic loading derived from samples collected at the same site (Arles, France) and at the beginning of our observation period (Schmidt et al., 2018; Constant, 2018) (Table 2). The total floating plastic waste, as macro- and micro-plastics "traveling" at the same time in the Rhone surface waters, could reach up to 8.5 $t \cdot y^{-1}$, considering our estimate and the higher-end estimate of micro-plastics from Schmidt et al. (2018). However, this estimation contrasts with the higher flow of plastics (mostly micro-plastics) measured in the Swiss part of the Rhone River (Faure et al., 2015), pointing to different loads of floating plastics upstream and downstream of the Rhone. Besides, our macro-plastic estimate are 1–4 orders of magnitude lower than the available modelling calculations of plastic waste export from the Rhone River, varying from 7 to ~1450 $t \cdot y^{-1}$ (Table 2) (Schmidt et al., 2017; Siegfried et al., 2017; Liubartseva et al., 2018). In contrast, our estimates are in the range or slightly higher than the modelling inputs calculated for the Rhone River downstream dams (0.01–0.14 $t \cdot y^{-1}$) (Lebreton et al., 2017), consistent with the hypothesis of higher loads of floating plastic upstream in the river basin, probably influenced by the existence of different litter sources and river transport conditions, including retention in dams. With the exception of the estimations from Lebreton et al. (2017), there is an important discrepancy between our export estimates derived from direct observation of floating items (plastic fragments ≥ 2.5 cm) and the existing theoretical estimations, which are mostly based on data from plastic production and waste in a given river catchment or geographical area, and based on scarce micro-plastics field data. The use of micro-plastic data can hardly be representative for the macro-plastics pool because of the sampling conditions, e.g. short-term deployment of ~20 min with 0.5–0.9 m width and 0.1–0.6 m height opening manta-nets (González et al., 2016). The available data also show that existing results from models, which have been partially or not at all validated with field observations due to the lack of data in most of the cases, can vary substantially among them, up to 5 orders of magnitude (Table 2).

Our estimate is lower compared to the 27 $t \cdot y^{-1}$ (mean value) of floating plastic debris reported for another French river (i.e., the Seine), based on items collection during April–July 2014 by using floating debris-retention booms (Gasperi et al., 2014) and even lower compared to a second study based on a longer data collection period in the same river (110–170 $t \cdot y^{-1}$) (Tramoy et al., 2019). However, about 16 million people live in the Seine catchment area (~73,000 km^2), including the megacity of Paris, whereas the population for the Rhone catchment area (~95,000 km^2), represents ~10 million people (Schmidt et al., 2017), and therefore a lower loading is expected in the latter. In addition, the fact that the retention booms used in these studies were all located on the river margins, supposedly macro-plastic accumulation areas as pointed out by van Emmerik et al. (2018), could also explain part of this variability. These facts illustrate one more time the importance of the data collection methodologies and the complexity in the comparison of existing data.

3.2. Environmental implications

The primary production in the NW Mediterranean Sea has been reported as largely affected by the Rhone River inputs (mostly by the large sedimentary material and nutrients inputs), also playing an important role in the marine ecosystem functioning in the entire Gulf of Lion due to the effective dispersion in the area (Raimbault and Durrieu de Madron, 2003; Durrieu de Madron et al., 2008). However, the effects of plastic waste in this ecosystem are largely unknown. Our work indicates that significant amounts of plastic waste may be delivered annually to the NW Mediterranean Sea from the Rhone River, and that floating macro-plastic loads are most probably only a part of the total plastic waste entering this ecosystem. Floating macro litter inputs from rivers include persistent and fragmented plastics that can have a longer term availability to marine animals and possibility to cause harm (Werner et al., 2016). Once they reach the marine environment, they can get stranded on beaches, sink in shallow bottoms, or travel long distances in the open sea, being accessible to a wide range of marine animals (Kühn et al., 2015) In addition to the possible "physical damages" (e.g. ingestion and entanglement) caused to the aquatic organisms, these fragments of different polymers could also represent new sources of dissolved organic carbon (DOC) (Romera-Castillo et al., 2018; Paluselli et al., 2019) and organic additives like PAEs and OPEs

Table 2
Compilation of existing plastic export estimations from the Rhone River to the NW Mediterranean Sea. Field studies are on surface waters only.

Geographical area	Period	Plastic size[a]	Type of study/sampling method	Export ($t \cdot y^{-1}$)	Reference
Rhone (Swiss part)	Oct. 2013	Micro-plastics	Field/Manta net	~208[b]	Faure et al. (2015)
Rhone (Arles, France)	Mar., Apr. 2016	Micro-plastics	Field/Manta net	~0.07–7.8[c]	Schmidt et al. (2018)
Rhone (Arles, France)	Oct. 2015–Oct. 2016	Micro-plastics	Field/Manta net	6.0	Constant (2018)
Rhone river basin	Year 2000	Micro-plastics	Numerical simulation	163	Schmidt et al. (2017)
Not specified	2013–2017	Micro-plastics	Numerical simulation	1454	Liubartseva et al. (2018)
Rhone river basin (downstream dams)	Not specified	Micro + macro-plastics	Numerical simulation	0.01–0.14	Lebreton et al. (2017)
Rhone river basin	Not specified	Micro + macro-plastics	Numerical simulation	7–16	Schmidt et al. (2017)
Rhone (Arles, France)	Sept. 2016–Sept. 2017	Macro-plastics	Field/visual observation	0.71	This study

[a] The microplastic sizes considered in the different studies may be different (see specific references for further details). We consider macro-plastics as fragments ≥ 2.5 cm for the purpose of this study.
[b] Estimated from the reported 570 $kg \cdot d^{-1}$.
[c] Estimated from the reported 0.20 and 21.32 $kg \cdot d^{-1}$.

(Paluselli et al., 2019). Indeed, a recent study reported from 5 to 54 $t \cdot y^{-1}$ of organic plastic additives, including PAEs, OPEs and bisphenols, exported by Rhone surface waters to the Gulf of Lion (Schmidt et al., n.d.). The latter suggests that the potential additive leaching from the combined estimated export of 8.5 $t \cdot y^{-1}$ for floating macro-plastics (this work) and micro-plastics (Schmidt et al., 2018) cannot explain the current levels of additives in the river dissolved water phase. However, the floating plastic waste seems to be only a fraction of the entire plastic pool in the water ecosystem, and the plastic stocks in the whole water column and sediments could contribute too to the "leaching source". A dedicated study aiming at establishing a first mass balance of organic plastic additives in the NW Mediterranean Sea is needed. Such assessment should consider also the additive inputs not directly linked to the leaching from plastic debris in the water column. For example, the atmospheric deposition of OPEs has been confirmed as an important input pathway in coastal and open Mediterranean Sea (Castro-Jiménez et al., 2014, 2018). Up to 1.1 $t \cdot y^{-1}$ of OPEs were estimated to be loaded from the atmosphere to the Gulf of Lion via dry deposition (Schmidt et al., n.d.). Finally, these inputs of macro-plastics and additives can contribute to the cocktail of pollutants that may affect the aquatic organisms and humans at a local/regional scale.

4. Conclusions

The first estimation of floating macro-plastics input from the Rhone River to the NW Mediterranean Sea supports the hypothesis of large European rivers as important pathways for plastic litter to coastal areas. Our data suggest that floating macro-litter represents only a fraction of the total plastic waste transported into the marine environment through rivers. An important uncertainty is associated to these estimations due to the high temporal variability. Small plastic fragments in the range of 2.5 to 50 cm are the most frequent litter observed in surface waters. Further, Single Use Plastics (SUP), like bags, bottles and cover/packaging are among the most abundant items, highlighting the relevance of their restriction at EU level, through the EU Plastic Strategy. The results of this investigation can be used to design mitigation measures and monitor their effectiveness. Regarding banning of SUP, this study can indicate the most common items and flux/loading values found in large Mediterranean rivers, establishing a baseline for future monitoring. The generated data can also help in the plastic pollution management at river basin scale, supporting actions aimed at intercepting the plastic before it gets to the marine environment.

Our results highlight also the current discrepancy between field observations and theoretical estimations. It is clear that both field observations and modelling simulations aiming at quantifying the plastic waste export to coastal areas, particularly from large European rivers draining into the Mediterranean Sea, like the Rhone River, are still incomplete. Improvements are needed in order to harmonize data collection methodologies for field studies and model validation. Macro-to-micro plastic transformation rates, and plastic item-to-mass conversion factors should be investigated for more accurate mass balances. Waterborne macro-plastics, traditionally described as a source of micro-plastics in rivers due to aging and fragmentation processes, should not be considered as the only source of the smallest plastic fragments. Other sources, like direct run-off and atmospheric inputs of micro-plastics, should be investigated. In addition, the role that waterborne plastic debris may play as contributing to the global stock of organic plastic additives in the water column should be further investigated also in relation to other potential sources of organic plastic additives like atmospheric deposition.

Acknowledgments

We would like to thank the project RIMMEL and G. Hanke from JRC for their logistic support. Observation campaigns were supported by the Service Atmosphère-Mer (SAM) platform from MIO, and received financial support from the Agence de l'Eau Rhône Méditerranée Corse projects Blue-POLUT and CAREMED and the Labex OT-Med (n° ANR-11-LABX-0061) – MEDPOP- Excellence Initiative of Aix-Marseille University - A*MIDEX (no ANR-11-IDEX-0001- 02). We thank Météo-France for providing the precipitation, wind speed and direction data from the Tour-du-Valant meteorological station.

Appendix A. Supplementary data

Supplementary data to this article can be found online at https://doi.org/10.1016/j.marpolbul.2019.05.067.

References

Addamo, A.M., Laroche, P., Hanke, G., 2017. Top marine beach litter items in Europe. A review and synthesis based on beach litter data. In: JRC Technical Reports, (EUR 29249 EN).
Arcangeli, A., Campana, I., Angeletti, D., Atzori, F., Azzolin, M., Carosso, L., Di Miccoli, V., Giacoletti, A., Gregorietti, M., Luperini, C., Paraboschi, M., Pellegrino, G., Ramazio, M., Sarà, G., Crosti, R., 2018. Amount, composition, and spatial distribution of floating macro litter along fixed trans-border transects in the Mediterranean basin. Mar. Pollut. Bull. 129, 545–554.
Blettler, M.C.M., Abrial, E., Khan, F.R., Sivri, N., Espinola, L.A., 2018. Freshwater plastic pollution: recognizing research biases and identifying knowledge gaps. Water Res.. 143, 416–424.
Castro-Jiménez, J., Berrojalbiz, N., Pizarro, M., Dachs, J., 2014. Organophosphate ester (OPE) flame retardants in the open Mediterranean and black seas atmosphere. Environmental Science & Technology 48, 3203–3209.
Castro-Jiménez, J., Barhoumi, B., Tedetti, M., Sempéré R., 2018. Atmospheric particle-bound organophosphate ester flame retardants and plasticizers in a North African Mediterranean coastal city (Bizerte, Tunisia). Sci. Total Environ. 642, 383–393.
Constant, M. 2018. Source, Transfert et Devenir des microplastiques (MP) en Mer Mediterranee Nord-Occidentale. PhD thesis. University of Perpginam-CEFREM, pp 277.
Cózar, A., Sanz-Martín, M., Martí, E., González-Gordillo, J. I., Ubeda, B., Á. Gálvez, J., Duarte, C. M., 2015. Plastic accumulation in the Mediterranean sea. PLoS One, 10(4). doi:https://doi.org/10.1371/journal.pone.0121762.
Crosti, R., Arcangeli, A., Campana, I., Paraboschi, M., González-Fernández, D., 2018.

'Down to the river': amount, composition, and economic sector of litter entering the marine compartment, through the Tiber river in the Western Mediterranean Sea. Rendiconti Lincei. Scienze Fisiche e Naturali 29, 859.
Di-Meglio, N., Campana, I., 2017. Floating macro-litter along the Mediterranean French coast: composition, density, distribution and overlap with cetacean range. Mar. Pollut. Bull. 118, 155–166.
Durrieu de Madron, X., Wiberg, P.L., Puig, P., 2008. Sediment dynamics in the Gulf of lions: the impact of extreme events. Cont. Shelf Res. 28:1867–1876.
EC JRC, 2013. European Commission Joint Research Centre, 2013. MSFD Technical Subgroup on Marine Litter (TSG-ML). Guidance on Monitoring of Marine Litter in European Seas. EUR 26113 EN - Joint Research Centre.
van Emmerik, T., Kieu-Le, T.-C., Loozen, M., van Oeveren, K., Strady, E., Bui, X.-T., Egger, M., Gasperi, J., Lebreton, L., Nguyen, P.-D., Schwarz, A., Slat, B., Tassin, B., 2018. A methodology to characterize riverine macroplastic emission into the ocean. Front. Mar. Sci. 5, 372. https://doi.org/10.3389/fmars.2018.00372.
Eriksen, M., Lebreton, L.C.M., Carson, H.S., Thiel, M., Moore, C.J., Borrero, J.C., et al., 2014. Plastic pollution in the world's oceans: more than 5 trillion plastic pieces weighing over 250,000 tons afloat at sea. PLoS One 9, 111913. https://doi.org/10.1371/journal.pone.0111913.
Eyrolle, F., Radakovitch, O., Raimbault, P., Charmasson, S., Antonelli, C., Ferrand, E., Aubert, D., Raccasi, G., Jacquet, S., Gurriaran, R., 2012 Consequences of hydrological events on the delivery of suspended sediment and associated radionuclides from the Rhône River to the Mediterranean Sea. J. Soils Sediments 12, 1479–1495.
Fabri, M.-C., Pedel, L., Beuck, L., Galgani, F., Hebbeln, D., Freiwald, A., 2014. Megafauna of vulnerable marine ecosystems in French Mediterranean submarine canyons: spatial distribution and anthropogenic impacts. Deep Sea Res. Part 2 Top. Stud. Oceanogr. 104, 184–207.
Faure, F., Saini, C., Potterand, G., Galgani, F., de Alencastro, L.F., Hagmann, P., 2015. An evaluation of surface micro- and mesoplastic pollution in pelagic ecosystems of the Western Mediterranean Sea. Environ. Sci. Pollut. Res. 22, 12190–7.
Galgani, F., Jaunet, S., Campillo, A., Guenegen, X., His, E., 1995. Distribution and abundance of debris on the continental shelf of the north-western Mediterranean Sea. Mar. Pollut. Bull. 30, 713–717.
Galgani, F., Souplet, A., Cadiou, Y., 1996. Accumulation of debris on the deep sea floor off the French Mediterranean coast. Mar. Ecol. Prog. Ser. 142, 225–234.
Galgani, F., Leaute, J.P., Moguedet, P., Souplet, A., Verin, Y., Carpentier, A., Goraguer, H., Latrouite, D., Andral, B., Cadiou, Y., Mahe, J.C., Poulard, J.C., Nerisson, P., 2000. Litter on the sea floor along European coasts. Mar. Pollut. Bull. 40, 516–527.
Gall, S.C., Thompson, R.C., 2015. The impact of debris on marine life. Mar. Pollut. Bull. 92, 170–179.
Gasperi, J., Dris, R., Bonin, T., Rocher, V., Tassin, B., 2014. Assessment of floating plastic debris in surface water along the Seine River. Environ. Pollut. 195, 163–166.
Gewert, B., Plassmann, M.M., MacLeod, M., 2015. Pathways for degradation of plastic polymers floating in the marine environment. Environ. Sci. Process. Impacts 17, 1513–1521.
González, D., Hanke, G., Tweehuysen, G., Bellert, B., Holzhauer, M., Palatinus, A., Hohenblum, P., and Oosterbaan, L., 2016. Riverine Litter Monitoring - Options and Recommendations. MSFD GES TG Marine Litter Thematic Report; JRC Technical Report; EUR 28307; doi:https://doi.org/10.2788/461233.
González-Fernández, D., Hanke, G., 2017. Toward a harmonized approach for monitoring of riverine floating macro litter inputs to the marine environment. Front. Mar. Sci. 4, 86. https://doi.org/10.3389/fmars.2017.00086.
González-Fernández, D., Hanke, G., and the RiLON network, Floating Macro Litter in European Rivers - Top Items, EUR 29383 EN, Publications Office of the European Union, Luxembourg, 2018, ISBN 978-92-79-96373-5, doi: https://doi.org/10.2760/316058, (JRC108172).
Guigue, C., Tedetti, M., Ferretto, N., Garcia, N., Méjanelle, L., Goutx, M., 2014. Spatial and seasonal variabilities of dissolved hydrocarbons in surface waters from the Northwestern Mediterranean Sea: results from one year intensive sampling. Sci. Total Environ. 466–467, 650–662.
Jambeck, J. R., Geyer, R., Wilcox, C., Siegler, T. R., Perryman, M., Andrady, A., Narayan, R., Law, K. L., 2015. Plastic waste inputs from land into the ocean. Science. 347, 768 − 771.
Kühn, S., Bravo Rebolledo, E.L., van Franeker, J.A., 2015. Deleterious effects of litter on marine life. In: Bergmann, M., Gutow, L., Klages, M. (Eds.), Marine Anthropogenic Litter. Springer, pp. 75–116 (http://edepot.wur.nl/344861).
Lahens, L., Strady, E., Kieu-Le, T. C., Dris, R., Boukerma, K., Rinnert, E., et al., 2018. Macroplastic and microplastic contamination assessment of a tropical river (Saigon River, Vietnam) transversed by a developing megacity. Environ. Pollut. 236, 661–671.
Lebreton, L. C. M., Zwet, J., van der Damsteeg, J.-W., Slat, B., Andrady, A., Reisser, J., 2017. River plastic emissions to the world's oceans. Nat. Commun. 8, ncomms15611.
Liubartseva, S., Coppini, G., Lecci, R., Clementi, E., 2018. Tracking plastics in the Mediterranean: 2D Lagrangian model. Marin. Pollut. Bull. 129, 151–162.
Morritt, D., Stefanoudis, P.V., Pearce, D., Crimmen, O.A., Clark, P.F., 2014. Plastic in the Thames: a river runs through it. Mar. Pollut. Bull. 78, 196–200.
Mourier, B., Desmet, M., Van Metre, P.C., Mahler, B.J., Perrodin, Y., Roux, G., Bedell, J.-P., Lefèvre, I., Babut, M., 2014. Historical records, sources, and spatial trends of PCBs along the Rhône River (France). Sci. Total Environ. 476–477, 568–576.
Paluselli, A., Aminot, Y., Galgani, F., Net, S., Sempéré, R., 2018. Occurrence of phthalate acid esters (PAEs) in the northwestern Mediterranean Sea and the Rhone River. Prog. Oceanogr. 163, 221–231.
Paluselli, A., Fauvelle, V., Galgani, F., Sempere, R., 2019. Phthalate Release from Plastic Fragments and Degradation in Seawater. Environ. Sci. Technol. 53, 166–175.
Poulier, G., Launay, M., Le Bescond, C., Thollet, F., Coquery, M., Le Coz, J., 2019. Combining flux monitoring and data reconstruction to establish annual budgets of suspended particulate matter, mercury and PCB in the Rhône River from Lake Geneva to the Mediterranean Sea. Sci. Total Environ. 658, 457–473.
Raimbault, P., Durrieu de Madron, X., 2003. Research activities in the Gulf of Lion (NW Mediterranean) within the 1997–2001 PNEC project. Oceanol Acta 26, 291–299.
Romera-Castillo, C., Pinto, M., Langer, T.M., Álvarez-Salgado, X.A., Herndl, G.J., 2018. Dissolved organic carbon leaching from plastics stimulates microbial activity in the ocean. Nat.Comm. 9, 1430. https://doi.org/10.1038/s41467-018-03798-5.
Rummel, C.D., Löder, M.G., Fricke, N.F., Lang, T., Griebeler, E.-M., Janke, M., Gerdts, G., 2016. Plastic ingestion by pelagic and demersal fish from the North Sea and Baltic Sea. Mar. Pollut. Bull. 102, 134–141.
Schmidt, C., Krauth, T., Wagner, S., 2017. Export of plastic debris by rivers into the sea. Environ. Sci. Technol. 51, 12,246–12,253.
Schmidt, N., Thibault, D., Galgani, F., Paluselli, A., Sempéré, R., 2018. Occurrence of microplastics in surface waters of the Gulf of Lion (NW Mediterranean Sea). Prog. Oceanogr. 163, 214–220.
Schmidt, N., Castro-Jiménez, J., Fauvelle, V., Sempéré, R. Organic plastic additives in the Rhone River surface waters (France) – occurrence and temporal variability. Submitted.
Sempéré, R., Cauwet, G., Randon, J., 1994. Ultrafiltration of seawater with a zirconium and aluminum oxide tubular membrane: application to the study of colloidal organic carbon distribution in an estuarine bottom nepheloid layer. Mar. Chem. 46 (1–2), 49–60.
Sempéré, R., Charriere, B., Cauwet, G., Van-Wambeke, F., 2000. Carbon inputs of the Rhône River to the Mediterranean Sea: biogeochemical implications. Global Biogeochem. Cy. 14, 669–681.
Sempéré, R., Charrière, B., Castro-Jiménez, J., Kawamura, K., Panagiotopoulos, C., 2018. Occurrence of α, ω-dicarboxylic acids and ω-oxoacids in surface waters of the Rhone River and fluxes into the Mediterranean Sea. Prog. Oceanogr. 163, 136–146.
Siegfried, M., Koelmans, A.A., Besseling, E., Kroeze, C., 2017. Export of microplastics from land to sea. A modelling approach. Water.Res. 127, 249–257.
Tramoy, R., Gasperi, J., Dris, R., Colasse, L., Fisson, C., Sananes, S., Rocher, V., Tasssin, B., 2019. Assessment of the Plastic Inputs From the Seine Basin to the Sea Using Statistical and Field Approaches. Front. Mar. Sci. 6, 151. https://doi.org/10.3389/fmars.2019.00151.
Werner, S., Budziak, A., van Franeker, J., Galgani, F., Hanke, G., Maes, T., Matiddi, M., Nilsson, P., Oosterbaan, L., Priestland, E., Thompson, R., Veiga, J. and Vlachogianni, T.; 2016; Harm caused by Marine Litter. MSFD GES TG Marine Litter - Thematic Report; JRC Technical report; EUR 28317 EN; doi:https://doi.org/10.2788/690366
Williams, A.T., Simmons, S.L., 1996. The degradation of plastic litter in rivers: implications for beaches. J. Coast. Conserv. 2, 63–72. https://doi.org/10.1007/BF02743038.

frontiers in Marine Science

METHODS
published: 31 August 2018
doi: 10.3389/fmars.2018.00295

One-Single Extraction Procedure for the Simultaneous Determination of a Wide Range of Polar and Nonpolar Organic Contaminants in Seawater

Vincent Fauvelle, Javier Castro-Jiménez, Natascha Schmidt, Benoit Carlez, Christos Panagiotopoulos and Richard Sempéré**

Aix-Marseille Univ., Université de Toulon, CNRS, IRD, Mediterranean Institute of Oceanography (M I O), Marseille, France

OPEN ACCESS

Edited by:
Juan Bellas, Instituto Español de Oceanografía (IEO), Spain

Reviewed by:
Víctor M. León, Instituto Español de Oceanografía, Centro Oceanográfico de Murcia, Spain
Monica F. Costa, Universidade Federal de Pernambuco, Brazil

***Correspondence:**
Vincent Fauvelle
vincent.fauvelle@mio.osupytheas.fr
Richard Sempéré
richard.sempere@mio.osupytheas.fr

Specialty section:
This article was submitted to Marine Pollution, a section of the journal Frontiers in Marine Science

Received: *14 May 2018*
Accepted: *31 July 2018*
Published: *31 August 2018*

Citation:
Fauvelle V, Castro-Jiménez J, Schmidt N, Carlez B, Panagiotopoulos C and Sempéré R (2018) One-Single Extraction Procedure for the Simultaneous Determination of a Wide Range of Polar and Nonpolar Organic Contaminants in Seawater. Front. Mar. Sci. 5:295. doi: 10.3389/fmars.2018.00295

A rapid analytical method including one-single solid-phase extraction (SPE) procedure followed by gas and liquid chromatography coupled with high resolution mass spectrometry detection (GC–MS and LC–HRMS respectively) was developed for the quantification of 40 organic compounds ($1.6 < \log K_{ow} < 9.5$) in seawater including both legacy and emerging contaminants, with a focus on the most common plastic organic additives. This new method allowed for the analyses of nine organophosphate esters (OPEs), seven phthalates (PAEs), six bisphenols (BPs), five perfluorinated compounds (PFCs), and thirteen legacy organochlorinated compounds (OCs, including polychlorobiphenyles and pesticides) with recoveries in the ranges of 57–124% for OPEs, 52–163% for PAEs, 64–118% for BPs, 63–124% for PFCs, and 40–95% for OCs. As a result of (i) strict cleanup protocols, (ii) material, and solvent selection, and (iii) the use of an ISO 6 cleanroom for sample treatment, the procedural blank levels were always lower than 5 ng L^{-1}, even for the most abundant and ubiquitous compounds like tris-(2-chloro, 1-methylethyl) phosphate (TCPP) and diethylhexyl phthalate (DEHP). The quantification limits were in the ranges of 0.03–0.75 ng L^{-1} for OPEs, 0.03–0.25 ng L^{-1} for PAEs, 0.1–5 ng L^{-1} for BPs, 0.1–8 ng L^{-1} for PFCs, and 0.02–1.1 ng L^{-1} for OCs, matching seawater analysis requirements. Dissolved water phase samples collected in Marseille Bay (NW Mediterranean Sea) were analyzed using the developed method reveling the concentration of PAEs up to 140 ng L^{-1} (DEHP) and that of OCs up to 70 ng L^{-1} (α-endosulfan). For the first time, we also provided the concentrations of OPEs (TCPP up to 450 ng L^{-1}), BPs (bisphenol S up to 123 ng L^{-1}), and PFCs (PFOS up to 5 ng L^{-1}) in this area. A sampling station close to the municipal waste water treatment plant outfall exhibited the highest concentration levels for all compounds.

Keywords: plastic additive, seawater, organic contaminants, legacy contaminants, Phtalates, bisphenol, organophosphate esters

INTRODUCTION

Over the past decades, the dramatic increase in chemical diversity, production volume, uses and sources has led to the widespread occurrence of organic contaminants in all waterbodies including marine environments and numerous living organisms (Sousa et al., 2017). Organochlorine legacy contaminants [OCs, e.g., polychlorinated biphenyls (PCBs), organochlorine pesticides

(OCPs)] together with emerging substances (e.g., flame retardants, other organic plastic additives, pharmaceuticals) are increasingly monitored in relation with stricter national and European regulations (Allan et al., 2006). Moreover, the persistence of emerging contaminants, such as perfluorinated flame retardants (PFCs), together with their ubiquitous detection and high toxicity resulting in sub-ppt EU Environmental Quality Standard (EQS) prompted growing concern (Kaserzon et al., 2012). In addition to the direct release of chemicals in the environment, several organic compounds, such as plastic additives, can be indirectly introduced in aquatic environment following leaching of marine litter such as plastic debris (Net et al., 2015b; Murphy et al., 2016; Suhrhoff and Scholz-Böttcher, 2016; Paluselli et al., 2018b). The release of organic compounds initially included in plastic materials, e.g., phthalates (PAEs), organophosphate esters (OPEs), and bisphenols (BPs) is otherwise identified among the most critical hazards associated with plastic discharge in the environment (Hermabessiere et al., 2017; Hahladakis et al., 2018).

Substantially most of the above-mentioned chemical families exhibit endocrine-disrupting properties and are thus potentially associated with both health and environmental deleterious effects whose mechanisms are largely unknown (Messerlian et al., 2017; Barrios-Estrada et al., 2018), especially for mixtures of contaminants (Kim-Tiam et al., 2016). Most of them are found in marine environmental compartments, sometimes significantly exceeding $\mu g\ L^{-1}$ level in estuarine waters (Chau et al., 2015; Zhang et al., 2018) or being close to it in coastal waters (Pojana et al., 2007; Hu et al., 2014; Paluselli et al., 2018b), whereas offshore waters generally exhibit ng L^{-1} or lower levels (Brumovský et al., 2017; Lammel et al., 2017; Paluselli et al., 2018a). The various classes of contaminants cited above may induce their toxic effect via direct contact or by biomagnifying in the marine food web from phyto- and zooplankton, which are mainly affected by the dissolved water phase fraction of the contaminants (Kim-Tiam et al., 2016).

Although a number of previous reports on a reliable trace-level detection of different families of organic contaminants in the dissolved water phase have been published (Holadová et al., 2007; Pojana et al., 2007; Kaserzon et al., 2012; Assoumani et al., 2013; Hu et al., 2014; Chau et al., 2015; Net et al., 2015a; Brumovský et al., 2017; Lammel et al., 2017; Li et al., 2017; Paluselli et al., 2018a), they focused on one class of chemicals, making analyses of several classes of organic contaminants time-consuming. Thus, reliable detection of a large set of organic contaminants from different chemical families and polarities in natural water is only scarcely reported (Chau et al., 2015). Although solid-phase extraction (SPE), commonly followed by gas and liquid chromatography (i.e., GC and LC, respectively) coupled with mass spectrometry (MS) analyses, is now accepted as a method of choice for all the contaminant families mentioned above (Pojana et al., 2007; Kaserzon et al., 2012; Hu et al., 2014; Chau et al., 2015; Net et al., 2015a; Brumovský et al., 2017; Lammel et al., 2017; Li et al., 2017; Paluselli et al., 2018a), their fractionated elution from a one-single extraction step for simultaneous GC and LC analyses has been investigated only scarcely to the best of our knowledge.

The aims of this study are (i) to propose a systematic strategy for SPE fractionated elution step able to extract simultaneously a wide range of contaminants ($1.6 < \log K_{ow} < 9.5$) from seawater dissolved fraction for subsequent LC–MS and GC–MS analysis, (ii) to validate the analytical method at environmentally relevant concentrations, and (iii) to apply the method to real samples in order to verify its performance, in line with existing requirements for seawater monitoring.

MATERIALS AND METHODS

Chemicals and Reagents

Hexane, ethyl acetate (EtOAc), dichloromethane (DCM), acetone, and toluene were purchased from Promochem (Picograde, LGC standard). MeOH was provided by Biosolve (ULC-MS grade), whereas ultrapure water (MQ) was obtained from a Millipore (resistivity > 18.2 MΩ) Milli-Q system. All standards and key physical-chemical properties are listed in **Table 1**. PAEs were obtained from Supelco (USA), BPs and native PFCs from AccuStandard (USA), and isotope labeled PFCs from Wellington Laboratories (Canada). Individual native OPE and OC standards and labeled 2,4-DDT-*d8*, 4,4-DDT-*d8*, and α-endosulfan-*d4* were purchased from Dr. Ehrenstorfer GmbH (Germany), whereas labeled standards of tri-n-butyl-*d27*-phosphate, triphenyl-d15-phosphate, tri-n-propyl-*d21*-phosphate, malathion-*d7*, α-HCH-*d6*, and γ-HCH-*d6* were obtained from C/D/N Isotopes Inc. (Canada) and tris(2-chloroisopropyl)-*d18*-phosphate, tris(1,3-dichloro-2-propyl)-*d15*-phosphate, tris(2-chloroethyl)-*d12*-phosphate, $^{13}C_{12}$-PCB-28,−118, and−180 were from Cambridge Isotope Laboratories, Inc. (USA). Monomolecular stock solutions (250–100 ng μL^{-1}) were prepared in toluene except for PFCs and BPs (acetone). Working mix solutions were prepared in isooctane or acetone by dilution to 10 ng μL^{-1}.

Solid Phase Extraction Procedure

The SPE method developed here is based on a previous procedure described for PAEs by Paluselli et al. (2018a) and optimized with a fractionated elution step in order to recover different contaminant classes (OPEs, PAEs, BPs, PFCs, and OCs). A 1 L subsurface seawater sample was collected in Marseille Bay with a stainless-steel beaker, filtered through a precombusted (450°C, 6 h) 0.7 µm glass fiber filter the same day, and stored at −20°C if extractions were not performed the same day. The whole SPE protocol was conducted on a manifold under vacuum (Supelco Visiprep®). SPE cartridges were prepared in the laboratory [Waters Oasis hydrophilic-lipophilic balance (HLB)® bulk sorbent, 30 µm, 250 mg, glass cartridge, polytetrafluoroethylene (PTFE) frits] and conditioned with 3 cycles of acetone (5 mL), EtOAc (5 mL), DCM (5 mL), and finally 10 mL of MQ. The freshly collected seawater samples were spiked with the corresponding surrogate mix (**Table 1**, 100 ng $sample^{-1}$) before the sample loading on the cartridges (10 mL min^{-1}, ∼2 h). A subsequent washing step (5 mL MQ) allowed removing salts from the cartridges. The cartridges were then dried under vacuum for ∼2 h in order to remove any residual water that may affect subsequent GC–MS analysis. Special attention was

TABLE 1 | Identification and physico-chemical properties of target substances.

Name	Full name	CAS	Description	Monoisotopic mass (g mol^{-1})	log K_{ow}
ORGANOPHOSPHATE ESTERS (OPEs)					
TPP	Tripropyl phosphate	513-08-6	A	224.1177	1.9
TiBP	Tri-iso-buthyl phosphate	126-71-6	A	266.1647	3.5
TnBP	tri-n-butyl phosphate	126-73-8	A	266.1647	4
TCEP	tris-(2-chloroethyl) phosphate	115-96-8	A	283.9539	1.8
TCPPs	tris-(2-chloro, 1-methylethyl) phosphate	13674-84-5	A	326.0008	2.6
TDCP	tris-(2-chloro-, 1-chloromethylethyl) phosphate	13674-87-8	A	427.8839	3.7
TPhP	triphenyl phosphate	115-86-6	A	326.0708	4.6
EHDPP	2- ethylhexyl-diphenyl phosphate	1241-94-7	A	362.1647	5.7
TEHP	tris(2-ethylhexyl) phosphate	78-42-2	A	434.3525	9.5
TBP-*d27*	Tri-n-butyl phosphate-*d27*	61196-26-7	S	293.3341	
TPhP-*d15*	Triphenyl phosphate-*d15*	1173020-30-8	S	341.1649	
TCPP-*d18*	Tris (2-chloroisopropyl) phosphate-*d18*	-	S	344.1138	
TDCP-*d15*	Tris (1,3-dichloro-2-propyl) phosphate-*d15*	1447569-77-8	S	442.9781	
TPrP-*d21*	Tri-n-propyl phosphate-*d21*	1219794-92-9	IS	245.2495	
TCEP-*d12*	Tris (2-chloroethyl) phosphate-*d12*	1276500-47-0	IS	296.0292	
MAL-*d7*	malathion-*d7*	352438-94-9	IS	337.0800	
PHTHALATES (PAEs)					
DMP	dimethyl phthalate	131-11-3	A	194.0579	1.6
DEP	diethyl phthalate	84-66-2	A	222.0892	2.5
DBP	di-n-butyl phthalte	84-74-2	A	278.1518	4.5
DiBP	diisobutyl phthalate	84-69-5	A	278.1518	4.1
DEHP	diethylhexyl phthalate	117-81-7	A	390.277	7.6
BBP	benzylbutyl phthalate	85-68-7	A	312.1362	4.7
DnOP	di-n-octyl phthalate	117-84-0	A	390.277	8.1
DEHP-*d4*	diethylhexyl phthalate-*d4*	93951-87-2	IS	394.3021	
DEP-*d4*	diethyl phthalate-*d4*	93952-12-6	IS	226.1143	
DnBP-*d4*	di-n-butyl phthalte-*d4*	93952-11-5	S	282.1769	
BISPHENOLS (BPs)					
BPA	bisphenol A	80-05-7	A	228.115	3.3
BPAF	bisphenol AF	14878-61-1	A	336.0585	4.5
BPAP	bisphenol AP	1571-75-1	A	290.1307	4.4
BPF	bisphenol F	620-92-8	A	200.0837	2.9
BPP	bisphenol P	2167-51-3	A	346.1933	6.1
BPS	bisphenol S	80-09-1	A	250.03	1.9
BPZ	bisphenol Z	843-55-0	A	268.1463	5.4
4nOP-*d17*	4-n-octylphenol-*d17*	1219794-55-4	S	223.2738	
BPA-*d16*	bisphenol A-*d16*	96210-87-6	IS	244.2154	
PERFLUORINATED COMPOUNDS (PFCs)					
PFHA	perfluoro hexanoic acid	307-24-4	A	313.9801	3.5
PFHS	perfluorohexane sulfonic acid	3871-99-6	A	399.9439	3.2
PFOA	perfluorooctanoic acid	335-67-1	A	413.9737	4.8
PFOS	perfluorooctane sulfonic acid	1763-23-1	A	499.9375	4.5
PFOSF	perfluoro octane sulfonyl fluoride	307-35-7	A	501.9332	7.8
PFHA-*13C5*	perfluoro hexanoic acid-$^{13}C_5$	–	IS	318.9969	
PFHS-*13C3*	perfluoro hexanesulfonate-$^{13}C_3$	–	IS	402.9539	
PFOS-*13C8*	perfluoro octanesulfonate-$^{13}C_8$	–	IS	507.9643	
ORGANOCHLORINATED (OCs)					
PCB-28	polychlorobyphenyl-28	7012-37-5	A	255.9613	5.6
PCB-52	polychlorobyphenyl-52	35693-99-3	A	289.9224	6.1

(Continued)

TABLE 1 | Continued

Name	Full name	CAS	Description	Monoisotopic mass (g mol^{-1})	log K_{ow}
PCB-101	polychlorobyphenyl-101	37680-73-2	A	323.8834	6.5
PCB-118	polychlorobyphenyl-118	31508-00-6	A	323.8834	7.1
PCB-138	polychlorobyphenyl-138	35065-28-2	A	357.8444	7.2
PCB-153	polychlorobyphenyl-153	35065-27-1	A	357.8444	7.2
PCB-180	polychlorobyphenyl-180	35065-29-3	A	391.8054	7.9
4,4-DDT	4,4-dichlorodiphenyltrichloroethane	50-29-3	A	351.9147	6.9
HCB	hexachlorobenzene	118-74-1	A	281.8131	5.7
α -HCH	alpha-hexachlorocyclohexane	319-84-6	A	287.8601	3.7
β-HCH	beta-hexachlorocyclohexane	319-85-7	A	287.8601	3.7
γ-HCH	gamma-hexachlorocyclohexane	58-89-9	A	287.8601	3.7
α-Endosulfan	alpha-endosulfan	959-98-8	A	403.8169	
α -HCH-*d6*	alpha-hexachlorocyclohexane-*d6*	–	S	293.8977	
2,4-DDT-*d8*	2,4-dichlorodiphenyltrichloroethan-*d8*	–	S	359.9649	
PCB-180 -*13C12*	polychlorobyphenyl-180-$^{13}C_{12}$	–	S	403.8457	
γ-HCH-*d6*	gamma-hexachlorohexane-*d6*	60556-82-3	IS	293.8977	
PCB-28-*13C12*	polychlorobyphenyl-28-$^{13}C_{12}$	–	IS	268.0016	
PCB-118-*13C12*	polychlorobyphenyl-118-$^{13}C_{12}$	–	IS	335.9237	
α-Endosulfan-d4	alpha-endosulfan-d4	203645-57-2	IS	407.8420	
4,4-DDT-d8	4,4-dichlorodiphenyltrichloroethane-d8	93952-18-2	IS	359.9649	

A, S, and IS correspond to analyte, surrogate, and internal standard, respectively.

paid to ensure complete dryness since poly(divinylbenzene-co-*N*-vinylpyrrolidone) (Oasis HLB) is more wettable than conventional poly(styrene-co-divinylbenzene) SPE sorbents. Four eluting fractions covering a wide range of solvent polarity were studied separately by implementing a multi-elution step following the polarity gradient, in order to give a general scheme for potential further contaminant inclusion: 5 mL hexane (F1), 5 mL hexane/DCM 50:50 (v/v) (F2), 5 mL EtOAc (F3), and then 5 mL MeOH (F4). Depending on the chemical family one fraction might not be needed, but we chose to keep these four fractions that include both polar and nonpolar, as well as protic and non-protic solvents. The four fractions were collected separately in pre-combusted 22 mL glass flasks, evaporated to ∼1 mL under gentle N_2 flux, transferred into 2 mL pre-combusted conical glass vials, spiked with an appropriate internal standard (IS) mixture (**Table 1**, 100 ng sample^{-1}), and evaporated again to a final volume of approximately 50 μL for the GC–MS analysis or 1000 μL for the LC–high-resolution mass spectrometry (HRMS) analysis. The concentration factors were 20,000 for the GC-MS analysis and 1,000 for the LC–HRMS analysis. Considering the injection volumes on GC (2 μL) and LC (10 μL), 40 and 10 mL seawater volume equivalents were injected on each instrument. The whole procedure was conducted in an International Standards Organization (ISO) 6 cleanroom, and strict quality assurance and quality control (QA/QC) procedures were implemented (see the QA/QC section).

GC–MS Analysis

According to the literature, PAE, OPE, and OC analyses were conducted with Agilent 7820A Series GC coupled with Agilent 5977E MS, operating in selected ion monitoring and electron impact (70 eV) modes. The separation was achieved in a 30 m × 0.25 mm internal diameter × 0.25 μm HP-5MS capillary column (Agilent J&W). All target contaminants were quantified by the IS procedure. **Supplementary Table 1** shows selected ions for detection and quantification for each compound. The injection volume was 2 μL, and the helium carrier gas flow was 1 mL min^{-1}. The temperatures of the MS transfer line, ion source, and quadrupole were set at 300, 230, and 150°C, respectively. For OPEs and PAEs, the following conditions were applied: the injector temperature was 270°C (splitless), and the oven was programmed from 90 to 132°C at 3°C min^{-1}, to 166°C at 10°C min^{-1}, to 175 at 1°C min^{-1} (holding time: 2 min), to 232°C at 2°C min^{-1}, and then to 300°C at 25°C min^{-1} (holding time: 5 min). For OCs, the injector temperature was 250°C (splitless), and the oven was programmed from 90 to 140°C at 25°C min^{-1} (holding time: 10 min), to 158°C at 1°C min^{-1}, to 188 at 20°C min^{-1}, to 208°C at 1°C min^{-1}, and then to 300°C at 25°C min^{-1} (holding time: 5 min).

LC–HRMS Analysis

Simultaneous quantification of BPs and PFCs was achieved by analyzing 10 μL with LC–electrospray ionization quadrupole

time of flight mass spectrometry (LC-ESI-QTOF, Agilent 1290 Infinity LC system coupled with Agilent 6530 Accurate-Mass Q-TOF, Agilent Technologies, Les Ulis, France). LC was chosen for BPs and PFCs according to the literature. Syringe was washed externally with 1 mL MeOH for 20 s before injection to avoid contamination of the injection port or the following samples. Separation was achieved on an Agilent Zorbax Eclipse XDB reversed phase column (50 mm × 2.1 mm, 1.8 µm), with a temperature of 30°C. Elution was performed with MQ (A) and MeOH (B) under gradient conditions: 0 min 95:5 A/B, 1 min 95:5 A/B, 10 min 0:100 A/B, 15 min 0:100 A/B, 15.1 min 95:5 A/B, and 20 min 95:5 A/B. The ESI interface was operated in the negative mode (3.5 kV capillary voltage), and MS TOF mass acquisition was performed in the range of 50–600 m/z at a rate of 1 spectrum s^{-1}. The ESI parameters were set as follows: 300°C gas temperature, 11 L min^{-1} drying gas, 40 psig nebulizer, 350°C sheath gas temperature, and 11 L min^{-1} sheath gas flow. The TOF parameters were: 1,500 V nozzle voltage, 175 V fragmentor voltage, 65 V skimmer voltage, and 750 V octopole voltage. Ion chromatogram extraction was performed with 10 ppm mass tolerance, based on the exact monoisotopic mass (**Table 1**) and retention time (**Supplementary Table 2**). A typical chromatogram for selected compounds is available in **Supplementary Figure 1**.

Application to Seawater Samples

The method was applied to real seawater samples collected at l'Estaque, Frioul, and Cortiou sites in May 2017 in the Marseille city coastal area (**Figure 1**) from R/V Antedon II, and followed the protocol described in the "SPE procedure" section. L'Estaque is under the influence of the commercial harbor, Frioul is considered the least impacted site, whereas the Cortiou station is around 150 m from the municipal wastewater treatment plant outfall (WWTP, 2.1 10^6 population equivalent capacity, 1 10^6 effective population).

QA/QC

Most of the target chemicals may be found ubiquitously in technical laboratory items at each stage of sample processing (sampling, filtration, SPE, analysis), in particular the emerging contaminants. As a result, several systematic precautions were taken throughout the sample preparation processes: a pre-combusted (i.e., 450°C for 6 h) aluminum foil was used to prevent direct contact between seawater and plastic items (e.g., bottle caps); stainless steel, pre-combusted glassware and PTFE were used instead of polyethylene and polypropylene materials; all samples were processed in an ISO class 6 cleanroom (22°C, +15 Pa cleanroom pressure, 50 vol h^{-1} brewing rate); all lab hood was cleaned with MeOH; all materials were covered with a pre-combusted aluminum foil; and the cartridges were covered during drying. PTFE might be a source of PFCs. Therefore, its use was limited to SPE cartridge frits and SPE sample loading lines, and each PFTE item was cleaned drastically with MeOH in order to lower PFC contamination to acceptable levels. Corresponding procedural blanks were performed.

Other precautions were taken for the analytical part: a ultra-high pressure liquid chromatography grade solvent was chosen, the LC syringe was washed externally with MeOH for 20 s before each injection, and the column was flushed with both MeOH and MQ included in the LC gradient for 5 min. The GC injection syringe was washed 10 times with DCM and isooctane before and after each individual injection in order to minimize cross-contamination at the GC injection port. The QA/QC were based on (i) procedural blank quantification for each SPE batch, (ii) instrumental blanks every five samples, (iii) surrogates' recovery evaluation for each individual sample, (iv) the use of appropriate IS quantification, and (v) initial method validation for recovery and the limit of quantification for a target chemical in the matrix of interest. The average procedural blanks ($n = 3$) ranged from < the limits of detection to 3.4 ng L^{-1} (average: 0.35 ng L^{-1}), exhibiting generally very low amounts of target analytes (**Supplementary Table 3**). No particular instrumental blanks or cross-contamination was

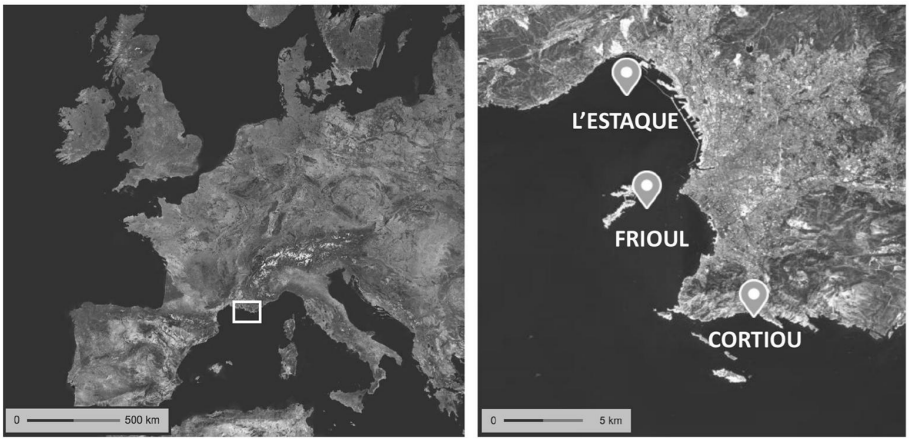

FIGURE 1 | Sampling locations in Marseille Bay. Map from the French National Institute of Geographic and Forestry Information.

TABLE 2 | Distribution of 40 target analytes in the four consecutive elution fractions.

	F_1: 5 mL Hexane	F_2: 5 mL Hexane/DCM 50:50 (v/v)	F_3: 5 mL EtOAc	F_4: 5 mL MeOH
ORGANOPHOSPHATE ESTERS (OPEs)				
TPP	10 ± 18	90 ± 18	0	0
TiBP	45 ± 40	55 ± 40	0	0
TnBP	19 ± 22	81 ± 22	0	0
TCEP	0	100	0	0
TCPPs	33 ± 58	67 ± 58	0	0
TDCP	0	100	0	0
TPhP	0	100	0	0
EHDPP	12 ± 17	88 ± 17	0	0
TEHP	47 ± 46	53 ± 46	0	0
PHTHALATES (PAEs)				
DMP	16 ± 27	84 ± 27	0	0
DEP	48 ± 35	52 ± 35	0	0
DBP	64 ± 35	35 ± 34	1 ± 1.1	0
DiBP	73 ± 26	26 ± 26	1 ± 0.8	0
DEHP	80 ± 19	20 ± 18	1 ± 0.5	0
BBP	10 ± 17	90 ± 17	0	0
DnOP	77 ± 21	22 ± 22	1 ± 0.8	0
BISPHENOLS (BPs)				
BPA	0	0	100	0
BPAF	0	0	34 ± 25	66 ± 25
BPAP	0	0	59 ± 19	41 ± 19
BPF	0	0	0	100
BPP	90 ± 17	10 ± 17	0	0
BPS	0	0	10 ± 10	90 ± 10
BPZ	0	0	0	100
PERFLUORINATED COMPOUNDS (PFCs)				
PFHA	0	0	9 ± 4	91 ± 4
PFHS	0	0	1 ± 1	99 ± 1
PFOA	0	0	0	100
PFOS	0	0	0	100
PFOSF	0	0	0	100
ORGANOCHLORINATED				
PCB-28	83 ± 11	12 ± 24	5 ± 11	0
PCB-52	91 ± 36	9 ± 27	0	0
PCB-101	92 ± 26	8 ± 35	0	0
PCB-118	93 ± 9	7 ± 22	0	0
PCB-138	89 ± 23	11 ± 12	0	0
PCB-153	92 ± 24	8 ± 26	0	0
PCB-180	91 ± 22	9 ± 30	0	0
4,4-DDT	77 ± 35	23 ± 25	0	0
HCB	100	0	0	0
α-HCH	85 ± 12	15 ± 26	0	0
β + γ-HCH	41 ± 28	58 ± 37	0	0
α-Endosulfan	100	0	0	0

The results are expressed as percent area of the sum of the areas found in the four fractions. The relative standard deviation is mentioned after each value (n = 3). Water Oasis HLB cartridges 250 mg, 1 L seawater sample.

observed during the GC–MS analyses. However, during the LC–HRMS analysis, we experienced instrumental blank issues, which were solved by a copious external syringe-washing step (MeOH flushing for 20 s) after each LC sampling. The nine isotope labeled surrogates (**Table 1**) added in the seawater samples before SPE showed acceptable recoveries in the range of 40–108% (**Table 3**). The LC matrix effects, i.e., ion suppression in the ESI source (Taylor, 2005), were always lower than 40% signal loss. These limited matrix effects were obtained by applying a lower SPE concentration factor than the one applied for the GC–MS analyses (1,000 vs. 20,000 see the "SPE procedure" section).

RESULTS AND DISCUSSION

SPE Optimization

The selection of an SPE sorbent that includes both polar and nonpolar moieties was the first requirement for retaining the whole range of target chemicals (1.6 < log Kow < 9.5). Among them, Oasis HLB is identified as the best candidate for extracting a wide range of contaminants (Kaserzon et al., 2012; Fauvelle et al., 2015; Net et al., 2015a). An important SPE step was the selection of an appropriate elution fraction. As our analytes cover a large polarity range, a preliminary fractionation experiment was

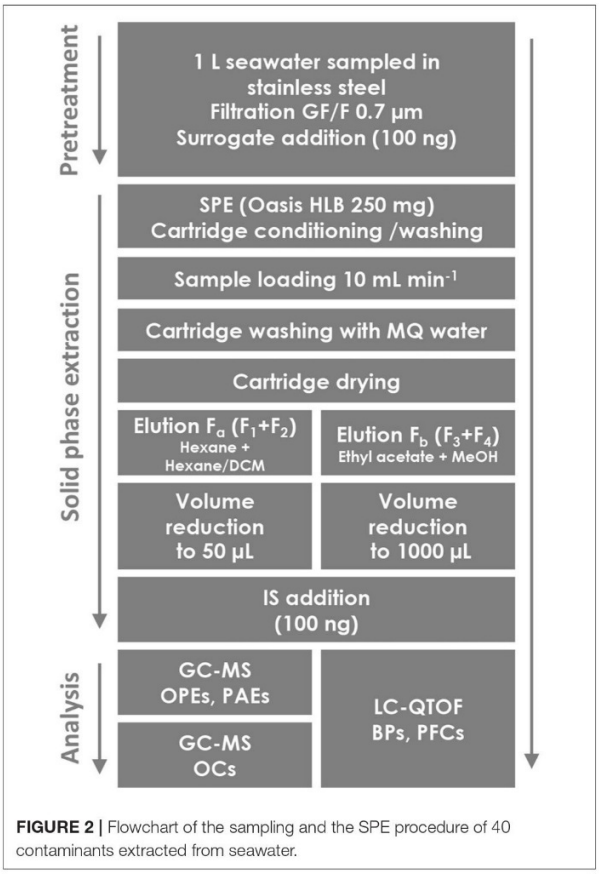

FIGURE 2 | Flowchart of the sampling and the SPE procedure of 40 contaminants extracted from seawater.

performed to better understand the HLB-to-solvent partitioning for each contaminant using a solvent polarity gradient: first nonpolar fraction (hexane), second slightly more polar fraction (hexane/DCM), third moderately polar fraction (EtOAc), and last polar fraction (MeOH). **Table 2** shows the distribution of all 40 target analytes in the four fractions defined in the "SPE procedure" section. OPEs were only found in F_1 and F_2 and not detected in F_3 and F_4. PAEs were mainly recovered in F_1 and F_2, whereas <1% was found in F_3, and they were not detected in F_4. OCs were also recovered predominantly in F_1 and F_2, while F_3 contained <5% of the total amount, and F_4 did not show detectable amounts. BPs were only found both in F_3 and F_4, except for BPP, which was detected only in F_1 and F_2. PFCs were otherwise only detected in F_3 and F_4. In summary, PAEs, OPEs, and OCs were recovered in the first two fractions, whereas BPs and PFCs were predominantly found in fractions F3 and F4. A limited number of PAEs and OCs were found in F3, with relative abundances always lower than 5%. One major exception for BPs was BPP, found mainly in F1, in line with its higher log K_{ow} value (i.e., 6.1, see **Table 1**).

Therefore, the final SPE protocol consisted in collecting F_1 with F_2 (called F_a thereafter) for the GC–MS analysis of OPEs, PAEs, and OCs and F_3 with F_4 (called F_b thereafter) for the LC–HRMS analysis of BPs and PFCs. As BPP was recovered in F_a, but analyzed by LC–HRMS, it was removed from the target list. A schematic view of the final protocol is available in **Figure 2**.

Method Validation

The final method was then validated at two environmentally relevant concentrations: 20 ng L^{-1} and 150 ng L^{-1}. Seawater samples (1 L) collected in the study area were spiked at the corresponding target concentrations with a mixture of native contaminants prepared in acetone (five replicates for each level, $n = 5$). Recoveries, the limits of quantification (LQs) are reported in **Table 3**. The LQs in pg injected were determined considering a signal/noise (S/N) ratio of >10 in the lowest calibration level, and the LQs in ng L^{-1} were derived from these values taking into account the corresponding SPE preconcentration factor. An acceptable sensitivity was reached working under the experimental conditions described above, with the LQs for the target contaminants ranging from 1 pg to 100 pg depending on the compound and the instrumental technique employed. The LQs in ng L^{-1} varied from 0.03 to 8 in seawater, with only five compounds having values ≥2 ng L^{-1}. The method recoveries for the native target contaminants (abbreviations are detailed in **Table 1**) and surrogates ranged from 57 ± 9 (TEHP) to 131 ± 16 (TCEP) for OPEs, from 52 ± 3 (DnOP) to 163 ± 131 (DEHP) for PAEs, from 88 ± 10 (BPAP) to 118 ± 26 (BPAF) for BPs, from 63 ± 9 (PFOSF) to 124 ± 5 (PFOA) for PFCs, and 48 ± 5 (PCB-180) to 133 ± 7 (α-endosulfan) for OCs. These values are in agreement with existing studies focusing on one chemical family: Hu et al. (2014) had recoveries between 67 and 118% for OPEs, Paluselli et al. (2018a) recovered PAEs in the range 95–110%, Pojana et al. (2007) found BPs in the range 50–98%, Kaserzon et al. (2012) determined recoveries between 36 and 129% for PFCs, and Lammel et al. (2017) found OCs in the range 75–103%. Similar recoveries were found for most compounds

TABLE 3 | Recoveries of the target contaminants ($n = 5$) with their associated standard deviation, LQs expressed as absolute amounts (pg) and ng L^{-1} in seawater.

Compound	Method recoveries in spiked seawater		LQ	
	20 ng L^{-1}	150 ng L^{-1}	(pg)	(ng L^{-1})
ORGANOPHOSPHATE ESTERS (OPEs)				
TPP	95 ± 9	108 ± 4	5	0.13
TiBP	119 ± 10	109 ± 5	1	0.03
TnBP	113 ± 16	107 ± 6	2	0.05
TCEP	124 ± 16	131 ± 5	10	0.19
TCPPs	122 ± 58	118 ± 4	10	0.25
TDCP	114 ± 9	120 ± 4	10	0.25
TPhP	111 ± 9	111 ± 4	5	0.10
EHDPP	74 ± 9	61 ± 6	5	0.13
TEHP	57 ± 9	61 ± 4	10	0.20
TBP-*d27*	88 ± 5	85 ± 4	2	0.05
TPhP-*d15*	91 ± 7	88 ± 4	5	0.13
TCPP-*d18*	109 ± 7	105 ± 10	30	0.75
TDCP-*d15*	111 ± 4	111 ± 15	11	0.28
PHTHALATES (PAEs)				
DMP	85 ± 5	80 ± 4	5	0.07
DEP	81 ± 8	82 ± 3	2	0.05
DiBP	137 ± 76	74 ± 15	1	0.03
DnBP	92 ± 7	82 ± 5	1	0.03
BBzP	82 ± 2	83 ± 4	5	0.09
DEHP	163 ± 131	73 ± 66	2	0.05
DnOP	57 ± 6	52 ± 3	10	0.25
DnBP-*d4*	92 ± 5	89 ± 1	1	0.03
BISPHENOLS (BPs)				
BPA	90 ± 22	88 ± 15	10	1.0
BPAF	112 ± 30	118 ± 26	1	0.1
BPAP	88 ± 13	92 ± 20	20	2.0
BPF	92 ± 19	90 ± 27	10	1.0
BPS	115 ± 9	112 ± 20	1	0.1
BPZ	96 ± 22	87 ± 17	50	5.0
4nOP-*d17*	64 ± 17	79 ± 4	30	3.0
PERFLUORINATED COMPOUNDS (PFCs)				
PFHA	69 ± 6	82 ± 2	80	8.0
PFHS	89 ± 10	73 ± 14	1	0.1
PFOA	113 ± 11	124 ± 5	20	2.0
PFOS	70 ± 9	85 ± 2	1	0.1
PFOSF	63 ± 9	76 ± 13	10	1.0
ORGANOCHLORINATED (OCs)				
PCB-28	70 ± 10	69 ± 9	10	0.18
PCB-52	75 ± 12	71 ± 3	12	0.31
PCB-101	63 ± 17	62 ± 4	15	0.38
PCB-118	63 ± 17	59 ± 4	10	0.25
PCB-138	60 ± 15	56 ± 4	20	0.42
PCB-153	70 ± 17	57 ± 3	20	0.46
PCB-180	53 ± 12	49 ± 3	20	0.50
HCB	48 ± 5	58 ± 3	12	0.29
α-HCH	76 ± 4	75 ± 1	20	0.49
β + γ-HCH	80 ± 3	81 ± 2	15	0.32
4,4-DDT	59 ± 15	55 ± 4	30	0.68
α-Endosulfan	110 ± 15	133 ± 7	45	1.07
α-HCH-*d6*	88 ± 7	95 ± 2	15	0.38
2,4-DDT-*d8*	69 ± 5	40 ± 2	1	0.02
^{13}C-PCB-180	65 ± 9	56 ± 1	20	0.45

at the two-environmental concentration tested. Therefore, most compounds showed acceptable recoveries. However, high relative standard deviations were found for DEHP and DiBP at the lower spiking level (i.e., 20 ng L^{-1}). The high recovery end observed could be due to a specific contamination of the spiked samples even if the blanks run in parallel did not show any significant contamination. Indeed, we measured a higher concentration of DEHP and DiBP in one single replicate, which explained the high relative standard deviations and recoveries for both compounds. Although many precautions were taken for minimizing contamination, some interference could still be attributed, for example, to random contamination of the SPE cartridges by residual plastic fibers present in the air. Therefore, we recommend analyzing duplicates of real samples to avoid false positive results, and thus we applied this strategy as described in the following section "Application to seawater samples." The recovery rates were not dependent on the compound polarity (e.g., nonpolar OCs showed a recovery range comparable to the one of more polar BPs), indicating that Oasis HLB is well adapted for our purpose.

Application to Seawater Samples

The method was applied to freshly collected marine samples from Marseille Bay at three sampling stations (**Figure 1**). The range of concentrations found at the three sites was between <LQ up to several hundreds of ng L^{-1}. Otherwise, concentrations close to LQ have been quantified, and accuracy was not affected. The duplicate samples were analyzed at each location (except for OCs, which were analyzed on a single replicate), and acceptable reproducibility was obtained at all sites, except for DEHP at the Cortiou station (79 and 132 ng L^{-1}). As DEHP LQ was substantially exceeded, the maximum analytical permissible error of 60% close to LQ (Lissalde et al., 2011) cannot explain fully the difference between both replicates. Therefore, this difference could also be attributed to laboratory contamination affecting one single sample from the duplicate. Among the 40 contaminants analyzed, 25 were found at least once (**Figure 3**). The three families of plastic organic additives exhibited the highest concentrations up to 462, 132, and 123 ng L^{-1} for the TCPP, DEHP, and BPS, respectively. Among the three sites, the highest concentrations of the targeted contaminants were found at Cortiou (150 m from Marseille WWTP outfall). The measured concentrations were generally in the range of those reported in previous studies in various marine environments (Pojana et al., 2007; Kaserzon et al., 2012; Hu et al., 2014; Chau et al., 2015; Net et al., 2015a; Brumovský et al., 2017; Lammel et al., 2017; Li et al., 2017; Paluselli et al., 2018a).

OPEs and PAEs represented from 78 to 85% of relative abundance of the five contaminant classes, whatever the site. OPEs were more abundant near the WWTP (~60% at the Cortiou site), whereas PAEs were the most abundant at the most remote site (68% at Frioul). TCPP was always the most abundant OPE, with a relative abundance among OPEs between 77 and 84%. The sum of DEHP and DiBP was always higher than 75% of the total PAE concentration. BPs represented from 1% (Frioul) to 14% (Cortiou) of the total target contaminant concentration. BPS was the most abundant BP near the WWTP at Cortiou (~90%), whereas BPA was the predominant BP in the other two sites (>80%). BPS was the most concentrated among all BPs (up to 123 ng L^{-1}, and 88% of all BPs), ahead of BPA, which points out the need for monitoring several compounds from each chemical family, for which less data is available. PFCs were quantified at very low levels in all samples (<1% of the total target contaminant concentration), with individual compound

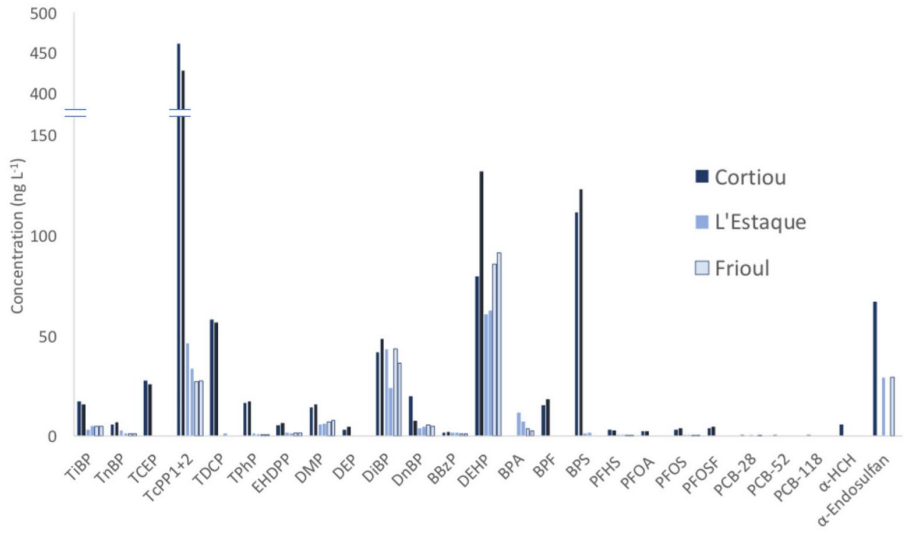

FIGURE 3 | Concentrations of contaminants found at the three sampling sites (Cortiou, L'Estaque, and Frioul) in the Bay of Marseille in May 2017. The duplicate samples are shown as two consecutive bars. The y-axis breaks between 150 and 400 ng L^{-1}. Not detected compounds are not shown. OCs were analyzed on one replicate at each site. The contaminant abbreviations are given in **Table 1**. Compounds are grouped by chemical family.

concentrations always lower than 5 ng L^{-1}, and only two OCs were found at concentrations clearly above the LQs (7–16% of the total target contaminant concentration depending on the site): α-endosulfan (30–70 ng L^{-1}, representing 90–100% of the 13 OCs concentration) and α -HCH (∼6 ng L^{-1}, representing <8% of OCs at all sites). PCBs-28,−52, and,−118 were found at very low concentration levels (0.4–0.6 ng L^{-1}) (**Supplementary Table 4**). The concentrations of the rest of OCs were below the LQs, most probably owing to the low amounts entering the bay and their preferential partitioning in the water particle phase (not considered in this study).

The EQSs from the European Union Water Framework Directive (WFD) in seawater are only available for DEHP (annual average: 1300 ng L^{-1}), PFOS/PFOA (annual average: 0.13 ng L^{-1}), and several OCs (annual average: from 4 to 300 ng L−1). Although an appropriate risk assessment cannot be conducted with the present data due to the limited number of samples, our results pointed PFOS as the most potentially harmful substance from our target list, exceeding the current EQS in seawater.

CONCLUSIONS

A reliable analytical method for a rapid measurement of five classes (OPEs, PAEs, BPs, PFCs, and OCs) of organic contaminants in natural seawater at trace levels was developed and validated. The method proposed in this study allowed the quantification of 40 organic contaminants presenting a wide range of physicochemical properties and sources in the environment, including both legacy and emerging contaminants. The implementation of a single SPE protocol using a sorbent, including polar and nonpolar moieties, allowed reaching acceptable performances both in terms of analyte recoveries and LQs. We proposed a systematic strategy for catching most of the organic contaminants, using the polarity gradient during the SPE elution step. Only ionizable organic substances could be missed because of the intrinsic properties of the selected sorbent, which could however been overcome by the use of mixed-mode ion exchange sorbents. This study focused mainly on plastic organic additives, which were found to be the most abundant contaminants in Marseille Bay, far ahead of conventional PCBs or OCPs. Therefore, our method represents a useful tool for screening and quantification of widely diffused plastic organic additives and indirect assessment of the impact of plastic waste on the dissolved seawater fraction, generally considered bioavailable.

AUTHORS CONTRIBUTIONS

VF, JC-J, and RS experimental design. NS and BC sampling. NS, BC, VF, and JC-J performed the experiments and analyses. VF, JC-J, RS, NS, and CP wrote the paper.

FUNDINGS

This study was financially supported by the JPI Oceans PLASTOX and Agence de l'Eau-CAREMED and Blue-POLUT projects. This research was also partially funded by the Labex OT-Med (no ANR-11-LABX-0061)—MEDPOP, funded by the French Government Investissements d'Avenir (ANR) through the AMIDEX project (no ANR-11-IDEX-0001-02). The project leading to this publication has also received funding from European FEDER Fund under project 1166-39417.

ACKNOWLEDGMENTS

The authors are grateful to Dorian Guillemain, Nagib Bhairy, Christian Grenz, Michel Lafont, and Deny Malengros from SAM-M I O platform and the crew and captain of the R/V Antedon II for operation at sea.

SUPPLEMENTARY MATERIAL

The Supplementary Material for this article can be found online at: https://www.frontiersin.org/articles/10.3389/fmars.2018.00295/full#supplementary-material

REFERENCES

Allan, I., Vrana, B., Greenwood, R., Mills, G., Knutsson, J., Holmberg, A., et al. (2006). Strategic monitoring for the European Water Framework Directive. *TrAC Trends Anal. Chem.* 25, 704–715. doi: 10.1016/j.trac.2006.05.009

Assoumani, A., Lissalde, S., Margoum, C., Mazzella, N., and Coquery, M. (2013). *In situ* application of stir bar sorptive extraction as a passive sampling technique for the monitoring of agricultural pesticides in surface waters. *Sci. Total Environ.* 463–464, 829–835. doi: 10.1016/j.scitotenv.2013.06.025

Barrios-Estrada, C., de Jesús Rostro-Alanis, M., Muñoz-Gutiérrez, B. D., Iqbal, H. M. N., Kannan, S., and Parra-Saldívar, R. (2018). Emergent contaminants: endocrine disruptors and their laccase-assisted degradation – a review. *Sci. Total Environ.* 612, 1516–1531. doi: 10.1016/j.scitotenv.2017.09.013

Brumovský, M., Bečanová, J., Kohoutek, J., Borghini, M., and Nizzetto, L. (2017). Contaminants of emerging concern in the open sea waters of the Western Mediterranean. *Environ. Pollut.* 229, 976–983. doi: 10.1016/j.envpol.2017.07.082

Chau, H. T. C., Kadokami, K., Duong, H. T., Kong, L., Nguyen, T. T., Nguyen, T. Q., et al. (2015). Occurrence of 1153 organic micropollutants in the aquatic environment of Vietnam. *Environ. Sci. Pollut. Res.* 25, 7147–7156. doi: 10.1007/s11356-015-5060-z

Fauvelle, V., Mazzella, N., Morin, S., Moreira, S., Delest, B., and Budzinski, H. (2015). Hydrophilic interaction liquid chromatography coupled with tandem mass spectrometry for acidic herbicides and metabolites analysis in fresh water. *Environ. Sci. Pollut. Res.* 22, 3988−3996. doi: 10.1007/s11356-014-2876-x

Hahladakis, J. N., Velis, C. A., Weber, R., Iacovidou, E., and Purnell, P. (2018). An overview of chemical additives present in plastics: migration, release, fate and environmental impact during their use, disposal and recycling. *J. Hazard. Mater.* 344, 179–199. doi: 10.1016/j.jhazmat.2017.10.014

Hermabessiere, L., Dehaut, A., Paul-Pont, I., Lacroix, C., Jezequel, R., Soudant, P., et al. (2017). Occurrence and effects of plastic additives on marine environments and organisms: a review. *Chemosphere* 182, 781–793. doi: 10.1016/j.chemosphere.2017.05.096

Holadová, K., Prokupková, G., Hajslová, J., and Poustka, J. (2007). Headspace solid-phase microextraction of phthalic acid esters from vegetable oil employing solvent based matrix modification. *Anal. Chim. Acta* 582, 24–33. doi: 10.1016/j.aca.2006.09.005

Hu, M., Li, J., Zhang, B., Cui, Q., Wei, S., and Yu, H. (2014). Regional distribution of halogenated organophosphate flame retardants in seawater

samples from three coastal cities in China. *Mar. Pollut. Bull.* 86, 569–574. doi: 10.1016/j.marpolbul.2014.06.009

Kaserzon, S. L., Kennedy, K., Hawker, D. W., Thompson, J., Carter, S., Roach, A. C., et al. (2012). Development and calibration of a passive sampler for perfluorinated alkyl carboxylates and sulfonates in water. *Environ. Sci. Technol.* 46, 4985–4993. doi: 10.1021/es300593a

Kim-Tiam, S., Fauvelle, V., Morin, S., and Mazzella, N. (2016). Improving toxicity assessment of pesticide mixtures: the use of polar passive sampling devices extracts in microalgae toxicity tests. *Front. Microbiol.* 7:1388. doi: 10.3389/fmicb.2016.01388

Lammel, G., Spitzy, A., Audy, O., Beckmann, S., Codling, G. P., Kretzschmann, L., et al. (2017). Organochlorine pesticides and polychlorinated biphenyls along an east-to-west gradient in subtropical North Atlantic surface water. *Environ. Sci. Pollut. Res.* 24, 11045–11052. doi: 10.1007/s11356-016-7429-z

Li, J., Xie, Z., Mi, W., Lai, S., Tian, C., Emeis, K. C., et al. (2017). *Organophosphate esters* in air, snow, and seawater in the North Atlantic and the Arctic. *Environ. Sci. Technol.* 51, 6887–6896. doi: 10.1021/acs.est.7b01289

Lissalde, S., Mazzella, N., Fauvelle, V., Delmas, F., Mazellier, P., and Legube, B. (2011). Liquid chromatography coupled with tandem mass spectrometry method for thirty-three pesticides in natural water and comparison of performance between classical solid phase extraction and passive sampling approaches. *J. Chromatogr. A* 1218, 1492–1502. doi: 10.1016/j.chroma.2011.01.040

Messerlian, C., Martinez, R. M., Hauser, R., and Baccarelli, A. A. (2017). 'Omics' and endocrine-disrupting chemicals — new paths forward. *Nat. Rev. Endocrinol.* 13, 740–748. doi: 10.1038/nrendo.2017.81.

Murphy, F., Ewins, C., Carbonnier, F., and Quinn, B. (2016). Wastewater Treatment Works (WwTW) as a source of microplastics in the aquatic environment. *Environ. Sci. Technol.* 50, 5800–5808. doi: 10.1021/acs.est.5b05416

Net, S., Delmont, A., Sempéré, R., Paluselli, A., and Ouddane, B. (2015a). Reliable quantification of phthalates in environmental matrices (air, water, sludge, sediment and soil): a review. *Sci. Total Environ.* 515–516, 162–180. doi: 10.1016/j.scitotenv.2015.02.013

Net, S., Sempéré, R., Delmont, A., Paluselli, A., and Ouddane, B. (2015b). Occurrence, fate, behavior and ecotoxicological state of phthalates in different environmental matrices. *Environ. Sci. Technol.* 49, 4019–4035. doi: 10.1021/es505233b

Paluselli, A., Aminot, Y., Galgani, F., Net, S., and Sempéré, R. (2018a). Occurrence of phthalate acid esters (PAEs) in the northwestern Mediterranean Sea and the Rhone River. *Prog. Oceanogr.* 163, 221–231. doi: 10.1016/j.pocean.2017.06.002

Paluselli, A., Fauvelle, V., Schmidt, N., Galgani, F., Net, S., and Sempéré, R. (2018b). Distribution of phthalates in Marseille Bay (NW Mediterranean Sea). *Sci. Total Environ.* 621, 578–587. doi: 10.1016/j.scitotenv.2017.11.306

Pojana, G., Gomiero, A., Jonkers, N., and Marcomini, A. (2007). Natural and synthetic endocrine disrupting compounds (EDCs) in water, sediment and biota of a coastal lagoon. *Environ. Int.* 33, 929–936. doi: 10.1016/j.envint.2007.05.003

Sousa, J. C. G., Ribeiro, A. R., Barbosa, M. O., Pereira, M. F. R., and Silva, A. M. T. (2017). A review on environmental monitoring of water organic pollutants identified by EU guidelines. *J. Hazard. Mater.* 344, 146–162. doi: 10.1016/j.jhazmat.2017.09.058

Suhrhoff, T. J., and Scholz-Böttcher, B. M. (2016). Qualitative impact of salinity, UV radiation and turbulence on leaching of organic plastic additives from four common plastics - a lab experiment. *Mar. Pollut. Bull.* 102, 84–94. doi: 10.1016/j.marpolbul.2015.11.054

Taylor, P. J. (2005). Matrix effects: the Achilles heel of quantitative high-performance liquid chromatography-electrospray-tandem mass spectrometry. *Clin. Biochem.* 38, 328–334. doi: 10.1016/j.clinbiochem.2004.11.007

Zhang, Z. M., Zhang, H. H., Zhang, J., Wang, Q. W., and Yang, G. P. (2018). Occurrence, distribution, and ecological risks of phthalate esters in the seawater and sediment of Changjiang River Estuary and its adjacent area. *Sci. Total Environ.* 619–620, 93–102. doi: 10.1016/j.scitotenv.2017.11.070

Conflict of Interest Statement: The authors declare that the research was conducted in the absence of any commercial or financial relationships that could be construed as a potential conflict of interest.

The reviewer VL and handling editor declared their shared affiliation at the time of the review.

Copyright © 2018 Fauvelle, Castro-Jiménez, Schmidt, Carlez, Panagiotopoulos and Sempéré. This is an open-access article distributed under the terms of the Creative Commons Attribution License (CC BY). The use, distribution or reproduction in other forums is permitted, provided the original author(s) and the copyright owner(s) are credited and that the original publication in this journal is cited, in accordance with accepted academic practice. No use, distribution or reproduction is permitted which does not comply with these terms.

Science of the Total Environment 621 (2018) 578–587

Contents lists available at ScienceDirect

Science of the Total Environment

journal homepage: www.elsevier.com/locate/scitotenv

Distribution of phthalates in Marseille Bay (NW Mediterranean Sea)

Andrea Paluselli [a], Vincent Fauvelle [a], Natascha Schmidt [a], François Galgani [b], Sopheak Net [c], Richard Sempéré [a,*]

[a] Aix-Marseille Univ., Université de Toulon, CNRS, IRD, MIO, Marseille, France
[b] IFREMER, Laboratoire Environnement Ressources, Provence Azur Corse (LER/PAC), Ifremer Centre de Méditerranée, ZP de Bregaillon, La Seyne sur Mer, France
[c] Université de Lille, Laboratoire LASIR, Villeneuve d'Ascq, France

HIGHLIGHTS

- Estimation of DMP, DEP, DiBP, DnBP, BzBP and DEHP concentration at Bay of Marseille.
- One year PAEs observations (2014) in the Bay of Marseille.
- Variation of PAE composition from surface to the bottom water.
- High PAEs concentration close to deep and bottom water.

GRAPHICAL ABSTRACT

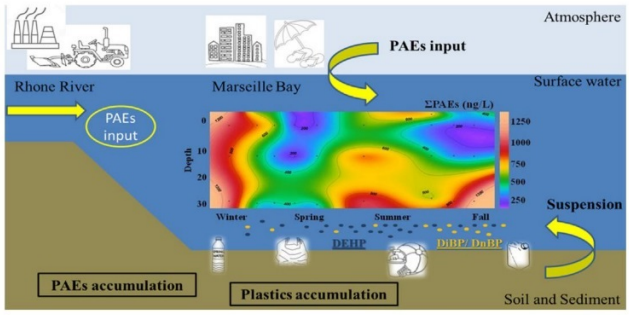

ARTICLE INFO

Article history:
Received 20 September 2017
Received in revised form 18 November 2017
Accepted 26 November 2017
Available online xxxx

Editor: Thomas Kevin V

Keywords:
Phthalates
DEHP
DMP
Seawater
Dissolved organic matter
Endocrine disruptors

ABSTRACT

Phthalic Acid Esters (PAEs) are a group of emerging organic contaminants that have become a serious issue because of their ubiquitous presence and hazardous impact on the marine environment worldwide. Seawater samples were collected monthly from December 2013 to November 2014 in the northwestern Mediterranean Sea (Marseille Bay). The samples were analyzed for dissolved organic carbon (DOC) as well as the molecular distribution of dissolved PAEs by using solid phase extraction followed by gas chromatography and mass spectrometry (GC/MS) analyses. The results demonstrated the occurrence of six PAEs, including dimethyl phthalate (DMP), diethyl phthalate (DEP), di-isobutyl phthalate (DiBP), di-n-butyl phthalate (DnBP), benzylbutyl phthalate (BzBP) and diethylhexyl phthalate (DEHP), with total concentrations ranging from 130 to 1330 ng L^{-1} (av. 522 ng L^{-1}). In Marseille Bay, the highest concentrations were detected in the bottom water from June to November 2014 and in the whole water column during the winter mixing period. This result suggests that resuspension of PAE-rich sediment, in relation to the accumulation of plastic debris above the seabed, or the higher degradation rate in the upper layer of the water column, plays a significant role in the PAE dynamics in coastal water. DEHP was the most abundant PAE in all of the surface samples and the summer bottom samples, followed by DiBP and DnBP, which also represent the largest fractions in the other bottom samples.

© 2017 Elsevier B.V. All rights reserved.

1. Introduction

Phthalates or phthalic acid esters (PAEs) are widely used in the manufacture and processing of plastic products such as plasticizers in a very broad range of industrial applications (Serôdio and Nogueria, 2006; Net

* Corresponding author.
E-mail address: richard.sempere@mio.osupytheas.fr (R. Sempéré).

https://doi.org/10.1016/j.scitotenv.2017.11.306
0048-9697/© 2017 Elsevier B.V. All rights reserved.

et al., 2015a). PAEs account for approximately 92% of produced plasticizers and represent the most produced and consumed plasticizers worldwide (Rahman and Brazel, 2004; He et al., 2013) since these compounds are used to improve the flexibility of polyvinyl chloride (PVC) resins (Kimber and Dearman, 2010; Net et al., 2015b). Other industrial applications include the manufacturing of cosmetics, insect repellents, insecticide carriers and propellants (Net et al., 2015a; Net et al., 2015b; Xie et al., 2007). PAEs of lower molecular weight (LMW-PAEs: C3-C6) are used as essential components of solvents, adhesives, waxes, pharmaceutical products, insecticide materials and cosmetics, whereas PAEs of higher molecular weight (HMW-PAEs: C7-C13) are instead used as additives to improve the flexibility and handling of industrial materials (Holahan and Smith, 2015; IARC, 2000; Halden, 2010). These compounds are suspected to enter the environment directly as emissions from household and industrial products, as released by wastewater from production and processing activity or the use and disposal of materials (Staples et al., 1997) as well as from plastic polymer migration (Andrady, 2011).

Previous studies have shown that PAEs are endocrine-disrupting chemicals with the capability of inducing significant effects on the reproduction of various organisms, including protozoans, mollusks, crustaceans, fishes and invertebrates (Andrady, 2011), on the ecosystem functioning (Kolena et al., 2014) and on human obesity and cancer development (Okamoto et al., 2011; Howdeshell et al., 2008; Buckley et al., 2016; Wang et al., 2016). Therefore, PAEs have become a matter of concern for their potential risk to health and the environment. Six PAEs (dimethyl phthalate (DMP), diethyl phthalate (DEP), di-n-butyl phthalate (DnBP), benzylbutyl phthalate (BzBP), diethylhexyl phthalate (DEHP) and di-n-octyl phthalate (DnOP)) have been included as priority pollutants of the US-EPA (United States Environmental Protection Agency, 2014), the European Union (EU) (Commission Staff Working Document on the Implementation of the Community Strategy for Endocrine Disrupters-A Range of Substances Suspected of Interfering with the Hormone System of Humans and Wildlife, 2007) and the Chinese water list (National Standard of the People's Republic of China, 2006). Accordingly, monitoring PAEs in the major environmental matrices has become a priority. After their introduction in the environment, they can reach marine water by wastewater and riverine inputs, and end up in the sediment via association with humic acid and adsorption onto particles and finally end up in the sediment (Bauer et al., 1998). Due to the physiochemical properties and biogeochemical cycling of PAEs, they have been detected in food, air, water, soil and sediment (Net et al., 2015b; Turner and Rawling, 2000; Fromme et al., 2002; Horn et al., 2004; Brossa et al., 2005; Teil et al., 2007; Xie et al., 2005; Xie et al., 2006; Zeng et al., 2008; Ferreira and Morita, 2012; Fu et al., 2009; Fu et al., 2013). However, there is a lack of data related to their sources, distribution in the whole water column as well as their transfer mechanisms from the molecular state to different living species.

The Mediterranean Sea being a semi-enclosed basin with slow turnover time of ~80 years implies a sensitive response to anthropogenic impact (The Mermex Group, 2011). Mediterranean rivers and primarily the Rhone River supply large amounts of freshwater, particles and organic carbon to the Mediterranean Sea (Sempéré et al., 2000; Panagiotopoulos et al., 2012). There is extensive urbanization particularly along the coastline as well as a number of highly industrialized spots all along the Mediterranean basin that are concentrated mainly in the northwestern Mediterranean Sea. All these activities as well as agricultural and domestic activities (The Mermex Group, 2011; UNEP Chemicals, 2002) generate a large volume of wastewater, which provides marine litter, microplastics (Deudero and Alomar, 2015; Collignon et al., 2012; Cozar et al., 2015; Faure et al., 2015; Pedrotti et al., 2016; Suaria et al., 2016; Ruiz-Orejon et al., 2016; Schmidt et al., submitted), anthropogenic molecules (Sicre et al., 2008; Sempéré et al., in press), persistent organic pollutants (POPs) and related contaminants such as polycyclic aromatic hydrocarbons (PAHs) and polychlorinated dibenzo-p-dioxins and dibenzofurans (PCDD/Fs) (The Mermex Group, 2011; Berrojalbiz et al., 2011; Castro-Jimenez et al., 2010) that impact the coastal marine ecosystems in unknown proportion. However, only a few studies have reported the occurrence of individual phthalates in the Mediterranean Sea (Brossa et al., 2005; Sanchez-Avila et al., 2012), and there is only one study dealing with the distribution of a series of PAEs in the Mediterranean basin (Paluselli et al., in press). The objectives of the present study are to investigate the composition and distribution of PAEs in the NW Mediterranean coastal seawater column and to ascertain their temporal trends on an annual basis.

2. Materials and methods

2.1. Study area, sampling, and dissolved organic carbon analyses

Seawater samples ($n = 72$) were collected with R/V Antedon from the SUNMEX station (Fig. 1) in the northwestern Mediterranean Sea in Marseille Bay (43°18′N, 05°22′E) from December 2013 to November 2014 at 1.5, 5, 15 and 30 m (with a bottom depth of 32–33 m) with a 12-L GO-FLO© (GENERAL OCEANICS) bottle previously rinsed with 1% hydrochloric acid and ultrapure water to avoid contamination. Immediately after sampling, the seawater samples were directly transferred from the GO-FLO© into 5-L precombusted (450 °C for 6 h) glass bottles closed with PTFE (polytetrafluoroethylene) lined screw caps, wrapped with aluminum foil and brought back to the laboratory within 4 h for processing. Four samples collected in October 2014 at Marseille Bay were already published (Paluselli et al., in press). The samples were filtrated through precombusted (450 °C for 6 h) GFF filters (47-mm filter diameter, rinsed with 2 L of Milli-Q water and 150 mL of sample prior to filtration) in a glass apparatus directly and transferred into 1-L glass bottles. After filtration, duplicate subsamples (10 mL) were collected for dissolved organic carbon (DOC) analyses with precombusted Pasteur pipettes, transferred into precombusted glass vials, poisoned with sulfuric acid to pH ~ 2 to avoid any biological activity, closed with PTFE-lined screw caps and stored in the dark at 4 °C. DOC concentrations were measured using a Shimadzu TOC-5000 carbon analyzer (Sempéré et al., 2008). The nominal analytical precision of the procedure was within 2%. The accuracy of the instrument and the system blank were determined by analyzing reference materials (D. Hansell, Rosenstiel School of Marine and Atmospheric Science, Miami, USA), including the Deep Seawater reference (DSR) and low carbon water (LCW) reference materials. The average DOC concentrations in the DSR and LCW reference standards were 45 ± 2 μM C, $n = 24$ and 1 ± 0.3 μM C, $n = 24$, respectively.

All glassware including Pasteur pipettes, glass bottles and glass filtration apparatus was previously cleaned in 1% hydrochloric acid bath, rinsed with ultrapure water and combusted at 450 °C for 6 h. All the GC/MS and DOC seawater analyses were conducted in duplicate in the MIO laboratory in Marseille within 6 months. Filtration of samples was conducted in the MIO ISO class 6 chemistry cleanroom (temperature: 22 °C; SAS pressure: + 15 Pa; SAS brewing rate: 30 vol/h; lab pressure: +30 Pa; brewing rate: 50 vol/h).

2.2. Phthalates analyses

Seven phthalates were studied including dimethyl phthalate (DMP), diethyl phthalate (DEP), di-isobutyl phthalate (DiBP), di-n-butyl phthalate (DnBP), benzylbutyl phthalate (BzBP), diethylhexyl phthalate (DEHP) and di-n-octyl phthalate (DnOP) (Fig. 2). The deuterated internal standards were: DEP-d4, DnBP-d4, DEHP-d4. All native and labeled standards were of high purity grade (>98%, 2000 μg mL^{-1} Supelco). Stock solutions were prepared in hexane and stored in the dark at 4 °C. Working solutions (unlabeled and labeled standards) were prepared by dilution of these solutions at 20 mg L^{-1}. All solvents were glass-distilled grade and supplied by Rathburn Chemicals Ltd. (Walkerburn, UK). Milli-Q water was produced on-site on a Milli-Q

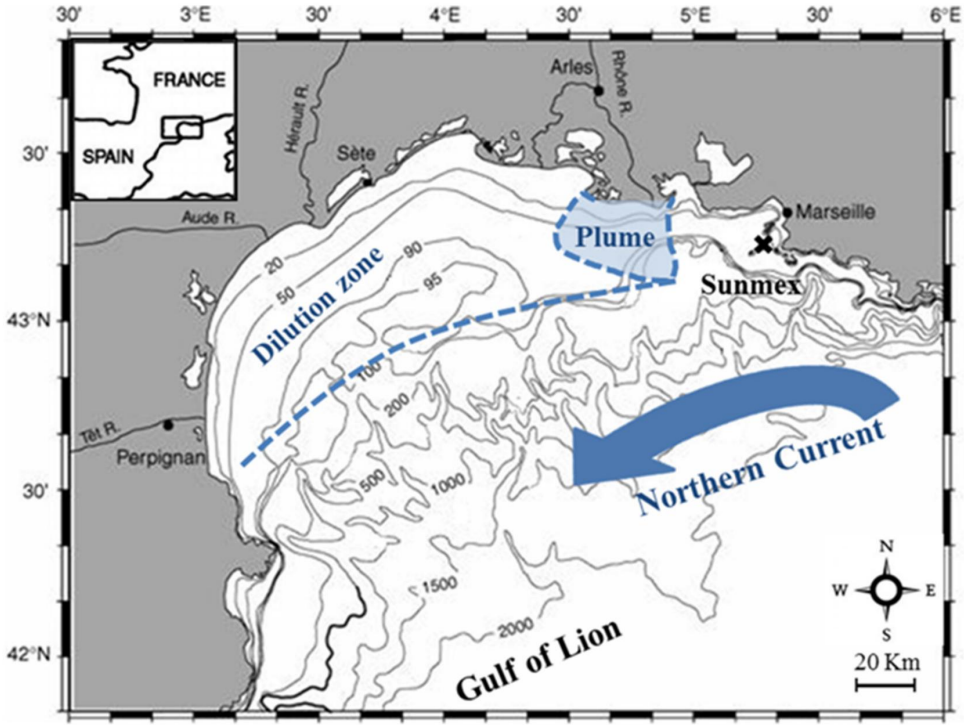

Fig. 1. Area of study. The map (adapted from Fraysse et al., 2014) shows the sampling stations in the Gulf of Lyon: SUNMEX (43°18′N, 05°22′E; depth 32 m) in the Bay of Marseille (December 2013–November 2014). Northern current is the main general circulation feature influencing the Gulf of Lyon with a geostrophic flux (calculated to 700 dbar) that varies throughout the year in a range of 0.9–1.8 Sv with its maximum in November or December (Sempéré et al., 2000). The Rhone River is the main fresh water supplier of the Mediterranean Sea with an average flow rate of 54 ± 12 km^3 $year^{-1}$ with maximum values in the fall period (Sempéré et al., 2000). In the studied period, the Rhone River flux ranged from 1300 to 2800 m3 s^{-1}.

system, Millipore (Molsheim, France) with resistivity higher than 18.2 MΩ cm (25 °C) and Total Organic Carbon <2 μg L^{-1}.

The extractions were performed following the method optimized for seawater PAE detection at trace levels (Paluselli et al., in press). PAEs were extracted by solid phase extraction (SPE) from seawater using a precombusted 6-mL glass reaction tube containing 200 mg of Oasis® HLB sorbent (Waters Corporation, 30 μm, 100 g). SPE was conducted on a Visiprep vacuum manifold from Sigma-Aldrich (Saint Quentin Fallavier, France). Before sample extraction, SPE cartridges were three times sequentially cleaned with 5 mL of acetone, 5 mL of dichloromethane, conditioned with 5 mL of ethyl acetate, 5 mL of acetone and 5 mL of ultrapure water prior sample processing. Seawater samples were spiked (for recovery estimate) with DEP-d4, DnBP-d4 and DEHP-d4 at 50, 200 and 400 ng L^{-1}, respectively, prior to loading onto SPE cartridges under

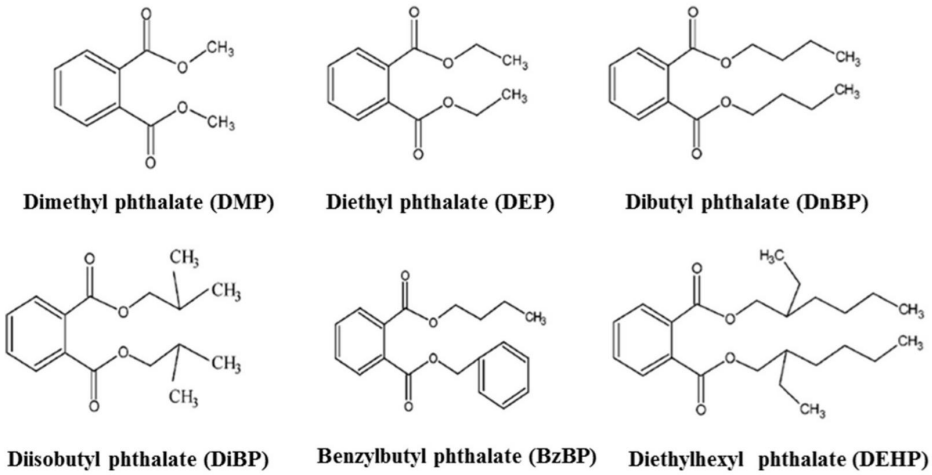

Fig. 2. Chemical structure of the 6 detected PAEs. Dimethyl phthalate (DMP; MW = 194.18), Diethyl phthalate (DEP; MW = 222.24), Dibutyl phthalate (DnBP; MW = 278.34), Diisobutyl phthalate (DiBP; MW = 278.34), Benzylbutyl phthalate (BzBP; MW = 312.36) and Diethylhexyl phthalate (DEHP; MW = 390.56).
Figure adapted from Xie et al., 2007.

vacuum at a flow rate of 5 to 10 mL min^{-1}. Then, 5 mL of ultrapure water was percolated to remove the remaining salt and air-dried for around 1 h under vacuum. PAEs were eluted into precombusted 10 mL-vials by a 2-step percolation of 3 mL of ethyl acetate. Ethyl acetate was gently evaporated to a final volume of 200 μL at room temperature under a gentle stream of nitrogen (purity >99,995%). Then, samples were immediately closed with PTFE lined screw caps rubbed with PTFE ribbon and stored before injection in the dark at −20 °C.

Analysis was performed using an Agilent Technologies 6850 GC system coupled to an Agilent Technologies 5975C mass spectrometer (GC/MS) operated with electron impact ionization (70 eV). Chromatographic separation was achieved on an Agilent HP-5MS capillary column (30 m × 0.25 mm, 0.25 μm film thickness) with the GC oven programmed at 70 °C for 1 min and then up to 230 °C at 30 °C min^{-1}, to 250 °C at 8 °C min^{-1} and to 280 °C at 30 °C min^{-1} with a final isotherm hold for 7.50 min. Helium was used as a carrier gas at a flow rate of 1.1 mL min^{-1}. Samples were manually injected (2 μL) on a splitless mode injector with a temperature set at 250 °C. The injector (Merlin Microseal system) was used as a low carryover septum and a gas purifier (Charcoal, CP17972) to prevent contamination during the injection. Data were acquired in single ion monitoring (SIM) mode for increased sensitivity with a dwell time of 100 ms. Data were collected and analyzed with the Agilent ChemStation software.

2.3. Quality control and quality assurance

For each batch of 12 samples, a method blank, a spiked blank and a sample duplicate were processed. The retention time and the response factors of GC/MS were assessed for each analytical sequence from daily control standards to ensure the most appropriate quantification. The average recoveries of PAEs spiked in seawater samples showed acceptable recovery for all phthalates, ranging from 97% ± 3% for DEP to 110% ± 7% for DiBP. Internal standard recoveries were estimates as 94% ± 2% for DEP-d4, 77% ± 3% for DnBP-d4 and 14% ± 2% for DEHP-d4. All material was produced in borosilicate glass previously kept in an acidic bath overnight (10% hydrochloric acid), rinsed with ultrapure water, combusted at 450 °C for 6 h and rinsed with methanol and dichloromethane before use. Extractions were carried out in controlled air conditions in an ISO class 6 chemistry cleanroom (temperature: 22 °C; SAS pressure: +15 Pa; SAS brewing rate: 30 vol/h; lab pressure: +30 Pa; brewing rate: 50 vol/h). Although precautions were considered to prevent sample contamination during the protocol, DEP, DiBP and occasionally DnBP were detected in the blanks at levels that remained below 0.07 ± 0.02 ng L^{-1}, 0.8 ± 0.3 ng L^{-1} and 0.7 ± 0.2 ng L^{-1}, respectively. DEHP was occasionally detected in blanks between the method detection limit (MDL) and the quantification detection limit (QDL). Limits of detection (LOD) were derived from the blanks and quantified as mean blanks plus three times the standard deviation of blanks, and they ranged from 0.11 ng L^{-1} for DMP to 1.67 ng L^{-1} for DEHP.

2.4. Statistics

Principal component analysis (PCA) was applied to reduce the multidimensional nature of the dataset and to evaluate the interrelationships among the PAEs, sites and sampling periods. PCA was performed using the individual phthalate concentrations (i.e. DEHP, DiBP) as PCA parameters. This data set was transformed in two smaller matrices that are linear combinations of the original data set. The number of observations in this study is 216, which permits the use of this statistical approach. The PCA statistics were performed using the statistical package XLSTAT 2010.2 (Addinsoft). Time series maps were made using the latest Ocean Data View version: ODV 4.7.4.

3. Results and discussion

3.1. General characteristics of the water column

The hydrological data (Fig. 3) are in line with previous well-known features in Marseille Bay and the local coastal area indicating that (Serôdio and Nogueria, 2006) the water column was well mixed during winter and fall periods, most of the time under the action of wind (Fraysse et al., 2014; Gatti et al., 2006; Barrier et al., 2016), whereas (Net et al., 2015a) the water began warming in May (16–17 °C) causing water stratification. It is noteworthy that lower salinity was observed in October–November 2014 probably in association with freshwater intrusion (Fig. 3b). The DOC distribution (Fig. 3e) showed a clear seasonal trend with a concentration range of 62.5–72.5 μM in winter-spring and 72.5–90 μM during summer-fall. Higher DOC values (79–81 μM) were observed in the spring water column as well as above the bottom in winter. As a byproduct of primary production, the DOC distribution highlighted higher concentrations in spring-summer following phytoplankton growth (Fig. 3d). The high DOC concentrations near the bottom and in the whole water column during winter might instead be explained by resuspension of rich organic sediment and subsequent mixing under the action of wind as previously reported from CDOM (colored dissolved organic matter) and DOC time series studies (Para et al., 2010; Sempéré et al., 2015). Such low DOC concentrations were comparable to those previously reported in open waters of the Mediterranean Sea (Doval et al., 1999; Dafner et al., 2001; Santinelli et al., 2012; Sempéré et al., 2002; Sempéré et al., 2003), with a stable annual mean of 67 ± 7 μMC at 2 m and 63 ± 6 μMC at 5 m.

3.2. Concentration and relative abundance of PAEs in Marseille Bay

All targeted PAEs were detected in all samples collected at SUNMEX station except DnOP. During the studied period, the sum of the 6 PAEs' concentrations in the water column (ΣPAEs) ranged from 130 to 1330 ng L^{-1} (av. 520 ng L^{-1}; Table 1; Fig. 3f) in Marseille Bay. The highest ΣPAEs concentrations were observed all along the well mixed water column in winter 2013 as well as near the bottom in the May–August and September–December 2014 periods (Fig. 3). By contrast, the lowest ΣPAEs concentrations were found in shallower waters between 0.5 and 15 m by the end of winter and in October–November 2014 where low salinities were observed (Fig. 3b). Note that the October–November 2014 period corresponds to possible freshwater intrusion into Marseille Bay (Gatti et al., 2006) as suggested by lower salinity values (Fig. 3b). In Marseille Bay, for 62 out of 72 samples, DEHP (9.3–91.6%) was the most abundant PAE, followed by DiBP (3.8–78%) and DnBP (2.1–44.8%) (Figs. 4–5; Table 1). By contrast, DMP, DEP and BzBP were the least abundant (0.2–2%) and can be considered minor species here.

Very limited data are available for the occurrence and fate of PAEs as a simultaneous series in marine waters and more specifically in both the Mediterranean Sea and river waters, making any comparison of ΣPAEs data with existing studies difficult. However we found that our data are consistent with literature. Indeed, examination of already published individual PAEs, indicated that our DEHP concentrations (20–920 ng L^{-1}; Table 1) were in the same range as values reported for NW Spanish coastal seawater (30–620 ng L^{-1}; (Sanchez-Avila et al., 2012)) and the southern coast of the UK (100–2200 ng L^{-1}; (Turner and Rawling, 2000)) but one order of magnitude lower than that for the Northern Mediterranean Spanish coast (Brossa et al., 2005). Noteworthy lower values were also reported in the North Sea for DEHP (0.5–5.3 ng L^{-1}), DMP as well as DEP (0.02–4.0 ng L^{-1}) (Teil et al., 2007; Dargnat et al., 2009). Similar concentrations of DEHP, 161–314 and 323–779 ng L^{-1}, were found in the Seine River whereas DMP concentrations were reported in the range of 2.5–5.5 ng L^{-1} in six Spanish rivers including Ebro River (Sanchez-Avila et al., 2012). DEP was detected in different studies in the Seine River (France) in a range slightly higher than our data, from 46 to 208 ng L^{-1} (Teil et al., 2007) to 71–181 ng L^{-1}. (Dargnat et

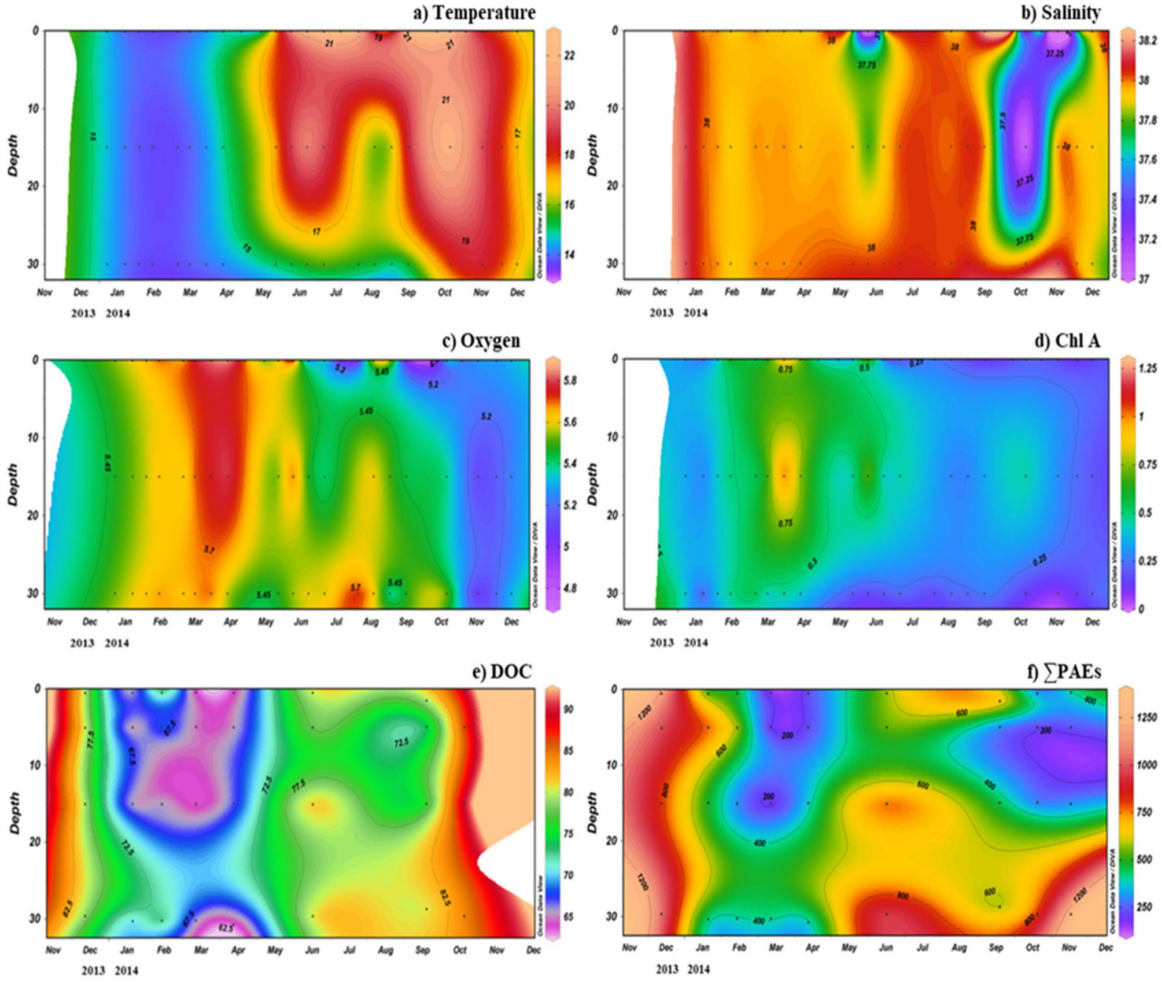

Fig. 3. a) Temperature (°C), b) salinity (PSU), c) oxygen (ml L^{-1}), d) chlorophyll A (μg L^{-1}), e) DOC (μM) and f) ∑ PAEs (ng L^{-1}) time-series at SUNMEX station (Bay of Marseille) from December 2013 to November 2014. Samples were collected at 1.5, 5, 15 and 30 m.

al., 2009) as well as 52–284 ng L^{-1} in 6 Spanish rivers (Sanchez-Avila et al., 2012). BzBP was also reported at low concentration in the range of 4.8–23 ng L^{-1} (Sanchez-Avila et al., 2012; Dargnat et al., 2009). Limited data are available for the distribution of PAEs in coastal seawater.

The contribution of carbon from PAEs to the DOC pool (PAE-C) accounted for 10–60 ppm. A comparison with other organic compounds within the DOC pool identified in the coastal Mediterranean Sea indicated that our PAE concentrations are in the same order of magnitude as the reported values of dissolved water phase PAHs (3–120 ng L^{-1}; (Berrojalbiz et al., 2011)), one of the most abundant classes of organic contaminants in the marine environment. Lower concentration range was reported for other organic pollutant as PFCs (0.07–4.55 ng L^{-1}; (Sanchez-Avila et al., 2012; Ahrens et al., 2010)) in NW Mediterranean Sea, PCB (2.2–82.4 pg L^{-1}; (Berrojalbiz et al., 2011)) in surface water of Mediterranean Sea and PBDE, another group of compounds used as additives in polymer, detected in Aegean Sea with concentration range of 4–6 pg L^{-1} (Lammel et al., 2015). PCDD/Fs was reported with two orders of magnitude lower than PAEs concentration (42.5–64.0 fg L^{-1}) (Castro-Jimenez et al., 2008). However, PAE concentrations are nevertheless two orders of magnitude lower than the sum of α,ω-dicarboxylic acids (20.7 ± 10.6 μg L^{-1}) and ω-oxoacids (11.7 ± 6.2 μg L^{-1}) in the Marseille coastal area (Tedetti et al., 2006) or in the Rhone River close to the Marseille Bay (Sempéré et al., in press).

3.3. PCA analysis

The grouping of samples by depth and season using principal component analysis (PCA) formed several clusters (samples scores, Fig. 6a) over PC1 and PC2 that represent 79.7% of the total information. Samples collected at Marseille Bay formed five well-identified clusters (Fig. 6a) including the fall samples in the lower left quadrant, the spring in the central left, the summer in the upper left, winter samples in the upper right quadrant and the bottom samples in the right quadrant. Of the biomarkers plotted, DMP, DEP and DnBP being positive on PC1 and most negative on PC2 form a compact cluster on the central-right quadrant and separated from DEHP located in the upper quadrant (positive on PC1 and PC2 factors) and from DiBP in the lower quadrant (positive on PC1 and negative on PC2). DEHP is a plasticizer used in the manufacture of PVC and other plastic products. On the other hand, the presence of LMW-PAEs in the same group is related to their common use as components of solvents, adhesives, pharmaceutical products, insecticide materials and cosmetics.

In brief, the PCA score plot therefore highlights that i) summer and winter groups have a similar pattern i.e. highest concentrations of DEHP, DMP and DEP, together with lowest concentrations of DiBP; ii) fall and spring groups are also very close on Fig. 6a: their intensity on both PC1 and PC2 axis are low and negative, meaning low Σ PAEs

Table 1
Concentration ranges, average concentrations and relative abundance of PAEs in Marseille Bay ($n = 72$) from December 2013 to November 2014 (samples were collected at 0.5, 5, 15 and 30 m depth).

	Depth (m)	Concentrations (ng L^{-1})		Relative abundance (%)	
		Range	Av. ± SD	Range	Av. ± SD
		Bay of Marseilles (Dec 2013–Nov 2014)			
Dimethyl phthalate (DMP)	0.5	0.9–6.9	2.8 ± 2.2	0.2–1.4	0.6 ± 0.3
	5	0.8–6.8	2.9 ± 2.0	0.3–1.1	0.7 ± 0.4
	15	0.8–7.7	2.7 ± 2.3	0.2–0.9	0.6 ± 0.3
	30	2.1–11.9	4.5 ± 2.1	0.2–1.2	0.7 ± 0.3
	Total	0.8–11.9	3.2 ± 2.4	0.2–1.4	0.6 ± 0.3
Diethyl phthalate (DEP)	0.5	3.4–25.7	11.8 ± 7.6	1.1–4.9	2.6 ± 1.4
	5	6.3–27.2	11.9 ± 7.9	1.1–10.2	3.4 ± 2.7
	15	3.3–45.5	13.9 ± 13.4	0.9–9.9	3.3 ± 2.7
	30	8.9–50.0	25.3 ± 12.6	0.9–5.1	3.8 ± 1.3
	Total	3.3–50.0	15.7 ± 12.5	0.9–10.2	3.3 ± 2.1
Diisobutyl phthalate (DiBP)	0.5	34.2–215.7	89.5 ± 70.3	4.3–68.0	24.3 ± 21.9
	5	30.1–155.3	62.0 ± 37.9	3.8–78.0	23.3 ± 23.1
	15	29.4–155.1	71.1 ± 39.6	4.7–64.2	20.2 ± 18.6
	30	50.8–383.4	188.5 ± 124.8	5.0–42.5	28.0 ± 11.5
	Total	27.5–383.4	102.7 ± 90.5	3.8–78.0	23.9 ± 18.7
Dibutyl phthalate (DnBP)	0.5	12.0–314.6	76.7 ± 66.7	2.6–26.3	11.1 ± 7.9
	5	14.0–196.5	58.3 ± 50.9	2.7–26.1	11.1 ± 7.3
	15	12.0–178.6	61.4 ± 48.9	2.8–42.1	14.2 ± 12.0
	30	21.0–596.0	173.8 ± 165.0	2.1–44.8	19.4 ± 13.7
	Total	12.0–596.0	83.2 ± 75.2	2.1–44.8	13.9 ± 10.7
Benzylbutyl phthalates (BzBP)	0.5	2.7–4.9	3.7 ± 0.7	0.4–2.0	1.0 ± 0.6
	5	2.6–4.6	3.6 ± 0.6	0.5–1.8	1.1 ± 0.5
	15	2.6–4.6	3.6 ± 0.6	0.5–1.8	1.0 ± 0.4
	30	3.6–6.1	4.4 ± 0.9	0.4–1.5	0.8 ± 0.4
	Total	2.6–6.1	3.8 ± 0.7	0.4–2.0	0.9 ± 0.5
Diethylhexyl phthalate (DEHP)	0.5	42.3–802.0	331.4 ± 257.1	18.5–89.3	61.0 ± 23.8
	5	15.8–714.0	317.0 ± 274.1	9.3–90.2	61.1 ± 24.7
	15	51.3–525.0	291.9 ± 221.5	21.2–91.1	61.4 ± 24.1
	30	130.0–923.8	328.6 ± 257.9	18.3–91.6	48.1 ± 23.9
	Total	15.8–923.8	317.2 ± 242.7	9.3–91.6	57.9 ± 23.8
Total PAEs		130.8–1330.7	522.7 ± 313.3	100	

concentration rather than a specific PAE mix; and iii) bottom samples are mainly driven by DiBP concentration, and are thus clearly separated from upper water layers whatever the season.

3.4. Potential sources and sinks of PAEs in the water column

The averaged concentrations of PAEs found in Marseille Bay (522.7 ± 313.3 ng L^{-1}) samples are significantly higher than that previously found offshore (maximum depth 2500 m) (135 ± 74 ng L^{-1}. (Paluselli et al., in press)) suggesting that the freshwater input and urban area provide a significant amount of PAEs to Marseille Bay. Our results also indicated i) significant seasonal variations of ΣPAEs in Marseille Bay suggesting variability in sources, degradation processes of PAEs occurring in coastal seawaters, and/or partitioning of PAEs onto particulate matter; ii) heterogeneous vertical distribution by the end of winter/spring and homogenous concentration in the whole water column in the winter period with a large ΣPAEs increase of concentration above the sea floor at different periods of the year.

3.4.1. Seasonal variation

Concerning seasonal variation in Marseille Bay, it is interesting to note that elevated concentration of PAEs (Fig. 3f) in summer coastal seawater nearby the Marseille urban area is concomitant with (Serôdio and Nogueria, 2006) the intense recreational coastal activities that reach their maximum during the summer on the beaches of Marseille, as well as (Net et al., 2015a) the elevated maritime traffic occurring during the tourist season between the ports of the coastal study area. As DEHP is predominant during the summer period (Figs. 4–5), it is likely that such summer activities preferentially generate inputs of DEHP-rich PAE into coastal seawater. It should be noticed that DEHP is the most abundant plasticizer for PVC, PVA and rubber materials that are widely used at sea through surfing, diving and swimming or left on the beaches such as food packaging, bags and sunscreen containers. The high turnover of cruise ships could also represent a significant source of DEHP for the coastal area. In Marseille Bay, the large variations of PAE concentrations in the first 25 m of the water column could be connected to variation of input and degradation processes as well. Few PAE-degrading bacteria have been isolated from marine environments (Gu et al., 2009) and a recent study suggests that the ability to degrade phthalate and its monoesters is widespread in Japanese seawater from bacteria related to 11 different genera (Iwaki et al., 2012). It is likely that prokaryotic degradation processes regulate the PAE concentration in the water column as well.

3.4.2. Higher concentration near the bottom

Interestingly, we found that PAE concentrations are quite elevated above the bottom being, in most cases, higher than the corresponding concentration on the sea surface (Figs. 3f–7), with the exclusion of winter 2013 and September for which PAE concentrations are similar in the whole water column probably because of winter mixing under the action of Mistral wind (Fraysse et al., 2014). Such an accumulation of ΣPAEs near the bottom has already been reported in a previous study in offshore Mediterranean seawater at 2000 m depth (Paluselli et al., in press). A gradient in the PAE concentration might be either due to i) preferential photochemical and/or prokaryotic degradation in the surface water column rather than in deeper seawater, giving rise to accumulation of PAEs above the seafloor, or ii) PAE input directly from the bottom by pure chemical diffusion and/or advection phenomena (resuspension of sediment or bioturbation).

Surface water column photochemical degradation is certainly more effective in the first meters of the water column whereas prokaryotic degradation is likely to be more efficient above the sediment. Although PAE-degrading bacteria have been isolated from marine environments (Gu et al., 2009; Iwaki et al., 2012), preferential biodegradation in the

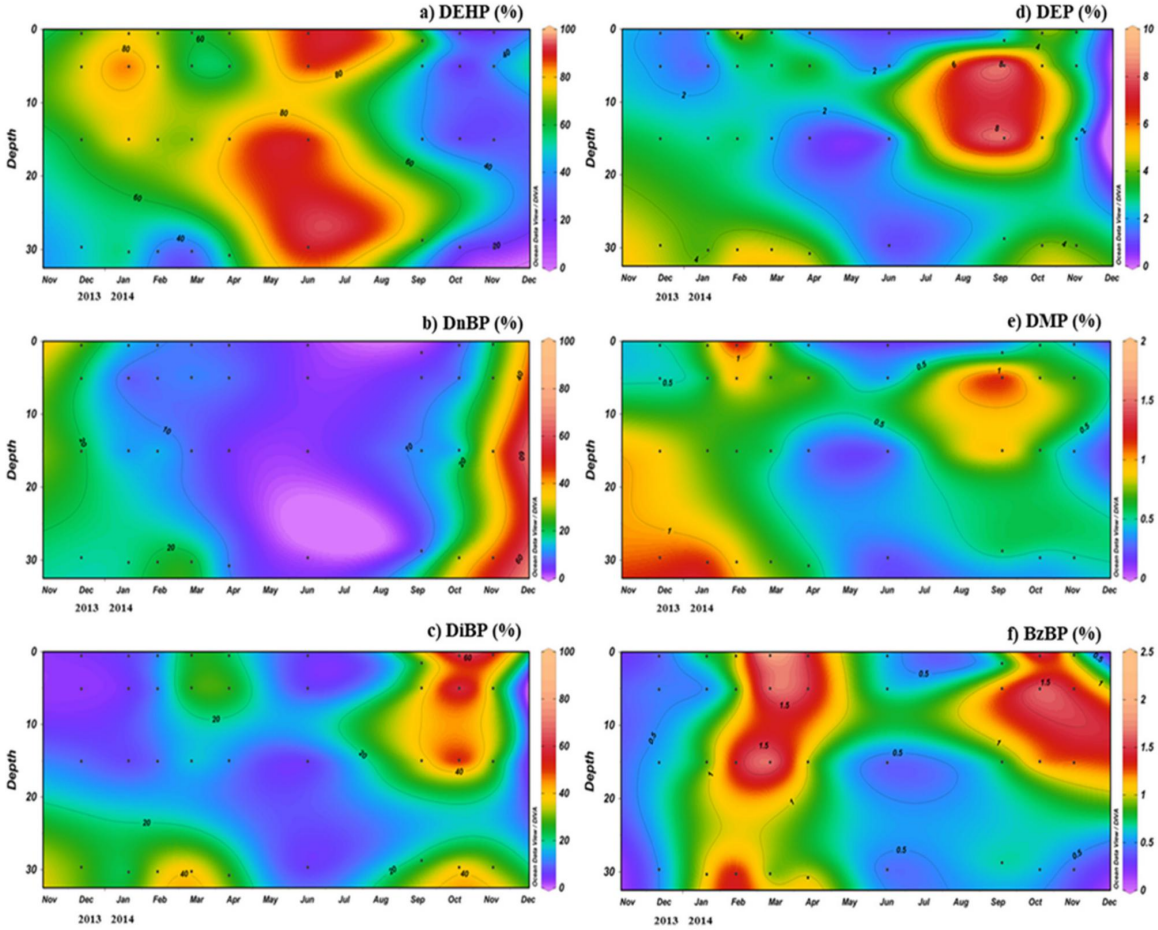

Fig. 4. Relative abundances for DEHP (a), DnBP (b), DiBP (c), DEP (d), DMP (e) and BzBP (f) at SUNMEX station in Marseille Bay from December 2013 to November 2014.

water column rather than above the bottom is very unlikely. Therefore, only photochemical degradation may explain such PAE concentration gradient along the vertical gradient.

This vertical gradient might also be connected to a concentration of plastic debris above the sea floor that may releases various chemical additives including phthalates into surrounding waters during their degradation as stated before. Indeed, accumulation of debris with a large proportion of plastic material has been observed several times, by trawling sampling and by video quantification based on recordings at the sea floor of the French Mediterranean coast including Marseille Bay (Galgani et al., 1995; Galgani et al., 1996; Galgani et al., 2000), the Rhone River plume area as well as canyons and continental slopes in the northwestern Mediterranean (Fabri et al., 2014). In most cases, plastic bags accounted for >90% of the total debris (Galgani et al., 1995) and in particular in the eastern canyons of the Gulf of Lion (Galgani et al., 2000) close to Marseille. Such debris are likely PAE-producer candidates. Chemical diffusion from sediment, or sediment resuspension/bioturbation could though explain higher PAE concentration close to the sediment. Resuspension episodes of PAE-rich sediment in the water column (originating from wind-driven turbulence and hydrodynamic features (Lapouyade, 2001) such as upwelling above the seafloor as previously reported for CDOM and DOC in Marseille Bay (Para et al., 2010)) are possible. However, higher DOC concentrations were not observed close to the sediment (Fig. 3e), supporting poor physical transport from the sediment toward the water column. Transport by chemical diffusion would therefore be predominant, in case PAEs input came from the sediment.

Interestingly, in Marseille Bay bottom samples, DiBP and DnBP relative abundance values were predominant over DEHP or higher (compared to surface waters) and match the period of high concentration of total PAEs. Indeed, in surface water samples, the relative abundance of DEHP, DnBP and DiBP averaged 66 ± 18%, 11 ± 6% and 21 ± 15%, respectively, whereas these values averaged 48 ± 21%, 21 ± 12% and 32 ± 14%, respectively, in bottom samples during the year (Fig. 5). A possible explanation would be a higher degradation rate of LMW-PAEs close to the atmosphere/water interface due to higher organisms' density, as suggested by Yuan et al., 2010. The predominance (or higher relative abundance) of DnBP and DiBP versus DEHP in deep-water samples is in line with previous observations at a deep offshore station (z = 2400 m) (Paluselli et al., in press). The variation of PAE relative abundance near the bottom could also be explained considering the higher hydrophobicity of DEHP ($\log K_{ow}$ = 7.54, SPARC) compared with DnBP and DEP ($\log K_{ow}$ = 4.63 and 2.51, respectively, SPARC), which could determine different grades of PAE repartition between sediment and water, making available a smaller dissolved fraction of DEHP and suggesting that DEP and even DnBP mainly exist under freely dissolved phase compared with DEHP. The higher desorption rate of these phthalate, with the exception of DEHP and DMP, in the interface sediment/water was already observed in a previous study (Mackintosh et al., 2006).

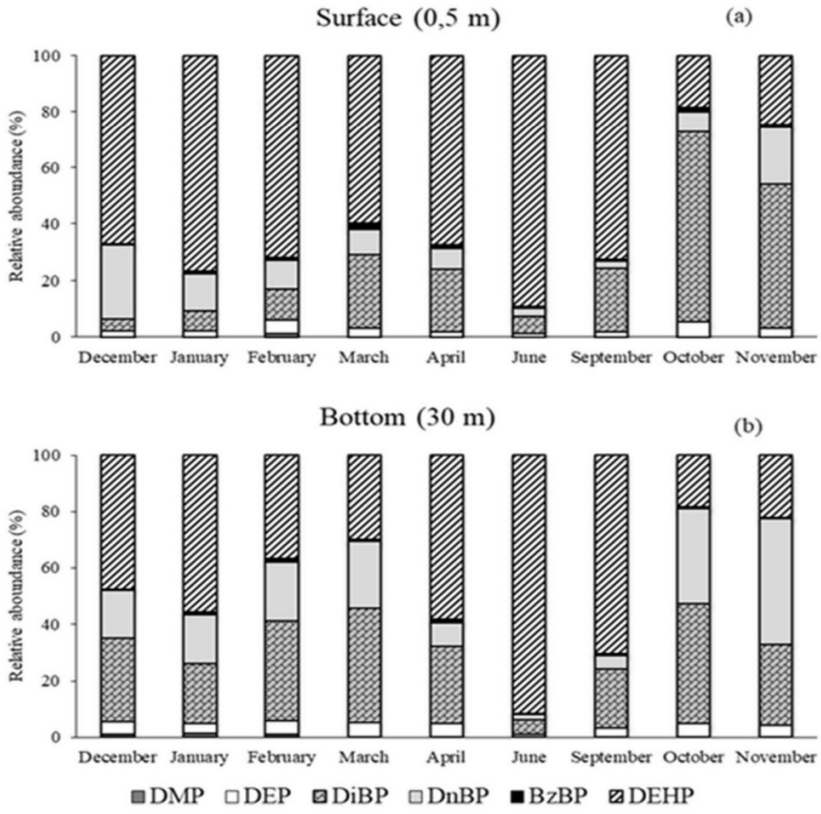

Fig. 5. Relative abundance of PAEs in surface (0.5 m; a) and bottom (30 m; b) seawater samples collected at SUNMEX station in Marseille Bay from December 2013 to November 2014.

Surprisingly, a significant decrease of DEHP concentration and relative abundance was observed after the summer (October/November 2014) (Figs. 4–5). The change in relative abundance during fall, even on the surface, was due to an increase of DiBP and to a lesser extent DnBP and could be associated with potential resuspension as we observed only high PAE concentration in bottom samples. Note that

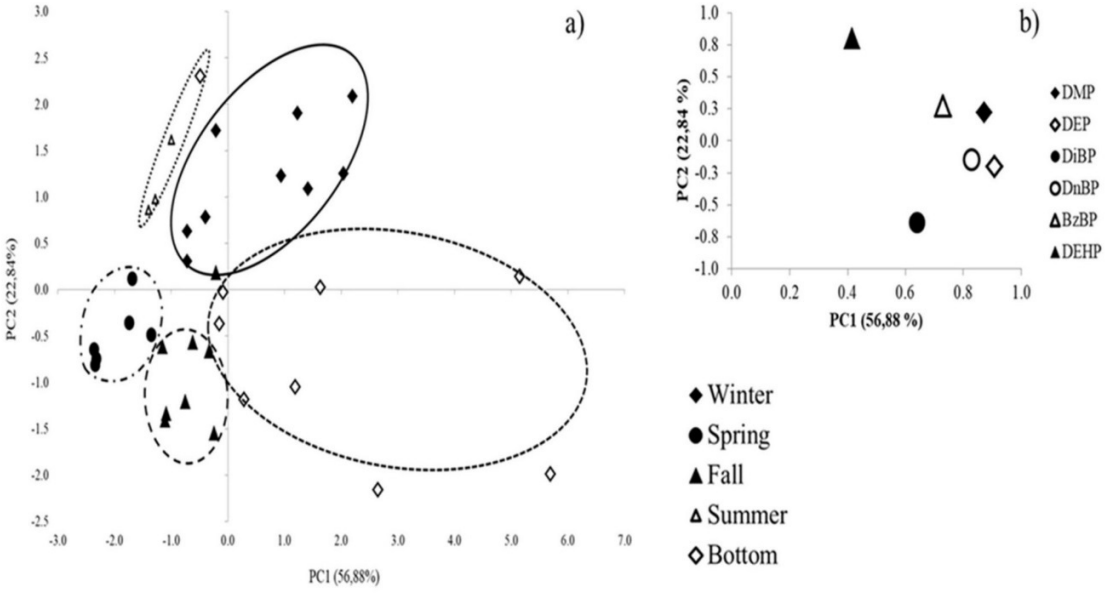

Fig. 6. Principal components analysis (PCA) for PAEs in the study area was applied to reduce the multidimensional nature of the dataset and to evaluate the interrelationships among the PAEs, sites and sampling periods. The PCA statistics were performed using the statistical package XLSTAT 2010.2 (Addinsoft). In (a) the sample scores, whereas in (b) the variable loadings of the PCA. The variance accounted for by each principal component is shown in parentheses after the axis label.

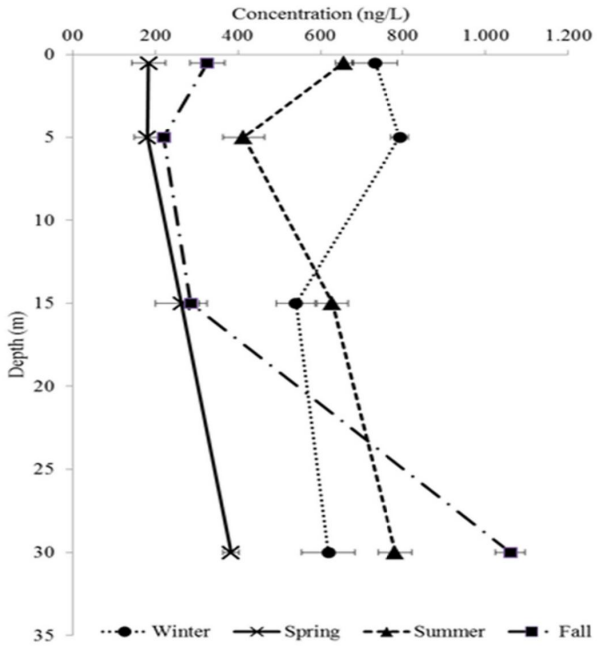

Fig. 7. ∑PAEs vertical profile at Bay of Marseille in 4 seasons (average values) of 2014.

the variable intensity of the resuspension processes might be favored by the Northern Current entering into the Gulf of Lyon and being particularly high from October to May (Lapouyade, 2001) intensifying the inputs and shelf/slope exchange processes including turbulent mixing and vertical flux on the continental slope (Lapouyade, 2001; Monaco et al., 1999). In these circumstances exchange with the deep bottom, already observed to be rich in plastic debris, could represent a seasonal source of PAEs for the Bay of Marseille at the end of the stratification season, especially in the eastern canyons close to Marseille. This area was already noticed to accumulate most of the debris in the Gulf of Lyon, especially plastic bags (Galgani et al., 1995; Galgani et al., 1996). Our data together with others studies, suggest sediment resuspension as an important process explaining the heterogeneous vertical distribution. However, additional specific experiments are needed to confirm such hypothesis.

4. Conclusion

This study provides the first complete data on PAEs concentration levels in the Bay of Marseille (NW Mediterranean Sea). In addition, the first estimation of the PAEs annual occurrence and PAEs vertical distribution were reported here. The Marseille Bay, which is highly populated, displays levels of contamination of the same order of magnitude as other coastal area (NW Spanish coast, UK southern coast, Seine River; (Turner and Rawling, 2000; Brossa et al., 2005; Teil et al., 2007; Sanchez-Avila et al., 2012; Dargnat et al., 2009)). DEHP was detected as the predominant PAE congener in spring/summer season at Marseille area in the whole water column, whereas DiBP and DnBP were found to be abundant when close to the seafloor and especially in fall/winter season in the study areas. DMP, DEP and BzBP represent a minor fraction of PAEs pool and DnOP was never detected in the analyzed samples. The highest PAEs concentrations were detected close to the bottom and we have hypothesized a connection with the plastic debris accumulated over the seafloor and with PAEs in the sediment.

More research regarding PAEs input from plastic, and PAEs presence in the sediment should be implemented in the future to better identify the sources of the PAEs in the water column. Furthermore, more investigation is needed on the level of PAEs transfer to food web, for a better risk assessment and management policy.

Acknowledgments

This study was conducted as part of the project PLASTOX-JPI-Ocean, PlasticMicro-EC2CO and MERMEX/MISTRALS LAbex-OTMed projects and supported by 'Pole Mer Méditerranée'. This study is a contribution to the international SOLAS and LOICZ projects. We acknowledge the financial support from the PACA region, which provided a PhD scholarship for A. Paluselli. The authors are grateful to the crews of the R/V *Antedon II* and SAM-M I O platform for operation at sea as well as Patrick Raimbault, Nagib Bhairy for hydrological data and sampling and Anne Delmont for help in sampling and DOC analyses. Reviewers are kindly acknowledged for improving the revised version of the MS. The project leading to this publication has received funding from European FEDER Fund under project 1166-39417. A PhD scholarship for N. Schmidt was provided by Agence de l'Eau.

References

Ahrens, L., Gerwinski, W., Theobald, N., Ebinghaus, R., 2010. Sources of polyfluoroalkyl compounds in the North Sea, Baltic Sea and Norwegian Sea: evidence from their spatial distribution in surface water. Mar. Pollut. Bull. 60 (2), 255–260.

Andrady, A.L., 2011. Microplastics in the marine environment. Mar. Pollut. Bull. 62 (8), 1596–1605.

Barrier, N., Petrenko, A.A., Ourmières, Y., 2016. Strong intrusions of the Northern Mediterranean Current on the eastern Gulf of Lion: insights from in-situ observations and high resolution numerical modeling. Ocean Dyn. 66 (3), 313–327.

Bauer, M.J., Herrmann, R., Martin, A., Zellmann, H., 1998. Chemodynamics, transport behavior and treatment of phthalic acid esters in municipal landfill leachates. Water Sci. Technol. 38 (2), 185–192.

Berrojalbiz, N., Dachs, J., Ojeda, M.J., Valle, M.C., Castro-Jimenez, J., Wollgast, J., Ghiani, M., Hanke, G., Zaldivar, J.M., 2011. Biogeochemical and physical controls on concentrations of polycyclic aromatic hydrocarbons in water and plankton of the Mediterranean and Black Sea. Glob. Biogeochem. Cycles 25 (4).

Brossa, L., Marcé, R., Borrull, F., Pocurull, E., 2005. Occurrence of twenty-six endocrine-disrupting compounds in environmental water samples from Catalogna, Spain. Environ. Toxicol. Chem. 24, 261–267.

Buckley, J.P., Engel, S.M., Mendez, M.A., Richardson, D.B., Daniels, J.L., Calafat, A.M., Wolff, M.S., Herring, A.H., 2016. Prenatal phthalate exposures and childhood fat mass in a New York City cohort. Environ. Health Perspect. 124 (4), 507–513.

Castro-Jimenez, J., Deviller, G., Ghiani, M., Loos, R., Mariani, G., Skejo, H., Umlauf, G., Wollgast, J., Laugier, T., Heas-Moisan, K., Leaute, F., Munschy, C., Tixier, C., Tronczynski, J., 2008. PCDD/F and PCB multi-media ambient concentrations, congener patterns and occurrence in a Mediterranean coastal lagoon (Etang de Thau, France). Environ. Pollut. 156 (1), 123–125.

Castro-Jimenez, J., Eisenreich, S.J., Ghiani, M., Mariani, G., Skejo, H., Umlauf, G., Wollgast, J., Zaldivar, J.M., Berrojalbiz, N., Reuter, H.I., Dachs, J., 2010. Atmospheric occurrence and deposition of polychlorinated dibenzo-p-dioxins and dibenofurans (PCDD/Fs) in the open Mediterranean Sea. Environ. Sci. Technol. 44 (14), 5456–5463.

Collignon, A., Hecq, J.-H., Galgani, F., Voisin, P., Collard, F., Goffart, A., 2012. Neustonic microplastic and zooplankton in the North Western Mediterranean Sea. Mar. Pollut. Bull. 64, 861–864.

Commission Staff Working Document on the Implementation of the Community Strategy for Endocrine Disrupters-A Range of Substances Suspected of Interfering with the Hormone System of Humans and Wildlife. CEC (Commission of the European Communities), Brussels.

Cozar, A., Sanz-Martin, M., Marti, E., Gonzalez-Gordillo, J.I., Ubeda, B., Galvez, J.A., Irigoien, X., Duarte, C.M., 2015. Plastic accumulation in the Mediterranean Sea. PLoS ONE 10 (4).

Dafner, E., Sempéré, R., Bryden, H.L., 2001. Total organic carbon distribution and budget through the Strait of Gibraltar in April 1998. Mar. Chem. 73 (3-4), 233–252.

Dargnat, C., Teil, M.J., Chevreuil, M., Blanchard, M., 2009. Phthalate removal throughout wastewater treatment plant: case study of Marne Aval station (France). Sci. Total Environ. 407, 1235–1244.

Deudero, S., Alomar, C., 2015. Mediterranean marine biodiversity under threat: reviewing influence of marine litter on species. Mar. Pollut. Bull. 98 (1-2), 58–68.

Doval, M.D., Perez, F.F., Berdalet, E., 1999. Dissolved and particulate organic carbon and nitrogen in the Northwestern Mediterranean. Deep-Sea Res. Part I Oceanogr. Res. Pap. 46 (3), 511–537.

Fabri, M.-C., Pedel, L., Beuck, L., Galgani, F., Hebbeln, D., Freiwald, A., 2014. Megafauna of vulnerable marine ecosystems in French mediterranean submarine canyons: Spatial distribution and anthropogenic impacts. Deep Sea Res. Part 2 Top. Stud. Oceanogr. 104, 184–207.

Faure, F., Demars, C., Wieser, O., Kunz, M., De Alencastro, L.F., 2015. Plastic pollution in Swiss surface waters: nature and concentrations, interaction with pollutants. Environ. Chem. 12 (5), 582–591.

Ferreira, I.D., Morita, D.M., 2012. Ex-situ bioremediation of Brazilian soil contaminated with plasticizers process wastes. Braz. J. Chem. Eng. 29 (1), 77–86.

Fraysse, M., Pairaud, I., Ross, O.N., Faure, V.M., Pinazo, C., 2014. Intrusion of Rhone River diluted water into the Bay of Marseille: generation processes and impacts on ecosystem functioning. J. Geophys. Res. 119 (10), 6535–6556.
Fromme, H., Kuchler, T., Otto, T., Pilz, K., Muller, L., Wenzel, A., 2002. Occurrence of phthalates and bisphenol A and F in the environment. Water Res. 36, 1429–1438.
Fu, P., Kawamura, K., Barrie, L.A., 2009. Photochemical and other source of organic compounds in the Canadian high Artic aerosol pollution during winter-spring. Environ. Sci. Technol. 43, 286–292.
Fu, P., Kawamura, K., Chen, J., Charrière, B., Sempéré, R., 2013. Organic molecular composition of marine aerosols over the Arctic Ocean in summer: contributions of primary emission and secondary aerosol formation. Biogeosciences 10, 653–667.
Galgani, F., Jaunet, S., Campillo, A., Guenegen, X., His, E., 1995. Distribution and abundance of debris on the continental shelf of the north-western Mediterranean Sea. Mar. Pollut. Bull. 30 (11), 713–717.
Galgani, F., Souplet, A., Cadiou, Y., 1996. Accumulation of debris on the deep sea floor off the French Mediterranean coast. Mar. Ecol. Prog. Ser. 142 (1-3), 225–234.
Galgani, F., Leaute, J.P., Moguedet, P., Souplet, A., Verin, Y., Carpentier, A., Goraguer, H., Latrouite, D., Andral, B., Cadiou, Y., Mahe, J.C., Poulard, J.C., Nerisson, P., 2000. Litter on the sea floor along European coasts. Mar. Pollut. Bull. 40 (6), 516–527.
Gatti, J., Petrenko, A., Devenon, J.L., Leredde, Y., Ulses, C., 2006. The Rhone River dilution zone present in the northeastern shelf of the Gulf of Lion in December 2003. Cont. Shelf Res. 26 (15), 1794–1805.
Gu, J., Han, B., Duan, S., Zhao, Z., Wang, Y., 2009. Degradation of the endocrine-disrupting dimethyl phthalate carboxylic ester by *Sphingomonas yanoikuyae* DOS01 isolated from the South China Sea and the biochemical pathway. Int. Biodeterior. Biodegrad. 63 (4), 450–455.
Halden, R.U., 2010. Plastics and health risks. Annu. Rev. Public Health 31, 179–194.
He, W., Qin, N., Kong, X., Liu, W., He, Q., Ouyang, H., Yang, C., Jiang, Y., Wang, Q., Yang, B., Xu, F., 2013. Spatio-temporal distributions and the ecological and health risks of phthalate esters (PAEs) in the surface water of a large, shallow Chinese lake. Sci. Total Environ. 461–462, 672–680.
Holahan, M.R., Smith, C.A., 2015. Phthalates and neurotoxic effects on hippocampal network plasticity. Neuro Toxicology 48, 21–34.
Horn, O., Nalli, S., Cooper, D., Nicell, J., 2004. Plasticizer metabolites in the environment. Water Res. 38, 3693–3698.
Howdeshell, K.I., Rider, C.V., Wilson, V.S., Gray Jr., L.E., 2008. Mechanisms of action of phthalate esters, individually and in combination, to induce abnormal reproductive development in male laboratory rats. Environ. Res. 108 (2), 168–176.
IARC, 2000. Some industrial chemicals, di(2-ethylhexyl) phthalate. IARC Monogr. Eval. Carcinog. Risks Hum. 77, 41–148.
Iwaki, H., Nishimura, A., Hasegawa, Y., 2012. Isolation and characterization of marine bacteria capable of utilizing phthalate. World J. Microbiol. Biotechnol. 28 (3), 1321–1325.
Kimber, I., Dearman, R.J., 2010. An assessment of the ability of phthalates to influence immune and allergic responses. Toxicology 271 (3), 73–82.
Kolena, B., Petrovivova, I., Pilka, T., Pucherova, Z., Munk, M., Matula, B., Vankova, V., Petlus, P., Jenisova, Z., Rozova, Z., Wimmerova, S., Trnovec, T., 2014. Phthalate exposure and health-related outcomes in specific types of work environment. Int. J. Environ. Res. Public Health 11 (6), 5628–5639.
Lammel, G., Audy, O., Besis, A., Efstathiou, C., Eleftheriasis, K., Kohoutek, J., Kukucka, P., Mulder, M.D., Pribylova, P., Prokes, R., Rusina, T.P., Samara, C., Sofuoglu, A., Sofuoglu, S., Tasdemir, Y., Vassilatou, V., Voutsa, D., Vrana, B., 2015. Air and seawater pollution and air-sea gas exchange of persistent toxic substances in the Aegean Sea: spatial trendes of PAHs, PCBs, OCPs and PBDEs. Environ. Sci. Pollut. Res. 22 (15), 11301–11313.
Lapouyade, A., 2001. Durrieu de Madron, X. Seasonal variability of the advective transport of particulate matter and organic carbon in the Gulf of Lion (NW Mediterranean). Oceanol. Acta 24 (3), 295–312.
Mackintosh, C., Maldonado, J., Ikonomou, M.A., Gobas, P.C., 2006. Sorption of phthalate esters and PCBs in a marine ecosystem. Environ. Sci. Technol. 40, 3481–3488.
Monaco, A., Durrieu de Madron, X., Radakovitch, O., Heussner, J., Carbonne, J., 1999. Origin and variability of downward biogeochemical fluxes on the Rhone continental margin (NW Mediterranean). Deep-Sea Res. Part I Oceanogr. Res. Pap. 46 (9), 1483–1511.
National Standard of the People's Republic of China, 2006. Standard for Drinking Water Quality. GB. p. 5749.
Net, S., Delmont, A., Sempéré, R., Paluselli, A., Ouddane, B., 2015a. Reliable quantification of phthalates in environmental matrices (air, water, sludge, sediment and soil): a review. Sci. Total Environ. 515–516:162–180. https://doi.org/10.1016/j.scitotenv.2015.02.013.
Net, S., Sempéré, R., Delmont, A., Paluselli, A., Ouddane, B., 2015b. Occurrence, fate, behavior and ecotoxicological state of phthalates in different environmental matrices. Environ. Sci. Technol. 49 (7), 4019–4035.
Okamoto, Y., Ueda, K., Kojima, N., 2011. Potential risks of phthalates esters: acquisition of endocrine-disrupting activity during environmental and metabolic processing. J. Health Sci. 57, 497–503.
Paluselli, A., Aminot, Y., Galgani, F., Net, S., Sempéré, R., 2017. Occurrence of phthalate acid esters (PAEs) in the northwestern Mediterranean Sea and the Rhone River. Prog. Oceanogr. (in press). https://doi.org/10.1016/j.pocean.2017.06.002.
Panagiotopoulos, C., Sempéré, R., Para, J., Raimbault, P., Rabouille, C., Charrière, B., 2012. The composition and flux of particulate and dissolved carbohydrates from the Rhone River into the Mediterranean Sea. Biogeosciences 9, 1827–1844.
Para, J., Coble, P.G., Charrière, B., Tedetti, M., Fontana, C., Sempéré, R., 2010. Fluorescence and absorption properties of chromophoric dissolved organic matter (CDOM) in coastal surface waters of the northwestern Mediterranean Sea, influence of the Rhône Rive not completer. Biogeosciences 7, 4083–4103.
Pedrotti, M.L., Petit, S., Elineau, A., Bruzaud, S., Crebassa, J.C., Dumontet, B., Marti, E., Gorsky, G., Cozar, A., 2016. Changes in the floating plastic pollution of the Mediterranean Sea in relation to the distance to land. PLoS ONE 11 (8).
Rahman, M., Brazel, C.S., 2004. The plasticizer market: an assessment of traditional plasticizers and research trends to meet new challenges. Prog. Polym. Sci. 29, 1223–1248.
Ruiz-Orejon, L.F., Sarda, R., Ramis-Pujol, J., 2016. Floating plastic debris in the Central and Western Mediterranean Sea. Mar. Environ. Res. 120, 136–144.
Sanchez-Avila, J., Tauler, R., Lacorte, S., 2012. Organic micropollutants in coastal waters from NW Mediterranean Sea: Sources distribution and potential risk. Environ. Int. 46, 50–62.
Santinelli, C., Sempéré, R., Van-Wambeke, F., Charriere, B., Seritti, A., 2012. Organic carbon dynamics in the Mediterranean Sea: an integrated study. Glob. Biogeochem. Cycles 26.
Schmidt, N., Thibault, D., Galgani, F., Paluselli, A., Sempéré, R., 2017. Occurrence of microplastics and potential contribution of phthalates in the surface waters of the Gulf of Lion (NW Mediterranean Sea). Prog. Oceanogr. https://doi.org/10.1016/j.pocean.2017.11.010 (in press).
Sempéré, R., Charrière, B., Van Wambeke, F., Cauwet, G., 2000. Carbon inputs of the Rhône river to the Mediterranean Sea: biogeochemical implications. Glob. Biogeochem. Cycles 14 (2), 669–681.
Sempéré, R., Panagiotopoulos, C., Lafont, R., Marroni, B., Van Wambeke, F., 2002. Total organic dynamics in the Aegean Sea. J. Mar. Syst. 33-34, 355–364.
Sempéré, R., Dafner, E., Van Wambeke, F., Lefevre, D., Magen, C., Allegre, S., Bruyant, F., Bianchi, M., Prieur, L., 2003. Distribution and cycling of total organic carbon across the Almeria-Oran Front in the Mediterranean Sea: implications for carbon cycling in the western basin. J. Geophys. Res. 108.
Sempéré, R., Tedetti, M., Panagiotopoulos, C., Charrière, B., Van Wambeke, F., 2008. Distribution and bacterial availability of dissolved neutral sugars in the South East Pacific. Biogeosciences 5, 1165–1173.
Sempéré, R., Para, J., Tedetti, M., Chattière, B., Mallet, M., 2015. Variability of Solar radiation and CDOM in Surface Coastal Waters of the Northwestern Mediterranean Sea. Photochem. Photobiol. 91 (4) (851–561).
Sempéré, R., Charrière, B., Castro-Jimenez, J., Kawamura, K., Panagiotopoulos, C., 2017. Occurrence of α, ω-dicarboxylic acids and ω-oxoacids in the surface waters of the Rhone River and fluxes into the Mediterranea Sea. Prog. Oceanogr. (in press). https://doi.org/10.1016/j.pocean.2017.07.002.
Serôdio, P., Nogueria, J.M.F., 2006. Considerations on ultra-trace analysis of phthalates in drinking water. Water Res. 40 (13), 2572–2582.
Sicre, M.A., Fernandes, M.B., Pont, D., 2008. Poly-aromatic hydrocarbon (PAH) inputs from the Rhone River to the Mediterranean Sea in relation with the hydrological cycle: impact of floods. Mar. Pollut. Bull. 56 (11), 1935–1942.
Staples, C.A., Peterson, D.R., Parkerton, T.F., Adams, W.J., 1997. The environmental fate of phthalate esters: a literature review. Chemosphere 35 (4), 667–749.
Suaria, G., Avio, C.G., Mineo, A., Lattin, G.L., Magaldi, M.G., Belmonte, G., Moore, C.J., Regoli, F., Aliani, S., 2016. The Mediterranean plastic soup: synthetic polymers in Mediterranean surface waters. Nat. Sci. Rep. 6, 37551.
Tedetti, M., Kawamura, K., Charriere, B., Chevalier, N., Sempéré, R., 2006. Determination of low molecular weight dicarboxylic and ketocarboxylic acids in seawater samples. Anal. Chem. 78, 6012–6018.
Teil, M., Blanchard, M., Dargnat, C., Larcher-Tiphagne, K., Chevreuil, M., 2007. Occurrence of phthalates diesters in river of the Paris district (France). Hydrol. Process. 21, 2515–2525.
The Mermex Group, 2011. Marine ecosystems responses to climatic and anthropogenic forcings in the Mediterranean. Prog. Oceanogr. 91, 97–166.
Turner, A., Rawling, M.C., 2000. The behaviour of di-(2-ethylhexyl) phthalate in estuaries. Mar. Chem. 68 (3), 203–217.
UNEP Chemicals, 2002. Regionally based assessment of persistent toxic substances. Mediterranean Regional Report. UNEP, Geneve.
United States Environmental Protection Agency, December 2014. 40 CFR Part 423, Appendix A. https://www.epa.gov/sites/production/files/2015-09/documents/priority-pollutant-list-epa.pdf.
Wang, Y., Zeng, Q., Sun, Y., You, L., Wang, P., Li, M., Yang, P., Li, J., Huang, Z., Wang, C., Li, S., Dan, Y., Li, Y., 2016. Phthalate exposure in association with serum hormone levels, sperm DNA damage and spermatozoa apoptosis: a cross-sectional study in China. Environ. Res. 150, 557–565.
Xie, Z., Ebinghaus, R., Temme, C., Caba, A., Ruck, W., 2005. Atmospheric concentrations and air–sea exchanges of phthalates in the North Sea (German Bight). Atmos. Environ. 39, 3209–3219.
Xie, Z., Selzer, J., Ebinghaus, R., Caba, A., Ruck, W., 2006. Development and validation of a method for the determination of trace alkylphenols and phthalates in the atmosphere. Anal. Chim. Acta 565, 198–207.
Xie, Z., Ebinghaus, R., Temme, C., Lohmann, R., Caba, A., Ruck, W., 2007. Occurrence and air-sea exchange of phthalates in the Arctic. Environ. Sci. Technol. 41, 4555–4560.
Yuan, S., Huang, I., Chang, B., 2010. Biodegradation of dibutyl phthalate and di-(2-ethylhexyl) phthalate and microbial community changes in mangrove sediment. J. Hazard. Mater. 184 (1-3), 826–831.
Zeng, F., Cui, K., Xie, Z., Liu, M., Li, Y., Lin, Y., Zeng, Z., Li, F., 2008. Occurrence of phthalate esters in water and sediment of urban lakes in a subtropical city, Guangzhou, South China. Environ. Int. 34, 372–380.

ANNEXES

Annex
Chapter I

Supplementary Table 1 Information on the sampling sites and microplastic counts (MPs) as well as environmental data (seawater temperature, wind and current mean speeds and directions, precipitation) for each sampling date.

Sample site	ID	GPS coordinates	Sampling Date	Manta net mesh size (µm)	MPs (items km^{-2})	Seawater temperature (°C)	Wind		Current		Rainfall (mm)
							Mean Speed (m s^{-1})	Direction	Mean Speed (m s^{-1})	Direction	
North Current	#1	42°48'25.6" N 6°04'39.5" E	17/02/14	780	164,032 8,947 202,803	14	6.1	W	0.25	S	-
			10/03/14	780	915,598 102,893 377,274	15	1.9	SE	0.40	W	-
			24/06/15	780	11,930 22,368	20	4.4	S/SE	0.35	N	-
			22/12/15	780	101,402	15	0.8	E/SE	0.35	W	0.2
Marseille	#2	43°16'04.0" N 5°20'01.0" E	17/06/14	780	1,161,646 317,626	20	2.5	NW	0.05	-	-
	#3	43°18'00.5" N 5°19'17.0" E	21/01/16	780	17,894	13	1.4	NE	0.05	SW	-
			11/02/16	780	23,859	13	1.9	N/NE	0.05	S	-
			25/02/16	780	10,438	13	1.9	NE	0.10	-	-
			07/03/16	330	37,280 10,438	13	6.1	NW	0.15	SE	-
			09/03/16	330	14,912	12	3.1	NW	0.05	-	-
			17/03/16	330	26,842	13	5.6	SE	0.50	NW	2.0
			14/04/16	330	22,368	15	2.5	NW	0.10	N	-
	#4	43°15'45.9" N 5°17'58.0" E	21/01/16	780	11,930	13	1.4	NE	0.05	SW	-
			11/02/16	780	11,930	13	1.9	N/NE	0.05	S	-
			25/02/16	780	8,947	13	1.9	NE	0.10	-	-
			07/03/16	330	5,965	13	6.1	NW	0.15	SE	-

					7,456					
			09/03/16	330	7,456	12	3.1	NW	0.05	-	-
			17/03/16	330	14,912	13	5.6	SE	0.50	NW	2.0
			14/04/16	330	8,947	15	2.5	NW	0.10	N	-
Rhône River plume	#5	43°19'15.4" N 4°51'20.5" E	18/03/14	780	61,139 59,648 152,103 399,642	12	3.6	S	0.80	NW	-
			06/05/14	780	52,192 46,227 99,911 32,806	14	3.1	SE	0.60	N	-
Rhône River	#6	43°40'37.1" N 4°37'13.8" E	19/03/14	780	26,842 37,280	7	1.4	N	-	-	-
			09/04/14	780	44,736 31,315 7,456	11	2.5	N	-	-	1.0
			07/05/14	780	43,245	15	2.5	N/NW	-	-	-
			11/06/14	780	14,912	17	3.1	N/NE	-	-	-
			19/06/14	780	68,595	17	3.9	N	-	-	-

Sources: Surface current speed and direction were extracted from the Mars 3D model (http://marc.ifremer.fr), wind speed and directions and seawater temperature data from http://www.infoclimat.fr and rainfall information from http://www.meteofrance.com .

Annex
Chapter II

Text S1: Method details concerning GC-MS and LC-HRMS analysis.

GC-MS analysis (Organophosphate ester and phthalate analysis)

GC analyses were conducted with an Agilent 7820A Series GC coupled with an Agilent 5977E MS, operating in selected ion monitoring (SIM) and electron impact (EI, 70 eV) modes. The separation was achieved in a 30 m x 0.25 mm i.d. x 0.25 µm HP-5MS capillary column (Agilent J&W). All target contaminants were quantified by the internal standard (IS) procedure. The injection volume was of 2 µL and the helium carrier gas flow was 1 mL min^{-1}. The temperatures of the MS transfer line and the ion source and the quadrupole were set at 300, 230 and 150 ºC, respectively. The following conditions were applied: injector temperature: 270 ºC (splitless) and the oven was programmed from 90 ºC to 132 ºC at 3 ºC min^{-1}, to 166 ºC at 10 ºC min^{-1}, to 175 at 1 ºC min^{-1} (holding time 2 min), to 232 ºC at 2 ºC min^{-1}, and then to 300 °C at 25 ºC min^{-1} (holding time 5 min).

LC-HRMS analysis (Bisphenol analysis)

10 µL of the extract were injected for the quantification of BPs using LC-electrospray ionization quadrupole time of flight mass spectrometry (LC-ESI-QTOF, Agilent 1290 Infinity LC system coupled with Agilent 6530 Accurate-Mass Q-TOF, Agilent Technologies, Les Ulis, France). The syringe was washed externally with MeOH for 20 seconds before injection to avoid contamination of injection port or following samples. Separation was achieved on an Agilent Zorbax Eclipse XDB reversed phase column (50 mm x 2.1 mm, 1.8 µm), with temperature set at 30 °C. Elution was performed with MQ (A) and MeOH (B) under gradient conditions: 0 min 95:5 A/B, 1 min 95:5 A/B, 10 min 0:100 A/B, 15 min 0:100 A/B, 15.1 min 95:5 A/B, 20 min 95:5 A/B. ESI interface was operated in negative mode (3.5 kV capillary voltage), and MS TOF mass acquisition was performed in the range 50-600 m/z at a rate of 1 spectrum s^{-1}. ESI parameters were set as follows: 300 °C gas temperature, 11 L min^{-1} drying gas, 40 psig nebulizer, 350 °C sheath gas temperature, 11 L min-1 sheath gas flow. TOF parameters were: 1500 V nozzle voltage, 175 V fragmentor voltage, 65 V skimmer voltage, 750 V octopole voltage. Ion chromatogram extraction was performed with 10 ppm mass tolerance, based on exact monoisotopic mass and retention time.

Table S1: Abbreviation, full name and CAS number of each compound as well as their monoisotopic masses and log K_{ow} values.

Name	Full name	CAS	Monoisotopic mass (g mol^{-1})	log K_{ow}
Organophosphate esters (OPEs)				
TPP	Tripropyl phosphate	513-08-6	224.1177	1.9
TiBP	Tri-iso-buthyl phosphate	126-71-6	266.1647	3.5
TnBP	Tri-n-butyl phosphate	126-73-8	266.1647	4
TCEP	Tris-(2-chloroethyl) phosphate	115-96-8	283.9539	1.8
TCPP	Tris-(2-chloro, 1-methylethyl) phosphate	13674-84-5	326.0008	2.6
TDCP	Tris-(2-chloro-, 1-chloromethylethyl) phosphate	13674-87-8	427.8839	3.7
TPhP	Triphenyl phosphate	115-86-6	326.0708	4.6
EHDPP	2-ethylhexyl-diphenyl phosphate	1241-94-7	362.1647	5.7
TEHP	Tris(2-ethylhexyl) phosphate	78-42-2	434.3525	9.5
TBP-*d27*	Tri-n-butyl phosphate-*d27*	61196-26-7	293.3341	
TPhP-*d15*	Triphenyl phosphate-*d15*	1173020-30-8	341.1649	
TCPP-*d18*	Tris (2-chloroisopropyl) phosphate-*d18*	-	344.1138	
TDCP-*d15*	Tris (1,3-dichloro-2-propyl) phosphate-*d15*	1447569-77-8	442.9781	
TPrP-*d21*	Tri-n-propyl phosphate-*d21*	1219794-92-9	245.2495	
TCEP-*d12*	Tris (2-chloroethyl) phosphate-*d12*	1276500-47-0	296.0292	
MAL-*d7*	Malathion-*d7*	352438-94-9	337.0800	
Phthalates (PAEs)				
DMP	dimethyl phthalate	131-11-3	194.0579	1.6
DEP	diethyl phthalate	84-66-2	222.0892	2.5
DBP	di-n-butyl phthalte	84-74-2	278.1518	4.5
DiBP	diisobutyl phthalate	84-69-5	278.1518	4.1
DEHP	diethylhexyl phthalate	117-81-7	390.277	7.6
BzBP	benzylbutyl phthalate	85-68-7	312.1362	4.7
DnOP	di-n-octyl phthalate	117-84-0	390.277	8.1
DEHP-*d4*	diethylhexyl phthalate-*d4*	93951-87-2	394.3021	
DEP-*d4*	diethyl phthalate-*d4*	93952-12-6	226.1143	
DnBP-*d4*	di-n-butyl phthalte-*d4*	93952-11-5	282.1769	

Bisphenols (BPs)

BPA	bisphenol A	80-05-7	228.115	3.3
BPAF	bisphenol AF	14878-61-1	336.0585	4.5
BPAP	bisphenol AP	1571-75-1	290.1307	4.4
BPF	bisphenol F	620-92-8	200.0837	2.9
BPS	bisphenol S	80-09-1	250.03	1.9
BPZ	bisphenol Z	843-55-0	268.1463	5.4
4nOP-*d17*	4-n-octylphenol-*d17*	1219794-55-4	223.2738	
BPA-*d16*	bisphenol A-*d16*	96210-87-6	244.2154	

Table S2: Quantification limits (LOQ) of native and surrogate compounds. The LOQs in pg injected (instrumental LOQs) were determined considering a signal/noise (S/N) ratio of >10 in the lowest calibration level. The LOQs in ng L^{-1} (method LOQs) were derived from these values taking into account the corresponding SPE preconcentration factor.

Compound	LOQ	
	(pg)	(ng L^{-1})
Organophosphate esters (OPEs)		
TPP	5	0.13
TiBP	1	0.03
TnBP	2	0.05
TCEP	10	0.19
TCPP	10	0.25
TDCP	10	0.25
TPhP	5	0.10
EHDPP	5	0.13
TEHP	10	0.20
TBP-*d27*	2	0.05
TPhP-*d15*	5	0.13
TCPP-*d18*	30	0.75
TDCP-*d15*	11	0.28
Phthalates (PAEs)		
DMP	5	0.07
DEP	2	0.05
DiBP	1	0.03
DnBP	1	0.03
BzBP	5	0.09
DEHP	2	0.05
DnOP	10	0.25
DnBP-*d4*	1	0.03
Bisphenols (BPs)		
BPA	10	1.0
BPAF	1	0.1
BPAP	20	2.0
BPF	10	1.0
BPS	1	0.1
BPZ	50	5.0
4nOP-*d17*	30	3.0

Table S3: Relative abundances (in %) of Σ_7 PAEs, Σ_9 OPEs, Σ_6 BPs and individual PAEs and OPEs in Rhône River water samples. Individual BPs are not shown, since BPS was the only BP detected.

	05/23/17	06/22/17	08/24/17	09/19/17	11/03/17	11/30/17	12/12/17	01/05/18	02/13/18	03/01/18	04/09/18
Sums											
$\sum_7$ PAEs	69.7	49.5	64.8	65.5	65.5	56.7	78.0	74.7	72.2	61.5	43.8
$\sum_9$ OPEs	29.2	47.9	34.2	32.0	31.8	41.4	20.7	22.2	27.0	36.6	51.6
$\sum_6$ BPs	1.1	2.6	1.0	2.5	2.8	1.9	1.3	3.1	0.9	1.9	4.7
Individual PAEs											
DMP	0.5	0.5	0.6	0.4	0.5	0.5	0.4	0.4	0.5	0.7	0.9
DEP	8.2	9.5	3.6	4.1	7.4	7.2	4.5	4.1	6.0	14.7	7.1
DiBP	8.7	20.2	13.8	7.3	22.0	7.1	3.2	4.5	16.1	31.9	11.5
DnBP	3.7	5.1	4.0	11.6	5.2	5.2	22.3	11.3	9.5	22.6	7.5
BzBP	n.d.	n.d.	n.d.	n.d.	n.d.	0.2	0.1	0.2	0.1	0.2	0.5
DEHP	78.9	64.7	78.0	76.6	65.0	79.3	69.4	79.6	67.4	29.5	71.8
DnOP	n.d.	n.d.	n.d.	n.d.	n.d.	0.4	0.1	n.d.	0.3	0.4	0.7
Individual OPEs											
TPP	2.1	1.1	2.3	n.d.	4.4	5.8	4.7	8.0	3.9	3.9	9.3
TiBP	3.4	2.0	3.1	1.4	5.6	5.5	7.2	7.3	8.1	6.1	7.4
TnBP	8.2	56.8	6.7	25.5	4.8	12.8	8.5	5.2	5.7	8.8	12.9
TCEP	1.6	1.7	3.8	2.5	9.2	3.3	2.1	29.4	n.d.	13.0	21.3
TCPP	79.8	34.9	74.0	65.4	67.7	65.3	70.5	43.2	78.0	64.0	44.1
TDCP	2.5	1.9	3.9	3.3	6.3	4.3	4.7	3.7	2.8	2.9	2.8
TPhP	0.6	0.4	0.5	0.5	0.9	0.7	0.9	1.7	n.d.	n.d.	0.6
EHDPP	1.7	1.2	5.6	1.3	1.2	2.3	1.3	1.5	1.3	1.3	1.6
TEHP	n.d.	n.d.	n.d.	n.d.	n.d.	n.d.	n.d.	n.d.	n.d.	n.d.	n.d.

n.d. = not detected

Table S4: Correlation matrix of the studied parameters. Contaminants that were not detected at all during the sampling campaign are excluded. Strong correlations (correlation coefficients ≥ ± 0.70) are highlighted in bold letters. RD = River discharge, WT = water temperature.

	TPP	TiBP	TnBP	TCEP	TCPP	TDCP	TPhP	EHDPP	ΣOPEs	DMP	DEP	DiBP	DnBP	BBzP	DEHP	DnOP	ΣPAEs	BPS	DOC	POC	PON	RD	WT
TPP	**1.00**																						
TiBP	0.56	**1.00**																					
TnBP	-0.39	-0,54	**1.00**																				
TCEP	0.53	0.22	-0.36	**1.00**																			
TCPP	-0.40	-0.32	0.20	-0.67	**1.00**																		
TDCP	-0.07	-0.34	0.15	-0.62	0.63	**1.00**																	
TPhP	-0.14	-0.09	-0.06	-0.12	0.43	0.35	**1.00**																
EHDPP	-0.35	-0.55	0.08	-0.48	0.40	0.24	-0.36	**1.00**															
ΣOPEs	-0.46	-0.56	**0.77**	-.061	**0.77**	0.51	0.24	0.30	**1.00**														
DMP	-0.55	-0.11	0.04	-0.59	**0.78**	0.29	0.52	0.23	0.49	**1.00**													
DEP	-0.39	0.13	0.16	-0.34	0.61	0.15	0.57	-0.11	0.50	**0.75**	**1.00**												
DiBP	-0.59	-0.09	0.19	-0.11	0.30	0.11	0.10	0.00	0.30	0.32	0.63	**1.00**											
DnBP	-0.05	0.20	-0.08	-0.17	0.16	0.21	0.47	-0.30	0.03	0.52	0.26	-0.04	**1.00**										
BBzP	0.21	0.38	0.60	-0.52	0.44	0.60	-0.22	0.37	**0.71**	0.36	0.59	0.22	0.45	**1.00**									
DEHP	-0.36	-0.34	0.08	-0.57	**0.73**	0.48	**0.77**	0.18	0.49	**0.77**	0.35	-0.15	0.43	-0.14	**1.00**								
DnOP	-0.28	-0.39	-0.14	0.55	0.13	-0.49	-0.55	0.02	0.08	-0.22	0.34	**0.75**	-0.54	-0.28	-0.67	**1.00**							
ΣPAEs	-0.46	-0.25	0.09	-0.57	**0.75**	0.49	**0.76**	0.07	0.51	**0.88**	0.54	0.06	0.61	0.12	**0.95**	-0.50	**1.00**						
BPS	0.16	-0.56	0.56	0.06	0.27	0.46	0.47	-0.22	0.59	0.02	0.05	-0.04	0.18	0.20	0.36	-0.52	0.34	**1.00**					
DOC	0.44	0.65	**-0.76**	0.40	-0.49	-0.36	0.19	-0.40	**-0.82**	-0.13	-0.34	-0.65	0.42	0.02	-0.04	-0.61	-0.04	-0.43	**1.00**				
POC	0.36	0.11	-0.33	0.57	-0.34	-0.53	0.35	-0.28	-0.39	-0.14	-0.11	-0.51	-0.10	-0.39	0.09	-0.26	-0.03	0.02	0.51	**1.00**			
PON	0.45	0.16	-0.32	**0.74**	-0.64	-0.59	0.19	-0.43	-0.58	-0.38	-0.37	-0.57	0.05	-0.35	-0.14	-0.43	-0.22	0.05	0.65	**0.90**	**1.00**		
RD	0.42	0.37	-0.35	0.60	-0.61	-0.59	0.21	-0.53	-0.60	-0.20	-0.24	-0.55	0.35	-0.20	-0.07	**-0.75**	-0.08	-0.05	**0.78**	**0.78**	**0.93**	**1.00**	
WT	-0.55	**-0.85**	0.64	-0.53	0.46	0.36	-0.19	0.66	**0.70**	0.22	0.02	0.11	-0.33	-0.24	0.34	-0.48	0.23	0.37	**-0.89**	-0.31	-0.45	-0.60	**1.00**

Table S5: Contaminant fluxes calculated based on individual contaminant concentrations and river discharge data.

Sampling date	River discharge (m^3 s^{-1})	Σ PAEs (ng L^{-1})	Σ OPEs (ng L^{-1})	Σ BPs (ng L^{-1})	PAE flux (kg day^{-1})	OPE flux (kg day^{-1})	BP flux (kg day^{-1})	Total flux (kg day^{-1})
05/23/2017	1116	513	215	8	49	21	0.8	70.8
06/22/2017	785	251	243	13	17	16	0.9	33.9
08/24/2017	470	269	142	4	11	6	0.2	17.2
09/19/2017	626	541	265	21	29	14	1.1	44.1
11/03/2017	460	262	127	11	10	5	0.4	15.4
11/30/2017	1026	217	159	7	19	14	0.7	33.7
12/12/2017	2772	483	128	8	116	31	2.0	149.0
01/05/2018	3960	285	85	12	97	29	4.0	130.0
02/13/2018	1521	294	110	4	39	14	0.5	53.5
03/01/2018	1566	245	146	8	33	20	1.0	54.0
04/09/2018	2340	97	114	10	20	23	2.1	45.1

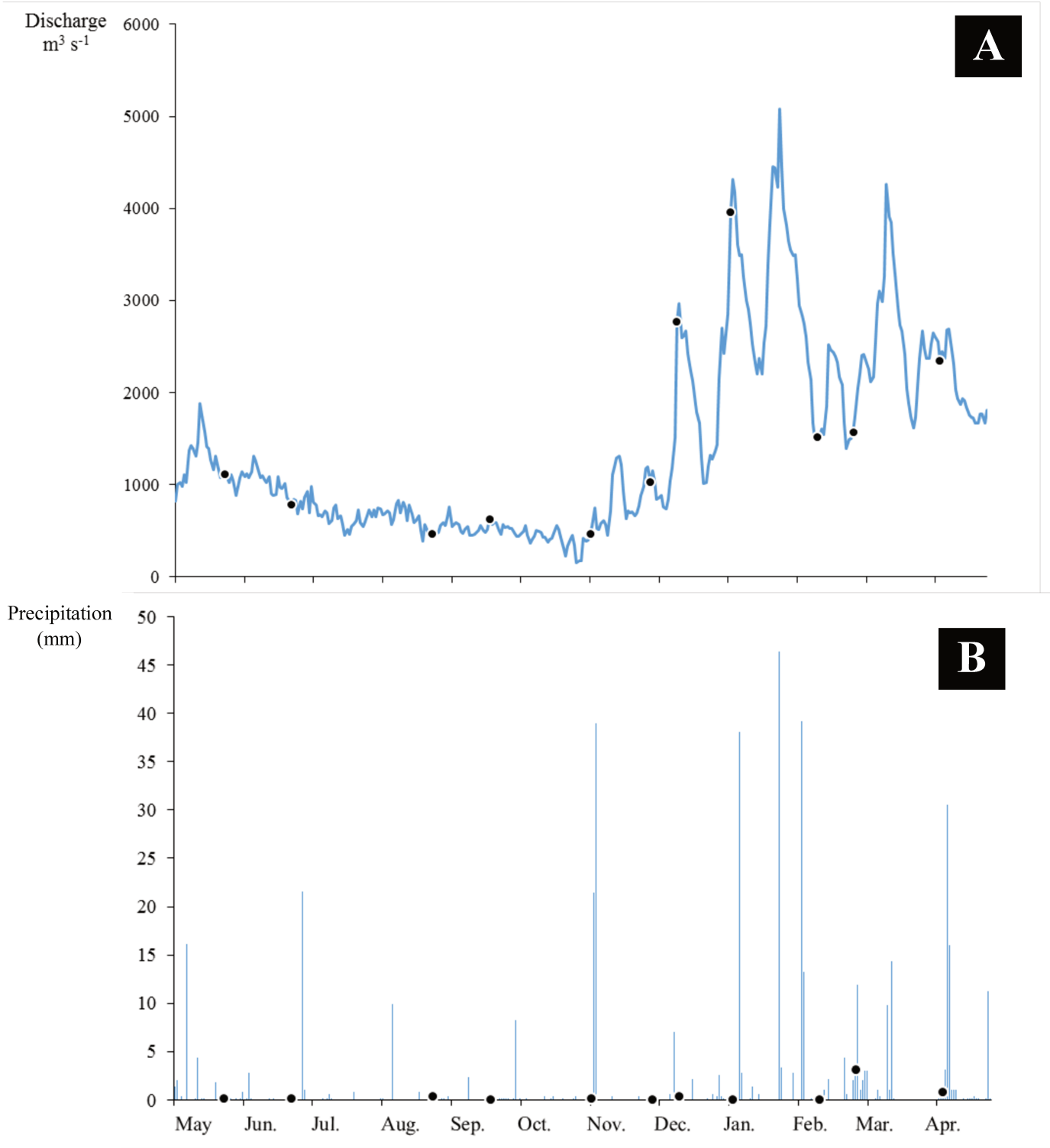

Figure S1: (A) Daily river flow (in m^3 s^{-1}) and (B) daily precipitation (in mm) during the sampling period (May 2017 - April 2018). Black dots indicate sampling events. As before, it is considered that the flow in Arles (sampling station; discharge shown in this figure) corresponds

to ~90% of the flow measured in Tarascon. Precipitation was measured by the French weather service METEO-FRANCE in the commune of Arles, approximately 25 km south of our sampling station.

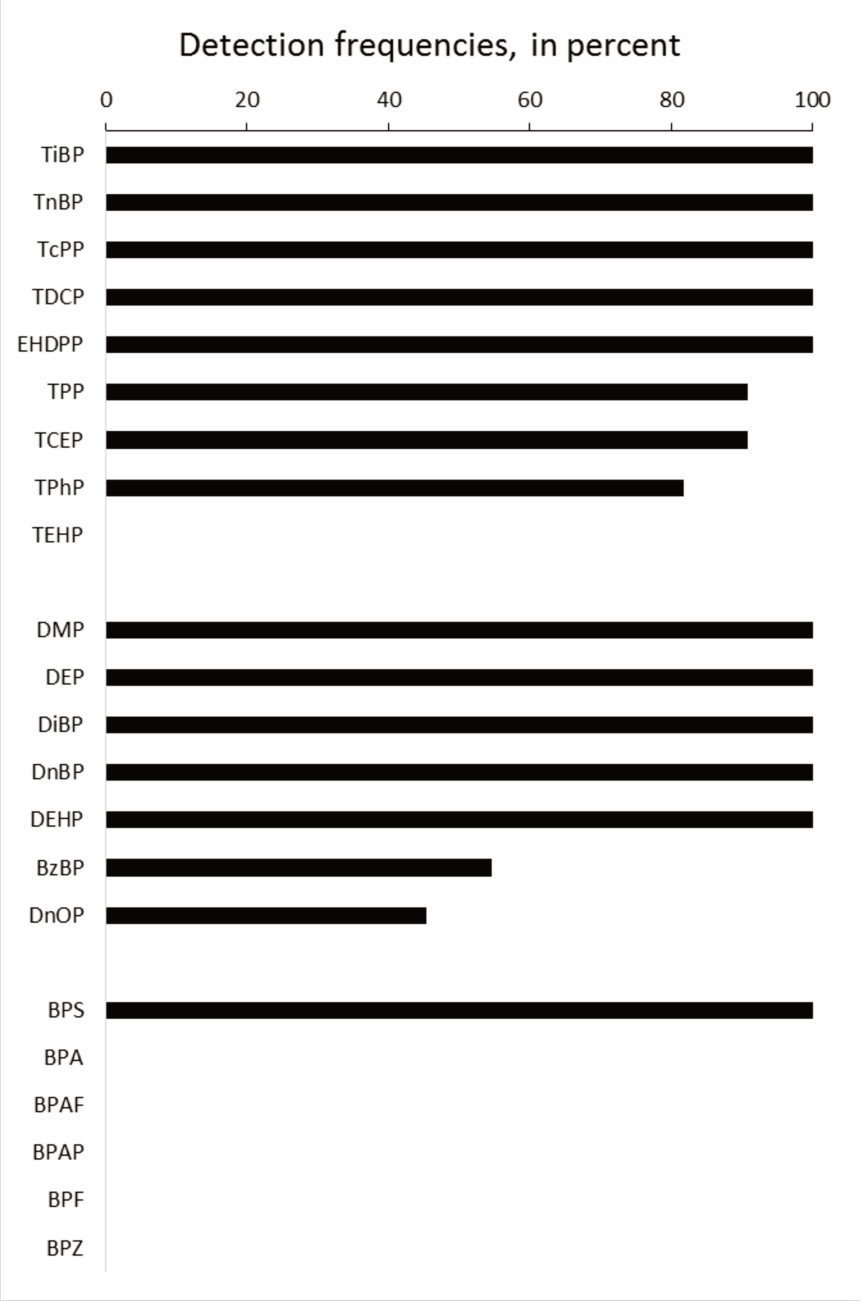

Figure S2: Detection frequencies (in %) of single contaminants.

Annex
Chapter III

Text S1: Method details concerning LC-HRMS injection.

LC-HRMS analysis

10 µL of the extract were injected for the quantification of PFAS using LC-electrospray ionization quadrupole time of flight mass spectrometry (LC-ESI-QTOF, Agilent 1290 Infinity LC system coupled with Agilent 6530 Accurate-Mass Q-TOF, Agilent Technologies, Les Ulis, France). The syringe was washed externally with MeOH for 20 seconds before injection to avoid contamination of injection port or following samples. Separation was achieved on an Agilent Zorbax Eclipse XDB reversed phase column (50 mm x 2.1 mm, 1.8 µm), with temperature set at 30 °C. Elution was performed with MQ (A) and MeOH (B) under gradient conditions: 0 min 95:5 A/B, 1 min 95:5 A/B, 10 min 0:100 A/B, 15 min 0:100 A/B, 15.1 min 95:5 A/B, 20 min 95:5 A/B. ESI interface was operated in negative mode (3.5 kV capillary voltage), and MS TOF mass acquisition was performed in the range 50-600 m/z at a rate of 1 spectrum s^{-1}. ESI parameters were set as follows: 300 °C gas temperature, 11 L min^{-1} drying gas, 40 psig nebulizer, 350 °C sheath gas temperature, 11 L min^{-1} sheath gas flow. TOF parameters were: 1500 V nozzle voltage, 175 V fragmentor voltage, 65 V skimmer voltage, 750 V octopole voltage. Ion chromatogram extraction was performed with 10 ppm mass tolerance, and ± 0.5 min retention time window, based on exact monoisotopic mass and retention time.

Table S1: Station name, sampling date, salinity, temperature, river discharge, DOC, POC and PON data.

Station	Date	Salinity	Temperature (°C)	River discharge ($m^3 s^{-1}$)	DOC (µM)	POC (µg L^{-1})	PON (µg L^{-1})
Rhone River	12/04/2017	-	16.0	805	109	n.a.	n.a.
Rhone River	23/05/2017	-	18.3	1116	114	1217	76
Rhone River	22/06/2017	-	24.6	785	83	235	53
Rhone River	12/07/2017	-	25.2	773	80	273	59
Rhone River	24/08/2017	-	23.5	470	117	268	47
Rhone River	19/09/2017	-	20.9	626	100	286	50
Rhone River	03/11/2017	-	14.0	460	118	185	48
Rhone River	30/11/2017	-	9.4	1026	134	570	74
Rhone River	12/12/2017	-	8.2	2772	164	505	112
Rhone River	05/01/2018	-	8.6	3960	162	2134	303
Rhone River	13/02/2018	-	7.3	1521	145	477	85
Rhone River	01/03/2018	-	5.0	1566	n.a.	417	83
Rhone River	09/04/2018	-	11.7	2340	131	1044	170
Cortiou	09/05/2017	37.0	14.6	-	222	1601	316
Cortiou	06/07/2017	37.7	17.2	-	183	1224	231
Cortiou	08/09/2017	34.1	15.6	-	130	722	159
Cortiou	15/11/2017	37.5	14.4	-	173	1011	191
Cortiou	24/01/2018	31.1	13.5	-	243	987	202
Cortiou	20/03/2018	34.1	13.3	-	141	974	196
L'Estaque	09/05/2017	38.2	14.3	-	68	100	96
L'Estaque	06/07/2017	38.1	18.8	-	n.a.	144	62
L'Estaque	08/09/2017	38.2	15.3	-	76	110	46
L'Estaque	15/11/2017	38.3	14.7	-	65	61	25
L'Estaque	24/01/2018	37.8	13.3	-	66	74	20
L'Estaque	20/03/2018	38.4	13.0	-	67	227	22
Frioul	09/05/2017	38.2	14.6	-	66	158	106
Frioul	06/07/2017	38.2	17.8	-	70	98	64
Frioul	08/09/2017	38.1	15.7	-	84	58	26
Frioul	15/11/2017	38.3	14.7	-	62	54	17
Frioul	24/01/2018	38.3	13.3	-	69	107	38
Frioul	20/03/2018	38.5	13.1	-	73	267	22

n.a. = not available

Table S2: Analytical details for LC-HRMS determination of the 4 target PFAS.

	Monoisotopic mass	Ionic form analyzed	Retention time	Theoretical m/z	Mean m/z measured	Error measured
	g mol-1		min			ppm
PFHxA	313.9801	[M-H+]	7.1	312.9728	312.9717	3.5
PFHxS	399.9439	[M-H+]	7.8	398.9366	398.9345	5.3
PFOA	413.9737	[M-H+]	8.4	412.9664	412.9659	1.2
PFOS	499.9375	[M-H+]	8.7	498.9302	498.9271	6.2
PFHxA 13C	318.9969	[M-H+]	7.1	317.9896	317.9913	5.3
PFOS 13C	507.9643	[M-H+]	8.7	506.9571	506.9599	5.5

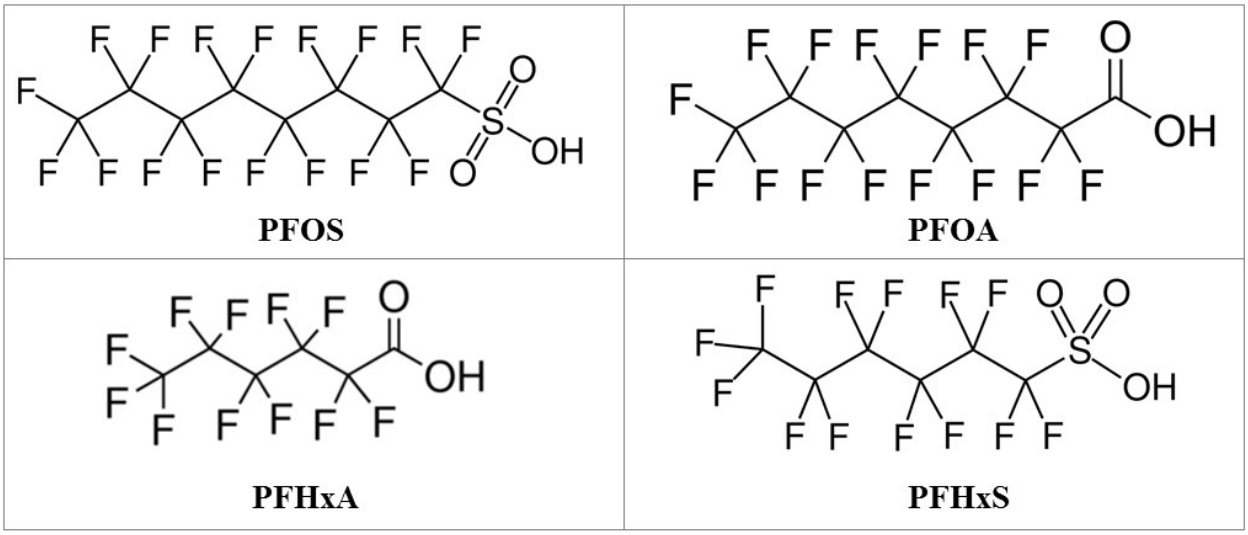

Figure S1: Chemical structures of the four PFAS analyzed in this study.

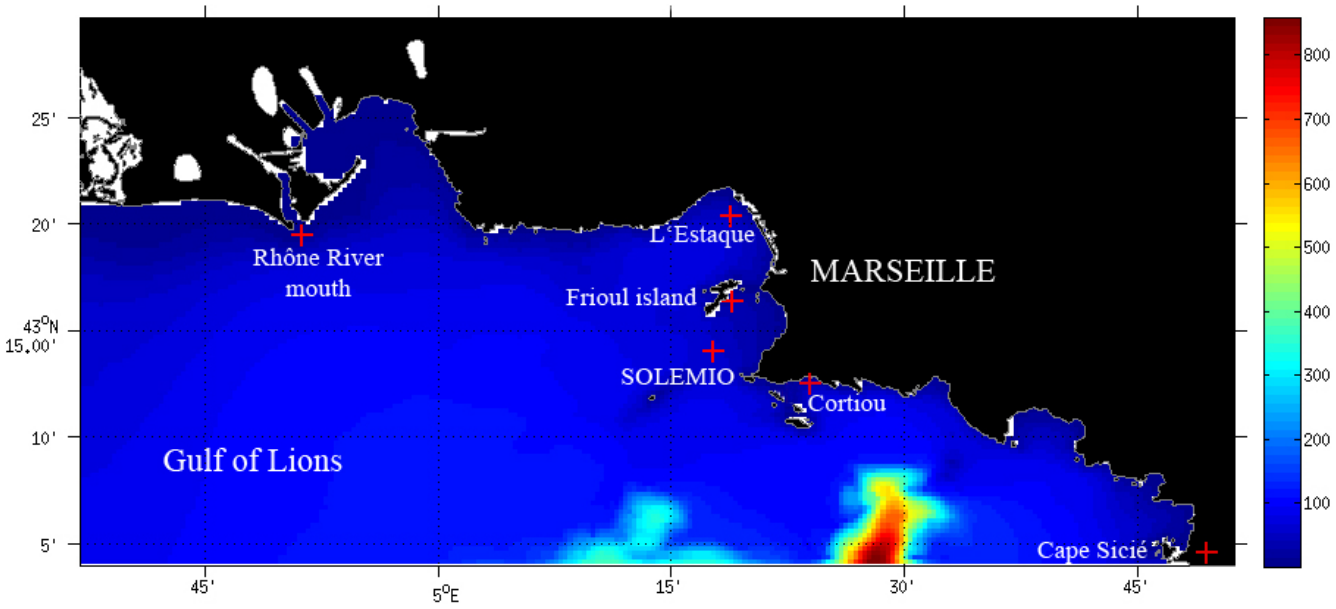

Figure S2: Bathymetric (in m) map of the area covered by the MARS3D model. The three marine sampling stations (L'Estaque, Frioul island, Cortiou) are indicated as well as the Rhône River mouth, Cape Sicié and the SOLEMIO station used in the meteorological WRF model.

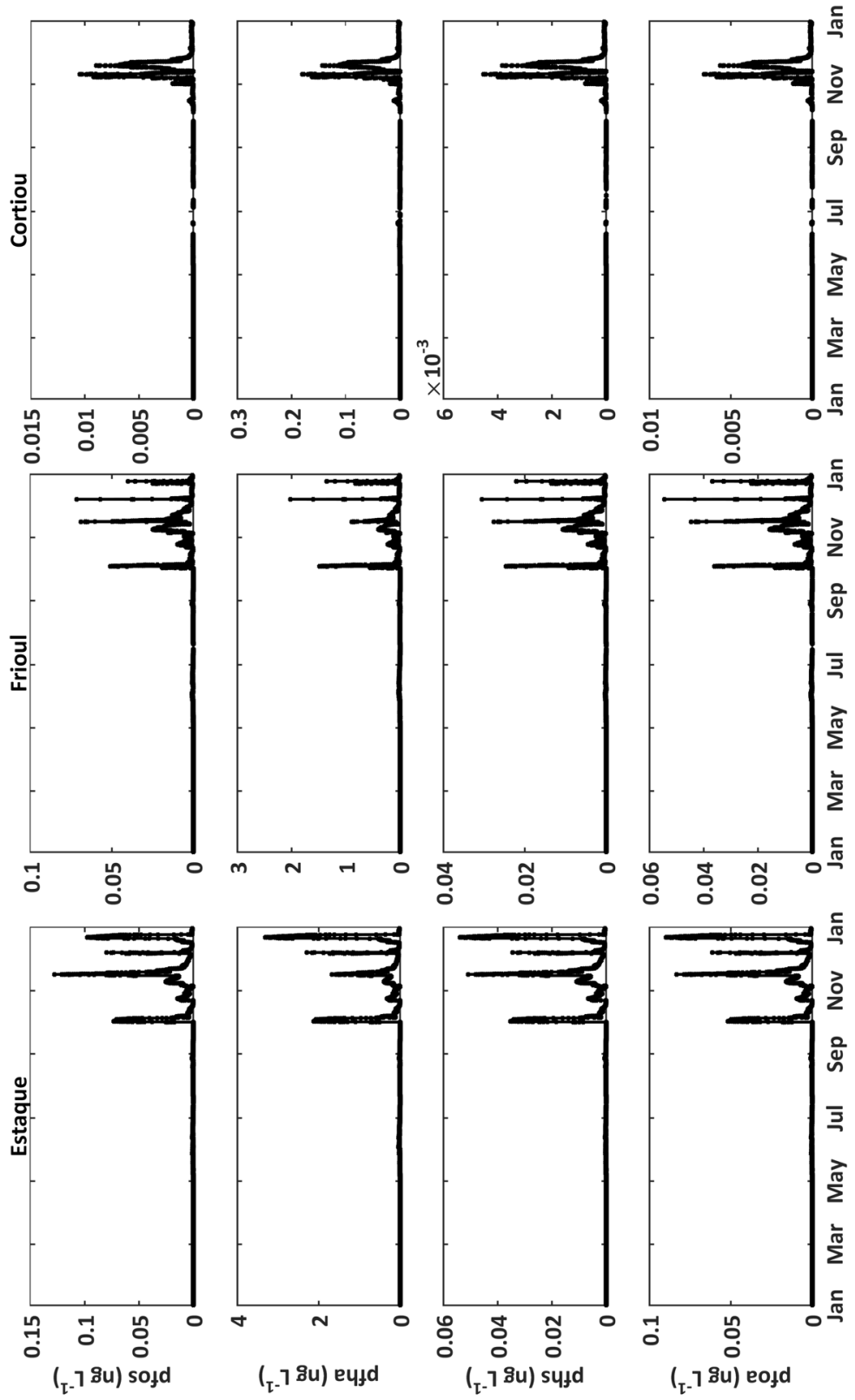

Figure S3: Simulated PFOS, PFHxA, PFHxS and PFOA concentrations (in ng L^{-1}) in L'Estaque, Frioul and Cortiou stations through inputs from the Rhône River. In the simulation, inputs from the Rhône River started in April, in accordance with the beginning of the sampling campaign and chemical analysis.

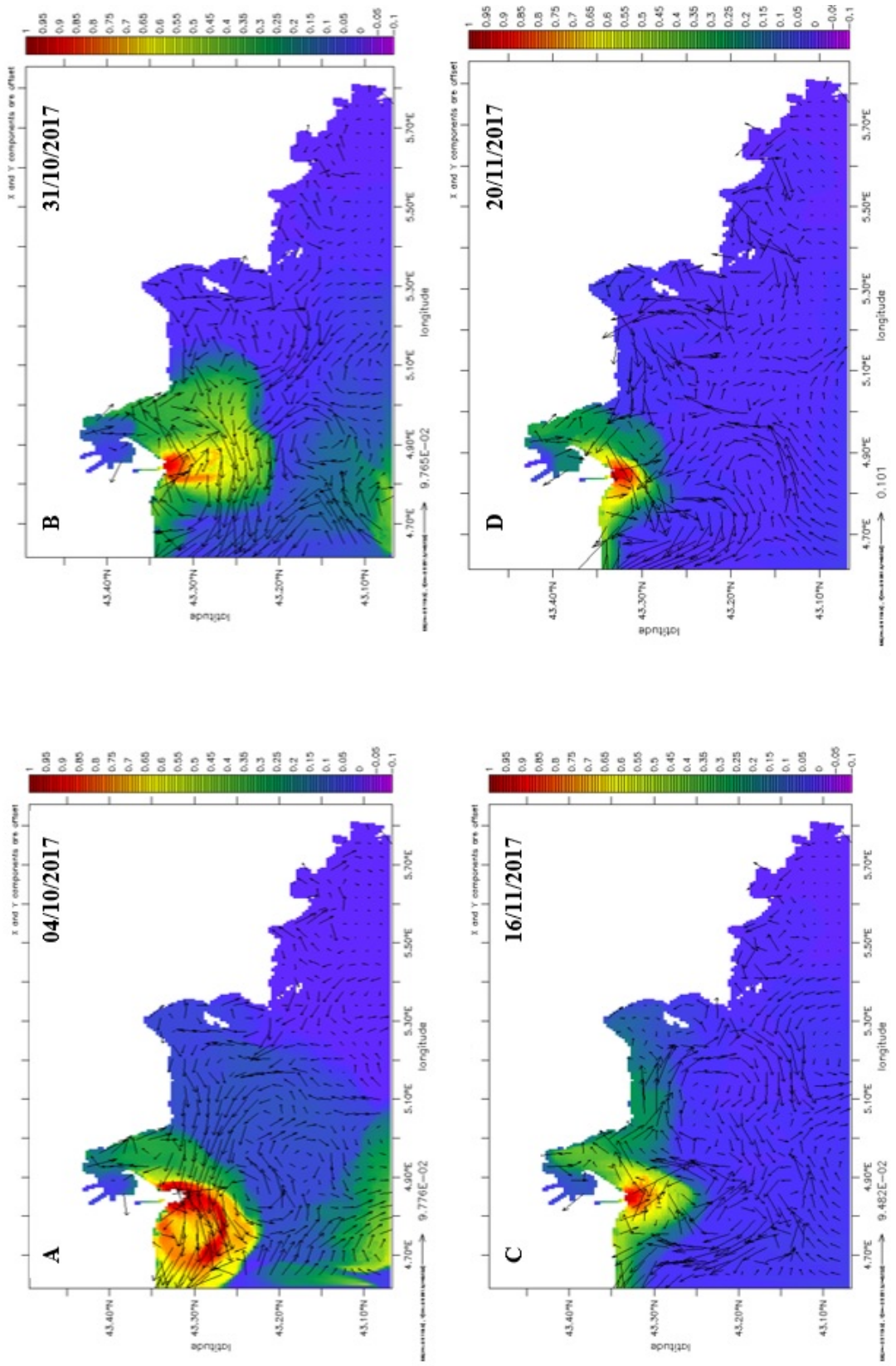

Figure S3: Maps displaying the barotropic currents (black arrows) on the four selected simulation dates as well as the simulated PFOS concentrations (in ng L^{-1}; color bar). Note that dark red values can also represent concentrations > 1 ng L^{-1}.

Annex
Chapter IV

Table S1: Summary of salinity (0.5 m and bottom), temperature (0.5 m and bottom) and depth for each sampling date and sampling station.

Date	ID	Station	Salinity (0.5 m)	Temperature (°C) (0.5 m)	Depth (m)	Salinity (bottom)	Temperature (°C) (bottom)
09/05/2017	S1	L'Estaque	38.2	14.3	42	38.2	14.1
		Frioul	38.2	14.6	35	38.2	14.1
		Cortiou	37.0	14.6	12	38.2	14.3
06/07/2017	S2	L'Estaque	38.0	19.0	33	38.2	14.4
		Frioul	38.2	17.8	34	38.2	14.6
		Cortiou	37.7	17.2	16	38.1	16.0
08/09/2017	S3	L'Estaque	38.2	15.3	40	38.2	14.5
		Frioul	38.1	15.7	35	38.2	14.7
		Cortiou	34.8	15.4	20	38.2	14.5
15/11/2017	S4	L'Estaque	38.3	14.7	44	38.3	14.2
		Frioul	38.3	14.7	33	38.4	14.1
		Cortiou	37.5	14.4	12	38.2	14.5
24/01/2018	S5	L'Estaque	37.8	13.3	43	38.2	13.0
		Frioul	38.3	13.3	34	38.2	13.3
		Cortiou	31.1	13.5	15	38.2	13.4
20/03/2018	S6	L'Estaque	38.4	13.0	42	38.3	13.0
		Frioul	38.5	13.1	34	38.3	13.0
		Cortiou	34.1	13.3	23	38.3	13.2

Table S2: Recoveries (in %) of seven PAEs and nine OPEs in sediment and zooplankton samples (in triplicate).

	Sediment	n = 3	Zooplankton	n = 3
	Recovery (%)	STD (%)	Recovery (%)	STD (%)
DMP	72	1	59	9
DEP	68	3	58	2
DiBP	86	2	69	5
DnBP	103	5	73	5
BzBP	95	4	68	10
DEHP	78	3	97	29
DnOP	103	2	74	6
TPP	63	7	61	11
TiBP	87	4	61	6
TnBP	81	4	75	8
TCEP	46	6	42	9
TCPP	57	28	62	5
TDCP	68	21	44	21
TPhP	71	1	53	11
EHDPP	104	2	81	11
TEHP	99	1	89	12

Table S3: Concentrations of target compounds found in blanks. For water samples, the mean of 2-3 blanks per extraction batch is reported. Concentrations are given in ng L^{-1} (water) or ng g^{-1} (sediment and zooplankton), respectively.

Compound / Matrix	**Water**			**Sediment**					**Zooplankton**					
	BLK 1	BLK 2	BLK 3	BLK 1	BLK 2	BLK 3	BLK 4	BLK 5	BLK 1	BLK 2	BLK 3	BLK 4	BLK 5	BLK 6
DMP	1.52	n.d.	n.d.	n.d.	n.d.	n.d.	n.d.	n.d.	<LOQ	<LOQ	n.d.	n.d.	n.d.	n.d.
DEP	n.d.	2.05	n.d.	1.02	<LOQ	<LOQ	<LOQ	<LOQ	1.18	<LOQ	1.69	1.52	2.01	1.49
DiBP	3.11	24.98	16.53	7.41	5.98	2.35	2.27	1.97	1.75	4.95	2.46	2.41	2.53	5.53
DnBP	1.49	n.d.	n.d.	1.18	0.97	<LOQ	<LOQ	0.97	<LOQ	3.96	<LOQ	1.04	1.04	3.61
BBzP	n.d.	n.d.	n.d.	n.d.	n.d.	n.d.	n.d.	n.d.	n.d.	n.d.	n.d.	n.d.	n.d.	n.d.
DEHP	n.d.	n.d.	34.72	4.45	3.42	10.01	3.70	9.77	7.96	4.81	16.87	22.71	7.36	39.21
DnOP	n.d.	n.d.	n.d.	1.64	n.d.	<LOQ	n.d.	<LOQ	n.d.	n.d.	n.d.	n.d.	n.d.	n.d.
TPP	n.d.	n.d.	n.d.	n.d.	n.d.	n.d.	n.d.	n.d.	n.d.	n.d.	n.d.	n.d.	n.d.	n.d.
TiBP	<LOQ	n.d.	<LOQ	n.d.	n.d.	n.d.	n.d.	n.d.	n.d.	n.d.	n.d.	n.d.	n.d.	n.d.
TnBP	<LOQ	n.d.	n.d.	n.d.	n.d.	n.d.	n.d.	n.d.	<LOQ	<LOQ	<LOQ	<LOQ	<LOQ	n.d.
TCEP	n.d.	n.d.	n.d.	n.d.	n.d.	n.d.	n.d.	n.d.	1.49	1.55	1.54	3.30	n.d.	n.d.
TCPP	4.43	4.11	3.78	8.85	7.28	10.97	9.15	8.60	2.02	1.81	2.09	2.01	14.88	20.53
TDCP	n.d.	n.d.	n.d.	n.d.	n.d.	n.d.	n.d.	n.d.	1.31	1.18	4.53	n.d.	2.55	3.81
TPhP	<LOQ	n.d.	n.d.	n.d.	n.d.	n.d.	n.d.	n.d.	n.d.	n.d.	n.d.	n.d.	n.d.	n.d.
EHDPP	<LOQ	<LOQ	<LOQ	<LOQ	<LOQ	<LOQ	<LOQ	<LOQ	<LOQ	n.d.	n.d.	<LOQ	<LOQ	n.d.
TEHP	n.d.	n.d.	n.d.	n.d.	n.d.	n.d.	n.d.	n.d.	n.d.	n.d.	n.d.	n.d.	n.d.	n.d.

n.d. = not detected, LOQ = limit of quantification

Table S4: Average and median bioconcentration factors (BCF) for seven phthalates and nine organophosphate esters, calculated for the three zooplankton size classes.

	Average			**Median**		
	> 1 mm	*<1 mm, >500 µm*	*<500 µm, >150 µm*	*> 1 mm*	*<1 mm, >500 µm*	*<500 µm, >150 µm*
DMP	32,829	3,359	7,805	8,733	1,880	3,250
DEP	518	523	697	410	359	519
DnBP	5,384	3,770	5,680	3,480	2,654	1,902
DiBP	979	275	690	687	264	350
BzBP	30,547	29,354	25,699	31,857	25,500	23,333
DEHP	6,944	5,942	13,216	3,567	2,455	4,556
DnOP	55,653	47,122	100,294	65,500	33,747	50,000
TPP	n.a.	n.a.	n.a.	n.a.	n.a.	n.a.
TiBP	183,125	27,255	138,400	28,133	8,533	7,211
TnBP	4,250	2,771	6,481	2,100	1,257	2,460
TCEP	25,009	79,596	50,671	1,834	14,414	22,737
TCPP	1,636	2,839	3,363	1,754	868	1,618
TDCP	6,216	27,976	84,756	4,724	3,335	5,847
TPhP	4,579	9,442	7,306	1,730	3,934	1,147
EHDPP	7,448	11,508	24,281	6,107	6,191	12,633
TEHP	n.a.	41,922	116,933	n.a.	11,167	116,933

n.a. = not available.

Annex
Chapter V

Supporting Information for
The Amazon River – a major source of organic plastic additives to the tropical North Atlantic?

Natascha Schmidt [1], Vincent Fauvelle [1], Anouck Ody [1], Javier Castro-Jiménez [1], Julien Jouanno [2], Thomas Changeux [1], Thierry Thibaut [1], Richard Sempéré [1,*]

[1] *Aix-Marseille Univ., Toulon Univ., CNRS, IRD, Mediterranean Institute of Oceanography (M I O), Marseille, France*
[2] *LEGOS, Université de Toulouse, IRD, CNRS, CNES, UPS, Toulouse, France*
* corresponding author; E-Mail: richard.sempere@mio.osupytheas.fr

CONTENTS: 26 pages including 1 text, 6 figures and 7 tables.

SUPPLEMENTARY TEXTS
Text S1: Method details concerning GC-MS and LC-HRMS analysis.

SUPPLEMENTARY FIGURES
Figure S1: Comparisons between salinity maps of each station and different sizes of seeded particle patches (5 km, 10 km, 16 km, 25 km and 50 km).
Figure S2: Detection frequencies (in %) of all 20 organic compounds analyzed.
Figure S3: Spatial salinity distribution of the surface waters of the study area during each sampling day.
Figure S4: Spatial distribution of Kd490 (unit 1/m) in October 2017.
Figure S5: Backwards trajectories of all stations.
Figure S6: Air mass backward trajectories modelled for each sampling station using the NOAA HYSPLIT Model.

SUPPLEMENTARY TABLES
Table S1: GPS positions of the sampling stations, collection dates and surface salinity.
Table S2: Quantification and confirmation ions of OPEs (GC/MS).
Table S3: $[M-H]^-$ values for BPs and PFCs quantification by LC-HRMS Agilent LC-QTOF 6530.
Table S4: Limits of quantification (LOQ) expressed as absolute amounts (pg) and ng L^{-1} in seawater.
Table S5: Concentrations (in ng L^{-1}) of all 20 molecules analyzed for each sampling station as well as extraction, transport and laboratory blank values.
Table S6: Surrogate recovery rates (in %) for each sampling station and the extraction blanks.
Table S7: Sensitivity tests results for radii from 5 to 25 km and densities from 0.5 to 2.5 particles km^{-2}.

SUPPLEMENTARY TEXTS

Text S1: Method details concerning GC-MS and LC-HRMS analysis.

GC-MS analysis (Organophosphate ester analysis)

GC analyses were conducted with an Agilent 7820A Series GC coupled with an Agilent 5977E MS, operating in SIM and electron impact (EI, 70 eV) modes. The separation was achieved in a 30 m x 0.25 mm i.d. x 0.25 µm HP-5MS capillary column (Agilent J&W). All target contaminants were quantified by the internal standard (IS) procedure. The injection volume was 2 µL and the helium carrier gas flow was 1 mL min^{-1}. The temperatures of the MS transfer line, the ion source and the quadrupole was set to 300, 230 and 150 ºC, respectively. The following conditions were applied: injector temperature: 270 ºC (splitless) and the oven was programmed from 90 ºC to 132 ºC at 3 ºC min^{-1}, to 166 ºC at 10 ºC min^{-1}, to 175 at 1 ºC min^{-1} (holding time 2 min), to 232 ºC at 2 ºC min^{-1}, and then to 300 °C at 25 ºC min^{-1} (holding time 5 min).

LC-QTOF analysis (bisphenol and perfluorinated compound analysis)

Ten microliters of the extract were injected for simultaneous quantification of BPs and PFCs using LC-electrospray ionization quadrupole time of flight mass spectrometry (LC-ESI-QTOF, Agilent 1290 Infinity LC system coupled with Agilent 6530 Accurate-Mass Q-TOF, Agilent Technologies, Les Ulis, France). The syringe was washed externally with MeOH for 20 s before injection to avoid contamination of the injection port or following samples. Separation was achieved on an Agilent Zorbax Eclipse XDB reversed phase column (50 mm x 2.1 mm, 1.8 µm), with the temperature set at 30 °C. Elution was performed with MQ (A) and MeOH (B) under gradient conditions: 0 min 95:5 A/B, 1 min 95:5 A/B, 10 min 0:100 A/B, 15 min 0:100 A/B, 15.1 min 95:5 A/B, 20 min 95:5 A/B. ESI interface was operated in negative mode (3.5 kV capillary voltage), and MS TOF mass acquisition was performed in the range of 50-600 m/z at a rate of 1 spectrum s^{-1}. ESI parameters were set as follows: 300 °C gas temperature, 11 L min^{-1} drying gas, 40 psig nebulizer, 350 °C sheath gas temperature, 11 L min^{-1} sheath gas flow. TOF parameters were: 1500 V nozzle voltage, 175 V fragmentor voltage, 65 V skimmer voltage, 750 V octopole voltage. Ion chromatogram extraction was performed with 10 ppm mass tolerance, based on exact monoisotopic mass and retention time.

SUPPLEMENTARY FIGURES

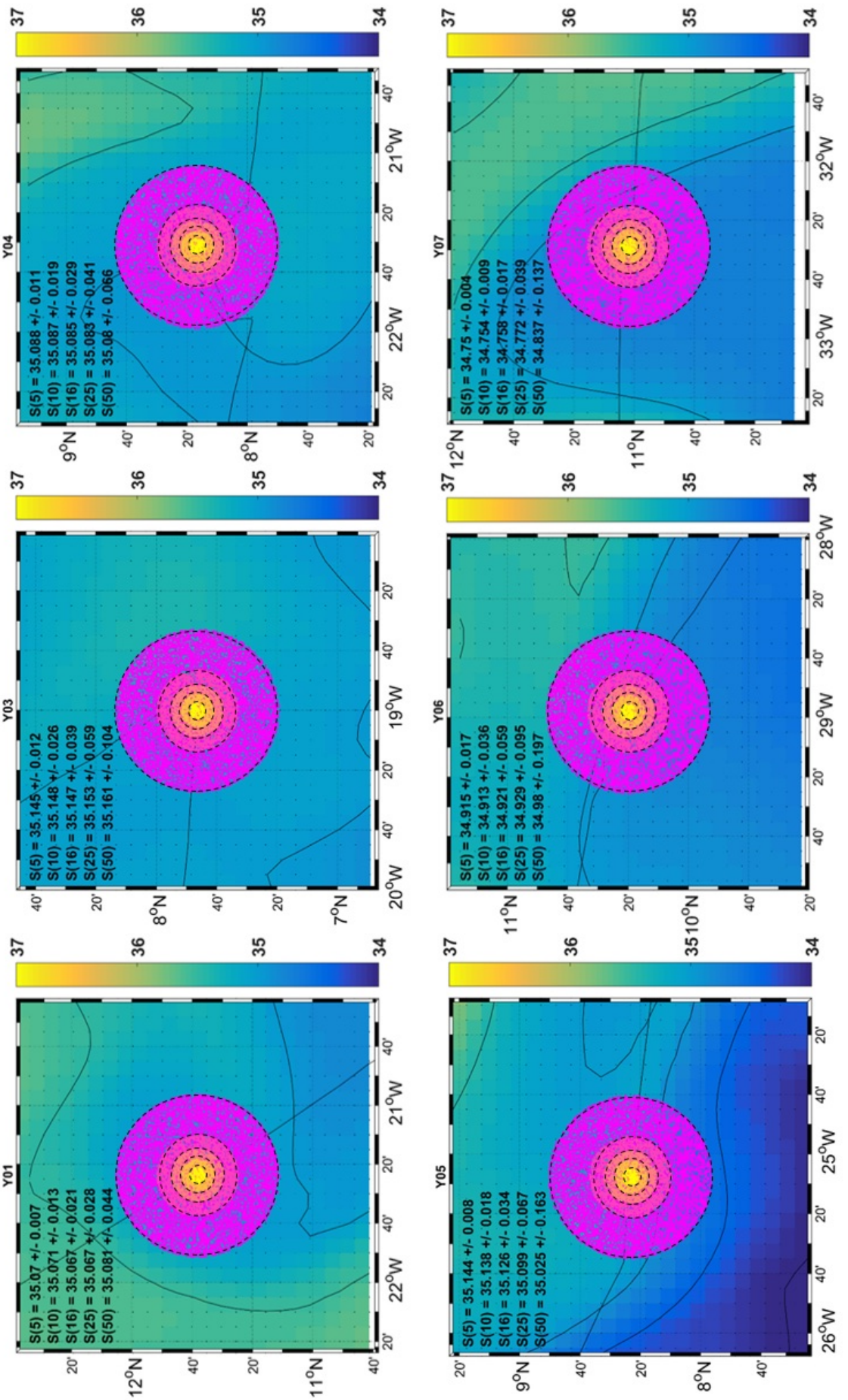

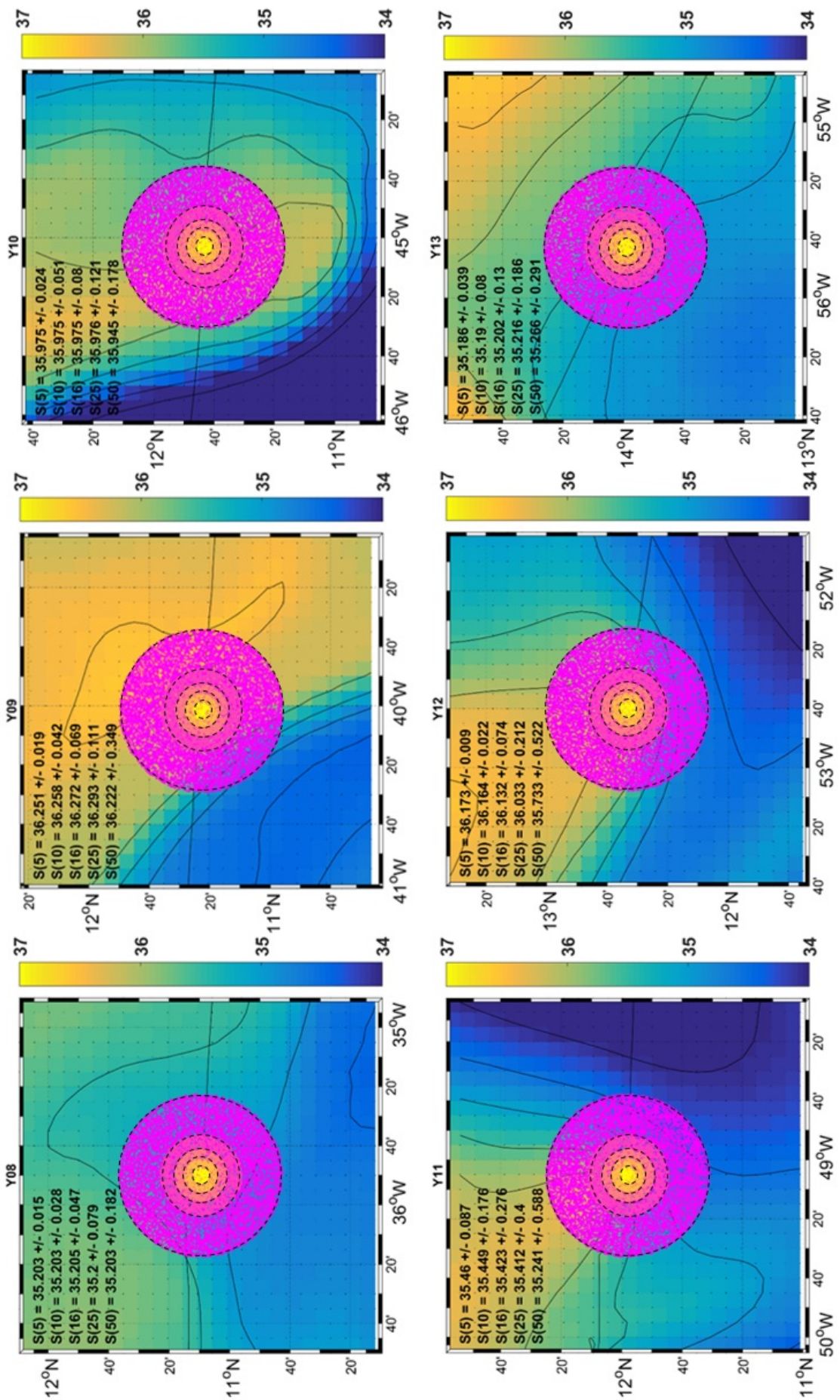
Y08
S(5) = 35.203 +/- 0.015
S(10) = 35.203 +/- 0.028
S(16) = 35.205 +/- 0.047
S(25) = 35.2 +/- 0.079
S(50) = 35.203 +/- 0.182
Y09
S(5) = 36.251 +/- 0.019
S(10) = 36.258 +/- 0.042
S(16) = 36.272 +/- 0.069
S(25) = 36.293 +/- 0.111
S(50) = 36.222 +/- 0.349
Y10
S(5) = 35.975 +/- 0.024
S(10) = 35.975 +/- 0.051
S(16) = 35.975 +/- 0.08
S(25) = 35.976 +/- 0.121
S(50) = 35.945 +/- 0.178
Y11
S(5) = 35.46 +/- 0.087
S(10) = 35.449 +/- 0.176
S(16) = 35.423 +/- 0.276
S(25) = 35.412 +/- 0.4
S(50) = 35.241 +/- 0.588
Y12
S(5) = 36.173 +/- 0.009
S(10) = 36.164 +/- 0.022
S(16) = 36.132 +/- 0.074
S(25) = 36.033 +/- 0.212
S(50) = 35.733 +/- 0.522
Y13
S(5) = 35.186 +/- 0.039
S(10) = 35.19 +/- 0.08
S(16) = 35.202 +/- 0.13
S(25) = 35.216 +/- 0.186
S(50) = 35.266 +/- 0.291

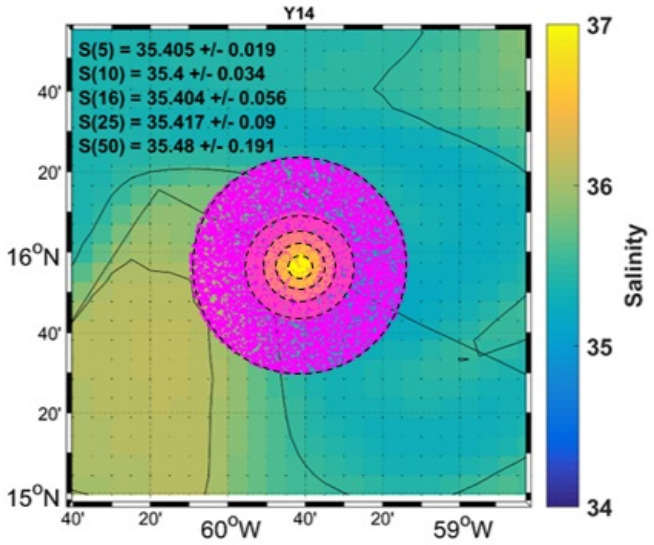

Figure S1: Comparisons between salinity maps of stations Y01-Y14 and different sizes of seeded particle patches (5 km, 10 km, 16 km, 25 km and 50 km). For each patch size, the mean salinity inside the patch and the standard deviation are reported. Black solid lines represent salinity contours for salinity values of 34, 35, 36 and 37. It can be observed that for a patch radius of 50 km, the particles are seeded over a high range of salinities, likely representing different water masses.



Figure S2: Detection frequencies (in %) of the 20 organic compounds analyzed. Abbreviations: TPP: Tripropyl phosphate, TiBP: Tri-iso-buthyl phosphate, TnBP: Tri-n-butyl phosphate, TCEP: Tris-(2-chloroethyl) phosphate, TCPP: Tris-(2-chloro, 1-methylethyl) phosphate, TDCP: Tris-(2-chloro-, 1-chloromethylethyl) phosphate, TPhP: Triphenyl phosphate, EHDPP: 2-ethylhexyl-diphenyl phosphate, TEHP: Tris(2-ethylhexyl) phosphate, BPA: Bisphenol A, BPAF: Bisphenol AF, BPAP: Bisphenol AP, BPF: Bisphenol F, BPS: Bisphenol S, BPZ: Bisphenol Z, PFHA: Perfluoro hexanoic acid, PFHS: Perfluorohexane sulfonic acid, PFOA: Perfluorooctanoic acid, PFOS: Perfluorooctane sulfonic acid, PFOSF: Perfluoro octane sulfonyl fluoride.

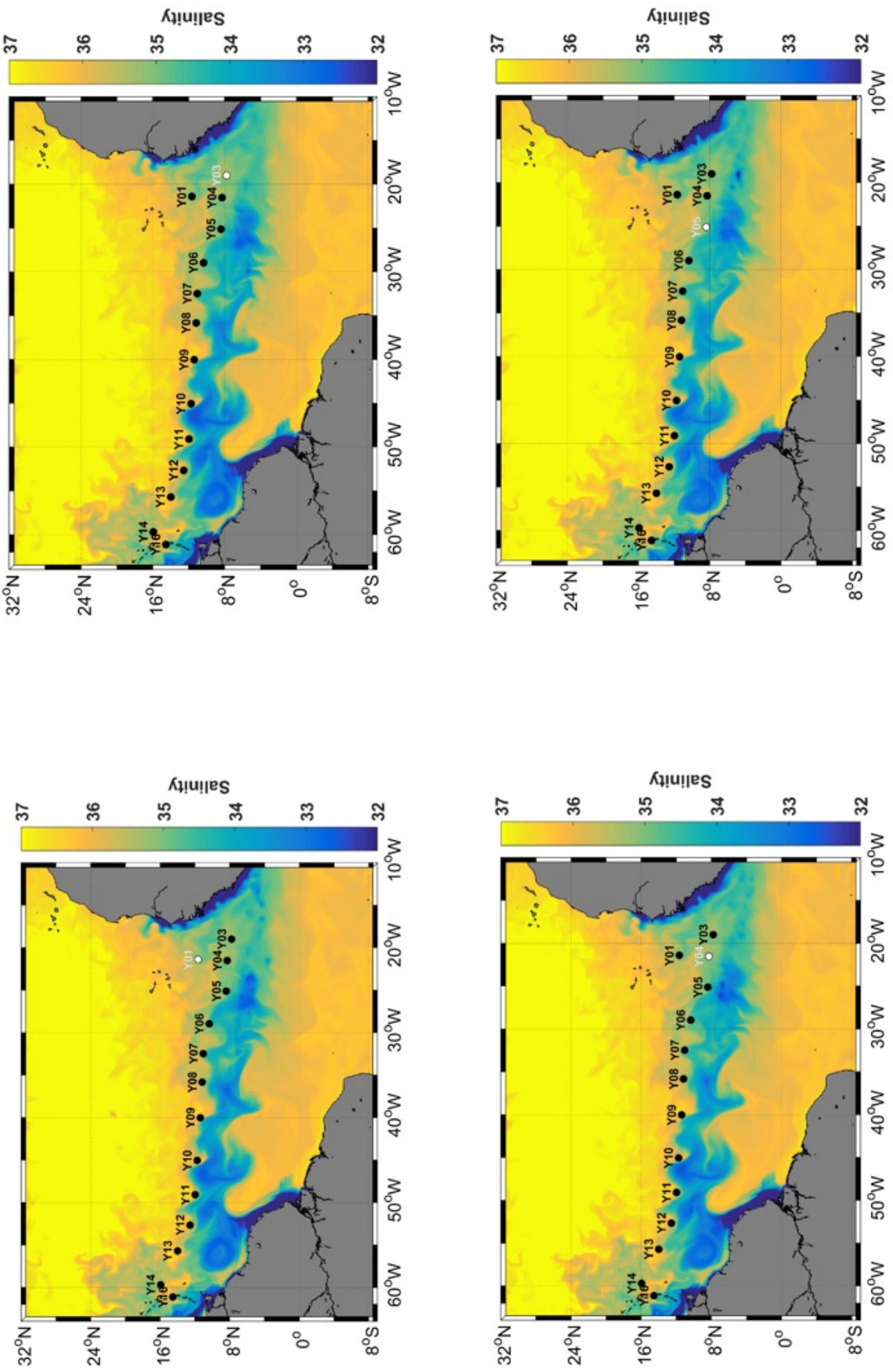
Salinity
37
36
35
34
33
32
32°N
24°N
16°N
8°N
0°
8°S
60°W
50°W
40°W
30°W
20°W
10°W
Y01
Y02
Y03
Y04
Y05
Y06
Y07
Y08
Y09
Y10
Y11
Y12
Y13
Y14
Y15

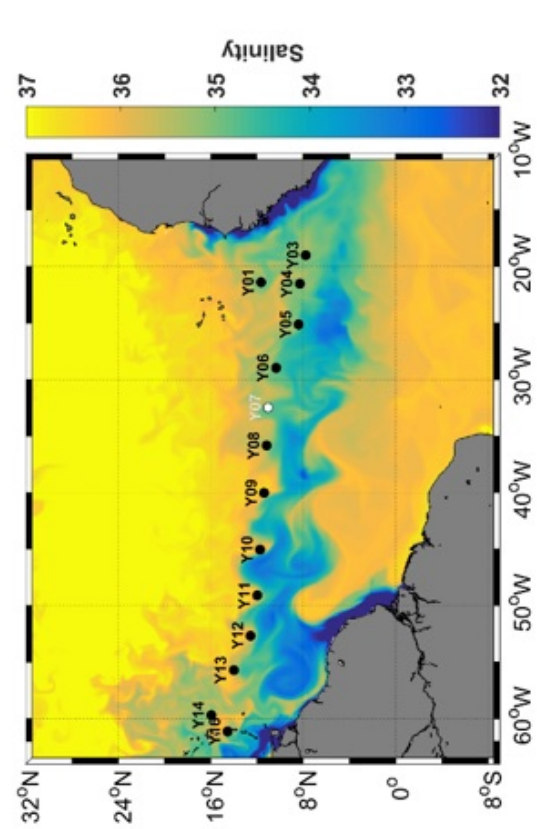
Salinity
37
36
35
34
33
32
32°N
24°N
16°N
8°N
0°
8°S
60°W
50°W
40°W
30°W
20°W
10°W
Y01
Y03
Y04
Y05
Y06
Y07
Y08
Y09
Y10
Y11
Y12
Y13
Y14
Y15

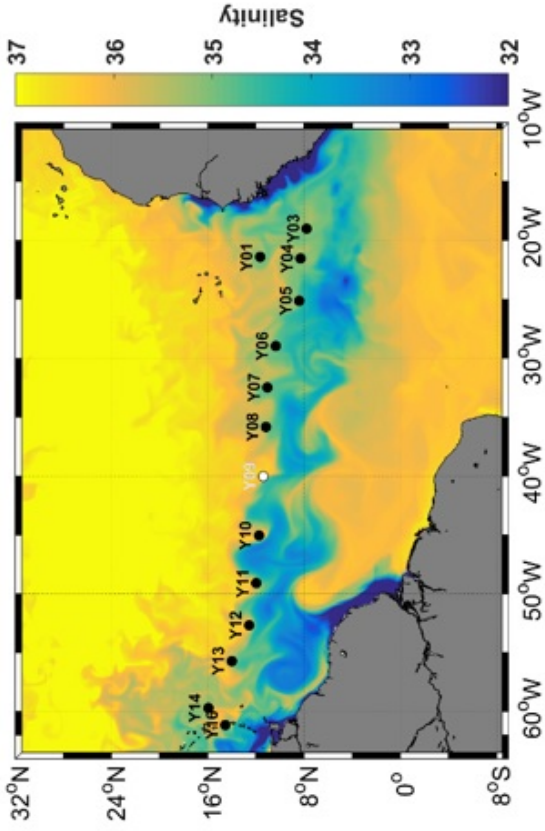
Salinity
37
36
35
34
33
32
32°N
24°N
16°N
8°N
0°
8°S
60°W
50°W
40°W
30°W
20°W
10°W
Y01
Y03
Y04
Y05
Y06
Y07
Y08
Y09
Y10
Y11
Y12
Y13
Y14
Y15

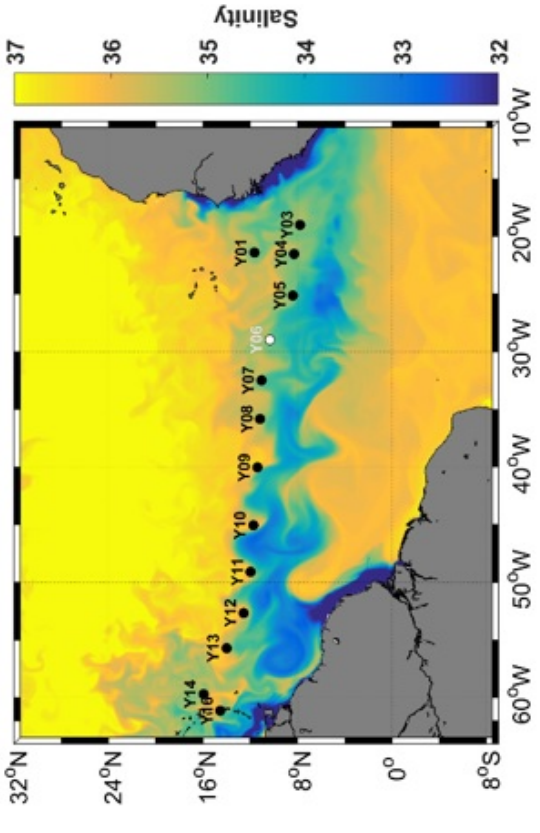
Salinity
37
36
35
34
33
32
32°N
24°N
16°N
8°N
0°
8°S
60°W
50°W
40°W
30°W
20°W
10°W
Y01
Y03
Y04
Y05
Y06
Y07
Y08
Y09
Y10
Y11
Y12
Y13
Y14
Y15

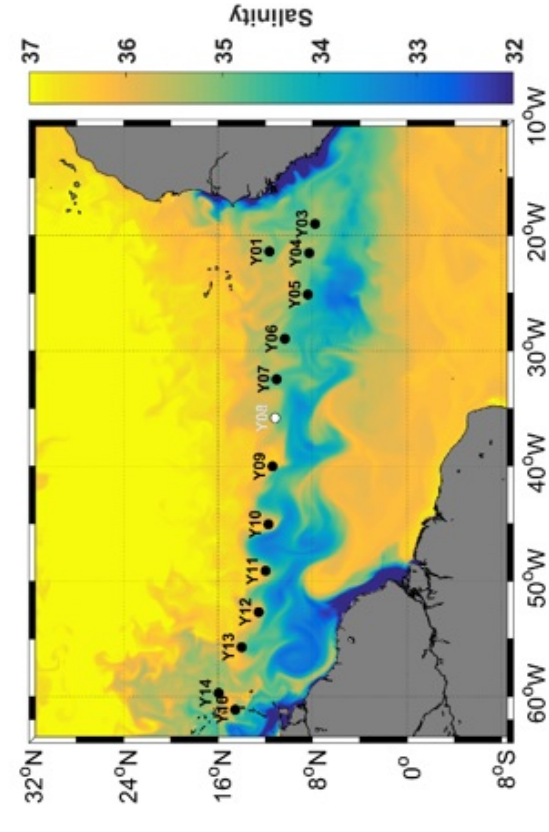
Salinity
37
36
35
34
33
32
32°N
24°N
16°N
8°N
0°
8°S
60°W
50°W
40°W
30°W
20°W
10°W
Y01
Y03
Y04
Y05
Y06
Y07
Y08
Y09
Y10
Y11
Y12
Y13
Y14
Y15

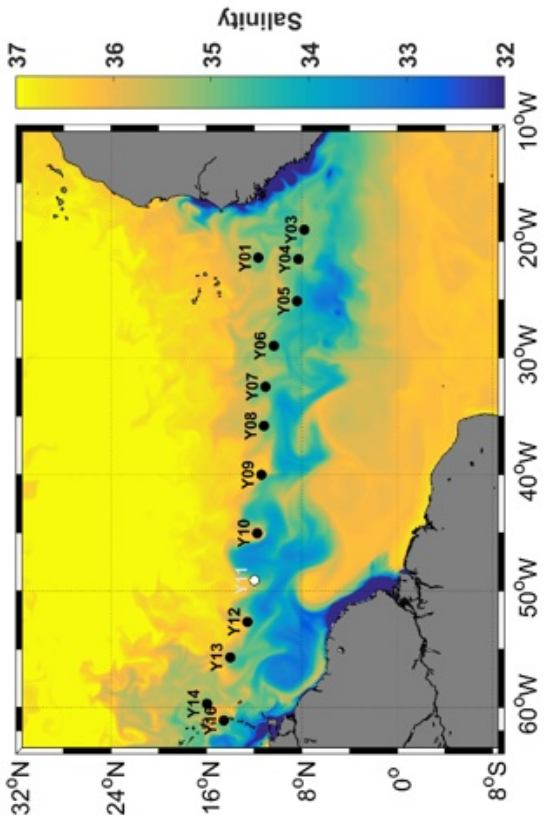
Salinity
37
36
35
34
33
32
10°W
20°W
30°W
40°W
50°W
60°W
32°N
24°N
16°N
8°N
0°
8°S
Y01
Y03
Y04
Y05
Y06
Y07
Y08
Y09
Y10
Y11
Y12
Y13
Y14

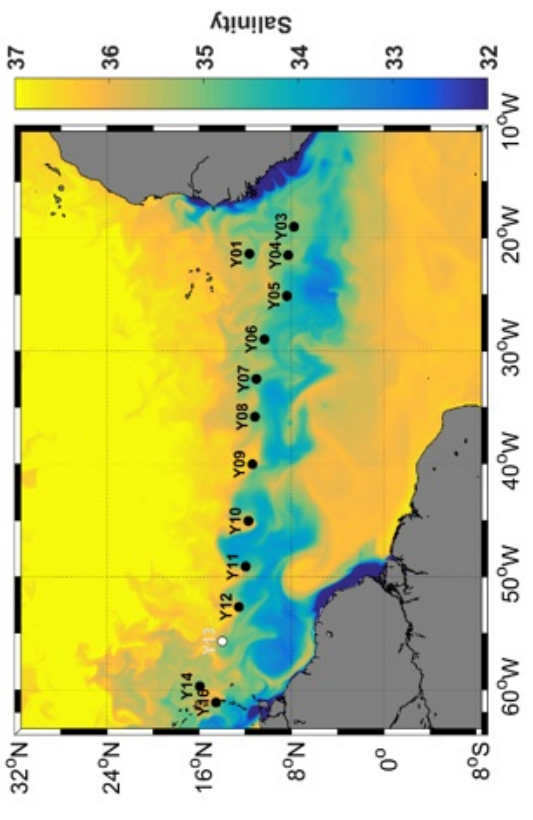
Salinity
37
36
35
34
33
32
10°W
20°W
30°W
40°W
50°W
60°W
32°N
24°N
16°N
8°N
0°
8°S
Y01
Y03
Y04
Y05
Y06
Y07
Y08
Y09
Y10
Y11
Y12
Y13
Y14

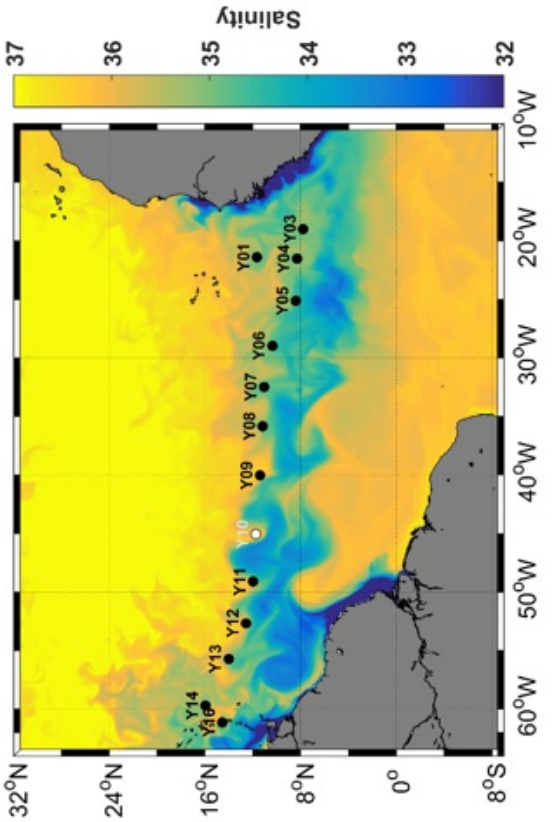
Salinity
37
36
35
34
33
32
10°W
20°W
30°W
40°W
50°W
60°W
32°N
24°N
16°N
8°N
0°
8°S
Y01
Y03
Y04
Y05
Y06
Y07
Y08
Y09
Y10
Y11
Y12
Y13
Y14

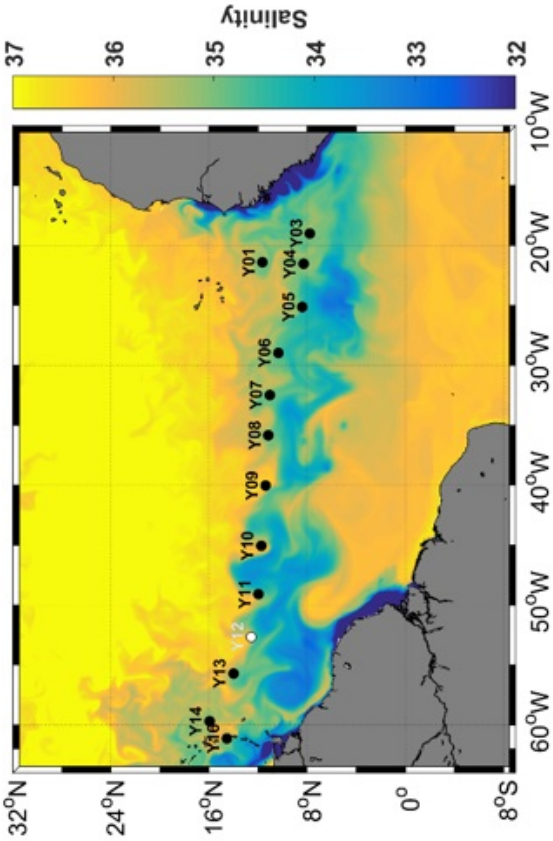
Salinity
37
36
35
34
33
32
10°W
20°W
30°W
40°W
50°W
60°W
32°N
24°N
16°N
8°N
0°
8°S
Y01
Y03
Y04
Y05
Y06
Y07
Y08
Y09
Y10
Y11
Y12
Y13
Y14

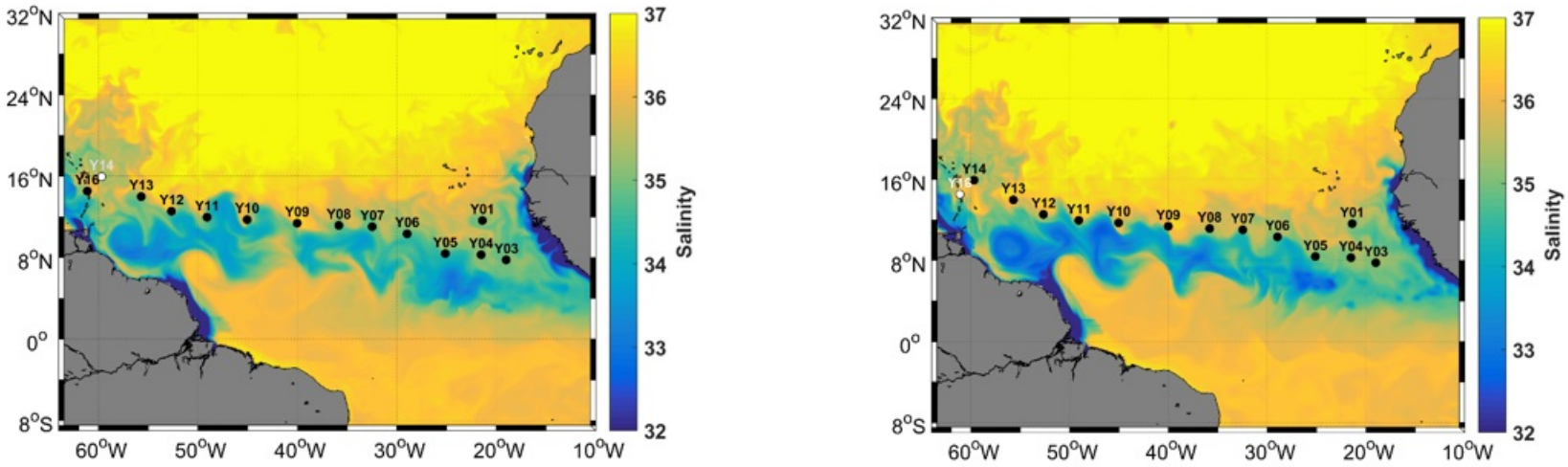

Figure S3: Spatial salinity distribution of the surface waters of the study area during each sampling day. The stations indicated in white are the ones sampled the day from which the MERCATOR salinity data originates.

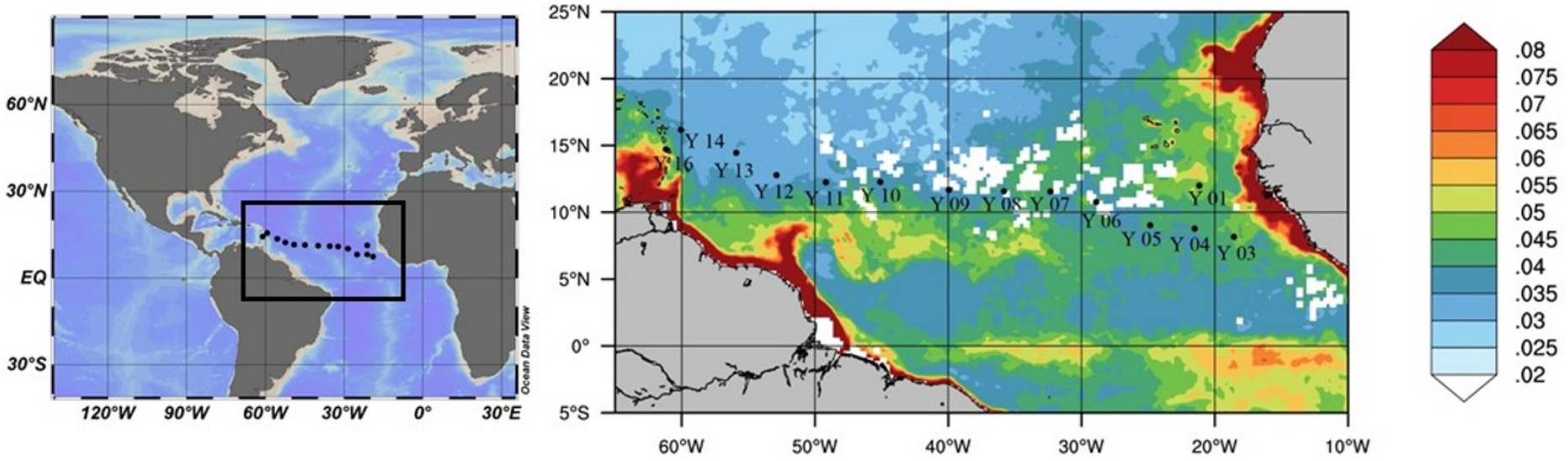

Figure S4: Map showing the position of the sampling area (left) and a zoom (right) showing the sampling stations with the spatial distribution of Kd490 (unit 1/m) in October 2017. Kd490 is a proxy for colored suspended matter and can be used to assess the chlorophyll a distribution.

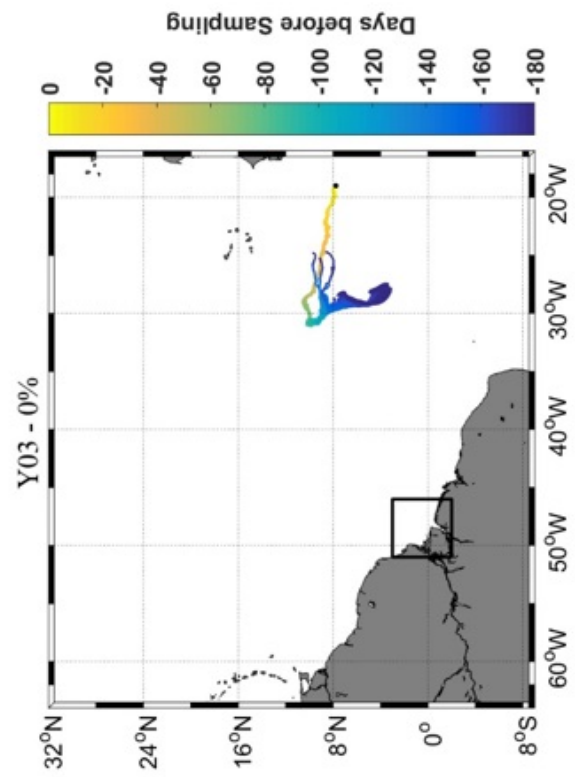
Y03 - 0%
Days before Sampling
0
-20
-40
-60
-80
-100
-120
-140
-160
-180
32°N
24°N
16°N
8°N
0°
8°S
60°W
50°W
40°W
30°W
20°W

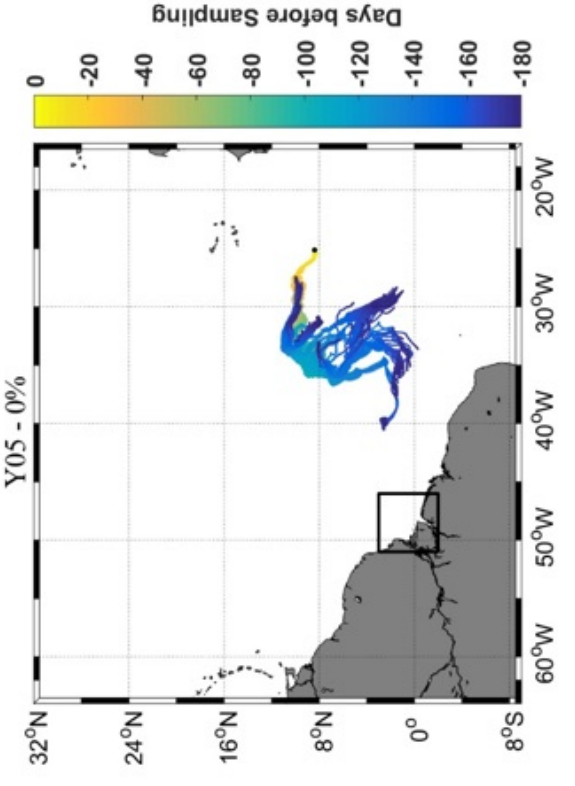
Y05 - 0%
Days before Sampling
0
-20
-40
-60
-80
-100
-120
-140
-160
-180
32°N
24°N
16°N
8°N
0°
8°S
60°W
50°W
40°W
30°W
20°W

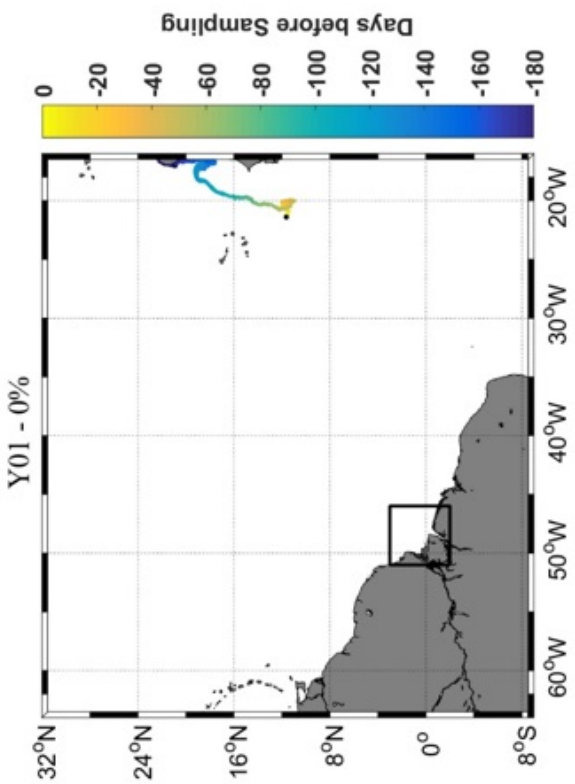
Y01 - 0%
Days before Sampling
0
-20
-40
-60
-80
-100
-120
-140
-160
-180
32°N
24°N
16°N
8°N
0°
8°S
60°W
50°W
40°W
30°W
20°W

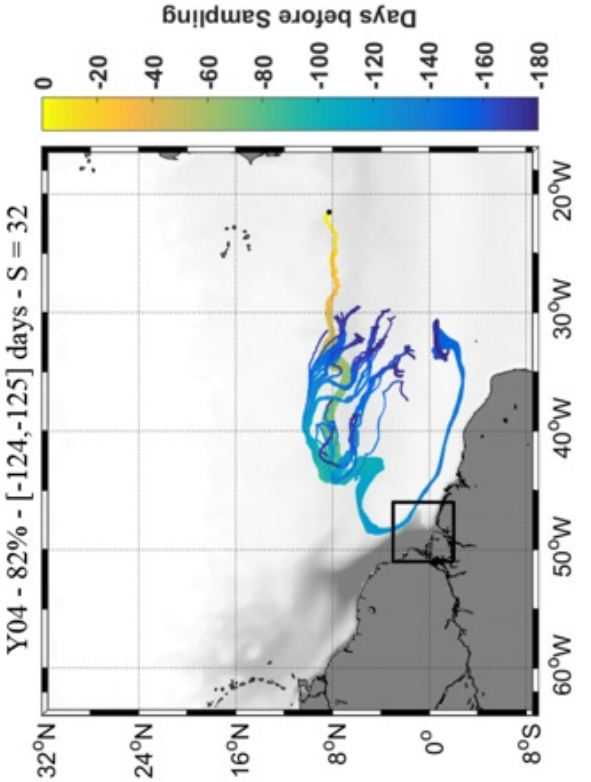
Y04 - 82% - [-124,-125] days - S = 32
Days before Sampling
0
-20
-40
-60
-80
-100
-120
-140
-160
-180
32°N
24°N
16°N
8°N
0°
8°S
60°W
50°W
40°W
30°W
20°W

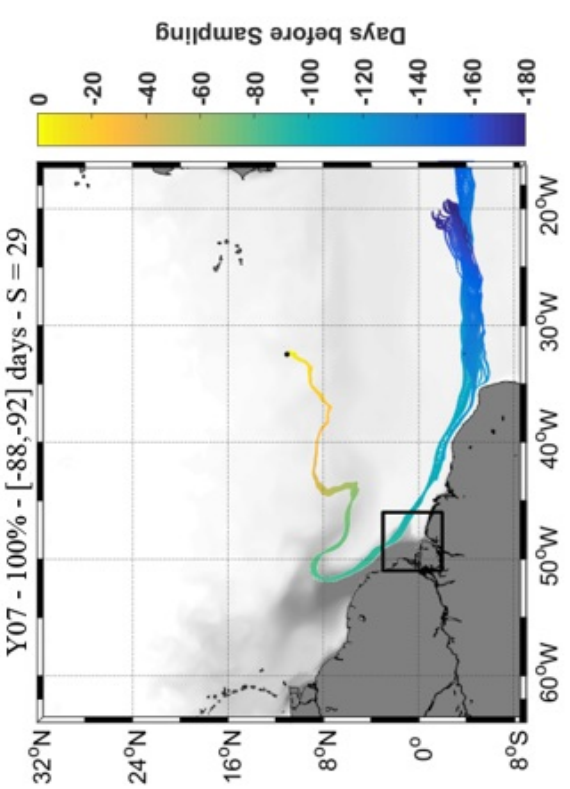
Y07 - 100% - [-88,-92] days - S = 29
Days before Sampling
0
-20
-40
-60
-80
-100
-120
-140
-160
-180
32°N
24°N
16°N
8°N
0°
8°S
60°W
50°W
40°W
30°W
20°W

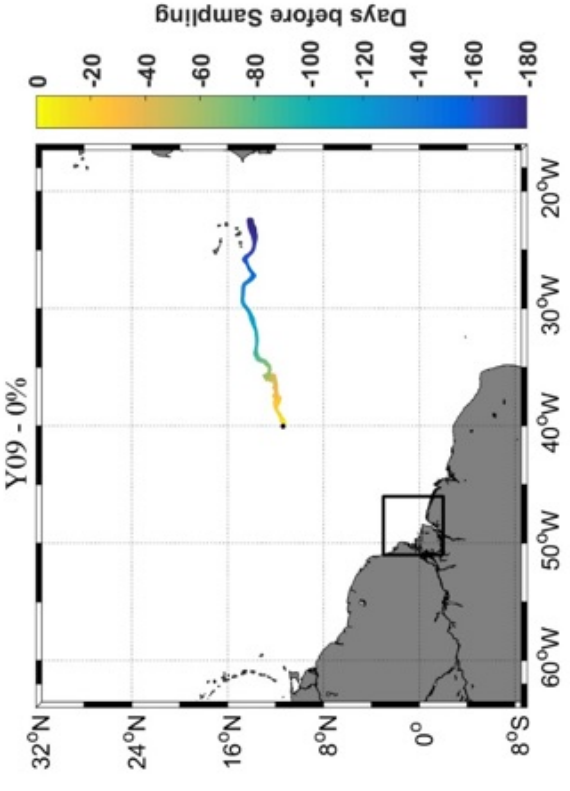
Y09 - 0%
Days before Sampling
0
-20
-40
-60
-80
-100
-120
-140
-160
-180
32°N
24°N
16°N
8°N
0°
8°S
60°W
50°W
40°W
30°W
20°W

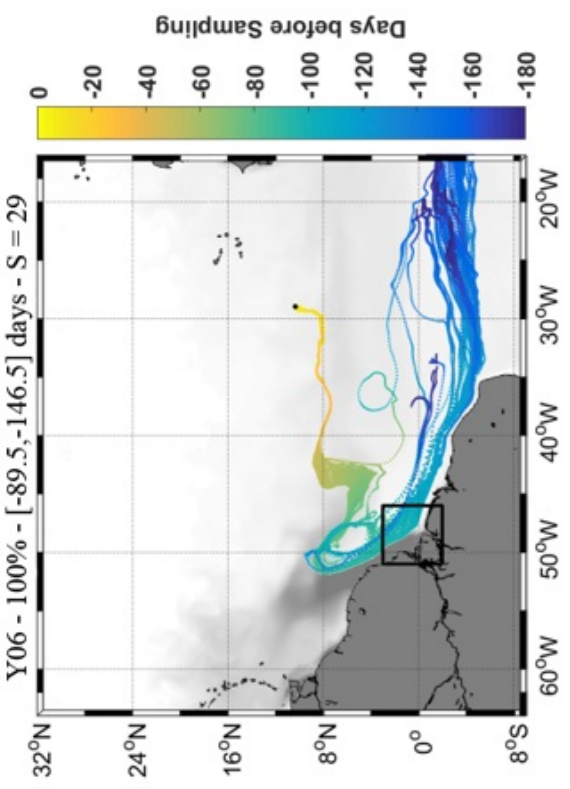
Y06 - 100% - [-89.5,-146.5] days - S = 29
Days before Sampling
0
-20
-40
-60
-80
-100
-120
-140
-160
-180
32°N
24°N
16°N
8°N
0°
8°S
60°W
50°W
40°W
30°W
20°W

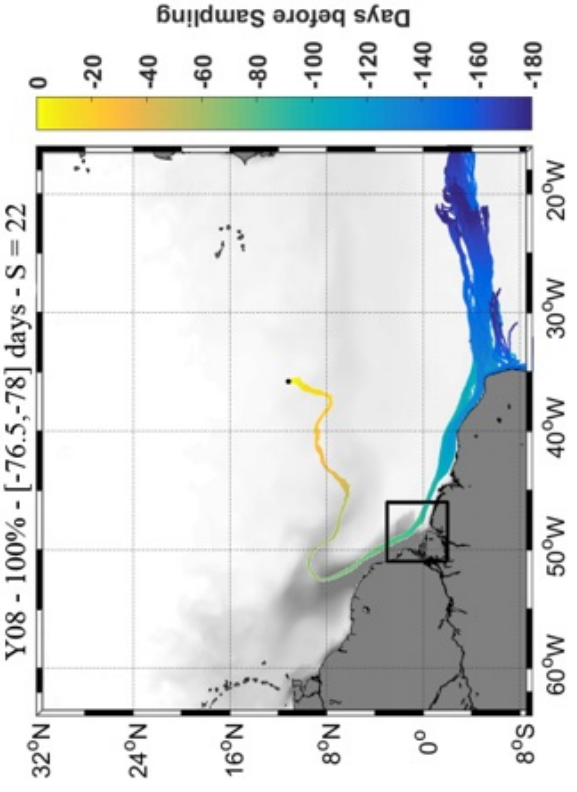
Y08 - 100% - [-76.5,-78] days - S = 22
Days before Sampling
0
-20
-40
-60
-80
-100
-120
-140
-160
-180
32°N
24°N
16°N
8°N
0°
8°S
60°W
50°W
40°W
30°W
20°W

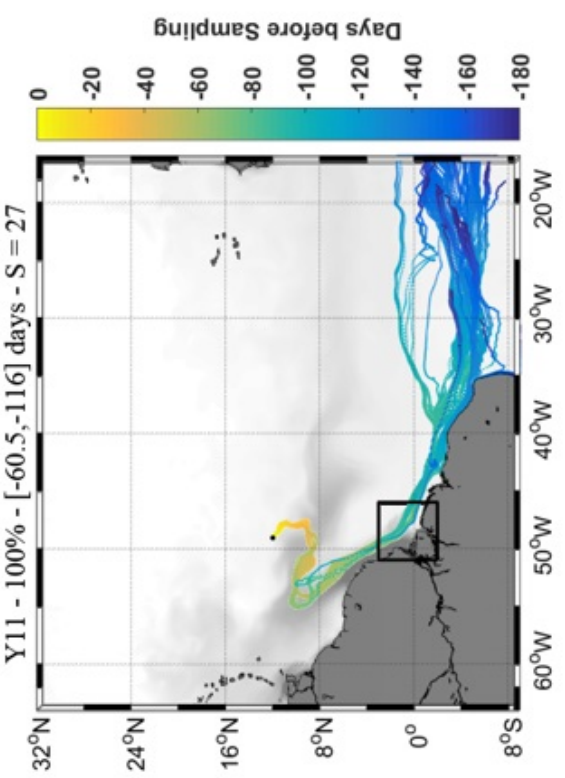
Y11 - 100% - [-60.5,-116] days - S = 27
Days before Sampling
0
-20
-40
-60
-80
-100
-120
-140
-160
-180
32°N
24°N
16°N
8°N
0°
8°S
60°W
50°W
40°W
30°W
20°W

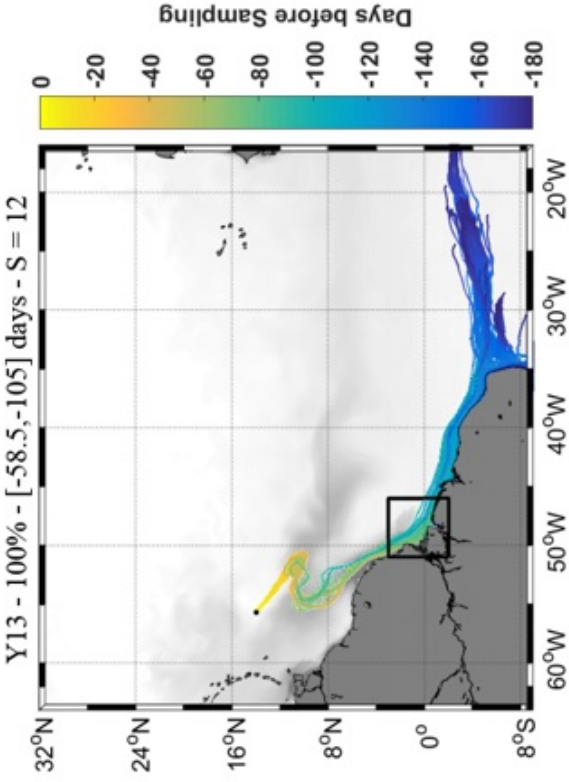
Y13 - 100% - [-58.5,-105] days - S = 12
Days before Sampling
0
-20
-40
-60
-80
-100
-120
-140
-160
-180
32°N
24°N
16°N
8°N
0°
8°S
60°W
50°W
40°W
30°W
20°W

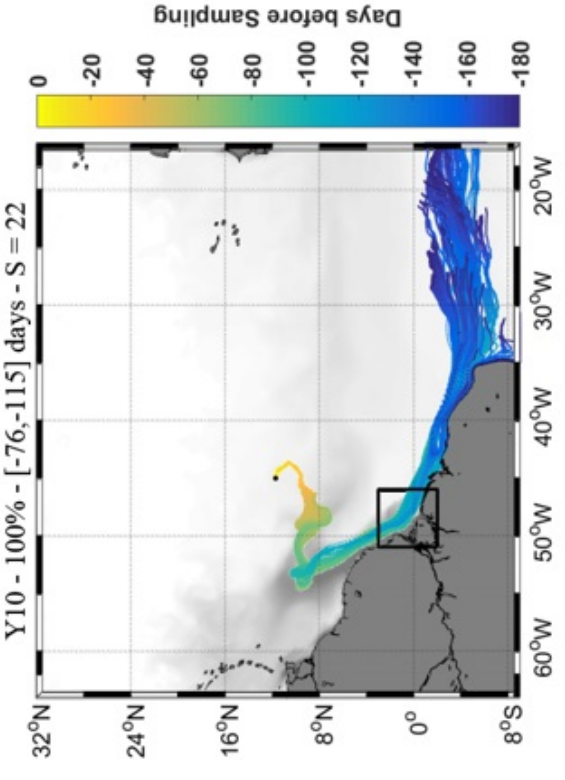
Y10 - 100% - [-76,-115] days - S = 22
Days before Sampling
0
-20
-40
-60
-80
-100
-120
-140
-160
-180
32°N
24°N
16°N
8°N
0°
8°S
60°W
50°W
40°W
30°W
20°W

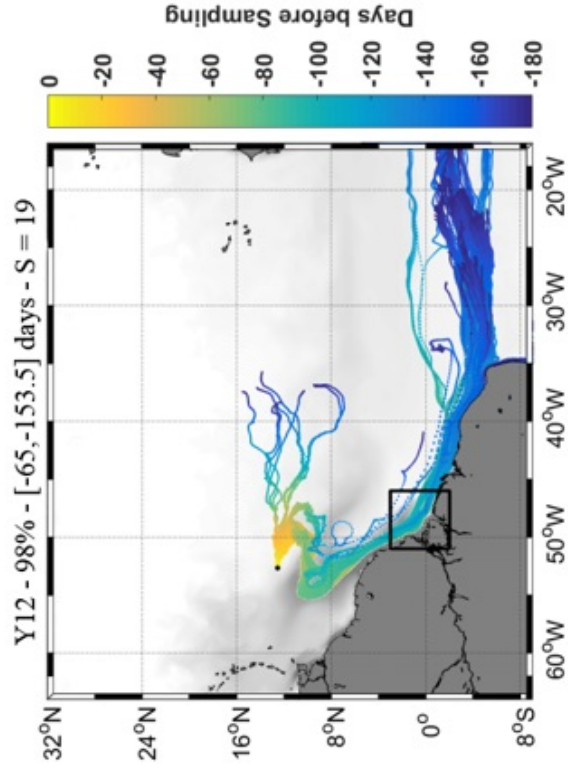
Y12 - 98% - [-65,-153.5] days - S = 19
Days before Sampling
0
-20
-40
-60
-80
-100
-120
-140
-160
-180
32°N
24°N
16°N
8°N
0°
8°S
60°W
50°W
40°W
30°W
20°W

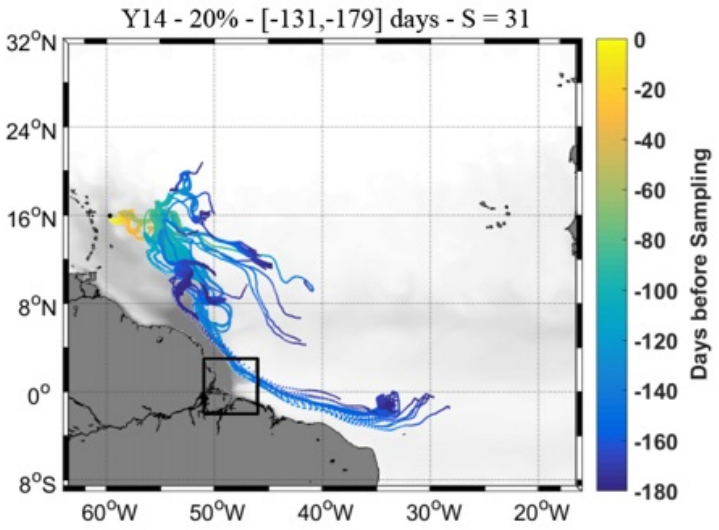

Figure S5: Water mass backwards trajectories of all stations (Y01-Y14, from upper left to lower right) except Y16, which is too close to the coast for reliable simulation results. Each map has a caption indicating the station ID, the percentage of particles that passed through the black box (indicating the Amazon Estuary) and the number of days that passed between the sampling of the water masses and their journey in the black box (indicated in brackets). The minimum of salinity (S) reached by particles during their journey in the black box is indicated as well as the river plume (in grey).

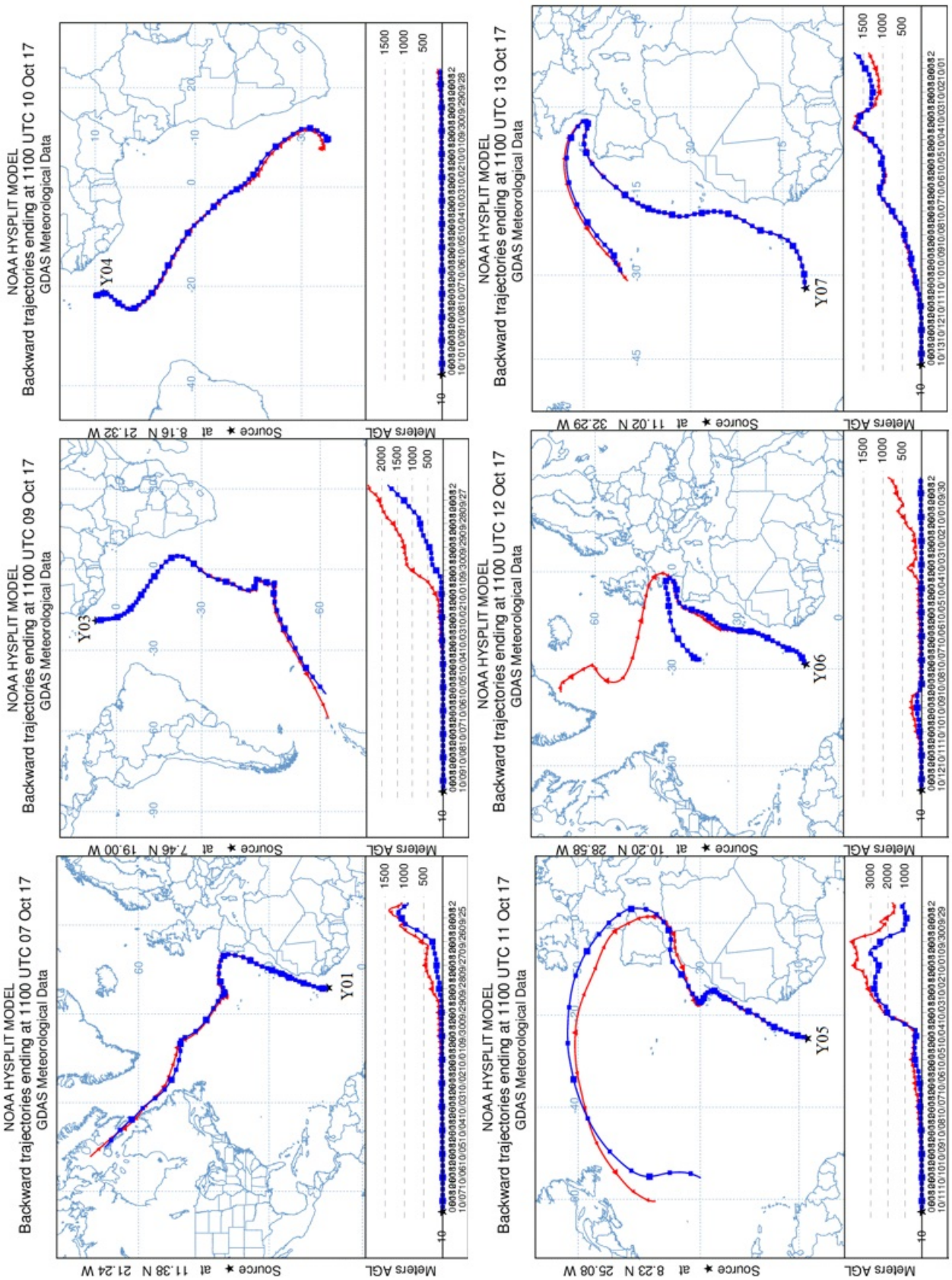
NOAA HYSPLIT MODEL
Backward trajectories ending at 1100 UTC 07 Oct 17
GDAS Meteorological Data
Y01
Source ★ at 11.38 N 21.24 W
Meters AGL
NOAA HYSPLIT MODEL
Backward trajectories ending at 1100 UTC 09 Oct 17
GDAS Meteorological Data
Y03
Source ★ at 7.46 N 19.00 W
Meters AGL
NOAA HYSPLIT MODEL
Backward trajectories ending at 1100 UTC 10 Oct 17
GDAS Meteorological Data
Y04
Source ★ at 8.16 N 21.32 W
Meters AGL
NOAA HYSPLIT MODEL
Backward trajectories ending at 1100 UTC 11 Oct 17
GDAS Meteorological Data
Y05
Source ★ at 8.23 N 25.08 W
Meters AGL
NOAA HYSPLIT MODEL
Backward trajectories ending at 1100 UTC 12 Oct 17
GDAS Meteorological Data
Y06
Source ★ at 10.20 N 28.58 W
Meters AGL
NOAA HYSPLIT MODEL
Backward trajectories ending at 1100 UTC 13 Oct 17
GDAS Meteorological Data
Y07
Source ★ at 11.02 N 32.29 W
Meters AGL

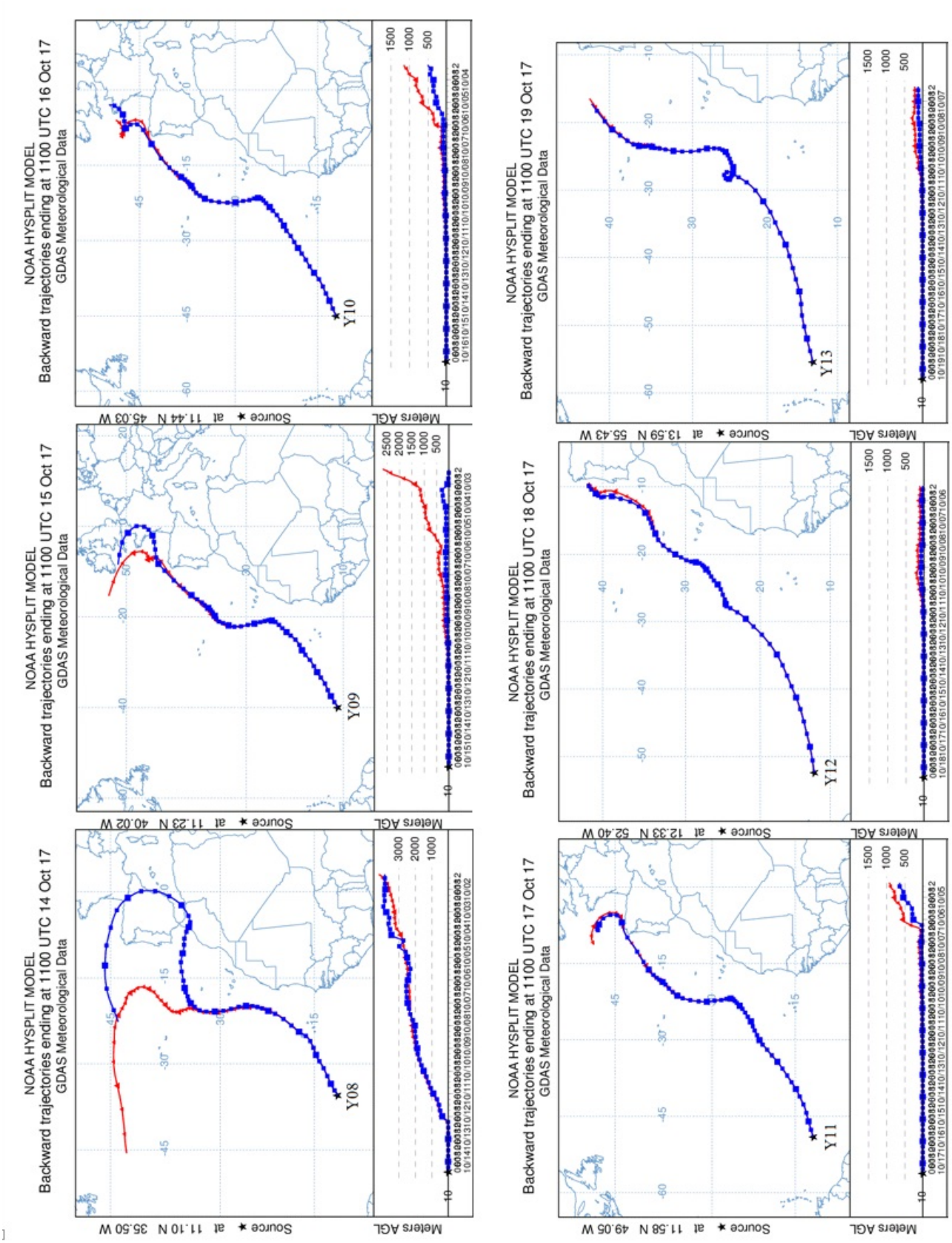
NOAA HYSPLIT MODEL
Backward trajectories ending at 1100 UTC 14 Oct 17
GDAS Meteorological Data
Source ★ at 11.10 N 35.50 W
Meters AGL
Y08
NOAA HYSPLIT MODEL
Backward trajectories ending at 1100 UTC 15 Oct 17
GDAS Meteorological Data
Source ★ at 11.23 N 40.02 W
Meters AGL
Y09
NOAA HYSPLIT MODEL
Backward trajectories ending at 1100 UTC 16 Oct 17
GDAS Meteorological Data
Source ★ at 11.44 N 45.03 W
Meters AGL
Y10
NOAA HYSPLIT MODEL
Backward trajectories ending at 1100 UTC 17 Oct 17
GDAS Meteorological Data
Source ★ at 11.58 N 49.05 W
Meters AGL
Y11
NOAA HYSPLIT MODEL
Backward trajectories ending at 1100 UTC 18 Oct 17
GDAS Meteorological Data
Source ★ at 12.33 N 52.40 W
Meters AGL
Y12
NOAA HYSPLIT MODEL
Backward trajectories ending at 1100 UTC 19 Oct 17
GDAS Meteorological Data
Source ★ at 13.59 N 55.43 W
Meters AGL
Y13

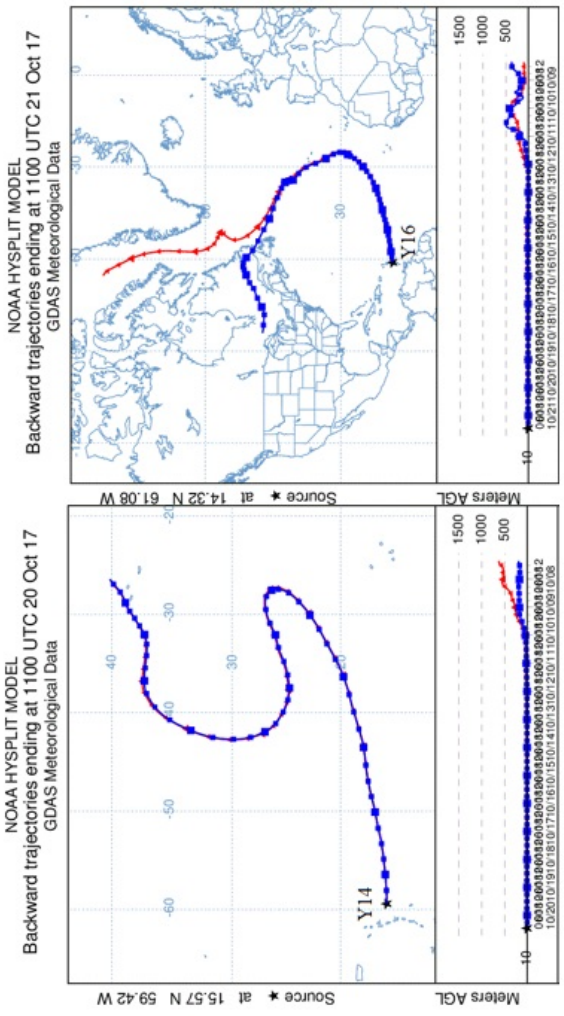

Figure S6: Air mass backward trajectories modelled for each sampling station using the NOAA HYSPLIT Model (https://www.arl.noaa.gov/hysplit/hysplit/). Black stars indicate the location of the sampling stations. The model was set to start at 10 m altitude and to run for 315 hours

SUPPLEMENTARY TABLES

Table S1: GPS positions of the sampling stations, collection dates and surface salinity.

Station ID	Latitude	Longitude	Date	Salinity
Y 01	11°38.2081' N	21°23.8295' W	10/07/2017	34.4
Y 03	7°46.3369' N	19°00.1133' W	10/09/2017	34.8
Y 04	8°16.5055' N	21°31.5612' W	10/10/2017	33.8
Y 05	8°23.2678' N	25°07.6840' W	10/11/2017	35.1
Y 06	10°19.9553' N	28°58.0255' W	10/12/2017	34.6
Y 07	11°01.9355' N	32°28.8749' W	10/13/2017	34.3
Y 08	11°09.4697' N	35°50.0678' W	10/14/2017	34.8
Y 09	11°22.7072' N	40°01.6629' W	10/15/2017	34.7
Y 10	11°43.4907' N	45°03.1796' W	10/16/2017	35.0
Y 11	11°57.9510' N	49°05.2901' W	10/17/2017	34.5
Y 12	12°33.1485' N	52°40.1368' W	10/18/2017	34.6
Y 13	13°59.3505' N	55°42.7139' W	10/19/2017	35.1
Y 14	15°56.6274' N	59°41.6454' W	10/20/2017	33.7
Y 16	14°32.1003' N	61°07.9776' W	10/21/2017	33.2

Table S2: Quantification and confirmation ions of OPEs (GC/MS).

Compound	Full name	Q1	Q2	Q3	Q4
TPP	Tripropyl phosphate	99	141	123	183
TiBP	Tri-iso-buthyl phosphate	99	155	139	
TnBP	Tri-n-butyl phosphate	99	155	211	
TCEP	Tris-(2-chloroethyl) phosphate	249	251	143	99
TCPP-1	Tris-(2-chloro, 1-methylethyl) phosphate	125	99	157	277
TCPP-2	Tris-(2-chloro, 1-methylethyl) phosphate	125	99	157	277
TDCP	Tris-(2-chloro-, 1-chloromethylethyl) phosphate	191	99	381	209
TPhP	Triphenyl phosphate	326	325	215	170
EHDPP	2-ethylhexyl-diphenyl phosphate	251	250	326	
TEHP	Tris(2-ethylhexyl) phosphate	99	113	112	
TBP-*d27*	Tri-n-butyl-d27 phosphate	103	167	231	
TPhP-*d15*	Triphenyl-d15 phosphate	341	339	223	180
TCPP-*d18*	Tris-(2-chloro, 1-methylethyl)-d18 phosphate	131	164	193	
TDCP-*d15*	Tris-(2-chloro-, 1-chloromethylethyl)-d15 phosphate	197	199	217	394
TPrP-*d21*	Tri-n-propyl-d21 phosphate	103	131	151	199
TCEP-*d12*	Tris-(2-chloroethyl)-d12 phosphate	261	263	148	231
MAL-*d7*	Malathion-d7	174	131	128	164

Table S3: $[M-H]^-$ values for BPs and PFCs quantification by LC-HRMS Agilent LC-QTOF 6530.

Compound	Full name	[M-H]-
BPA	Bisphenol A	227.1078
BPAF	Bisphenol AF	335.0512
BPAP	Bisphenol AP	289.1234
BPF	Bisphenol F	199.0765
BPS	Bisphenol S	249.0227
BPZ	Bisphenol Z	267.1391
BPA-*d16*	Bisphenol A-d16	243.2082
PFHA	Perfluoro hexanoic acid	312.9728
PFHS	Perfluorohexane sulfonic acid	398.9366
PFOA	Perfluorooctanoic acid	412.9664
PFOS	Perfluorooctane sulfonic acid	498.9302
PFOSF	Perfluorooctane sulfonyl fluoride	500.9259
PFHA-*13C*	Perfluoro hexanoic acid-13C	317.9896
PFHS-*13C*	Perfluorohexane sulfonic acid-13C	401.9467
PFOA-*13C*	Perfluorooctanoic acid-13C	420.9933
PFOS-*13C*	Perfluorooctane sulfonic acid-13C	506.9571

Table S4: Limits of quantification (LOQ) expressed as absolute amounts (pg) and ng L^{-1} in seawater.

Compound	LOQ	
	(pg)	(ng L^{-1})
TPP (CAS 513-08-6)	5	0.13
TiBP (CAS 126-71-6)	1	0.03
TnBP (CAS 126-73-8)	2	0.05
TCEP (CAS 115-96-8)	10	0.19
TCPP (CAS 13674-84-5)	10	0.25
TDCP (CAS 13674-87-8)	10	0.25
TPhP (CAS 115-86-6)	5	0.10
EHDPP (CAS 1241-94-7)	5	0.13
TEHP (CAS 78-42-2)	10	0.20
TBP-*d27* (CAS 61196-26-7)	2	0.05
TPhP-*d15* (CAS 1173020-30-8)	5	0.13
TCPP-*d18*	30	0.75
TDCP-*d15* (CAS 1447569-77-8)	11	0.28
BPA (CAS 80-05-7)	10	1.0
BPAF (CAS 14878-61-1)	1	0.1
BPAP (CAS 1571-75-1)	20	2.0
BPF (CAS 620-92-8)	10	1.0
BPS (CAS 80-09-1)	1	0.1
BPZ (CAS 843-55-0)	50	5.0
PFHA (CAS 307-24-4)	80	8.0
PFHS (CAS 3871-99-6)	1	0.1
PFOA (CAS 335-67-1)	20	2.0
PFOS (CAS 1763-23-1)	1	0.1
PFOSF (CAS 307-35-7)	10	1.0

Table S5: Concentrations (in ng L^{-1}) of all 20 molecules analyzed for each sampling station as well as extraction, transport and laboratory blank values. Sampling station data are already blank-corrected. For each sampling station, the average of the concentrations measured in the two replicates is given.

	Extraction Blank	*Extraction Blank*	*Extraction Blank*	*Transport Blank*	*Laboratory Blank*	*Y 01*	*Y 03*	*Y 04*	*Y 05*	*Y 06*	*Y 07*	*Y 08*	*Y 09*	*Y 10*	*Y 11*	*Y 12*	*Y 13*	*Y 14*	*Y 16*
TPP	n.d.	n.d.	n.d.	n.d.	n.d.	n.d.	n.d.	n.d.	n.d.	n.d.	n.d.	n.d.	n.d.	n.d.	n.d.	n.d.	n.d.	n.d.	n.d.
TiBP	<LOQ	n.d.	n.d.	n.d.	n.d.	3.9	6.5	1.8	2.7	2.0	5.2	6.2	11	33	38	30	17	1.7	<LOQ
TnBP	n.d.	n.d.	n.d.	n.d.	n.d.	n.d.	n.d.	n.d.	n.d.	n.d.	n.d.	n.d.	n.d.	n.d.	n.d.	n.d.	n.d.	n.d.	n.d.
TCEP	n.d.	n.d.	n.d.	n.d.	n.d.	<LOQ	1.0	<LOQ	<LOQ	<LOQ	<LOQ	<LOQ	1.3	n.d.	1.6	1.2	1.6	<LOQ	<LOQ
TCPP	29	7.9	31	5.4	6.7	203	248	141	142	205	290	577	466	921	1300	966	596	104	74
TDCP	n.d.	n.d.	n.d.	n.d.	n.d.	n.d.	n.d.	n.d.	n.d.	n.d.	n.d.	n.d.	n.d.	n.d.	n.d.	n.d.	n.d.	n.d.	n.d.
TPhP	<LOQ	<LOQ	<LOQ	n.d.	<LOQ	2.2	6.9	1.5	1.0	<LOQ	<LOQ	<LOQ	1.3	<LOQ	1.5	1.6	1.3	<LOQ	<LOQ
EHDPP	<LOQ	<LOQ	<LOQ	<LOQ	<LOQ	2.4	5.4	2.4	1.2	<LOQ	<LOQ	<LOQ	1.2	1.0	<LOQ	<LOQ	<LOQ	<LOQ	<LOQ
TEHP	n.d.	n.d.	n.d.	15	16	<LOQ	<LOQ	n.d.	n.d.	n.d.	n.d.	n.d.	n.d.	n.d.	n.d.	n.d.	n.d.	n.d.	n.d.
Σ_9 OPEs	**29**	**7.9**	**31**	**20.4**	**22.7**	**211.5**	**267.8**	**146.7**	**146.9**	**207.0**	**295.2**	**583.2**	**480.8**	**955.0**	**1341.1**	**998.8**	**615.9**	**105.7**	**74.0**
BPA	1.0	1.0.	<LOQ	n.d.	n.d.	1.2	n.d.	n.d.	n.d.	n.d.	n.d.	<LOQ	1.8	1.8	<LOQ	<LOQ	<LOQ	n.d.	n.d.
BPAF	<LOQ	<LOQ	1.0	<LOQ	<LOQ	n.d.	n.d.	n.d.	n.d.	n.d.	n.d.	n.d.	n.d.	n.d.	n.d.	n.d.	n.d.	n.d.	n.d.
BPAP	n.d.	<LOQ	<LOQ	<LOQ	<LOQ	n.d.	n.d.	n.d.	n.d.	n.d.	n.d.	n.d.	n.d.	n.d.	n.d.	n.d.	n.d.	n.d.	n.d.
BPF	<LOQ	<LOQ	<LOQ	<LOQ	<LOQ	n.d.	n.d.	n.d.	n.d.	n.d.	n.d.	n.d.	n.d.	n.d.	n.d.	n.d.	n.d.	n.d.	n.d.
BPS	<LOQ	n.d.	<LOQ	n.d.	n.d.	n.d.	n.d.	n.d.	n.d.	n.d.	n.d.	<LOQ	n.d.	1.1	<LOQ	n.d.	n.d.	n.d.	n.d.
BPZ	n.d.	n.d.	n.d.	n.d.	n.d.	n.d.	n.d.	n.d.	n.d.	n.d.	n.d.	n.d.	n.d.	n.d.	n.d.	n.d.	n.d.	n.d.	n.d.
Σ_6 BPs	**1.0**	**1.0**	**1.0**			**1.2**							**1.8**	**2.9**					
PFHA	2.2	<LOQ	1.0	<LOQ	<LOQ	n.d.	n.d.	n.d.	n.d.	n.d.	n.d.	n.d.	n.d.	9.7	16	11	n.d.	n.d.	n.d.
PFHS	n.d.	n.d.	n.d.	n.d.	n.d.	n.d.	n.d.	n.d.	n.d.	n.d.	n.d.	n.d.	n.d.	n.d.	4.4	n.d.	n.d.	n.d.	n.d.
PFOA	<LOQ	n.d.	n.d.	n.d.	n.d.	n.d.	n.d.	n.d.	n.d.	n.d.	n.d.	n.d.	n.d.	n.d.	2.9	n.d.	n.d.	n.d.	n.d.
PFOS	<LOQ	n.d.	<LOQ	<LOQ	<LOQ	n.d.	n.d.	n.d.	n.d.	n.d.	n.d.	n.d.	n.d.	n.d.	2.3	n.d.	n.d.	n.d.	n.d.
PFOSF	n.d.	n.d.	n.d.	<LOQ	<LOQ	n.d.	n.d.	n.d.	n.d.	n.d.	n.d.	n.d.	n.d.	n.d.	n.d.	n.d.	n.d.	n.d.	n.d.
Σ_5 PFCs	**2.2**		**1.0**											**9.7**	**25.6**	**11.0**			
Total						**212.7**	**267.8**	**146.7**	**146.9**	**207.0**	**295.2**	**583.2**	**482.6**	**967.6**	**1366.7**	**1009.8**	**615.9**	**105.7**	**74.0**

n.d. = not detected; LOQ = limit of quantification

Abbreviations: TPP: Tripropyl phosphate, TiBP: Tri-iso-buthyl phosphate, TnBP: Tri-n-butyl phosphate, TCEP: Tris-(2-chloroethyl) phosphate, TCPP: Tris-(2-chloro, 1-methylethyl) phosphate, TDCP: Tris-(2-chloro-, 1-chloromethylethyl) phosphate, TPhP: Triphenyl phosphate, EHDPP: 2-ethylhexyl-diphenyl phosphate, TEHP: Tris(2-ethylhexyl) phosphate, BPA: Bisphenol A, BPAF: Bisphenol AF, BPAP: Bisphenol AP, BPF: Bisphenol F, BPS: Bisphenol S, BPZ: Bisphenol Z, PFHA: Perfluoro hexanoic acid, PFHS: Perfluorohexane sulfonic acid, PFOA: Perfluorooctanoic acid, PFOS: Perfluorooctane sulfonic acid, PFOSF: Perfluorooctane sulfonyl fluoride.

Table S6: Surrogate recovery rates (in %) for each sampling station and the extraction blanks. Transport and laboratory blanks were not spiked with surrogate standards, which is why no data are available in this case.

	Extraction Blank	*Extraction Blank*	*Extraction Blank*	*Transport Blank*	*Laboratory Blank*	*Y 01*	*Y 03*	*Y 04*	*Y 05*	*Y 06*	*Y 07*	*Y 08*	*Y 09*	*Y 10*	*Y 11*	*Y 12*	*Y 13*	*Y 14*	*Y 16*
D27-TBP	83.0	84.4	77.6	n.a.	n.a.	87.7	74.9	81.6	75.8	64.4	74.4	72.1	79.9	82.7	82.0	87.7	86.2	63.2	82.2
D18-TCPP	63.8	62.4	62.2	n.a.	n.a.	69.5	67.3	66.7	68.5	67.8	74.5	69.4	71.6	73.4	75.5	79.1	67.0	59.8	72.1
D15-TDCP	106.9	89.1	54.4	n.a.	n.a.	76.0	74.9	81.5	69.2	63.3	74.4	71.3	80.4	64.8	71.1	81.9	82.8	67.0	85.1
D15-TPhP	94.4	82.6	63.2	n.a.	n.a.	64.5	62.0	69.9	56.5	48.7	67.4	61.7	73.3	62.0	71.9	101.9	82.8	77.8	83.5

n.a. = not available

Abbreviations: D27-TBP: D27-Tri-n-butyl phosphate, D18-TCPP: D18-Tris (2-chloroisopropyl) phosphate, D15-TDCP: D15-Tris (1,3-dichloro-2-propyl) phosphate, D15-TPhP: D15-Triphenyl phosphate.

Table S7: Sensitivity tests results for radii from 5 to 25 km and densities from 0.5 to 2.5 particles km^{-2}.

	0.5 particles km^{-2}		1.3 particles km^{-2}		2.5 particles km^{-2}		Sensitivity
Y 01	% of particles	travel time (days)	% of particles	travel time (days)	% of particles	travel time (days)	
5 km	0%		0%		0%		0 %
10 km	0%		0%		0%		
16 km	0%		0%		0%		
25 km	0%		0%		0%		
Y 03							
5 km	0%		0%		0%		0%
10 km	0%		0%		0%		
16 km	0%		0%		0%		
25 km	0%		0%		0%		
Y 04							
5 km	100%	[-124,-125]	100%	[-124,-125]	100%	[-124,-125]	40%
10 km	74%	[-124,-125]	82%	[-124,-125]	80%	[-124,-125]	
16 km	67%	[-124,-126]	70%	[-124,-125]	68%	[-124,-128]	
25 km	60%	[-124,-180]	60%	[-124,-126]	61%	[-124,-127]	
Y 05							
5 km	0%		0%		0%		8%
10 km	0%		0%		0%		
16 km	0%		0%		0%		
25 km	7%	[-92,-126]	8%	[-92,-126]	7%	[-92,-126]	
Y 06							
5 km	100%	[-90,-146]	100%	[-90,-113]	100%	[-90,-146]	0%
10 km	100%	[-90,-146]	100%	[-89,-147]	100%	[-83,-151]	
16 km	100%	[-88,-151]	100%	[-88,-147]	100%	[-84,-147]	
25 km	100%	[-88,-147]	100%	[-82,-148]	100%	[-81,-162]	
Y 07							
5 km	100%	[-88,-92]	100%	[-88,-92]	100%	[-88,-92]	0%
10 km	100%	[-88,-92]	100%	[-88,-92]	100%	[-88,-92]	
16 km	100%	[-88,-92]	100%	[-88,-92]	100%	[-88,-92]	
25 km	100%	[-88,-114]	100%	[-88,-117]	100%	[-88,-127]	
Y 08							
5 km	100%	[-77,-78]	100%	[-76,-78]	100%	[-76,-78]	0%
10 km	100%	[-76,-78]	100%	[-76,-78]	100%	[-76,-78]	
16 km	100%	[-76,-78]	100%	[-76,-78]	100%	[-76,-78]	
25 km	100%	[-76,-85]	100%	[-76,-85]	100%	[-76,-85]	
Y 09							
5 km	0%		0%		0%		0%
10 km	0%		0%		0%		
16 km	0%		0%		0%		
25 km	0%		0%		0%		
Y 10							
5 km	100%	[-76,-115]	100%	[-76,-115]	100%	[-76,-115]	4%
10 km	100%	[-76,-115]	100%	[-76,-115]	100%	[-76,-120]	
16 km	100%	[-76,-115]	100%	[-76,-115]	100%	[-76,-115]	
25 km	96%	[-76,-119]	96%	[-76,-119]	96%	[-76,-119]	
Y 11							
5 km	100%	[-61,-65]	100%	[-61,-65]	100%	[-61,-65]	3%
10 km	100%	[-60,-91]	100%	[-60,-116]	100%	[-60,-116]	
16 km	100%	[-60,-115]	100%	[-60,-96]	100%	[-60,-116]	
25 km	97%	[-60,-116]	97%	[-60,-122]	97%	[-60,-120]	
Y 12							
5 km	100%	[-66,-105]	100%	[-65,-111]	100%	[-65,-139]	8%
10 km	99%	[-65,-140]	98%	[-65,-154]	97%	[-65,-153]	
16 km	93%	[-52,-140]	92%	[-52,-153]	92%	[-52,-159]	
25 km	94%	[-37,-159]	95%	[-37,-140]	95%	[-37,-159]	
Y 13							
5 km	100%	[-59,-81]	100%	[-59,-106]	100%	[-59,-107]	0%
10 km	100%	[-58,-106]	100%	[-58,-105]	100%	[-58,-106]	
16 km	100%	[-57,-107]	100%	[-57,-107]	100%	[-57,-107]	
25 km	100%	[-54,-107]	100%	[-54,-107]	100%	[-54,-107]	
Y 14							
5 km	33%	[-138,-141]	30%	[-138,-156]	29%	[-132,-159]	26%
10 km	23%	[-133,-156]	20%	[-131,-179]	21%	[-131,-174]	
16 km	23%	[-78,-157]	26%	[-78,-168]	25%	[-78,-179]	
25 km	46%	[-78,-175]	46%	[-78,-180]	46%	[-78,-179]	